universität wien

DISSERTATION

Titel der Dissertation

Regulation of meiotic progression in *Arabidopsis*

Verfasserin

Mgr. Petra Bulánková

angestrebter akademischer Grad

Doktorin der Naturwissenschaften (Dr. rer.nat.)

Wien, 2010

Studienkennzahl lt. Studienblatt:	A 091 490
Dissertationsgebiet lt. Studienblatt:	Molekulare Biologie,
Betreuerin / Betreuer:	Dr. Karel Riha

ABSTRACT

Meiosis is a specialized cell division necessary for sexual reproduction. Although the fundamental regulatory mechanisms are shared with mitosis, meiosis has several crucial characteristics that require a different regulation. Whereas in mitotic cell cycle is cell division always preceded by DNA replication, during meiosis a diploid maternal cell undergoes two subsequent rounds of chromosome segregation in the absence of DNA synthesis, which results in formation of four haploid daughter cells. Therefore the cell cycle machinery has to be modified to repress DNA replication after the first meiotic division. This is achieved by mechanisms that retain elevated levels of cyclin-dependent kinase (cdk) activity after meiosis I. However, complete cdk inactivation must occur after the second nuclear division to allow for exit from meiosis. Mechanisms that govern the differential regulation of transition from high to low cdk activity after the first and second meiotic divisions are still poorly understood. To understand regulation of meiotic cell cycle in plants, one aim of my thesis was focused on characterization of the *SMG7* gene that is essential for meiotic exit. I developed a cytogenetic method to study the level of cdk activity in distinct stages of meiosis and I could show that the defect in *smg7* mutants is caused by a failure to downregulate cdk activity at meiotic exit. Therefore I tested whether inactivation of a meiotic cyclin alleviates anaphase II arrest in SMG7 deficient plants. *TAM* is an A-type cyclin, that is specifically expressed during first meiotic division and its deficiency causes premature exit from meiosis in interkinesis. Interestingly, I found that the *tam* phenotype is suppressed by inactivation of *SMG7*. Another protein important for meiotic exit is TDM1. I showed that the anaphase II arrest observed in *smg7* mutants is dependent on TDM1. In addition, *TDM1* is also epistatic to *TAM*. These data argue that while *TAM* is crucial for entry into the second meiotic division, progression through meiosis II has to be driven by another cdk-cyclin complex(es). To determine the core meiotic cell cycle machinery I focused the second part of my project on the identification of cyclins expressed during male meiosis in *Arabidopsis*. I generated marker lines for all 11 *Arabidopsis* B-type cyclins and found that three of them are expressed during meiosis. Further analysis indicated that two cyclins may represent not-conserved pseudogenes. I am currently investigating whether the only conserved protein -coding cyclin is partially responsible for a residual cdk activity in interkinesis and whether SMG7 is involved in regulation of its activity.

ZUSAMMENFASSUNG

Meiose, eine spezielle Art der Zellteilung, ist für die sexuelle Reproduktion notwendig. Obwohl die regulatorischen Mechanismen ähnlich jenen der Mitose sind, hat Meiose einige entscheidende Unterschiede in dessen Regulierung. In Mitose findet DNA Replikation immer vor der Zellteilung statt. In Meiose durchläuft eine diploide Mutterzelle eine zweifache Chromosomensegregation ohne vorheriger DNA Synthese, was in vier haploiden Tochterzellen resultiert. Die Zellzyklusmaschinerie muss so modifiziert werden, dass die DNA Replikation nach Meiose I unterdrückt wird, was durch ein erhöhtes Level an cyclin-dependent kinase (cdk) Aktivität erzielt wird. Nach der zweiten nuklearenTeilung muss eine komplette cdk Inaktivierung erfolgen, um die Meiose zu beenden. Die Mechanismen der unterschiedlichen Regulierung von cdk nach der 1. und 2. meiotischen Teilung sind noch unklar. Um die Regulierung der Meiose in Pflanzen besser zu verstehen, war ein Ziel meines Dokorrats die Charakterisierung des *SMG7* Genes, welches für den Meioseaustritt essenziell ist. Ich habe eine zytogenetische Methode entwickelt, die das Aktivitätslevel von cdk in verschiedenen meiotischen Phasen bestimmt und zeigte, dass der Defekt in *smg7* Mutanten auf einer mangelnden Herunterregulierung der cdk Aktivität bei Meioseaustritt basiert. Ich testete ob die Inaktivierung eines meiotischen Zyklins den Anaphase II Arrest in *smg7* Mutanten verringert. *TAM* ist ein A-Typ Zyklin, das während Meiose I exprimiert wird und dessen Fehlen zu einem verfrühten Meioseaustritt in Interkinese führt. Ich konnte zeigen, dass dieser *tam* Phenotyp durch die Inaktivierung von *SMG7* unterdrückt wird. Ein weiteres Protein das für den Meioseaustritt wichtig ist, ist TDM1 und ich demonstrierte, dass der Anaphase II Arrest der *smg7* Mutanten von TDM1 abhängt. Außerdem ist *TDM1* epistatisch zu *TAM*. Dies weist darauf hin, dass *TAM* für den Eintritt in Meiose II entscheidend ist, aber für den Verlauf der Meiose II andere cdk-Zyklin Komlexe verantwortlich sind. Im zweiten Teil meines Projektes fokussierte ich auf die Identifikation von Zyklinen, die während der männlichen Meiose in *Arabidopsis* exprimiert werden. Ich entwickelte Markerlinien für alle 11 *Arabidopsis* B-Typ Zykline und zeigte, dass drei Linien in Meiose exprimiert werden. Weitere Analysen weisen darauf hin, dass zwei Zykline unkonservierte Pseudogene sind.

Zurzeit untersuche ich, ob das einzige konservierte Protein-kodierende Zyklin für eine Restaktivität der cdk in der Interkinese verantwortlich ist und ob SMG7 in der Regulierung dieser Aktivität beteiligt ist.

TABLE OF CONTENTS

ABSTRACT

ZUSAMMENFASSUNG

1. INTRODUCTION……...…….....…1

1.1. Cell cycle…….….....1

1.2. Cell cycle regulation…….....2

1.3. Regulation of progression trough M-phase……..…….....4

1.4. Meiosis……..……..…….…..7

1.5. Regulation of meiotic activity during interkinesis in distinct model organism.….....9

1.5.1. *Xenopus laevis*

1.5.2. *Saccharomyces cerevisiae*

1.5.3. *Schizosaccharomyces pombe*

1.6. Meiotic cell cycle in *Arabidopsis thaliana*.……...…..12

1.7. Role of *SMG7* during meiosis in *Arabidopsis thaliana* …….....14

1.8. Goals of this thesis…….……....…….....15

2. RESULTS……..……...…...16

2.1. Spindle checkpoint functionality in *smg7* mutants ……...…...…….……..16

2.1.1. Conditions for effective induction of spindle checkpoint in *Arabidopsis*

2.1.2. Induction of spindle checkpoint in meiosis

2.2. Inhibition of proteasome by MG115 can mimic *smg7* phenotype……..……....27

2.3. CDK activity in meiosis...……..…….....28

2.3.1. Background

2.3.2. Which *Arabidopsis* cdk is involved in regulation of meiotic cell cycle?

2.3.3. Localization of CDKA;1:YFP construct in *Arabidopsis* meiocytes

2.3.4. Test of antibodies against phosphorylated threonine 161 in *CDKA;1* t-loop
2.3.5. Cytogenetic detection of active CDKA;1
2.4. *SMG7* dysfunction suppresses premature meiotic exit in *TAM* deficient plants.....39
2.4.1. *tam-2 null* allele causes exit after first meiotic division
2.4.2. Localization of TAM:GUS protein
2.4.3. Genetic interaction between *SMG7* and *TAM* gene
2.5. Anaphase arrest in *smg7* mutants is dependent on TDM1 protein…….…...52
2.5.1. *TDM1* mutant phenotype
2.5.2. *smg7 tdm1* double mutant
2.5.3. TDM1 protein localization
2.6. Premature exit in *tam* null mutants depends on *TDM1*…….....61
2.7. Screen for meiotic B-type cyclins in *Arabidopsis* ……...…....64
2.7.1. B-type cyclins in *Arabidopsis*
2.7.2. Detection of cyclin expression in plant tissues
2.7.3. Subcellular localization B-type cyclins by immunocytology
2.7.3.1. Expression in mitotic cells
2.7.3.2. Expression in meiotic cells
2.7.4. Characterization of cyclins expressed in meiosis

3. DISCUSSION……...……..…….…….....90

3.1. *SMG7* is required for down-regulation of cdk activity during meiotic anaphase ……..……...…….....90
3.2. TDM1 protein is required for anaphase arrest in *SMG7* mutant plants.……...…...93
3.3. Neither *smg7* anaphase arrest nor *tdm1* re-entry into the third meiosis require TAM activity…….…….....96
3.4. Two cyclin pseudogenes and *CYCLIN B3;1* are expressed during meiosis in *Arabidopsis thaliana*…….....102

4. CONCLUSION……...……..…….…….……...….107

5. MATERIAL AND METHODS……..……....109

5.1. Plant material……..…….…….……...…….....…109

5.1.1. Plant cultivation
5.1.2. *In vitro* plant culture
5.1.3. T-DNA insertion lines
5.2. Genotyping……...…110
5.2.1. Allele specific PCR for *tam-1* allele:
5.3. Crossing……...…112
5.4. Analysis of gene expression……...…….....113
5.4.1. RNA isolation
5.4.2. RNA concentration and integrity control
5.4.2.1. RNA concentration estimation
5.4.2.2. RNA mini gel
5.4.3. RT-PCR
5.4.3.1. DNAse treatment
5.4.3.2. cDNA synthesis
5.4.3.3. PCR amplification of cDNAs
5.4.4. 3´ RACE
5.5. Generation of transgenic lines……..……...…118
5.5.1. Cloning strategy for TAM:GUS and TDM:GUS constructs
5.5.2. Cloning strategy for CYCLIN B:GUS constructs
5.5.3. Cloning of TAM:GUS and TDM1:GUS constructs
5.5.3.1.1. PCR amplification of inserts
5.5.3.1.2. Cloning to pENTR/D/TOPO vector
5.5.3.1.3. Heat-shock transformation of *Escherichia coli*
5.5.3.1.4. Glycerol stock preparation and plasmid extraction
5.5.3.1.5. Verification of plasmids by restriction digest
5.5.3.1.6. Sequencing of plasmids
5.5.3.1.7. Gateway recombination to pMDC163 vector
5.5.4. Cloning of CYCLIN B : GUS constructs
5.5.4.1.1. PCR amplification of inserts
5.5.4.1.2. Cloning to pCR2.1 TOPO vector
5.5.4.1.3. Restriction cloning to pCBK04 vector
5.5.5. Electroporation of plasmid to *Agrobacterium tumefaciens*
5.5.6. Transformation of plants with *Agrobacterium tumefaciens*
5.5.7. Selection of representative plant lines
5.6. Alexander staining…….....129

5.7. Histochemical GUS staining…….....…130
5.8. Transpiration stream delivery …….....130
5.9. Cytogenetic analysis……...…….....131
5.9.1. Preparation of slides for scoring mitotic and meiotic stages
5.9.2. Preparation of slides for detection of CDKA:YFP and immunodetection from inflorescences
5.9.3. Preparation of slides for immunodetection in cells from roots
5.9.4. Immunodetection
5.10. Analysis of ploidy……..…….....133
5.11. Protein analysis……...…….....134
5.11.1. Protein extraction
5.11.2. Western blot
5.11.3. Antibody specificity testing with competitive peptides
5.11.4. Phosphatase treatment
5.12. *In silico* analysis……..….…….....136
5.12.1. Annotation of *Arabidopsis lyrata* B-type cyclins

6. REFERENCEES……...…….....137

7. ABBREVIATIONS……...…….....151

8. ACKNOWLEDGEMENT……...…….....153

9. CURRICULUM VITAE……...…….....155

1. INTRODUCTION

1.1. Cell cycle

Cell cycle is series of events necessary for proper cell reproduction. Cell division is a fundamental feature of all living organism. In unicellular organisms cell division results in a formation of a new organism, whereas in multicellular organism it contributes to a development and regeneration of tissues and organs.

Most cell divisions generate two daughter cells with equal DNA contents. To maintain the DNA content, it is necessary that DNA replication that takes place during ´S´ or synthesis phase precedes the cell division during ´M´ or mitotic phase. S and M phase are usually separated by two gap phases ´G1´ and ´G2´, where cell growth and synthesis of molecules necessary for further progression occur. Cells that are not dividing are in G0 or ´quiescent´ phase. The length of the individual cell cycle phases, and presence or absence of gap phases varies between distinct cell types or organisms. In addition some specialized cells in multicellular organism may undergo endoreduplication cycle where M phase is skipped. Despite these differences, the key features of progression trough cell cycle and the key molecules that drive it, are conserved in eukaryotes. As inappropriate progression trough cell cycle could have fatal consequences, all cells have a regulatory network that surveys the correct order of events and eventually delays or stops cell cycle progression trough numerous checkpoints until all ongoing processes are correctly finished.

Studies in frog oocytes showed that M-phase can be completed in enucleated cells and, therefore, the factors required for M-phase progression have to be present in cytoplasm (reviewed in Duesbery and Vande Woude 1998). In 1971 Masui and Markert demonstrated existence of a specific cytoplasmic factor called `Maturation promoting factor – MPF` that is crucial for cell cycle progression. They showed that cytoplasm from hormonally stimulated enucleated oocytes can stimulate untreated oocytes for progression trough meiosis. Moreover, cytoplasm from an oocyte which was stimulated by MFP containing cytoplasm from another oocyte could subsequently activate other untreated oocytes (Masui and Markert 1971; Duesbery and Vande Woude 1998). Later on, work in Paul Nurse and Tim Hunts labs showed that the MFP consists of cyclin-dependent kinase (cdk) and cyclin (Nurse and Thuriaux 1980; Evans et al. 1983). Whereas cyclin-dependent kinases are stable, protein levels of cyclins oscillate with each round of cell cycle. Extensive research in this area has established the current textbook model of cell cycle

regulation. It was shown that the necessary condition for activity of cyclin-dependent kinase is binding of a cyclin (Pines and Hunter 1989). Complexes consisting of a cyclin-dependent kinase and of a cyclin, or so-called cdk complexes, are the key molecules that drive progression trough cell cycle by phosphorylating down-stream substrates. These substrates include proteins involved in inhibition of cell cycle progression which are inactivated upon phosphorylation like pRb protein or proteins that positively regulate cell cycle progression that are activated by this phosphorylation like transcription factor B-Myb. There is a great variability in the number of cyclins and cdks in different eukaryotic organisms. Although it was shown, that one single cdk complex is sufficient to drive progression trough mitotic cell cycle in fission yeast (Fisher and Nurse 1996), most organisms use specific cdk complexes for distinct stages of the cell cycle.

1.2. Cell cycle regulation

The regulation of cell cycle is extremely complex and there are species or even cell type specific differences in the details of this regulation. Therefore in the following text are summarized only very basic principles of cell cycle regulation which are relevant for further understanding of work described in this thesis. Because nomenclature for genes and proteins differs in distinct model organism, all names of genes and protein that are shared by different organism are in following text written with first letter in uppercase (example: Wee1). All names that have already become a general name describing a wide and conserved group of genes/ proteins are written with all letters in the lowercase (example: cdk, the only exception is anaphase-promoting complex APC). Names of proteins from a particular organism are written according to rules relevant for this organism (example *SMG7* gene in *Arabidopsis*).

Principles of cdk activity regulation

In general, the coordination of cell cycle with environmental and developmental signals is assured through regulation of activity of cdk-cyclin complexes. Cyclin dependent kinases belong to the family of serine/threonine protein kinases. Most known cdks are small proteins around 34 kDa that are inactive as monomers. Activation of a cdk requires conformation change that liberates ATP binding site and the access of substrates to the catalytic site. First condition important for activity is binding of a cyclin. The cyclin binding motif PSTAIRE is highly conserved in the cdk family and its interaction with cyclin induces the first change in the conformation of cdk. The second condition for cdk activation is phosphorylation of so-called t-

loop or activation loop. Phosphorylation of a particular threonine in t-loop is carried by cyclin activating kinase (cak), which is itself also a cyclin dependent kinase. This activating phosphorylation further changes the conformation of cdk-cyclin complex which is now fully active.

Negative regulation of cdk complexes can occur at several levels. First, there is a range of cdk complex inhibitors. In animals, the proteins from Cip/Kip family can bind both cdk and cyclin in a cdk complex and inhibit the activity by blocking the ATP binding site and conformation change in the active cdk site. Other mechanism for inhibition of cdk activity is inhibiting phosphorylation of the cdk in so-called p-loop. This phosphorylation is carried by conserved Wee1 and related Myt1 kinase at tyrosine 15, and in some organism also at threonine 14. Again, this phosphorylation changes locally conformation of cdk and interferes with ATP –binding site. This phosphorylation can be removed by phosphatases from the Cdc25 family. Following text summarizes regulation of cdk complexes activity in distinct stages of a cell cycle.

Progression trough cell cycle

In a very simplified model based on work in yeast, *Drosophila* and mammalian cell culture, the entry into a new round of cell cycle starts in G1 phase. The start of a new cell cycle is triggered by external signals from its environment and also by internal factors that are integrated by cell. It induces elimination of effect from cell cycle inhibitory proteins such as pRb and p21, and stimulates synthesis of G1/S cyclins. The main G1 cyclins are D-type or E-type cyclins in animals, and Cln cyclins in *Saccharomyces cerevisiae*. G1/S cyclins subsequently initiate synthesis of proteins required for DNA replication, as well as of S phase cyclins and their activation. Later on, as S phase proceeds, the G1 cdk complexes initiate their own inactivation by mediating degradation of G1 cyclins through ubiquitination by SCF ubiquitin ligase pathway (Lanker et al. 1996; Won and Reed 1996; Welcker et al. 2003). Cyclins regulating S phase differ between species. In *Drosophila* and *Xenopus* embryos the major S-phase cyclin is Cyclin E (Chevalier et al. 1996; Lilly and Spradling 1996; Strausfeld et al. 1996; Follette et al. 1998; Hinchcliffe et al. 1999) whereas in cultured mammalian cells it is Cyclin A. S-phase cyclins in budding yeast are the Clb5 and Clb6 cyclins that are also important for M-phase (Schwob and Nasmyth 1993; Cross et al. 1999). DNA replication requires also activity of another kinase called Cdc7 which is distantly related to cyclin dependent kinases and associates with Dbf4 cyclin (Bousset and Diffley 1998; Donaldson et al. 1998). To ensure that DNA replication takes place only once per cell cycle, the assembly of pre-replicative complexes at origins of replication

is allowed only under the condition of low or none cdk activity, which occurs during exit from M-phase and early G1 phase (reviewed in Waga and Stillman 1998; Bell and Dutta 2002). After activation of origins of replication in S phase, the pre-replicative complex is disassembled and its reassembly is prevented by high cdk activity until the following G1 phase (Dahmann et al. 1995). Another important event that takes place during DNA replication and which is important for chromosome segregation in M phases, is establishment of cohesion of sister chromatids. The entry to mitosis is allowed only after DNA replication was completed and all components necessary for cell division like centrosomes or spindle pole body were duplicated. In most eukaryotes, this is controlled by checkpoint that operates during G2 phase (reviewed in Elledge 1996). The only known exception is budding yeast, where the G2 phase rather overlaps with M phase and therefore cells with DNA damage stop only at metaphase due to spindle checkpoint (Rhind and Russell 1998). G2 phase further allows accumulation of B-type cyclin-cdk complexes, which are the key complexes for the following M-phase. Because M-phase is of special importance for this work, it is described in more details in the next chapter.

1.3. Regulation of progression trough M-phase

M-phase is the final phase of a cell cycle when cell divides. It consists of a nuclear division - mitosis, and cell division – cytokinesis. These divisions are under very strict control in order to divide genetic material equally between daughter cells. During M-phase, cells undergo the most apparent morphological changes. Replicated chromosomes begin to condense together with spindle assembly during prophase followed by nuclear envelope breakdown and migration of chromosomes to centre of a spindle during prometaphase. In metaphase, chromosomes are aligned in the metaphase plate with all chromosomes attached to both poles of spindle. This is monitored by spindle checkpoint that inhibits further mitotic progression until all chromosomes are properly bioriented (or attached to the spindle). During anaphase, sister chromatids separate and are pulled apart by spindle to the opposite poles of a cell. During telophase, the divided chromatids decondense, spindle disassembles and new nuclear envelop forms. The cell division starts usually simultaneously with progression trough anaphase or telophase. In animals, cleavage plane is specified shortly after anaphase onset. An actin-myosin contractile ring constricts the cell membrane and forms so-called cleavage furrow that moves inwards to the centre of a cell. At the late stages of cytokinesis is formed a structure called midbody, which defines the site where the cell is finally cleaved (reviewed in Glotzer 2001). In contrast, plant cells have a cell wall and therefore the mechanism of cytokinesis significantly differs from the animal model. Plant cell divides by formation of a cell plate in the midzone between separating

nuclei. This requires formation of phragmoplast that is required for trafficking of vesicles that will form a plasma membrane or carries a cell wall material. These vesicles fuse together at the cell plate and are transformed into new membrane. Afterwards a components of a cell wall such as callose and cellulose are deposited (reviewed in Jurgens 2005).

Such complicated processes require very precise regulation. The key cdk complexes that drive progression through mitosis are A and B-type cyclins with their associated cdks. The exact function of A-type cyclins in mitosis has not been yet fully understood. Animal A-type cyclins that play a critical role during progression through S-phase, appear to be also important at the mitotic entry. They are essential for mitotic entry in *Drosophila* and mammalian somatic cells, but dispensable in *Xenopus* eggs that can enter mitosis without cyclin A (Lehner and O'Farrell 1990; Walker and Maller 1991; Kim and Ferrell 2007). The B-type cyclins which are sometimes called mitotic cyclins play a central role in M-phase regulation. At the entry into mitosis, cyclin B-cdk complexes are kept inactive by phosphorylation of threonine 14 and tyrosine 15 in the p-loop by Wee1 and Myt1 kinases (reviewed in Nurse 1990) This phosphorylation can be counteracted by Cdc25 phosphatase. It was shown that in mammalian cells is Cyclin A required for accumulations of active cdk-cyclin B complexes through inactivating Wee1 kinase (Fung et al. 2007; Deibler and Kirschner 2010) and thereby allowing Cdc25 phosphatase to remove inhibitory phosphorylation. Activated cyclin B-cdk complexes together with polo-like kinases phosphorylate downstream targets including proteins important for chromosome condensation, nuclear envelop breakdown, spindle assembly, and thereby promote the major events of prophase, prometaphase and metaphase. The cyclin B-cdk activity peaks at metaphase when all chromosomes are align at metaphase spindle.

Important mitotic transition is initiation of chromosome separation. Correct attachment of chromosomes to spindle is monitored by spindle checkpoint (reviewed in Musacchio and Hardwick 2002; Pinsky and Biggins 2005). Incorrectly attached kinetochores generate a signal which prevents activation of anaphase promoting complex (APC). APC is an ubiquitin-protein ligase that targets proteins for degradation by 26S proteasome (reviewed Peters 2006). It is of a central importance for mitosis as it triggers anaphase by destroying securin and promotes progression through anaphase and telophase by mediating proteolytic degradation of mitotic cyclins. In contrast to SCF-ubiquitin-protein ligases, APC is activated by binding of co-factors, mainly Cdc20 and Cdh1. At least a fraction of the APC^{cdc20} is activated already during late prophase and destroys Cyclin A and some other targets, recognition of which by APC is not inhibited by the spindle checkpoint (Di Fiore and Pines 2010; den Elzen and Pines 2001;

Wolthuis et al. 2008). When all chromosomes are correctly attached to spindle, spindle checkpoint is released and APC becomes fully active. Activation of APC is critical for progression from metaphase to anaphase. Two main targets degradation of which is necessary condition for progression through anaphase are Securin and Cyclin B. Securin is a protein that inhibits Separase - a protease that cleaves cohesin that holds sister chromatids together - thereby allowing separation of sister chromatids to opposite poles of a cell by spindle. Degradation of Cyclin B results in decrease of cdk activity, which is a necessary condition for progression through anaphase. As the cdk activity drops down, target proteins are being dephosphorylated enabling chromosome decondensation, nuclear envelope assembly and other events that revert cells back to interphase. Dephosphorylation of cdk targets is in budding yeast carried out by Cdc14p phosphatase (reviewed in Stegmeier et al. 2002; Clifford et al. 2008b) which is activated by release from nucleolus by FEAR and MEN networks. It was shown that in other organism is dephosphorylation carried out by action of protein phosphatases PP1, PP2A, and calcineurin (reviewed in De Wulf et al. 2009).

Full deactivation of M phase cdk-cyclin is required to proceed to G1 phase and next round of cell cycle (Wolf et al. 2007)). Degradation of APC targets is based on motifs in their amino-acid sequences: so-called destruction box (D-box) and KEN-box (Glotzer et al. 1991; Pfleger and Kirschner 2000). These motifs are recognized by the core APC complex, but binding of APC activators Cdc20 and Cdh1 facilitates their recognition and subsequent protein ubiquitination. While the APC^{cdc20} is important for metaphase to anaphase transition, APC^{cdh1} activity is required later to maintain the M-phase cdks downregulated during G1 phase (reviewed in Fang et al. 1999; Skaar and Pagano 2008). This is further facilitated by cdk inhibitors that also suppress cdk activity during G1 phase (Sherr and Roberts 1999). In budding yeast, fission yeast and *Drosophila* are found functionally similar inhibitors Sic1p, Rum1p and Roughex respectively, which directly inhibit M-phase cdk activity in G1 phase. They do not inhibit G1 phase cdks and therefore do not block entry into a new cell cycle. Taken together, there are several mechanisms that ensure uni-directionality of cell cycle progression by down-regulating M-phase cdk activity after the onset of anaphase.

1.4. Meiosis

Meiosis is a modified cell division that is essential for sexual reproduction. For most eukaryotic organism is sexual reproduction a part of their life cycle. Although there are differences in sexual reproductive strategies such as existence of distinct sexes or hermaphrodism, the principal steps consist of 1) formation of haploid gametes and 2) their subsequent fusion with other gamete which leads to formation of a new diploid cell. In multicellular organisms this cell called zygote and its subsequent extensive divisions give rise to the whole organism. In some eukaryotes including algae, fungi, some protozoa and plants can this cell serve as dormant stage in non-hostile environment and then is called spore.

Meiosis is the reductional cell division which produces haploid gametes from diploid cells. This is accomplished by two subsequent nuclear divisions that follow only one round of DNA replication. The two nuclear segregations are separated by short stage called interkinesis. Therefore chromosome segregation during meiosis requires differential regulation of basic cell cycle related processes.

There are three key features that distinguish meiosis from mitosis: 1) homologous chromosomes pair and in most organism eventually recombine during prophase I, 2) the first meiotic division segregates the paired chromosomes that have kinetochores attached to the spindle in monopolar orientation and 3) chromosome segregation after the first meiotic division is not followed by S-phase, but chromosomes enter a second round of segregation after short interkinesis (reviewed in Marston and Amon 2004). Chromosome pairing and recombination are relatively well studied in variety of different organisms. In contrast very little is known about the regulation of meiotic cell cycle. There are several reasons why meiotic cell cycle progression has not yet been thoroughly studied. Although initiation of meiosis can be stimulated by external factors in unicellular organisms, meiosis is not synchronous in individual cells. Reliable protocols for synchronization of *S. cerevisiae* were developed only recently independently by groups of A. Amon and W. Zachariae (Carlile and Amon 2008; Matos et al. 2008). In multicellular organism, cells undergoing meiosis are not numerous and they are localized in specialized organs. Therefore, in these organisms, the regulation of meiotic cell cycle can be investigated only using genetic and cytogenetic approaches. The only exception between multicellular model organisms is *Xenopus laevis* which oocytes can be easily obtained in sufficient quantities. Moreover *Xenopus* oocytes provide a cell-free system, easy synchronization by hormones and possibility to directly detect

particular proteins or measure kinase activity. Therefore most of our current view on regulation of cdk activity in meiosis comes from studies on *Xenopus* (reviewed in Ohsumi et al. 2006; Philpott and Yew 2008).

Involvement of cdk complexes in regulation of meiotic progression became apparent from the very first cell cycle studies when it was confirmed that the `Maturation promoting factor – MPF` discovered by Masui and Markert, is in fact a cdk-cyclin complex (reviewed in Perez-Hidalgo et al. 2007). In most cases, the same cdk-cyclin complexes are required for somatic divisions and meiosis. The importance of cdk complexes in normal development of the organism complicates the investigation of their specific roles in meiosis. However, by dissecting functions of Cdc7-Dfb4 complex, it was possible to show that this complex is not only required during S phase, but it also initiate monopolar attachment and meiotic recombination in budding yeast (Matos et al. 2008). Although in most studied organism the major mitotic cyclins are required also for meiosis, there are several examples of meiosis-specific cyclins such as Rem1p in fission yeast, CYCLIN A1 and CYCLIN B3 in mammals and *CYCLIN SDS* in *Arabidopsis*, (Liu et al. 1998; Azumi et al. 2002; Nguyen et al. 2002a; Malapeira et al. 2005). Their absence usually results in mis-regulation of chromosome pairing and recombination.

Biochemical measurement of cdk activity during meiosis was so far possible only in yeast cells and *Xenopus* oocytes. These experiments established that there are two peaks of activity during meiosis - in metaphase I and metaphase II (Gerhart et al. 1984; Kanki and Donoghue 1991a; Minshull et al. 1991; Furuno et al. 1994; Carlile and Amon 2008; Tang et al. 2008). Interestingly, it seems that the cdk activity is higher in metaphase I than in metaphase II (Tang et al. 2008). To allow division of paired chromosomes in meiosis I and division of sister chromatids in meiosis II, cdk activity drops down during each anaphase. But a specific mechanism has to operate during interkinesis to assure that cdk activity is decreased to a level that allows chromosome decondensation and spindle rearrangement, but is still sufficient to prevent assembly of pre-replicative complexes and exit to G1 phase (Marston and Amon 2004). This mechanism has to be switched off after the second meiotic division, when exit to G1 phase takes place. Although this differential regulation of cdk activity seems to be valid for all studied species, the precise details of its regulation differ. Therefore, the current knowledge of cdk regulation during meiosis is summarized for best characterized model organisms separately.

1.5. Regulation of meiotic activity during interkinesis in distinct model organism

1.5.1. *Xenopus laevis*

Large *Xenopus* oocytes can be easily enucleated, manipulated by microinjections and synchronized by hormone treatments in quantities sufficient for biochemical analysis. Therefore *Xenopus* oocytes present the major source of information about the biochemistry of meiosis. Immature *Xenopus* oocytes store a large pool of mRNAs that are translated in three waves, according to their polyadenylation (reviewed in Radford et al. 2008). Immature oocytes are arrested in prophase I, but this arrest is released by progesterone treatment. Exposure to progesterone induces translation of stored mRNAs, which is necessary for subsequent progression through meiosis I and meiosis II up to metaphase II, when the oocyte remains arrested until fertilization (reviewed in Philpott and Yew 2008). Studies in the *Xenopus* oocytes showed that cdk is reactivated in interkinesis to suppress S-phase and to prevent exit from meiosis after the first meiotic division (Furuno et al. 1994). Cyclin re-synthesis between divisions was shown to be activated by the mos/MAPK pathway (Kanki and Donoghue 1991b; Furuno et al. 1994; Gross et al. 2000; Frank-Vaillant et al. 2001).

Xenopus genome encodes five B-type cyclins and with the exception cyclin B3, all are expressed in oocytes (Hochegger et al. 2001). It was shown after the hormonal stimulus with progesterone progression through the first division is driven by cyclin B2 and B5 which are stored in immature oocytes. Their degradation during anaphase I is counteracted by new cyclin synthesis, specifically of cyclins B1 and B4, which mRNAs are translated after meiosis I (Hochegger et al. 2001). However, cyclins are not the only proteins required for progesterone-induced oocyte maturation in *Xenopus*. It was shown that proteins from ringo/speedy family are another class of cdk activators involved in meiotic G2/M transition, despite not having amino acid sequence homology with cyclins (Ferby et al. 1999; Lenormand et al. 1999, reviewed in Nebreda 2006). emi2 protein is another player that was shown to be required for cyclin re-synthesis and metaphase II arrest (Ohe et al. 2007; Tung et al. 2007). emi2 is phosphorylated by MAPK cascade downstream of mos and this phosphorylation stimulates its association with APC that seems to be dependent on the D-box motif (Nishiyama et al. 2007). Therefore, emi2 possibly inhibits APC by blocking substrate access. Interestingly, emi2 binding to APC is inhibited by cdk phosphorylation on other residues than the ones that are targeted by mos/MAPK. Tang and colleagues (Tang et al. 2008) found that cdk activity is higher during metaphase I then in

metaphase II. They proposed that high cdk activity in metaphase I lead to degradation of emi2, and that only the drop of cdk activity during anaphase I allow emi2 re-synthesis. In these conditions emi2 contributes to cyclin re-synthesis by inhibiting APC. During metaphase II, in conditions of lower cdk activity than in metaphase I, emi2 is stabilized by the pp2a phosphatase and contributes to metaphase II arrest (Tang et al. 2008).

1.5.2. *Saccharomyces cerevisiae*

S. cerevisiae or budding yeast is one of the best studied model organisms in which were discovered several important regulatory mechanism of mitotic progression and chromosome segregation. The first screen for cell cycle mutants was carried in budding yeast already in 1970 by Hartwell and colleagues (Hartwell et al. 1970). Therefore, it is rather surprising that the precise regulation of cdk activity and of distinct cyclins were biochemically examined during meiosis only recently (Carlile and Amon 2008).

Sexual reproduction is in yeast induced by response to nutrient depletion. The meiotic program is induced by expression of Ime1p transcription factor, that triggers expression of early genes required for pre-meiotic DNA synthesis (Kassir et al. 1988; Mandel et al. 1994). One of them is Ime2p kinase that phosphorylates the cdk inhibitor Sic1p and allows activation of S-phase cdk complexes (Smith and Mitchell 1989; Dirick et al. 1998). Five out of six clb cyclins participate in meiotic progression; only the major mitotic cyclin Clb2p is absent during meiosis. Clb5p and Clb6p are required for pre-meiotic S-phase (Dirick et al. 1998; Stuart and Wittenberg 1998) and together with Cdc7-Dbf4 complexes for the initiation of homologous recombination (Henderson et al. 2006; Matos et al. 2008). Striking differences were found in the regulation of cyclin proteins and respective cdk activities during meiosis (Carlile and Amon 2008). The Clb5p protein and associated kinase activity peaks during metaphase I and metaphase II and declines during subsequent anaphases. Clb1p and Clb4p protein levels were stable throughout the whole meiosis until meiotic exit. Clb4p activity peaked twice, in metaphase I and in metaphase II, while the Clb1p activity was detectable only in metaphase I. This suggests that there is a cyclin destruction independent mechanism to down-regulate cdk activity during anaphase. mRNA of the cyclin Clb3p was present during both divisions, but it was translated only in the second meiotic division. This translation was regulated by 5´UTR. All these data indicate that progression through meiosis in *S. cerevisiae* requires several mechanisms that operate at level of translation and post-translational modifications.

1.5.3. *Schizosaccharomyces pombe*

Fission yeast is another organism that significantly contributed to understanding of cell cycle. Although it is possible to synchronize cell for examination of meiotic cell cycle by temperature-sensitive *pat1* mutation (Iino and Yamamoto 1985), the progression from metaphase I to meiotic exit is very quick and it is difficult to precisely determine stages of meiosis. Fission yeast has five cyclins: three of them regulate mitotic divisions: Cig1p and Cig2p control S phase (Connolly and Beach 1994; Obara-Ishihara and Okayama 1994; Martin-Castellanos et al. 1996), and Cdc13p is the M-phase cyclin (Booher and Beach 1988; Hagan et al. 1988). Nevertheless, it was shown that Cdc13p alone is sufficient for progression through mitotic cell cycle (Fisher and Nurse 1996). The *cdc13* gene is also essential for progression through meiosis I and II (Iino et al. 1995). The Cig2p cdk activity is present during first meiotic division and plays a minor role in completion of the second meiotic division (Borgne et al. 2002). Rem1p and Crs2p, the last two *S. pombe* cyclins, are meiotically expressed. Interestingly *cig2* as well as the *rem1* and *crs1* transcripts exhibit meiosis-specific splicing (Borgne et al. 2002; Averbeck et al. 2005; Malapeira et al. 2005; Moldon et al. 2008). In case of *rem1* and *crs1*, this splicing prevents their expression during mitotic divisions, which could be toxic for cells. Both cyclins are regulated also on transcriptional level, so the amount of transcripts in vegetative cells is very low. It was shown that forced expression of Rem1p during mitotic cell cycle results in G1 arrest caused by a mitotic catastrophe due to division without fully replicated DNA (Malapeira et al. 2005). Rem1p was shown to be required for meiotic gene conversion. Similarly, translation of the last cyclin *crs1* is prevented in vegetative cells by intron retention (Averbeck et al. 2005), as its contrived expression in mitotic cells causes cell cycle arrest resulting in cells containing hypercondensed DNA and abnormal nuclear segregation (Averbeck et al. 2005). The precise role of distinct cyclins during meiosis is still not clear, but their activity appears to be at least partially retained in interkinesis. A mechanism that protects cyclins from complete destruction after first meiotic division has been elucidated recently. The key component of this mechanism is *mes1* gene that is also regulated by splicing. Mes1p is substrate of APC that is degraded at the same time as cyclin Cdc13p (Izawa et al. 2005). However, Mes1p is not only APC substrate, but its binding also sequesters Cdc20p and thereby partially inhibits APC. This mutual inhibition between Mes1p and APC prevents total degradation of Cdc13p and decrease of cdk activity during interkinesis (Izawa et al. 2005; Kimata et al. 2008).

1.6. Meiotic cell cycle in *Arabidopsis thaliana*

Arabidopsis is the major plant model for study of meiosis as it allows combination of genetic and cytogenetic approaches. Similar to other model organisms, meiosis in *Arabidopsis* starts with long prophase stage when homologous chromosomes undergo pairing and recombination. It was estimated that it takes 30 hours from S phase until end of pachytene, whereas the rest of meiosis takes only 3 hours (Armstrong et al. 2003). Pairs of homologous chromosomes are divided during the first division which is followed by interkinesis. In *Arabidopsis*, the two nuclei completely decondense, spindle is rearranged, but there is no cell wall formation. Sister chromatids divide in the second meiotic division resulting in formation of four haploid nuclei. In male meiosis, the four haploid nuclei are divided by simultaneous cytokinesis and released as individual microspores. Each microspore further undergo two mitotic divisions and differentiate in trinuclear pollen (Borg and Twell 2010). In female meiosis, three of four haploid cells produced by meiosis undergo programmed cell death (Armstrong and Jones 2001), and mature female gametophyte is produced by three consecutive mitotic divisions of the single surviving haploid nuclei.

There is a great number of known genes involved in pairing of homologous chromosomes and recombination (reviewed in Mercier and Grelon 2008), but only few mutants were shown to directly influence meiotic cell cycle progression. One of them is the major *Arabidopsis* cyclin-dependent kinase *CDKA;1*. *CDKA;1* is an essential gene and it is the only *Arabidopsis* cdk which can rescue *S. pombe cdc2* mutation (Ferreira et al. 1991; Hirayama et al. 1991). A hypomorphic *cdka;1* allele conferring decreased cdk activity was produced by substitution of threonine 161, which phosphorylation is necessary for cdk activity, with a phosphomimicry residuum (Dissmeyer et al. 2007; Harashima et al. 2007). This phosphomimicry allele can still rescue lethal null mutation in vegetative growth, but results in failed chromosome pairing and pre-mature cell wall formation in interkinesis. This indicates that, as in mitosis, cdks play the central role in meiotic progression and particularly *CDKA;1* is required.

There are only two meiotic cyclins known so far. One of them, *CYCLIN SDS*, was shown to be required for pairing of homologous chromosome (Azumi et al. 2002). The second cyclin, *TAM*, is involved in regulation of progression from the first to the second meiotic division (Magnard et al. 2001; Azumi et al. 2002; Wang et al. 2004b). *TAM* was found in a screen for mutations affecting pollen development. The first described *tam-1* temperature sensitive allele showed low

frequency formation of abnormal pollen grains that were composed of two gametophytes within one exine (Magnard et al. 2001). It was shown that at restrictive temperatures *tam-1* mutant plants progress trough meiosis with a delay and during interkinesis form a cell wall between the two nuclei. After this stage called dyad, the two halves of dyad progressed into second meiotic division asynchronously. *TAM* was mapped and it was shown that it encodes an A-type cyclin, CYCLIN A1;2 (Wang et al. 2004b). Further, it was determined that *tam-1* temperature-sensitive allele is caused by a point mutation of a conserved amino acid in cyclin domain. Up to now, the precise roles, protein expression and associated activity of the CYCLIN SDS and TAM was not investigated. It is also not clear whether some of the other 50 predicted *Arabidopsis* cyclins participate in regulation of meiotic progression (Wang et al. 2004a).

Although the core components of the cell cycle machinery important for meiotic divisions are not known, several genes as *OSD1*, *TDM1* and *SMG7* seem to directly or indirectly modulate meiotic cdk activity. The exact function of these genes in meiosis is currently not clear, but their mutant phenotypes suggest requirement at a particular stage of meiotic cell cycle. Two of them, *OSD1* and *TDM1* genes encode a plant specific not-conserved proteins (Ross et al. 1997; Glover et al. 1998; Sanders et al. 1999; d'Erfurth et al. 2009), whereas *SMG7* is a factor of non-sense mediated RNA decay conserved in most eukaryotes (Riehs et al. 2008). Loss of *OSD1* causes cell wall formation during interkinesis and subsequent pre-mature meiotic exit after the first meiotic division (d'Erfurth et al. 2009). Therefore *OSD1*, similar as *TAM*, seems to be required for maintaining cdk activity between meiotic divisions.

TDM1 gene seems to be required at meiotic exit. *TDM1* was originally found in screen for genes causing male sterility (Chaudhury 1994). Mutant plants were shown to be completely male sterile and female fertile and without any obvious vegetative phenotype. Later on it was shown that dysfunction of *TDM1* results in attempt to divide unreplicated haploid nuclei after meiosis II (Ross et al. 1997). In wild-type meiosis, chromatids separated during anaphase II are decondensed and form four haploid nuclei in a tetrad stage. Tetrads are then divided by cytokinesis into haploid microspores. *tdm1* mutants form a regular tetrad stage, but it was observed that chromatids again re-condensed in a stage called metaphase III, stretched during anaphase III and then eventually decondensed in form of multiple unequal nuclei. As these experiments were done on DAPI stained meiotic squashes, it is not clear whether there is a spindle formation. *TDM1* gene was mapped and it was shown that this gene encodes a plant specific protein with a limited homology to xe-p9, a regulatory subunit of cdk from *Xenopus* (Glover et al. 1998).

Recently, a conserved factor of non-sense mediated RNA decay, *SMG7*, was shown to be indispensable for meiotic exit (Riehs et al. 2008). SMG7 dysfunction causes very unusual arrest in meiotic cell cycle and therefore, it would be especially interesting to determine its nature as it can help understanding the regulation of meiotic progression and its link to RNA metabolism.

1.7. Role of *SMG7* during meiosis in *Arabidopsis thaliana*

In all three discussed model organism: *Xenopus*, budding and fission yeast, posttranscriptional RNA metabolism and posttranscriptional processing seems to play an important role in meiosis. Work in our lab showed that a conserved factor of non-sense mediated RNA decay, called *SMG7,* is required for proper progression through the second meiotic anaphase and meiotic exit in *Arabidopsis* (Riehs et al. 2008)**.** Non-sense mediated RNA decay is a pathway that eliminates RNAs with premature stop codons (reviewed in Stalder and Muhlemann 2008). The role of *Arabidopsis SMG7* in this process was confirmed independently in our lab and by Kerenyi and colleagues (Kerenyi et al. 2008; Riehs et al. 2008). While *smg7* null mutant is lethal, hypomorphic alleles are viable, but completely sterile due to a meiotic arrest in anaphase II (Riehs et al. 2008). Although the meiotic progression seems to proceeds without defects until early anaphase II, no telophase II could be found in *smg7* mutants. Cells are arrested in an irregular anaphase II stage, which is characteristic by a persistent phosphorylation of histone H3 on serine 10, failure to decondense chromosomes and to reorganize the meiotic spindle. Such cell cycle defect is very unusual and only three causes of a similar phenotype have reported so far: 1) premature loss of sister chromatid cohesion in mutants depleted of shugoshin (Kitajima et al. 2004; Salic et al. 2004; McGuinness et al. 2005), 2) a failure to down regulate cdk activity due to stabilization of B-type cyclin lacking the D-box, or 3) defect in a specific APC activator (Holloway et al. 1993; Sigrist et al. 1995; Page and OrrWeaver 1996; Chu et al. 2001; Parry and O'Farrell 2001; Swan et al. 2005; Swan and Schupbach 2005; Wolf et al. 2006). Analysis of sister chromatid cohesion at centromeres by FISH excluded that the possibility that the arrest is caused by premature loss of cohesion and demonstrated that chromosomes normally aligned to metaphase plate (Riehs et al. 2008).

Thus, SMG7 function appears to be important after metaphase II. To test the second hypothesis that SMG7 directly or indirectly interferes with cell cycle machinery in meiosis, is not so easy due to lack of information about the core meiotic components of cdk complexes in *Arabidopsis*. However, to determine the exact role of SMG7 protein in progression through meiosis in

Arabidopsis will help to shed light on regulation of meiotic cell cycle and eventually the function of RNA metabolism.

1.8. Goals of this thesis

The main focuses of this thesis were following questions:

1. What causes anaphase II arrest in SMG7 deficient meiocytes?

2. What is the relation of *SMG7* to other genes known to play a role in regulation of meiotic cell cycle in *Arabidopsis*?

3. What are the core components of cell cycle machinery?

2. RESULTS

2.1. Spindle checkpoint functionality in *smg7* mutants

SMG7 mutation causes a specific arrest in anaphase II during meiotic division, but progression trough stages of meiosis that precede this arrest does not seem to be affected. To understand the nature of defect in anaphase II, we needed to clarify whether there is no alteration in meiosis progression in *smg7* meiocytes before anaphase II. The most important mechanism surveying the correct progression trough mitotic and meiotic divisions is spindle checkpoint, which prevents entry into anaphase until all chromosomes are properly attached to the spindle apparatus. To test spindle checkpoint in *smg7* mutants we decided to expose meiocytes to spindle poisons inhibiting spindle polymerization. In wild type, destabilization of spindle should result in accumulation of cells in metaphase and increased metaphase to anaphase ration. These inhibitors are widely used in cell biology, but so far, no detailed study was published about their effect on *Arabidopsis.* Therefore we first established condition for effective induction of spindle checkpoint in mitotic cell.

2.1.1. Conditions for effective induction of spindle checkpoint in *Arabidopsis*

We tested number of spindle inhibitors that are known to induce metaphase arrest in various plant species. These drugs and conditions included oryzalin, 8-hydroxyquinoline, colchicine, nocodazol, propyzamide and cold treatment. Furthermore, we also tested combination of some of the inhibitors to increase the effect of the treatment (table 2.1 - 2.9). To deliver these compounds into rapidly dividing cells in intact flowers, we used transpiration stream delivery method. We cut inflorescence stem 5 cm from flowers and dipped the base of the stem into a solution of respective inhibitor in water. A control treatment with water only was performed in parallel. After application of drug, we counted metaphase to anaphase ratio in squashed young buds. During the first treatment with oryzalin, we tested different time intervals: 2, 4 and 6 hours (table 2.2). As 2 hour treatment yielded only mild increase in metaphase to anaphase ratio compared to control experiment, we tested only 4 hour and 6 hour treatments for other inhibitors. Longer incubation times could result in possible adaptation to the inhibitor and cause side effects. Indeed we observed that in few cases a high dose applied for 6 hours resulted in lower metaphase to anaphase ratio than 4 hour treatment with a lower dose (table 2.2 and 2.9). For the cold treatment we applied for 6, 8 and 24 hours intervals to give enough time for physiological response. Very effective inhibitors were oryzalin, 8-hydroxyquinoline and nocodazol, where we could get

metaphase to anaphase ratio over value 3 after 4 hours, compared to control with 1,6 to 1,8 (table 2.2; table 2.4 and table 2.5). Cold treatment was also very effective but we chose not to use it because of difficulty to distinguish the effect of spindle checkpoint from other possible effects on cell metabolism (table 2.7). Surprisingly, widely used colchicine was not very effective, with all values under 2.4 (table 2.3). Finally we chose to test also a mix of inhibitors consisting of 2,5mM 8-hydroxyquinoline, 100µM oryzalin and 100µM colchicine (table 2.9). We counted separately metaphase to anaphase ratio in whole young buds and in anthers only as they were our target organs. Already 4 hour treatment resulted in 5,59 metaphase/anaphase ratio for whole buds and 4,62 for anthers. Although this value increased with time we finally decided that to use 4 hour treatment to minimize side effects. Thus, in our conditions, the most effective spindle checkpoint induction was obtained with a mix of 8-hydroxyquinoline, oryzalin and colchicine.

NEGATIVE CONTROL - WATER

Time in hours	metaphases	anaphases	metaphase : anaphase ratio
2 h	433	232	1,87
4 h	321	161	1,68
6 h	337	210	1,60

Table 2.1: Negative control treatment – water: Time of incubation and numbers of counted mitotic metaphases and anaphases after incubation of wild type plants in water

ORYZALIN

Time in hours	Concentration	metaphases	anaphases	metaphase : anaphase ratio
2 h	10µM	431	197	2,18
2 h	50µM	426	162	2,62
2 h	100µM	414	129	3,20
4 h	10µM	395	148	2,66
4 h	100µM	333	93	3,58
4 h	500 µM	366	170	2,15
6h	100µM	351	137	2,56
6h	500µM	380	150	2,53

Table 2.2: Treatment with oryzalin: Time of incubation, concentration used and numbers of counted mitotic metaphases and anaphases after incubation of wild type plants in oryzalin.

COLCHICINE

Time in hours	Concentration	metaphases	anaphases	metaphase : anaphase ratio
4 h	10 µM	332	141	2,35
4 h	100 µM	288	129	2,23
4 h	1 mM	324	147	2,2
6 h	10 µM	290	127	2,28
6 h	100 µM	325	138	2,35
6 h	1 mM	363	152	2,38

Table 2.3: Treatment with colchicine: Time of incubation, concentration used and numbers of counted mitotic metaphases and anaphases after incubation of wild type plants in colchicine

8-HYDROXYQUINOLINE

Time in hours	Concentration	metaphases	anaphases	metaphase : anaphase ratio
4 h	2,5 mM	275	89	3,1
4 h	10 mM	245	88	2,8
4 h	25 mM	288	97	2,96
6 h	2,5 mM	156	48	3,4
6 h	10 mM	241	68	3,5
6 h	25 mM	290	82	3,5

Table 2.4: Treatment with 8-hydroquinoline: Time, concentration and numbers of counted mitotic metaphases and anaphases after incubation of wild type plants in 8-hydroxyquinoline

NOCODAZOL

Time in hours	Concentration	metaphases	anaphases	metaphase : anaphase ratio
4 h	10 µM	307	109	2,81
4 h	100 µM	320	104	3,07
4 h	500 µM	181	56	3,23
6 h	10 µM	351	131	2,67
6 h	100 µM	337	99	3,4
6 h	500 µM	269	80	3,36

Table 2.5: Treatment with nocodazol: Time, concentration and numbers of counted mitotic metaphases and anaphases after incubation of wild type plants in nocodazol

PROPYZAMIDE

Time in hours	Concentration	metaphases	anaphases	metaphase : anaphase ratio	Note
4 h	1 µM	380	150	2,53	
4 h	10 µM	286	104	2,75	
6 h	1 µM	301	122	2,47	
6 h	10 µM	307	98	3,13	6 anaphases with bridges

Table 2.6: Treatment with propyzamide: Time, concentration and numbers of counted mitotic metaphases and anaphases after incubation of wild type plants in propyzamide

COLD TREATEMENT: 4°C

Time in hours	Concentration	metaphases	anaphases	metaphase : anaphase ratio	Examined in:
6 h	-	431	200	2,2	
6 h	-	83	33	2,51	Anthers
8 h	-	391	145	2,69	
8 h	-	101	28	3,6	Anthers
24 h	-	399	109	3,66	
24 h	-	133	28	4,7	Anthers

Table 2.7: Cold treatment: Time of incubation at 4°C and numbers of counted mitotic metaphases and anaphases after incubation of wild type plants

COLD (4°C) + 2,5 mM 8-HYDROXYQUINOLINE

Time in hours	metaphases	anaphases	metaphase : anaphase ratio
4 h	177	52	3,4
6 h	360	98	3,67
8 h	342	92	3,717
8 h	282	77	3,66

Table 2.8: Treatment of wild type plants with 8-hydroquinoline combined with cold treatment: Time of incubation at 4°C, concentration of 8-hydroxyquinoline and numbers of counted mitotic metaphases and anaphases after incubation

MIX of 2,5mM 8-HYDROXYQUINOLINE + 100µM ORYZALIN + 100µM COLCHICINE

Time in hours	metaphases	anaphases	metaphase : anaphase ratio	Examined in:
4 h	**341**	**61**	**5,59**	
4 h	157	34	4,62	Anthers
6 h	408	73	5,58	
6 h	129	26	4,96	Anthers
8 h	310	51	6,07	
8 h	220	26	8,46	Anthers

Table 2.9: Combined treatment of wild type plants with 2,5 mM 8-hydroquinoline, 100 µM oryzalin and 100µM colchicine: Time of incubation and numbers of counted mitotic metaphases and anaphases after incubation. Best metaphase: anaphase ration in shortest time is highlighted by bold font.

2.1.2. Induction of spindle checkpoint in meiosis

To test spindle checkpoint in meiocytes we started with wild type plants. We applied previously tested mix of inhibitors trough transpiration stream for 4 hours and eventually counted all meiotic stages. We included two independent negative control experiments with water only, to compare variability within negative control with difference to treated sample (table 2.10 - 2.12). In negative controls the metaphase I to anaphase I ratio was 1,0 and 1,4 whereas treatment with inhibitors yielded 28,6. In the case of metaphase II to anaphase II ratio, the difference between control values was higher (0,5 and 1,6) but the treatment again increased the ratio order of magnitude higher (11,8). We tested differences between samples with chi-square test (box 1). The test showed that whereas there is no difference between number of anaphases (anaphase I and anaphase II) in two non-treated wild type samples, there is a significant difference between non-treated and treated samples in wild type plants. Accordingly we can conclude that the application of spindle inhibitors resulted in accumulation of metaphases and induction of spindle checkpoint in meiosis.

WT - NEGATIVE CONTROL 1

Meiotic stage	M I	A I	Interkinesis	MII	A II	T II	Total	MI to AI ratio	MII to AII ratio
Number of meiocytes	61	44	127	27	17	26	302	1,4	1,6
% of total	20,2	14,6	42	8,9	5,6	8,6			

Table 2.10: Negative control WT 1 - incubation of wild type plants in water: Numbers of counted meiotic metaphases and anaphases after incubation, percentages and metaphase: anaphase ratios. MI- metaphase I; AI – anaphase I; MII – metaphase II; AII – anaphase II; TII – telophase II

WT - NEGATIVE CONTROL 2

Meiotic stage	M I	A I	Interkinesis	MII	A II	T II	Total	MI to AI ratio	MII to AII ratio
Number of meiocytes	29	29	134	7	13	5	217	1,0	0,53
% of total	13,3	13,3	61,8	3,2	5,9	2,3			

Table 2.11: Negative control WT 2 - incubation of wild type plants in water: numbers of counted meiotic metaphases and anaphases after incubation, percentages and metaphase: anaphase ratios. MI- metaphase I; AI – anaphase I; MII – metaphase II; AII – anaphase II; TII – telophase II

WT - TREATEMENT

Meiotic stage	M I	A I	Interkinesis	MII	A II	T II	Total	MI to AI ratio	MII to AII ratio
Number of meiocytes	86	3	77	47	4	7	224	28,6	11,75
% of total	38,4	1,3	34,4	20,9	1,8	3,1			

Table 2.12: Combined treatment of wild type plants with 2,5 mM 8-hydroquinoline, 100 µM oryzalin and 100µM colchicine: numbers of counted meiotic metaphases and anaphases after incubation, percentages and metaphase: anaphase ratios. MI- metaphase I; AI – anaphase I; MII – metaphase II; AII – anaphase II; TII –telophase II

To test spindle checkpoint induction in *smg7* mutants we treated in one control sample with water and one sample with inhibitor mix (tables 2.13- 2.14). Metaphase I to anaphase I ratio was in control sample 2,4 but in treated sample 25,5. This numbers corresponds to 10 fold increase already seen in wild type. During second meiotic division, metaphase to anaphase ration in non-treated sample was 0,4 and increased to 0,8 in sample with inhibitors. However, these numbers can be explained by the fact that *smg7* meiosis naturally arrests in anaphase II. As it was determined previously, 75% *smg7* meiocytes were found in aberrant anaphase II stage compared to 0% in wild type meiocytes (Riehs et al. 2008). The progression from starting and still regular anaphase to irregular arrested stage is gradual. Therefore we most likely cannot clearly distinguish between them and many of the counted anaphases started before application of the

inhibitor mix. If tested with chi-square test, the difference between observed and expected number of anaphases II is significant (box 1). This indicates that spindle checkpoint is intact in the second meiotic division. Our data also provide strong evidence for efficient spindle checkpoint in the first meiotic division. These data together with previous observation that centromeric sister chromatin cohesion is intact until metaphase II (Riehs et al. 2008) argue that meiosis in *smg7* mutants proceeds normally until metaphase II and suggest that SMG7 function is specifically required after onset of anaphase II.

smg7 NEGATIVE CONTROL

Meiotic stage	M I	A I	Interkinesis	MII	A II	T II	Total	MI to AI ratio	MII to AII ratio
Number of meiocytes	33	14	77	21	53	0	198	2,36	0,4
% of total	16,7	7,1	38,9	10,6	26,7				

Table 2.13: Negative control *smg7* - incubation of *smg7* plants in water: numbers of counted meiotic metaphases and anaphases after incubation, percentages and metaphase: anaphase ratios. MI- metaphase I; AI – anaphase I; MII – metaphase II; AII – anaphase II; TII –telophase II

smg7 TREATEMENT

Meiotic stage	M I	A I	Interkinesis	MII	A II	T II	Total	MI to AI ratio	MII to AII
Number of meiocytes	51	2	99	27	32	0	201	25,5	0,84
% of total	25,5	1,0	49,2	13,4	15,9				

Table 2.14: Combined treatment of *smg7*plants with 2,5 mM 8-hydroquinoline, 100 µM oryzalin and 100µM colchicine: numbers of counted meiotic metaphases and anaphases after incubation, percentages and metaphase: anaphase ratios. MI- metaphase I; AI – anaphase I; MII – metaphase II; AII – anaphase II; TII –telophase II

CHI - SQUARE TEST:

Chi-square is a statistical test commonly used to compare observed data with data we would expect to obtain according to a specific hypothesis.

The formula for calculating chi-square (χ^2) is:

$\chi^2 = (o-e)^2/e$

so, chi-square is the sum of the squared difference between observed (*o*) and the expected (*e*) data, divided by the expected data in all possible categories. Next is necessary to determine degrees of freedom (df). Degrees of freedom are calculated as the number of categories in minus 1. The resulting number is compared to a chi-square distribution table.

Our null hypothesis: there is no difference between treated and untreated samples

1. Hypothesis1: there is no significant difference in number of anaphases between two control non- treated wild type samples (NC1 and NC2):

In NC1 we have:
NC1 AI: 14,6%
NC1 AII: 5,6%

So if our null hypothesis is true, we would expect to have the same percentages of anaphase I and anaphase II in NC2 sample. Therefore we calculate the expected numbers of anaphases from the total number of meiocytes counted:

NC2 AI expected: 218 x 0,146 = 31,83 =*e1*
NC2 AII expected: 218 x 0,056 = 12,21=*e2*
Real numbers of observed anaphases are:
NC2 AI observed: 29 =*o1*
NC2 AII observed: 13 =*o2*
degrees of freedom: 1

$\chi 2 = (31,83-29)^2 / 31,83 + (12,21-13)^2 / 12,21$
$\chi 2 = 0,16 + 0,05$
$\chi 2 = 0,21 \ll 3,84$ (P=0,05)

Therefore there is no significant difference in number of anaphases between negative control samples in wild type.

2. Hypothesis 2: there is no difference non treated wild type samples (NC1 and NC2) and sample treated with tubulin inhibitors.

In non-treated samples we have:
NC AI: 14,6% and 13,3% - average: 13,95
NC AII: 5,6% and 5,9% - average: 5,75

So if our null hypothesis is true, we would expect to have the same percentages of anaphase I and anaphase II in treated sample. Therefore we calculate the expected numbers of anaphases from the total number of meiocytes counted:

AI expected: 13,95% : 224 x 0,1395 = 31,25 =*e1*
AII expected: 5,75% : 224 x 0,0575 = 12,88=*e2*
Real numbers of observed anaphases are:
Treatment AI: 3 =*o1*
Treatment AII: 4 =o*1*
degrees of freedom: 1

$\chi 2 = (31,25-3)^2 / 31,25 + (12,88-4)^2 / 12,88$
$\chi 2 = 25,54 + 6,12$
$\chi 2 = 31,66 \gg 3,84$ (P=0,05)

Therefore there is a significant difference between number of anaphases in negative control samples and sample treated with tubulin inhibitors in wild type.

3. Hypothesis 3: there is no difference in number of anaphases between non treated *smg7* sample and *smg7* sample treated with tubulin inhibitors

In non-treated sample we have:
NC AI: 7,1 %
NC AII: 26,7%

So if our null hypothesis is true, we would expect to have the same percentages of anaphase I and anaphase II in treated sample. Therefore we calculate the expected numbers of anaphases from the total number of meiocytes counted:

AI expected: 7,1% : 201 x 0,071 = 14,22 =*e1*
AII expected: 26,7% : 201 x 0,267 = 56,67=*e2*
Real numbers of observed anaphases are:
Treatment AI: 2 =*o1*
Treatment AII: 32 =*o2*
degrees of freedom: 1

$\chi 2 = (14,22-2)^2 / 14,22 + (56,67-32)^2 / 56,67$
$\chi 2 = 10,5 + 10,74$
$\chi 2 = 21,24 \gg 3,84$ (P=0,05)

Therefore there is a significant difference between number of anaphases in negative control samples and sample treated with tubulin inhibitors in *smg7*.

Box1: Chi-square test

2.2. Inhibition of proteasome by MG115 can mimic *smg7* phenotype

As already mentioned, there are only three described cases of the phenotype that is similar to *smg7* anaphase arrest. One of them is premature loss of sister chromatid cohesion due to shugoshin dysfunction. However, our previous experiments excluded premature sister chromatid cohesion to be the cause of observed arrest in *smg7* mutants (this work and Riehs et al. 2008). The other two conditions are related to inefficient cyclin degradation that is mediated by anaphase promoting complex (APC). First is mutation in the specific APC subunit *Cortex*, which causes arrest in metaphase II or aberrant anaphase II in *Drosophila* oocytes (Page and OrrWeaver 1996; Chu et al. 2001). Similar condition can be induced in mitotic cells by expressing cyclin B with mutated destruction box and therefore resistant to ubiquitination by APC which is required for degradation by proteasome.

We decided to test whether we can induce similar anaphase arrest in wild type meiocytes by inhibiting proteasome activity. Although all effects of proteolysis inhibition are not known we can expect that the effect would vary in different stages of cell division. In metaphase inhibition of proteasome should stabilize securin and cyclin B and cause accumulation of metaphases. During anaphase when separase is already activated and cohesin cleaved, inhibition of proteolysis should lead to stabilization of cyclin B and anaphase arrest. One of the most efficient and of specific inhibitors of proteasome is MG115 (Carbobenzoxy-L-leucyl-L-leucyl-L-norvalinal) that inhibits its chymotrypsin-like activity (Planchais et al. 2000). Therefore we decided to apply MG115 by transpiration stream to meiocytes and examine its impact on meiosis. We applied 50 μM and 500 μM MG115 dissolved in water for 4 hour, and water control in parallel. In 437 meiocytes scored in both experiments, we found 18 meiocytes that resembled anaphase II arrest stage in *smg7* mutants (8 in 50 mM; 10 in 500 μM) (figure 2.1). We never detected this phenotype in control experiments without MG115 (520 meiocytes scored). Therefore, we can conclude that inhibition of proteolysis mimics the *smg7* phenotype in meiocytes. As both so far described conditions resulting in similar phenotype are caused by failure to downregulate cdk activity, proteasome inhibition experiment suggests that this might be also a cause of anaphase II arrest in *smg7* mutants.

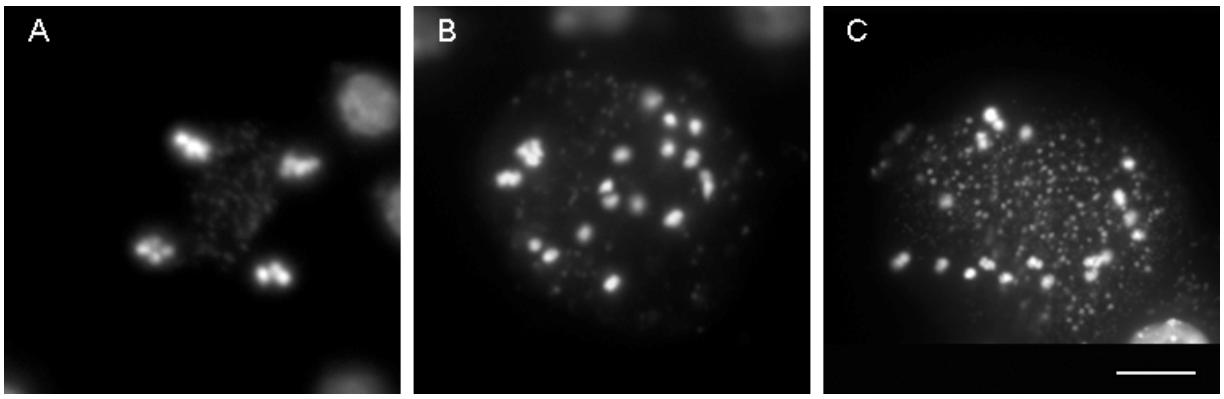

Figure 2.1 Treatment of wild type plants with MG115 mimics *smg7* anaphase II arrest. **(A)** Wild-type control treated with water: anaphase II **(B)** Wild-type meiocyte treated with MG115 contains randomly dispersed chromatids **(C)** *smg7* anaphase II arrest. Scale bar represents 5 µm.

2.3. CDK activity in meiosis

2.3.1. Background

Previous data support the idea that *SMG7* is required for progression trough anaphase II and meiotic exit. Extensive genetic and biochemical studies of mitotic cell cycle established that the necessary condition for anaphase progression is down-regulation of cdk activity and subsequent dephosphorylation of its substrates. Is anaphase II arrest in *smg7* mutant plants caused by defects in cdk down-regulation or aberrant substrate dephosphorylation? One way to address this question is to examine levels of cdk activity in *smg7* meiocytes. Therefore we decided to test the hypothesis whether the anaphase II arrest in *SMG7*-deficient meiocytes is accompanied by higher cdk activity.

Arabidopsis male meiosis takes place in young buds of size between 0.2 – 0.5 mm inside structures called anthers. An anther has four lobes each with approximately 30 meiocytes (Armstrong et al. 2001). Surrounding tissues are composed of several layers of highly dividing mitotic cells (Goldberg et al. 1993). Because of a small size of anthers, limited amount of meiocytes and high risk of cross – contamination with mitotically dividing cells it is impossible to dissect meiocytes in reasonable quantities and purity for biochemical analysis. For this reason we developed a cytogenetic method that allows us to compare relative cdk activity levels in different meiotic stages.

This assay is based on the differential phosphorylation of active and inactive cdk complexes.

Activity of cdk complexes depends on cyclin binding and it is also regulated by inhibiting and activating phosphorylations at different residues. Phosphorylation of the cdk t-loop on the conserved threonine changes conformation of the kinase that is necessary condition for cdk complex activity. Therefore we consider that activating phosphorylation of cdk complex reflects its activity and we decided to monitor this activating phosphorylation cytogenetically it *Arabidopsis* meiocytes.

2.3.2. Which *Arabidopsis* cdk is involved in regulation of meiotic cell cycle?

Arabidopsis contains several CDK related genes: one gene for A-type cdk called *CDKA;1*, and four genes for B type cdks: *CDKB1;1 CDKB1;2, CDKB2;1* and *CDKB2;2*. B-type cdks are a class of cdks specific for plants, they are non- essential, contain degenerated cyclin binding motif, and their role in meiosis was not so far examined. *CDKA;1* was shown to be an essential gene (Dissmeyer et al. 2007). *cdka;1* t-loop phosphomimicry mutant (T161D) is viable despite it has significantly decreased activity. Interestingly these plants are sterile as a consequence several defects in meiosis. All these findings suggest that CDKA;1 might provide most of the cdk activity needed for meiotic progression. Thus we have decided to localize *CDKA;1* in meiosis.

2.3.3. Localization of CDKA;1:YFP construct in *Arabidopsis* meiocytes

To perform CDKA;1 localization study, we used *CDKA;1:YFP* construct made in the laboratory of Dr. Arp Schnittger. In this construct the native promoter of *CDKA;1* drives expression of the *CDKA;1* cDNA fused with *YFP* (yellow fluorescent protein) at the C-terminus. In our studies we used the plants in which endogenous *CDKA;1* was disrupted and complemented by ectopically expressed *CDKA;1:YFP* (Dr. Arp Schnittger, personal communication). Because this construct fully complemented lethal *cdka;1* mutation, it appears to be fully functional.

We detected CDKA;1:YFP by direct fluorescence in squashes of anthers with nuclei stained by DAPI. Our observation confirmed that CDKA;1:YFP is a ubiquitously present. Interestingly we noticed differences in the localization in interphase and mitotic nuclei (figure 2.2). During interphase the signal seems to be concentrated on chromatin. In mitotic stages that are characterised by condensed chromatin (metaphase, anaphase) the CDKA;1:YFP signal was cytoplasmic and we could not detect signal on chromatin any more.

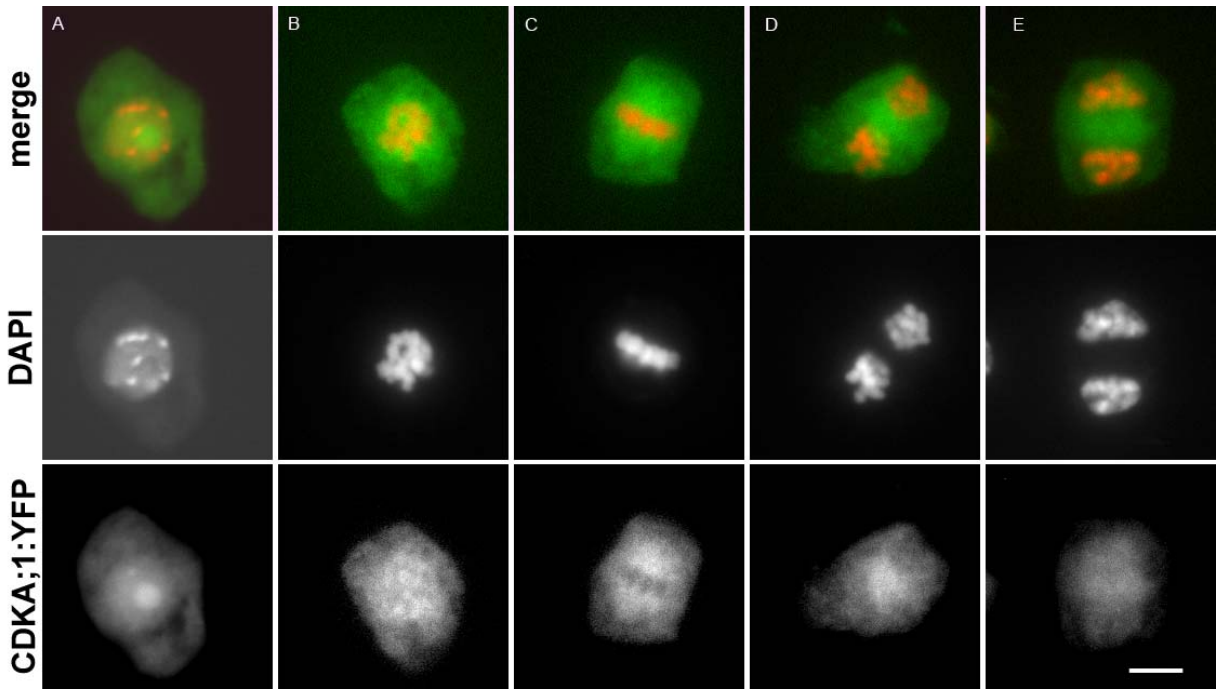

Figure 2.2. CDKA;1:YFP localization in somatic cells. For each stage is shown CDKA,1:YFP, DAPI staining of DNA and merged picture of CDKA;1:YFP signal (in green) and DNA counterstained with DAPI (in red). **(A)** interphase somatic cell **(B)** prophase **(C)** metaphase **(D)** anaphase **(E)** telophase. Scale bar represents 5 μm.

CDKA;1:YFP signal was also highly abundant during all meiotic stages (figure 2.3). The levels of CDKA;1:YFP protein did not appear to significantly change, but we observed similar changes in its localization as in mitosis. During prophase I, the signal from YFP was concentrated in an area around pairing chromosomes (figure 2.3A). In metaphase I the signal became cytoplasmic with slight enrichment around chromosomes in metaphase plate, reminding a position of a spindle (figure 2.3C). Similar enrichment was observed during anaphase I (figure 2.3D). In interkinesis CDKA;1:YFP signal reappears enriched on nuclei. This pattern was repeated during following stages of meiosis: signal becomes again cytoplasmic in metaphase II and anaphase II meiocytes, but after decondensation in tetrade stage has clearly mainly nuclear localization (figure 2.3 F-H). Based on all these observations we conclude that CDKA;1 is present in meiosis and the abundant signal indicates that it likely represents the major meiotic cdk.

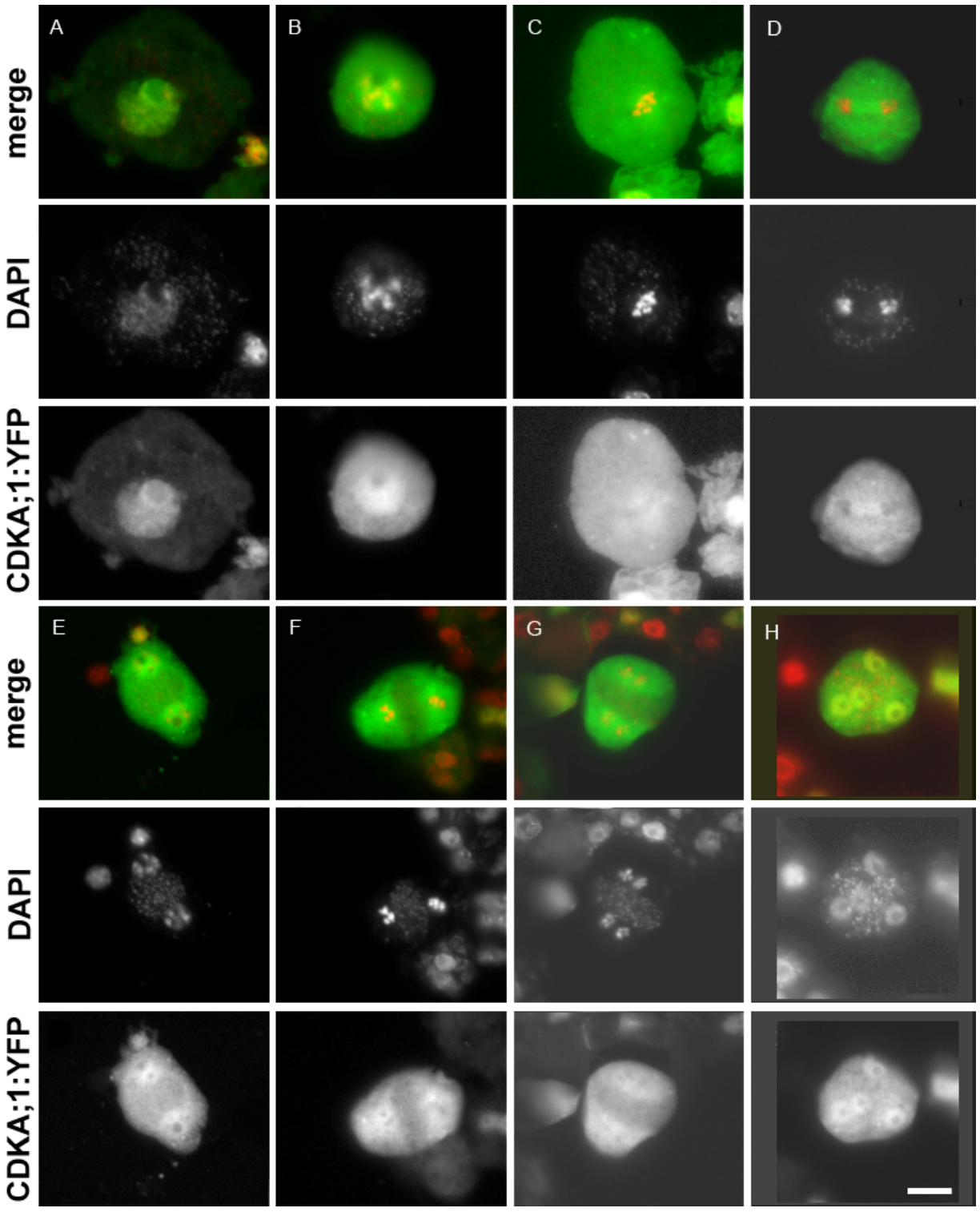

Figure 2.3: CDKA;1 localization during meiosis. For each stage is shown CDKA,1:YFP, DAPI staining of DNA and merged picture of CDKA;1:YFP signal (in green) and DNA counterstained with DAPI (in red). **(A)** pachytene, **(B)** diakinesis **(C)** metaphase I **(D)** anaphase I **(E)** interkinesis **(F)** metaphase II **(G)** anaphase II **(H)** telophase. Scale bar represents 10 µm.

2.3.4. Test of antibodies against phosphorylated threonine 161 in CDKA;1 t-loop

Antibodies against *Arabidopsis* CDKA;1 activating phosphorylation in the t-loop are not available. Comparison of t-loops of other cdks from different organism showed that the highest

sequence similarity has human CDK1 and CDK2 with 91% identity. As there are several substitutions in both CDKs, we have chosen commercially available antibody against threonine 160 phosphorylated isoform of CDK2, which has only two substituted amino acids whereas CDK1 contains six substitutions compared to CDKA;1 (figure 2.4). Because of these substitutions, it was necessary to test whether the antibody specifically recognizes *Arabidopsis* CDKA;1 phosphorylated at the threonine 161 in t-loop.

```
AtCDKA;1        148  GLARAFGIPVRTFTHEVVTLWYRA  171
HsCDK1          148  GLARAFGIPIRVYTHEAITLWYRS  171
HsCDK2          147  GLARAFGVPVRTYTHEVVTLWYRA  170
```

Figure 2.4: Alignment of t-loops from *Arabidopsis* CDKA;1 and human CDK1 and CDK2 t-loops. Numbers indicate the position of first and the last amino acid of the aligned peptides within protein. Human CDK1 and CDK2 have several isoforms, for this alignment was used peptide and coordinates from isoform 1 for both. Threonine 160/161 phosphorylated in active form of is shown in red colour, substitutions in human cdks compared to *Arabidopsis* CDKA;1 are in green colour. Note that in HsCDK2 the threonine is in position 160, whereas in CDKA;1 it is position 161.

Equal amounts of proteins from human HeLa cells, *Arabidopsis* wild type flowers and suspension culture and *CDKA;1:YFP* flowers were analysed by western-blot with antibody against cyclin binding motif PSTAIR to detect total cdk (figure 2.5A). Strong signal of approximately 34 kDa was detected in HeLa cell extract, wild type flowers and suspension culture, but the band in CDKA;1:YFP flower extract was shifted to 61 kDa (figure 2.5A). This reflects the size of fusion protein and demonstrates that *CDKA;1* is the only *Arabidopsis* cdk kinase with canonical cyclin binding PSTAIR motif detectable in *Arabidopsis* extracts. Next we analysed the same amounts of proteins with antibody against HsCDK2 phosphorylated threonine 160 to detect phosphorylated fraction of cdk. This blotting yielded similar but weaker pattern of detected bands (figure2.5A), that might reflect either that only relatively low amount of total cdk is phosphorylated or the antibody in not as efficient as the PSTAIR antibody.

Next, it was necessary to test phospho-specificity of the antibody by out-competing the signal with blocking peptide and phosphatase treatment. In this assays we used *CDKA;1:YFP* flower extract because it gave a stronger signal than extract from wild type flowers. Antibody used for detection was raised against a short peptide surrounding phosphorylated threonine 160 of human CDK2. To block the phospho-cdk specific signal we mixed increasing amounts of synthetic phosphorylated peptide and control non-phosphorylated blocking peptide with antibody (figure 2.5B). Whereas the signal from the antibody was detected in samples with 100 micrograms of

control peptide, 1 microgram of phosphorylated blocking peptide decreased signal almost completely (figure 2.5B). To confirm these data we isolated samples with and without phosphatase inhibitors and treated them with lambda-phosphatase (figure 2.5C). Only weak decrease in the signal intensity was observed in samples with phosphatase inhibitors. In contrast in sample without phosphatase inhibitors the signal was almost gone (figure 2.5C). Hence we conclude that the tested antibody is specifically detecting threonine 161 phosphorylated form of CDKA;1 in *Arabidopsis*. So in following text and figures this antibody will be referred as α-Thr161(p).

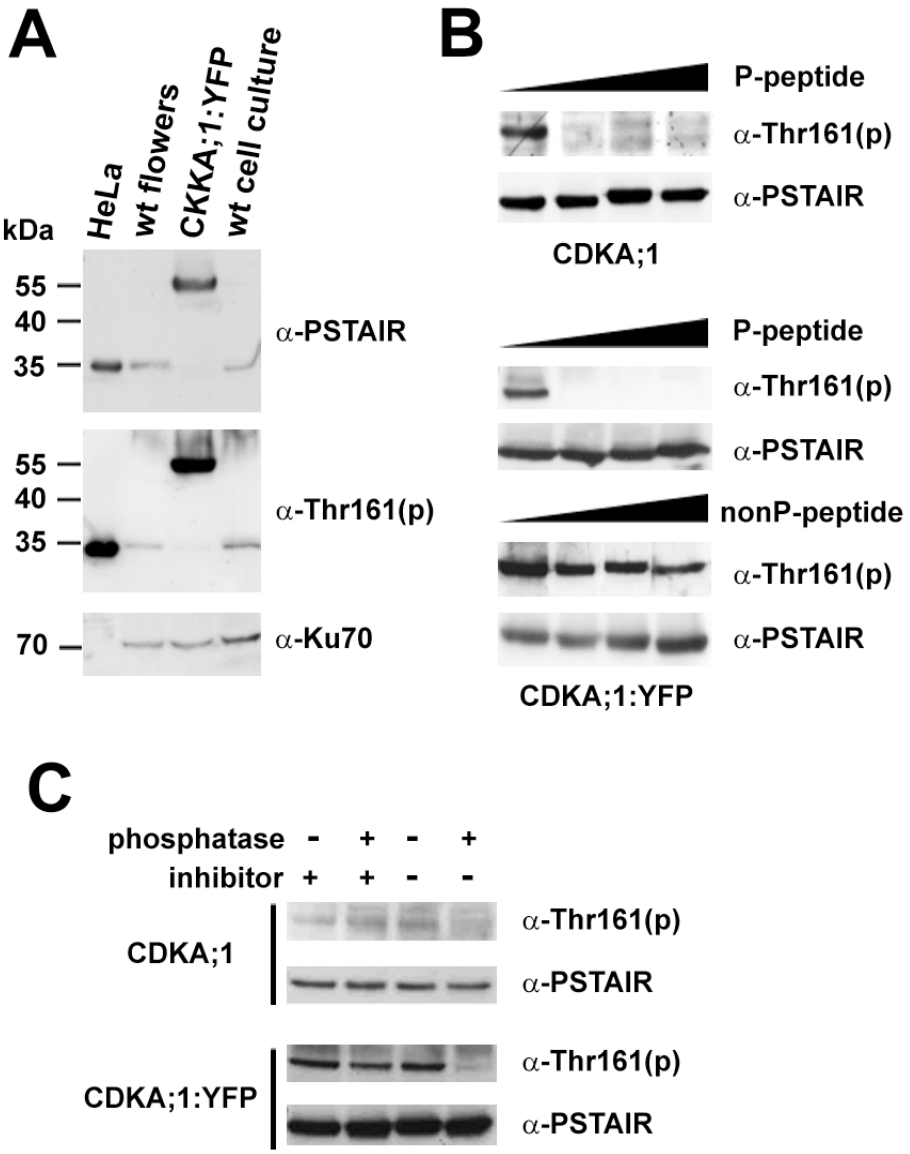

Figure 2.5: Detection of CDKA,1 phosphorylation by immunoblotting. **(A)** Immunodetection of phosphorylated HsCDK2, AtCDKA;1 and AtCDKA;1:YFP proteins in extracts from HeLa cells, *Arabidopsis* wild type inflorescences and suspension culture and from *CDKA;1:YFP* flowers **(B)** Immunodetection of Thr161 phosphorylation of CDKA;1 and CDKA;1:YFP in the presence of increasing concentration (0, 1, 10, 100 mg/mL) of phosphorylated (P) and nonphosphorylated (nonP) competitor peptides. Total CDKA;1 was detected with α-PSTAIR antibody as a loading control **(C)** The Thr161 phosphorylation signal is sensitive to phosphatase treatment. Protein extracts from wild-type and CDKA;1:YFP plants were pretreated with the Lambda protein phosphatase in the presence or absence of phosphatase inhibitors as indicated. Proteins were analyzed by immunoblotting with α-phospho- CDK2 (Thr160) and α-PSTAIR antibody.

2.3.5. Cytogenetic detection of active CDKA;1

After establishing specificity of α-Thr161(p) antibody we asked whether this antibody can be used for immunocytological detection of active cdk complexes in meiocytes prepared from squashes. To assure specific detection of phosphorylated cdks, a blocking non-phosphorylated peptide was always used in immunodetection experiments at concentration of 100 micrograms per 1 ml of antibody solution. We first focused on mitotic cells where Thr161 phosphorylation is expected to peak at metaphase. Indeed we observed mitotic cells with different levels of a signal (figure 2.6). The signal peaked in both wild type and CDKA;1:YFP complemented mitotic cells during metaphase and decreased during anaphase (figure 2.6 B,C). Localization of the CDKA;1:YFP distribution indicates that the total level of cdk appears to be unchanged. As expected, the Thr161 phospho specific signal colocalized with the signal of CDKA;1:YFP which was in interphase mainly nuclear, but during metaphase and anaphase cytoplasmic .

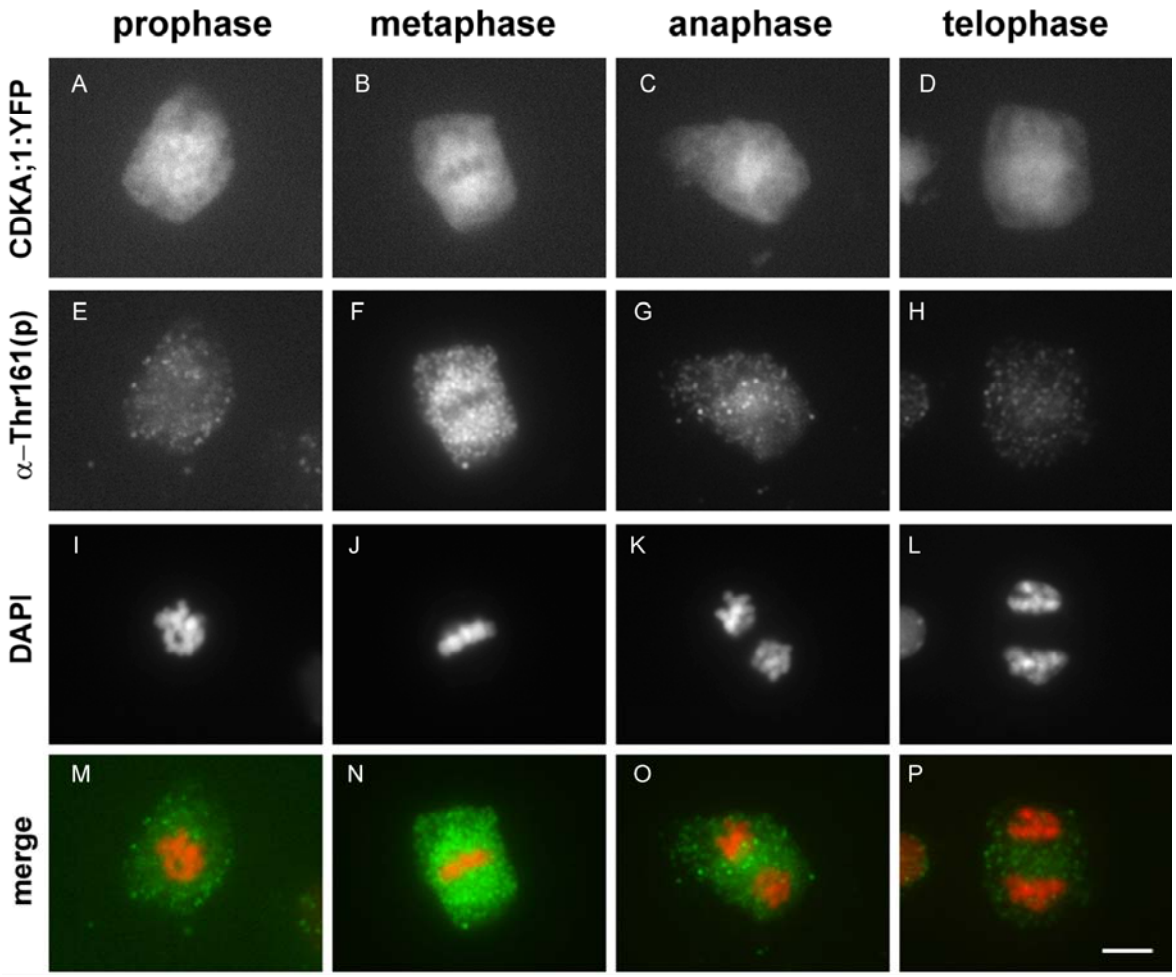

Figure 2.6: Immunolocalization of CDKA;1 phosphorylated on threonine 161 in somatic cells from flowers. **(A-D)** CDKA,1:YFP **(E-H)** Thr161 phosphorylation immunodetection **(I-L)** DAPI staining of DNA **(M-P)** merged pictures of Thr161 phosphorylation immunodetection (in green) and DNA counterstained with DAPI in red. **(A, E, I, M)** prophase **(B, F, J, K)** metaphase I **(C, G, K,O)** anaphase I **(D, H, L, P)** telophase. Scale bar represents 5 μm.

Similar localization pattern was also observed in meiosis. In contrast to the constitutively present CDKA;1 protein throughout meiosis, the Thr161 phosphorylation cycles, with the highest signal intensity in metaphase I and II (figure 2.7A). The phosphorylation level decreases during subsequent anaphases and telophases (figure 2.7A). Interestingly during interkinesis the Thr161-phospho signal was enriched in a zone of organellar band between the two nuclei, while the total CDKA;1:YFP shows nuclear localization and is excluded from the organellar band (figure 2.7A). This indicates that cdk activity is required in this area to prevent cell wall formation and cytokinesis. Quantitative comparison of signal intensities in immunodetection experiments is not easy as these values may be affected by numerous experimental variables. Therefore to ascertain oscillating signal intensity in distinct meiotic stages, we were directly comparing meiocytes in different stages that were located within the same field on a slide and we used always constant exposure times. As the observed pattern of signal from cdk activating phosphorylation in *Arabidopsis* meiocytes fits with expected relative cdk activity levels that were established by biochemical analysis in other organism (Iwabuchi et al. 2000; Carlile and Amon 2008), we can conclude that immunodetection of Thr161 phosphorylation reflects cycling of cdk activity in distinct meiotic stages. We observed an interesting pattern in tapetum cells that undergo karyokinesis but not cytokines, producing binuclear cells. The signal from α-Thr161(p) antibody was enriched in between the two nuclei, probably preventing cytokinesis that would normally be initiated in this part of cell (figure 2.8).

We next asked whether SMG7 deficient meiocytes arrested at anaphase II exhibit a high level of CDKA;1 phosphorylated at Thr161. To examine relative level of Thr161 phosphorylation in meiocytes from *smg7* deficient plants, *smg7* and *CDKA;1:YFP* anthers were squashed on the same slide (figure 2.9). Based on YFP fluoresce it was possible to distinguish wild-type CDKA;1:YFP meiocytes with normal levels of cdk activity from *smg7* meiocytes. No significant differences were observed in *smg7* meiosis until anaphase II. However, whereas the α-Thr161(p) signal decreased with progression trough anaphase II in CDKA;1:YFP plants, levels of Thr161 phosphorylation remained high in SMG7-deficient meiocytes that were arrested at the aberrant anaphase II (figure 2.7B and figure 2.9). Figure 2.9 shows an aberrant anaphase II from *smg7* in close proximity of a wild type telophase II, thereby allowing direct comparison of signals from α-Thr161(p) antibody.

Therefore we conclude that anaphase II arrest in *smg7* mutants is likely caused by a persisting high level of cdk activity. Thus, the SMG7 protein appears to be required for down-regulation of cdk activity at the end of meiosis.

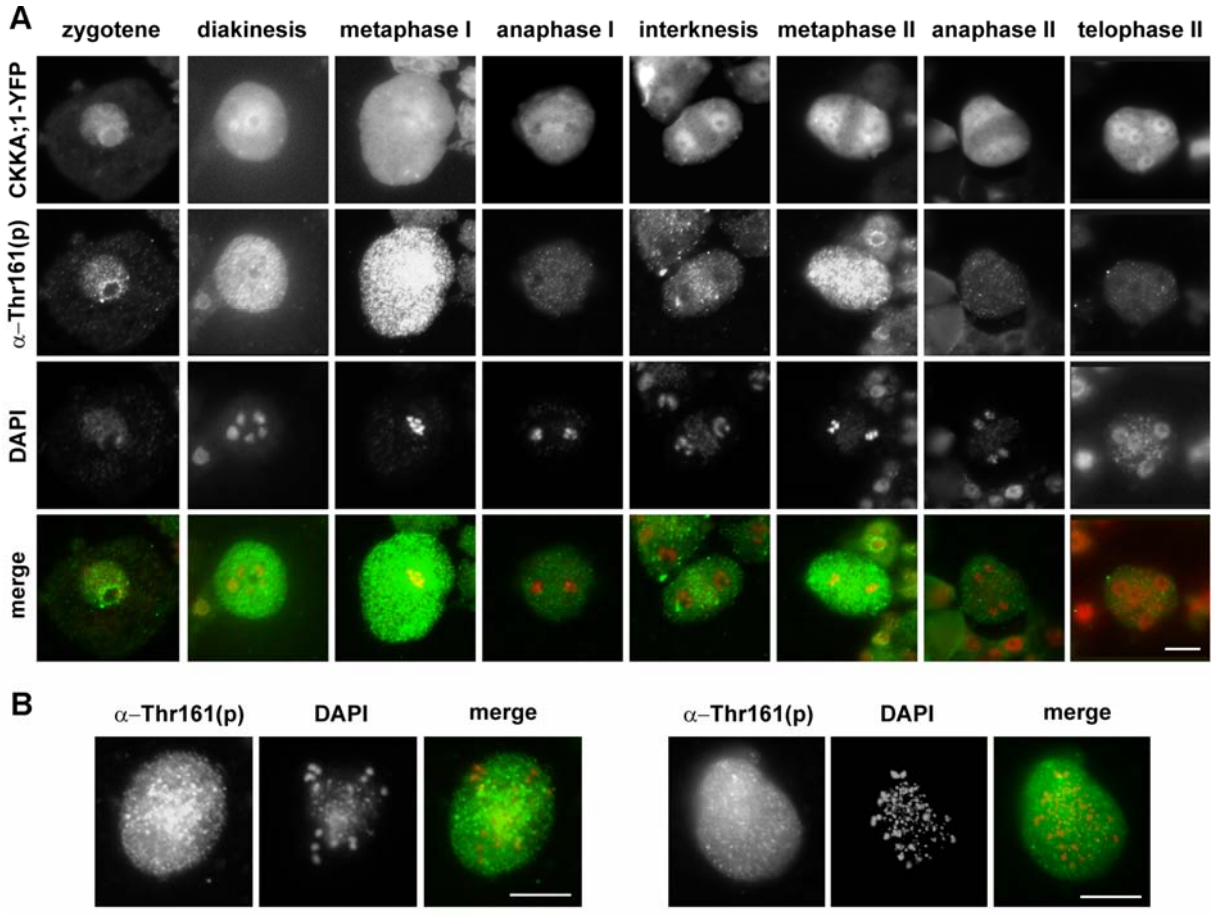

Figure 2.7: Immunolocalization of CDKA;1 phosphorylated on threonine 161 during progression of wild-type meiosis **(A)** and in *smg7* meiocytes arrested in anaphase II **(B).** Following stages of meiosis are shown: zygotene, diakinesis, metaphase I, anaphase I, interkinesis, metaphase II, anaphase II and telophase II. For each stage is shown CDKA,1:YFP, Thr161 phosphorylation immunodetection and DAPI staining of DNA and merged picture of Thr161 phosphorylation immunodetection (in green) and DNA counterstained with DAPI (in red). **(B)** CDKA;1 Thr161 phosphorylation in aberrant anaphase II of *smg7* mutants. Scale bar represents 10 μm.

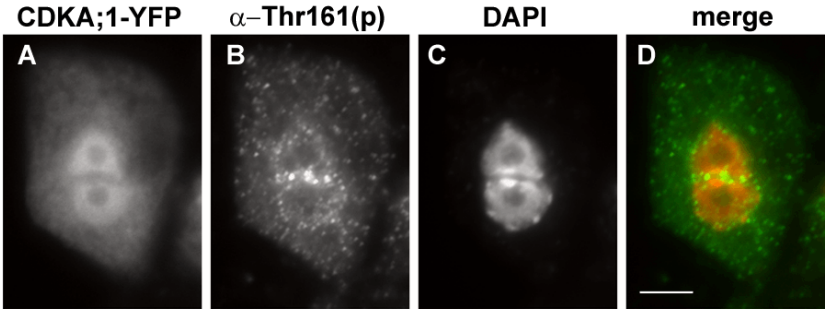

Figure 2.8: Immunolocalization of CDKA;1 phosphorylated on threonine 161 in wild-type tapetum cells. Note the band of Thr161 phosphorylation signal in between the two nuclei. **(A)** CDKA;1:YFP **(B)** Thr161 phosphorylation immunodetection **(C)** DAPI staining of DNA **(D)** merged picture of Thr161 immunodetection (in green) and DNA counterstained with DAPI in red. Scale bar represents 5 µm.

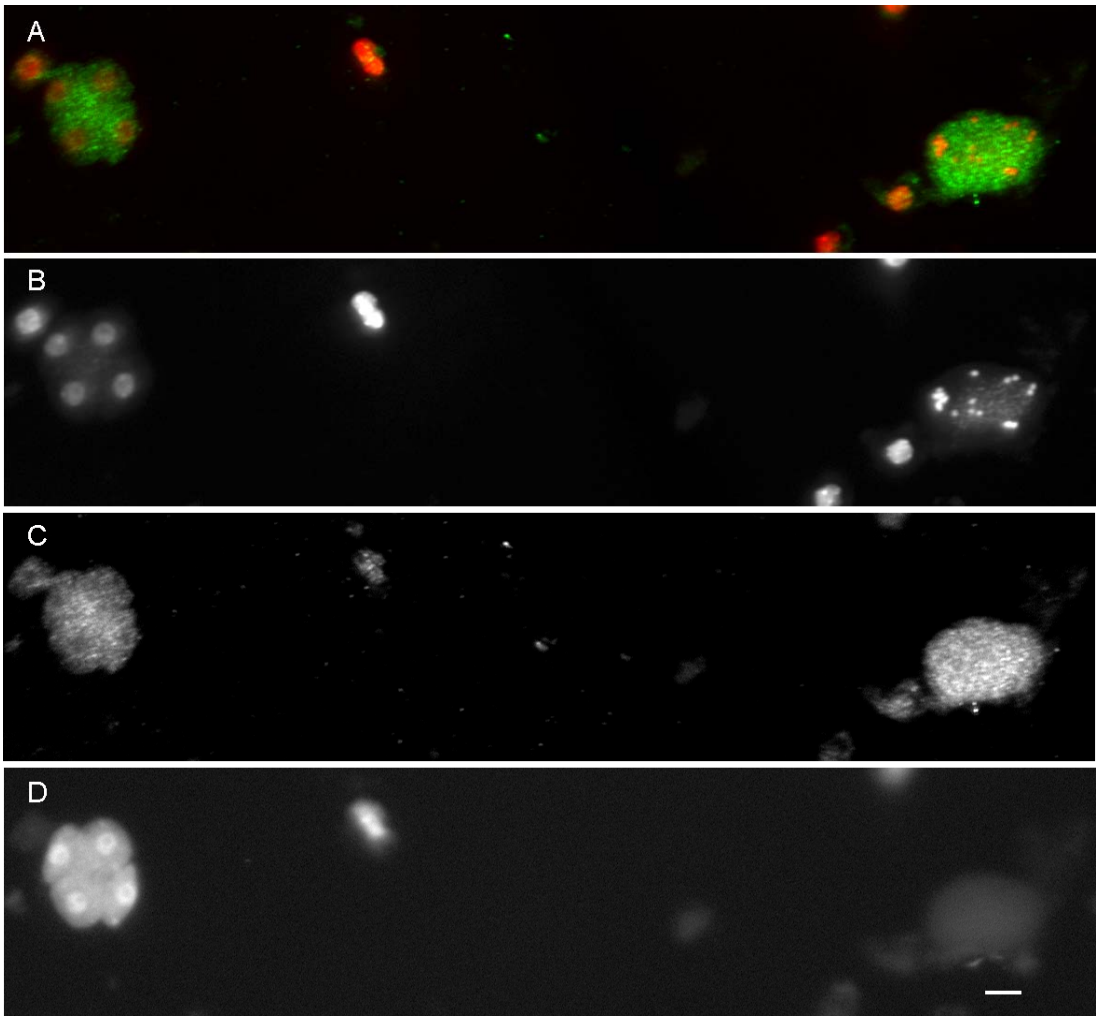

Figure 2.9: Comparison of CDKA;1 Thr161 phosphorylation signal in tetrade of CDKA;1:YFP plants with aberrant anaphase II in *smg7* mutants. PMCs from these plants were prepared on the same slide. CDKA;1:YFP meiocytes are distinguished from *smg7* meiocytes due to the presence of the YFP signal. Scale bar: 10 µm. **(A)** merged picture of Thr161 phosphorylation immunodetection (in green) and DNA counterstained with DAPI in red **(B)** DAPI staining of DNA **(C)** Thr161 immunodetection **(D)** YFP signal in CDKA,1:YFP cells. Scale bar represents 10 µm.

2.4. *SMG7* dysfunction suppresses premature meiotic exit in *TAM* deficient plants

To further prove that *smg7* anaphase II arrest is due to high levels of cdk activity we should be able to suppress this phenotype by experimentally decreasing cdk activity. *smg7* mutant phenotype is highly reminiscent of anaphase arrest caused by artificial expression of a non-degradable M-phase cyclin. Thereby the most suitable experimental approach would be to specifically remove/inactivate a meiotic cyclin that controls progression through the second meiotic division. As mentioned before, so far only two cyclins, *TAM* and *SDS*, have been identified in *Arabidopsis* so far. Mutation in *tam-1* causes delay in meiotic cell cycle and leads to premature cell wall formation in interkinesis (Magnard et al. 2001; Wang et al. 2004b). Therefore, we decided to focus on this cyclin. Interaction between *smg7* and *tam-1* was already investigated by Nina Riehs (Riha laboratory, GMI). However, because *tam-1* is a temperature sensitive point mutation allele, we wanted to analyse also a null allele of this cyclin.

2.4.1. *tam-2 null* allele causes exit after first meiotic division

To analyze complete knock-out of *TAM*, we ordered a line that was predicted to contain a T-DNA insertion in the *TAM* gene. We confirmed the presence of T-DNA left border insertion at the expected position in the 4th intron by polymerase chain reaction (PCR) and by sequencing the PCR product (figure2.10 A-B). However, we failed to amplify *TAM* genomic sequences upstream of the predicted site of insertion. Further set of PCRs revealed that the T-DNA insertion caused deletion of a large part of the *TAM* gene spanning the whole promoter region and first four exons (figure 2.10 A-B). Therefore, the T-DNA insertion led to deletion of the N-terminal part of the *TAM* gene. RT-PCR amplification of different parts of *TAM* cDNA yielded products of expected size in wild type but failed in amplification of proximal part of the cDNA in mutants. We could detect expression of the last part of the cDNA which is behind T-DNA insertion (figure 2.10 C). Nevertheless, as this mRNA does not contain large part of the *TAM* N-terminus including initiation codon and part of cyclin amino terminal domain which is required for binding to cyclin dependent kinase, we consider this allele to be null and we call it *tam-2*.

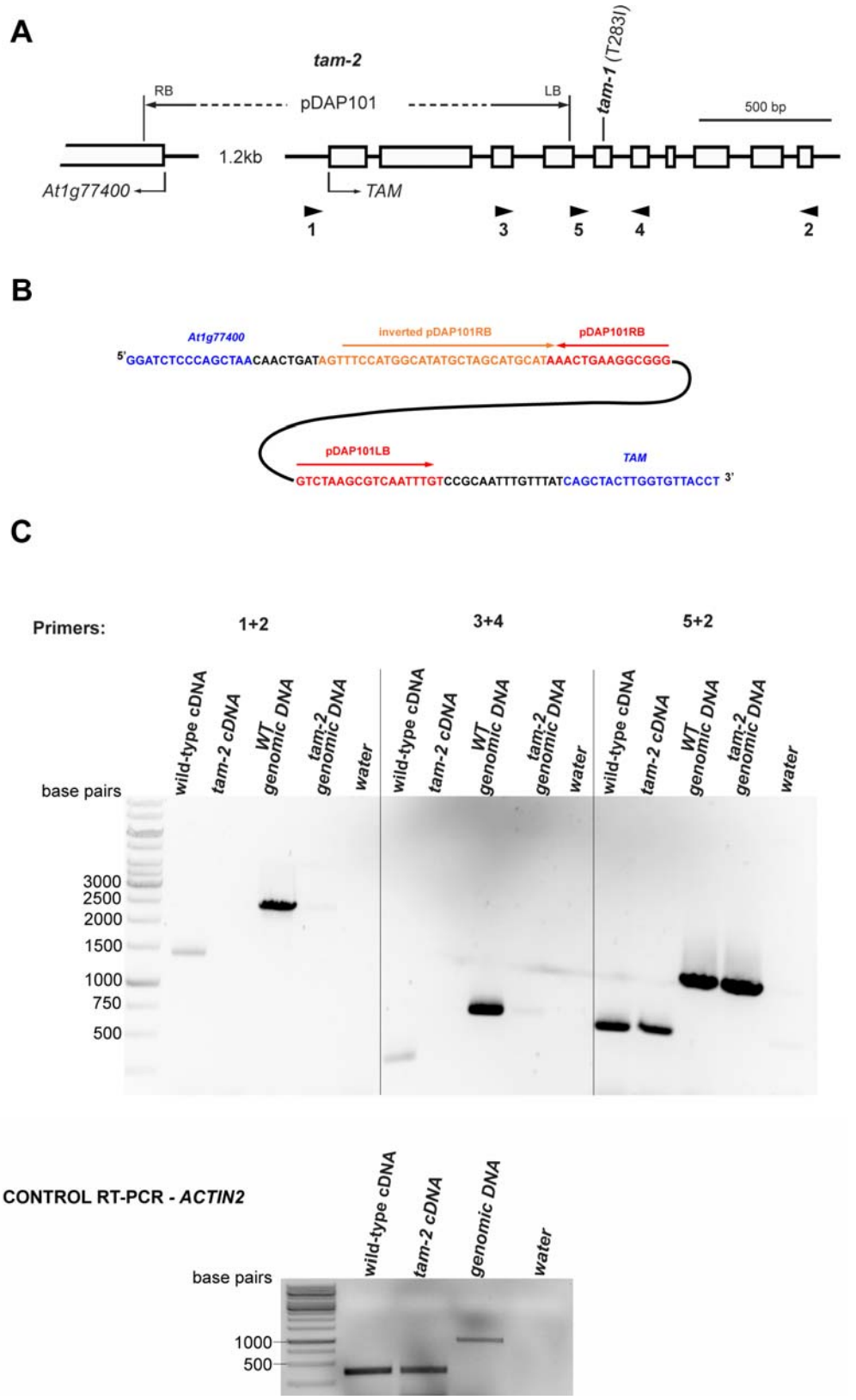

Figure 2.10: Molecular characterization of *tam-2* allele. **(A)** Diagram of *TAM* locus with marked positions of *tam-1* and *tam-2* alleles. Position of TAM primers used in RT-PCR analysis is indicated by arrowheads **(B)** Sequence of the junctions of T-DNA insertion within the *TAM* locus of the *tam-2* allele. *Arabidopsis* genomic DNA is marked in blue, T-DNA in red and orange and filler sequences at the fusion junction are marked in black. **(C)** Reverse transcription PCR analysis of RNA expression from the *TAM* locus in wild-type and *tam-2* mutants. Primers used in each PCR reaction are indicated. Control PCR reaction was performed on house-keeping gene *ACTIN2*.

Next, we examined male meiosis in *tam-2* mutant plants. Previous analysis of *tam-1* allele revealed delayed progression trough meiosis, cell wall formation in interkinesis resulting in formation of dyads, followed by asynchronous second division (Magnard et al. 2001; Wang et al. 2004b). Phenotype of *tam-2* mutants was more severe. While we could not detect any difference from wild type in stages between prophase I and interkinesis (figure 2.11 A-E), meiocytes underwent cytokinesis and formed dyads already after the first meiotic division (figure 2.11 F-H). In contrast to *tam-1* allele, we could not detect any stages of the second meiotic division in *tam-2* mutants. We counted abundance of meiotic stages from diakinesis to meiotic exit and detected only 3 tetrades in total 596 counted meiocytes, in contrast to wild type plants with 224 tetrades in 618 total meiocytes (table 2.15). This data suggest that *tam-2* mutants do not undergo second meiotic division and exit from meiosis in interkinesis. Therefore as a consequence, they should form a diploid spores which may lead to polyploid progeny. To test this hypothesis we measured ploidy of progeny of diploid *tam-2* mutant plants. Flow cytometry measurements showed that only 3 out of 18 plants were diploid and the remaining 15 plants were tetraploid (figure 2.11 I). We used also seeds from *tam-1* mutant plants grown at restrictive temperature to compare these two alleles. All 18 *tam-1* -/- progeny plants measured were diploid.

All these data provide evidence that in contrast to the point-mutation *tam-1* allele, the *tam-2* null allele causes exit after the first meiotic division. *TAM* is thereby required for meiosis I to meiosis II transition.

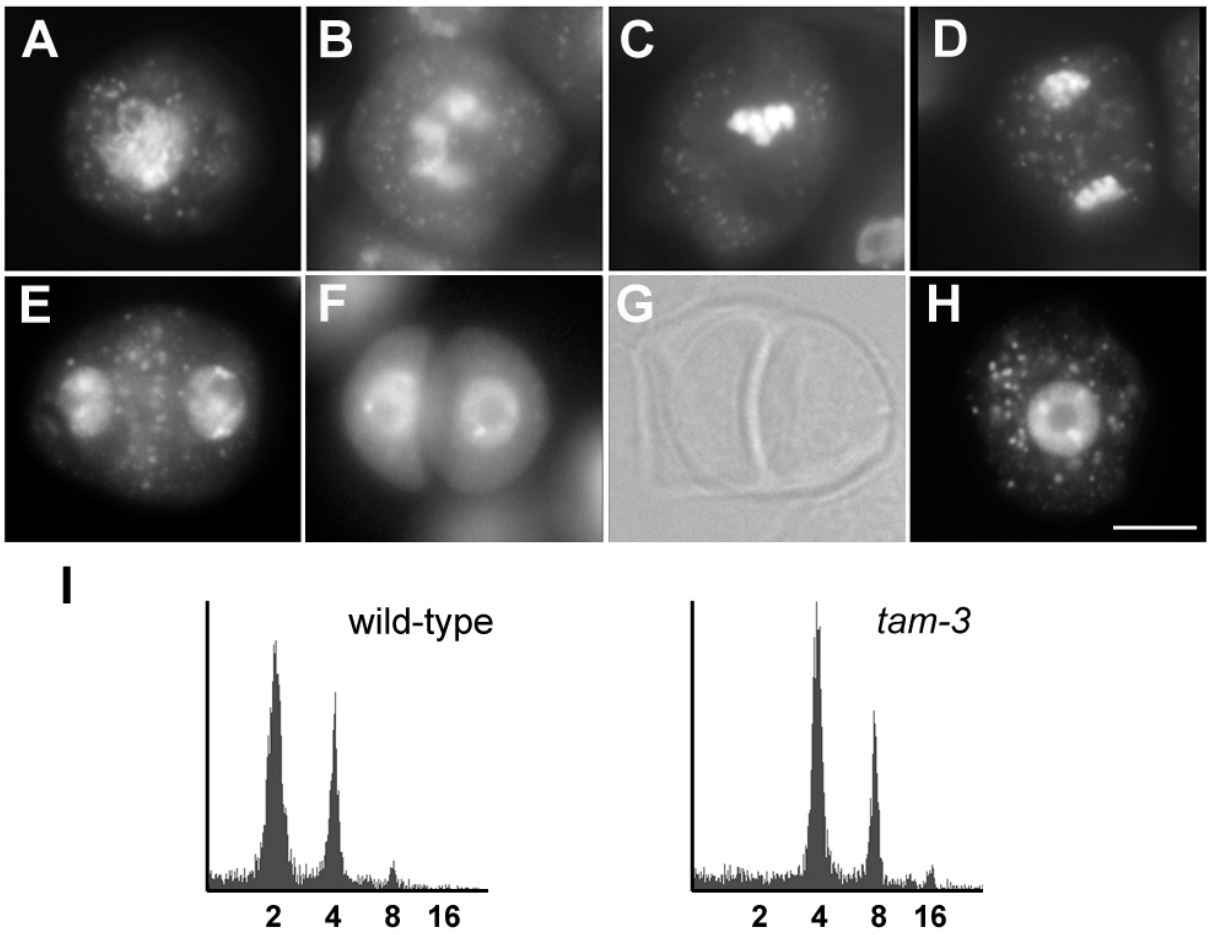

Figure 2.11: Cytogenetic characterization of premature meiotic exit in *tam-2* mutants. Meiotic chromosomes stained by DAPI from *tam-2* mutants **(A-H)** and ploidy analysis of wild-type and F3 *tam-2* mutant plants **(I)**. **(A)** Zygotene, **(B)** diakinesis, **(C)** metaphase I, **(D)** anaphase I, **(E)** interkinesis and **(F)** dyad visualized by DAPI staining **(H)** and by phase contrast **(G)**. Scale bar: 10 µm. **(I)** Flow cytometry analysis of DNA content in nuclei prepared from inflorescences of progeny of wild-type and *tam-2* plants.

2.4.2. Localization of TAM:GUS protein

TAM mutant phenotype suggests its role in interkinesis and progression from the first to second meiotic division. Since data from other species imply that A-type cyclins are mainly involved in regulation of meiotic S/G2 and prophase I, we decided to detect in which meiotic stages is *TAM* protein present. Localization of *TAM* was already examined by (Wang et al. 2004b), but methodology used in this study was not precise enough to determine exact meiotic stage at which TAM:GFP signal occurred. Moreover, broad expression of *TAM* examined by Wang and colleagues (Wang et al. 2004b) suggests that *TAM* may be involved also in control of mitotic divisions.

To detect expression of *TAM* in distinct plant tissues and during development, we decided to express C-terminal fusion of *TAM* with beta-glucuronidase (*GUS*) gene under *TAM* promoter. This construct was transformed to wild type plants. Tissue specific expression of TAM:GUS fusion protein was assayed in transgenic plants by histochemical GUS assay, while the subcellular localization of the protein was analyzed using immunodetection with anti-GUS antibody. We checked 17 independent T1 plants for histochemical GUS staining and chose four representative lines that were subsequently crossed with *TAM-2* heterozygous plants for complementation. We followed these 4 lines to T2 and T3 generation. Interestingly, one of the lines (#12) had a dominant negative phenotype causing meiotic exit in T2 plants suggesting that the transgene caused silencing of the endogenous *TAM* gene. TAM:GUS expression was generally localized to highly proliferating tissues (figure 2.12 A, B). In 10-days seedlings, *TAM* was expressed in root tips, in lateral roots, shoot apex, tips of cotyledons and young leaves (figure 2.12A). Within inflorescences the staining was prominent in young buds, anthers and in pistils of older buds (figure 2.12 B). This expression profile is in accord with previously published RT PCR expression data by Wang and collegues (Wang et al. 2004b) and expression profile published on Geneinvestigator (Hruz et al. 2008). Our histochemical staining together with published RT_PCR data demonstrates that *TAM* cyclin is not exclusively expressed only in meiosis.

To investigate the subcellular localization of *TAM:GUS* we used immunostaining with antibodies against *GUS* protein (figure 2.12C-F). For detection in somatic cells we squashed anthers and pistils from young flower buds. TAM:GUS signal was detected in mitotically dividing cells and in some cells in interkinesis (figure 2.12C). Because A-type cyclins are known to be expressed from S phase to mitosis, we suppose that these cells are in S or G2 phase. During mitosis, TAM was clearly detected in prophase, slightly weaker in metaphase and localized to cytoplasm (figure 2.12 D,E). The signal was completely lost during anaphase, reflecting likely a destruction of a cyclin by APC mediated polyubiqutination and degradation (figure 2.11 F).

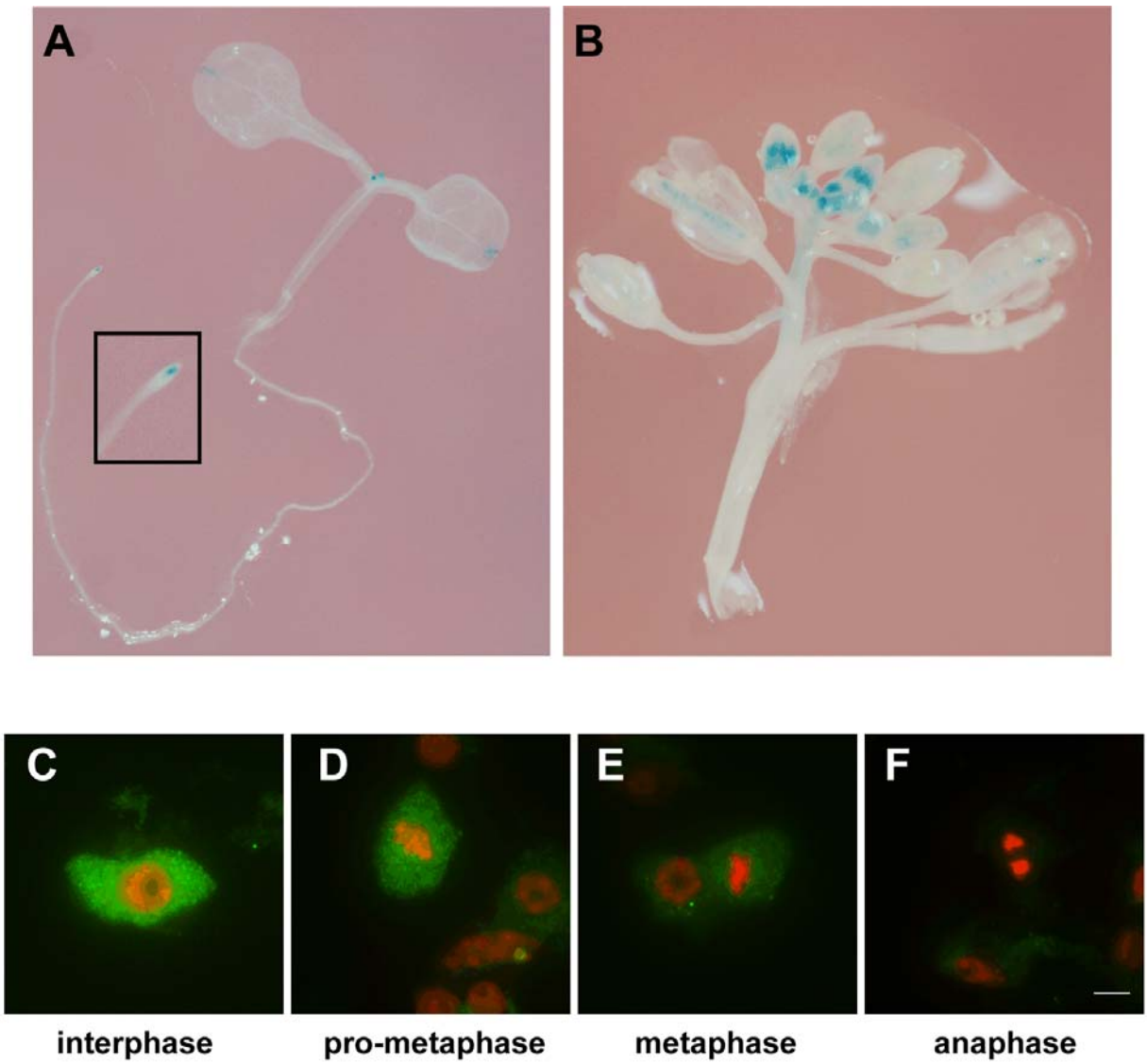

Figure 2.12: Expression of TAM:GUS fusion protein. **(A,B)** and immunolocalization of TAM:GUS in mitotic cells from floral buds **(C-F)**. Examination of TAM:GUS expression on **(A)** 10 days old seedlings and **(B)** inflorescences by using GUS histochemical assay. TAM:GUS expression is not restricted to meiotic tissues; it can be detected in root (inset) and shoot apical meristems, in the tips of cotyledons, and in meiotic as well as in postmeiotic floral buds. **(C-F)** Immunolocalization of TAM:GUS in mitotic cells from floral buds. FITC signal detecting TAM:GUS is indicated in green, DNA counterstained with DAPI in red. **(C)** interphase cells presumably in G2 phase, **(D)** prometaphase **(E)** metaphase **(F)** anaphase. Scale bar: 5 µm.

In meiosis, it was possible to detect TAM:GUS from the beginning of meiosis in leptotene (figure 2.13A), visibly increasing in during zygotene (figure 2.13B) and the strongest signal was detected pachytene stage (figure 2.13C). Localization was mainly cytoplasmic, although some weak signal could be recognized also in area where chromosome pairing occurred. Interestingly, strength of signal decreased during diplotene and diakinesis (figure 2.13D-E) and it was possible to recognize it in most but not all metaphases I (figure 2.13F). During anaphase I TAM:GUS completely disappeared and in later stages we could not detect any clear signal over background

(figure 2.13G-L). Therefore we conclude that TAM expression peaks in mitotic and meiotic prophase. This conclusion is consistent with expression data obtained from other organisms, where cyclin A is expressed during S, G2 and prophase and removed during metaphase independently of spindle checkpoint. Our data also suggest that TAM is specifically expressed in meiosis I, although we can not fully exclude a possibility that undetectable levels of TAM are present in interkinesis or during meiosis II.

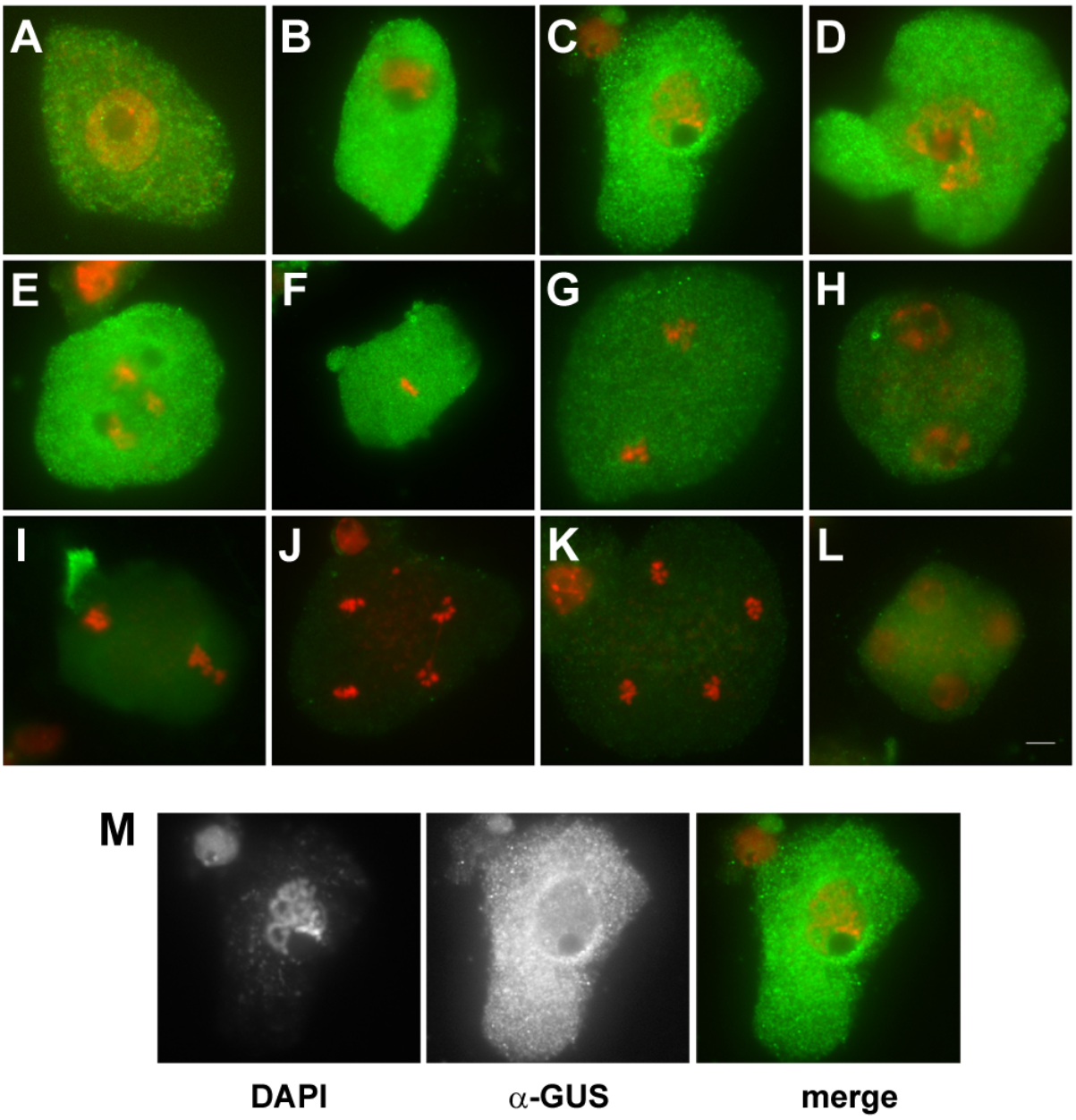

Figure 2.13: Immunolocalization of TAM:GUS during progression of meiosis. FITC signal detecting TAM:GUS is indicated in green, DNA counterstained with DAPI in red. **(A)** leptotene, **(B)** zygotene, **(C)** pachytene, **(D)** diplotene, **(E)** diakinesis, **(F)** metaphase I, **(G)** anaphase I, **(H)** interkinesis, **(I)** metaphase II, **(J)** anaphase II, **(K)** telophase II, **(L)** tetrade. **(M)** Same pachytene as in **(C)** shown as unmerged DAPI and FITC pictures. Scale bar: 5 μm.

2.4.3. Genetic interaction between *SMG7* and *TAM* gene

As already pointed, genetic interaction between *smg7* and *tam-1* mutant allele was previously described in our laboratory by Nina Riehs during her PhD (Riehs 2009). To compare interaction between *smg7* and point mutation *tam1* allele wit *smg7* interaction with null *tam-2* allele, it is necessary to shortly introduce these data.

smg7 tam-1 double mutants (data provided by Nina Riehs)

Growth phenotypes of double mutant *smg7 tam-1* were indistinguishable from *smg7* single mutants. Surprisingly, plants were also completely sterile. Cytogenetic analysis of meiosis showed that whereas there is a clearly detectable cell wall formation in *tam-1* single mutants (figure 2.14 A), in *smg7 tam-1* double mutants is this phenotype completely suppressed. Meiocytes continue into second meiotic division and during and they are arrested in aberrant anaphase II stage similar to *smg7* single mutants (figure 2.14 B). Therefore *smg7* mutation fully suppressed *tam-1* phenotype. But the most striking observation was unexpected impact of *smg7 tam-1* double mutation on progression trough interkinesis. Interkinesis-like stages with decondensed chromatin almost disappeared in double mutants; instead aberrant metaphase II – like stages were observed with fully condensed chromosomes but which were not aligned into metaphase plate (figure 2.14 B). To a further explore effects of *smg7 tam-1* double mutation on meiotic progression, abundance of individual cell cycle stages from metaphase I to anaphase II was counted for wild-type, *smg7* and *tam-1* single mutants and *smg7 tam-1* double mutant plants (figure 2.14 C). All plants were grown at 27 °C which is a restrictive temperature for *tam-1* allele. Whereas in wild-type plants interkinesis represents 32.9 % of all counted stages and in *smg7* 20.5%, in *tam-1* deficient plants up to 50,6 % of meiocytes are in interkinesis. In contrast, in *smg7 tam-1* double mutants only 1.3% of meiocytes in interkinesis could be identified. Instead, 9.8% of meiocytes showed an aberrant-metaphase II-like phenotype. This striking loss of interkinesis suggests that SMG7 protein is required for chromosome decondensation already during interkinesis in *tam-1* mutants. To elucidate whether residual activity of *tam-1* is point mutation plays a role in this impaired meiotic progression, we examined *smg7* interaction with null *tam-2* null allele.

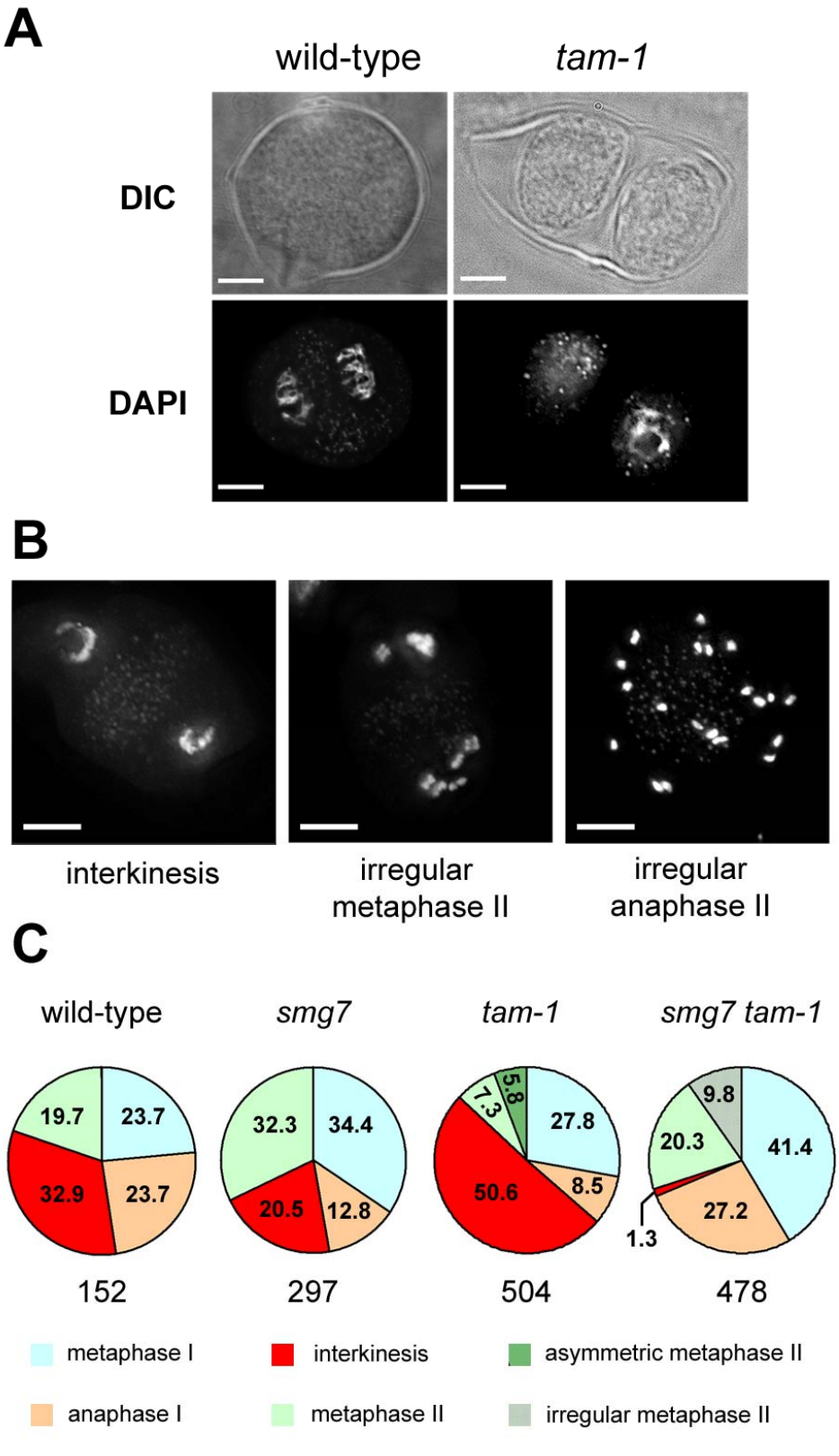

Figure 2.14 - data provided by Nina Riehs: Genetic analysis of *smg7* and *tam-1* interaction. **(A)** PMCs at interkinesis from wild-type and *tam-1* mutants shown in phase contrast (upper panel); nuclei are stained with DAPI (bottom panel). **(B)** Irregular behaviour of meiotic chromosomes in PMCs of *smg7 tam-1* double mutants. DNA is counterstained by DAPI. Bars in (A) and (B) represent 5 µm. **(C)** Frequency (in %) of meiotic stages from metaphase I to metaphase II in wild-type, *smg7-1*, *tam-1* and *smg7 tam-1* plants. All plants were kept at 28°C during flowering. The total number of meiocytes is indicated below each pie chart.

smg7 tam-2 double mutants

As shown above, *tam-2* has more severe phenotype than the *tam-1* allele. Hence it was of a big interest to determine whether *smg7* mutation will suppress also this allele. Therefore we crossed *SMG7* and *TAM-2* heterozygous plants and examined double mutants segregating in F2 generation. First observation of phenotype confirmed that *tam-2,* as previously shown for *tam-1* allele, does not have any effect on *smg7* vegetative phenotype. All double mutant plants were sterile and Alexander staining of anthers confirmed that they contain only few non-viable pollen grains similar to *smg7* single mutants (figure 2.15). Further cytological examination confirmed that *smg7* phenotype is dominant. Exit after first meiotic division was completely suppressed and all stages until anaphase II did not show any differences to wild type of *smg7* single mutants (figure 2.16 A-E). But anaphase II progression was clearly abolished and we never found a telophase II stage, instead we found a 20 chromatids phenotype typical for *smg7* (figure 2.16 F-H).

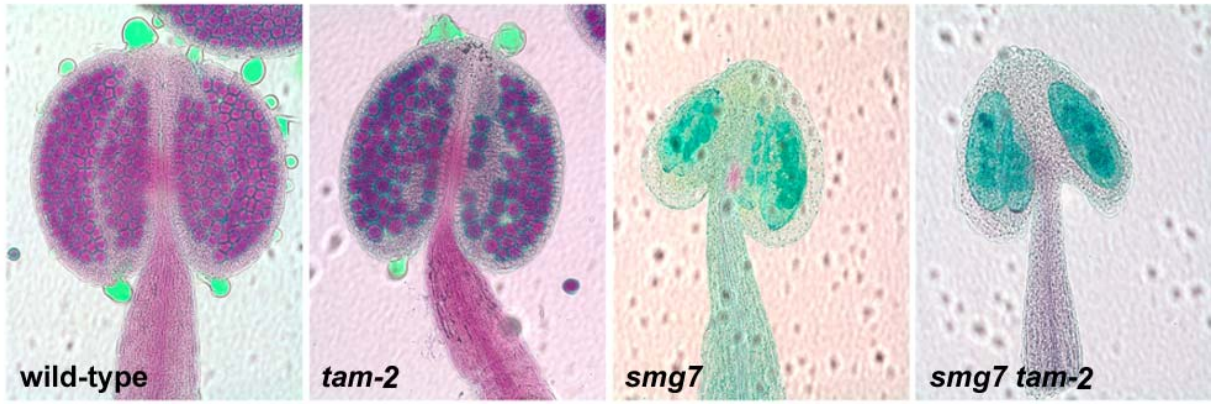

Figure 2.15: Pollen viability determined by Alexander staining of anthers. Viable pollen in wild-type and *tam-2* plants stain in red. No pollen is detected in anthers of *smg7* and *smg7 tam-2* mutants.

Thus *smg7* phenotype is completely dominant over *tam-2*. But the most striking observation was the difference between *smg7 tam-1* and *smg7 tam-2* double mutant phenotypes. Whereas in *smg7 tam-1* interkinesis shortened with almost no decondensation of chromosomes, *smg7 tam-2* had no phenotypic differences in interkinesis compared to wild type. To better describe this difference, we also counted frequency of meiotic stages from metaphase I to anaphase II in wild type, single *smg7* and *tam-2* mutants and *smg7 tam-2* double mutant (table 2.15). Whereas in *smg7 tam-1* only 6 interkinesis-like stages were observed out of 482 counted meiocytes (Nina Riehs, table 2.16), corresponding to 1,2%, in *smg7 tam-2* we found 32 out of 257 meiocytes,

representing 12%. We can not fully explain this difference; but we suppose that most likely balanced effects of *TAM* and *SMG7* are required for proper progression trough interkinesis.

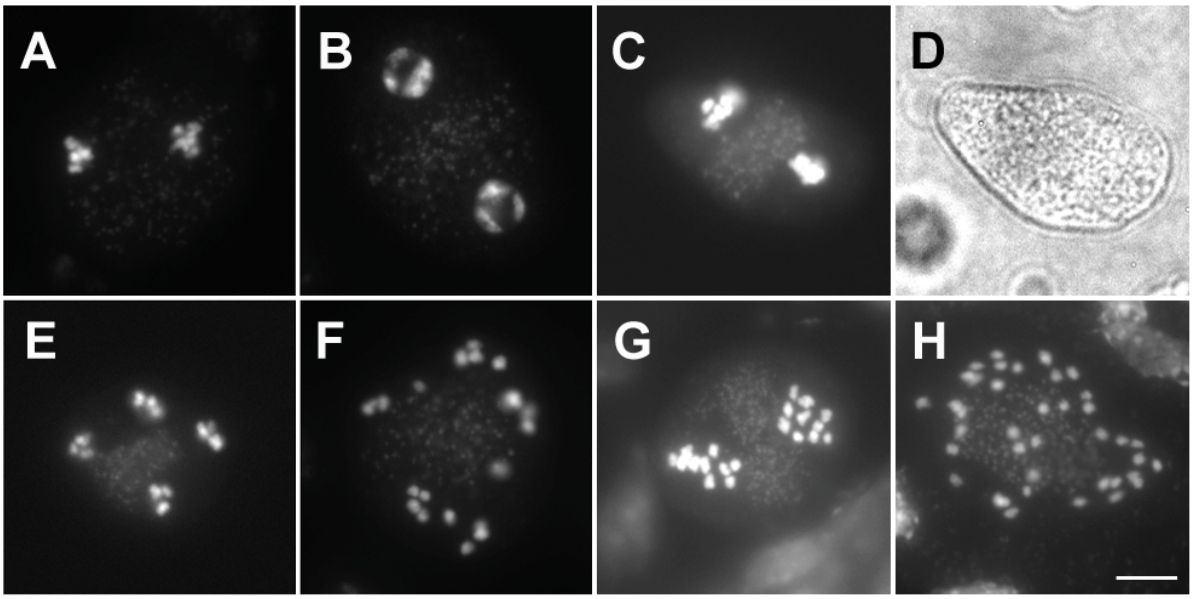

Figure 2.16: Meiosis in *smg7 tam-2* double mutants. Progression of meiosis from anaphase I is shown. **(A)** anaphase I, **(B)** interkinesis, **(C)** fluorescence **(D)** and phase contrast pictures of metaphase II, **(E)** anaphase II, **(F)** and irregular anaphase II. Metaphase II **(G)** and irregular anaphase II **(H)** from tetraploid *smg7 tam-2* double mutants. Scale bar: 10 µm.

Genotype	wild type Col0		*smg-7 -/-*		*tam-2-/-*		*smg7 tam-2-/-*	
	Number of meiocytes	**%**	Number of meiocytes	**%**	Number of meiocytes	**%**	Number of meiocytes	**%**
Metaphase I	151	**27%**	92	**34%**	119	**24%**	112	**44%**
Anaphase I	22	**4%**	22	**8%**	32	**6%**	33	**13%**
Interkinesis without cell wall	70	**13%**	56	**21%**	68	**14%**	32	**12%**
Interkinesis with cell wall					50	**10%**		
Dyad					221	**45%**		
Metaphase II	41	**7%**	86	**32%**			60	**23%**
Anaphase II	14	**3%**	14	**5%**			20	**8%**
Telophase II	12	**2%**						
Tetrade	244	**44%**			3	**1%**		
Anaphase II arrest (not counted to total number)			1368				1072	
Total meiocytes	554		270		493		257	

Table 2.15: Counting of meiotic stages in wild-type, *smg7*, *tam-2* and *smg7 tam-2* double mutant plants. Frequency (in %) of meiotic stages from MI to meiotic exit in wild-type, *smg7*, *tam-2* and *smg7 tam-2* plants is indicated.

Genotype	wild type Col0		*smg7 tam-1-/-*; 27°C counted by Nina Riehs		*smg7 tam-2-/-*	
	Number of meiocytes	**%**	Number of meiocytes	**%**	Number of meiocytes	**%**
Metaphase I	151	**27%**	198	**41%**	112	**44%**
Anaphase I	22	**4%**	130	**27%**	33	**13%**
Interkinesis without cell wall	**70**	**13%**	**6**	**1%**	**32**	**12%**
Metaphase II	41	**7%**	97	**20%**	60	**23%**
Anaphase II	14	**3%**	4	**1%**	20	**8%**
Asymmetric second division			47	**10%**		
Telophase II	12	**2%**				
Tetrade	244	**44%**				
Anaphase II arrest (not counted to total number)			Not counted		1072	
Total meiocytes	554		482		257	

Table 2.16: Comparison of frequencies of meiotic stages wild-type, *smg7 tam-1* grown at 27°C to induce *tam-1* phenotype and *smg7 tam-2* double mutant plants. Counted numbers of meiocytes in interkinesis are highlighted as there is the biggest difference between *smg7 tam-1* and *smg7 tam-2* double mutants.

2.5. Anaphase arrest in *smg7* mutants is dependent on TDM1 protein

Our data imply that while *TAM* is meiotic cyclin, it is most likely not involved in progression through meiosis II and does not affect meiotic exit. To understand role of *SMG7* at exit from meiosis, we performed detailed analysis of another gene required for proper meiotic exit in *Arabidopsis,* called *TDM1*. It was shown that *tdm1* mutants normally complete the second meiotic division, but then the resulting haploid nuclei attempt to undergo third division in male meiosis what causes male sterility. Female meiosis did not seem to be affected and *tdm1* mutants were female fertile (Ross et al. 1997). This phenotype implies that *TDM1* may be important for proper meiotic exit and that its function may be required at a later stage than function *SMG7.*

2.5.1. *TDM1* mutant phenotype

The first *TDM1* allele described by (Chaudhury 1994; Ross et al. 1997; Glover et al. 1998), *tdm1-1,* contains a T-DNA disruption in its C-terminal part and had a semi-dominant phenotype. The N-terminal part of the *tdm1-1* allele was shown to be transcribed, which most likely results in a production of truncated protein with partial dominant effect in heterozygous plants. To make sure that progression to third meiotic division is caused by *TDM1* dysfunction, we ordered another T-DNA allele. We verified that T-DNA insertion lies in *TDM1* gene by PCR and subsequent cloning and sequencing of T-DNA border lying inside the gene (figure 2.17). Because two additional *TDM1* alleles we re described in literature, we named this allele *tdm1-4*. Insertion of T-DNA in *tdm1-4* mutant allele is located in the first exon of the *TDM1* gene. As this T-DNA insertion disrupts the correct reading frame and contains a number of stop codons in all reading frames, we suppose that the expression of TDM1 protein is abolished. Plants homozygous for *tdm1-4* are male sterile, but no defect was found in heterozygous plants. So we suppose that this line presents a recessive null allele.

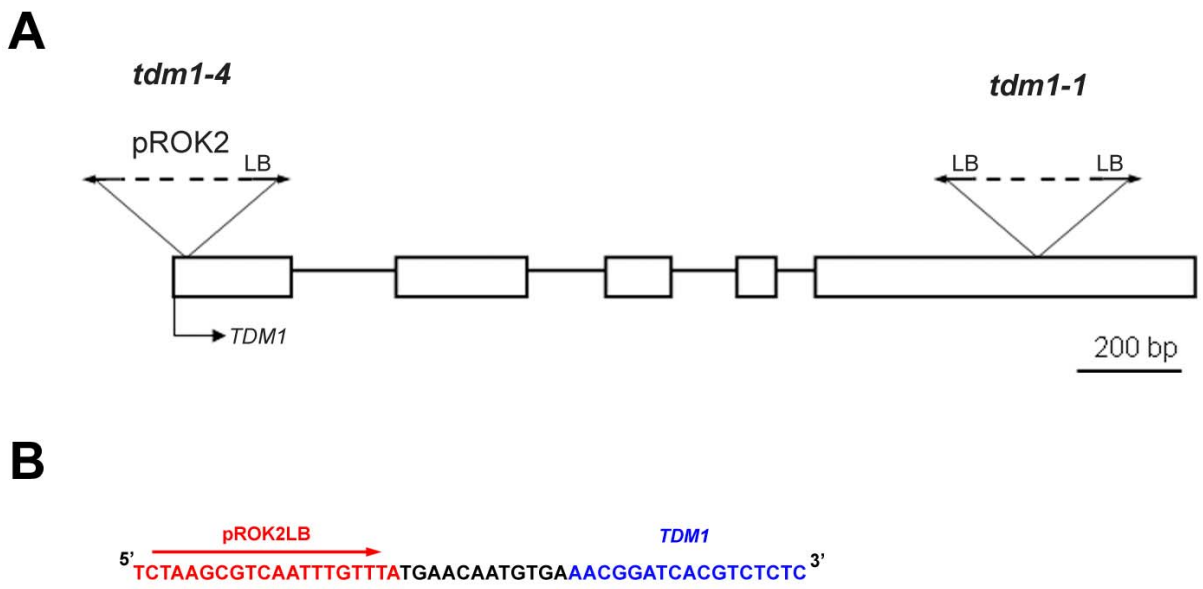

Figure 2.17: T-DNA insertions in the TDM1 gene. **(A)** Diagram of *TDM1* locus with marked positions of *tdm1-1* and *tdm1-4* alleles. *tdm1-1* insertion was annotated according to Glover et al. 1998 **(B)** Sequence of the junctions of T-DNA insertion within the *TDM1* locus of the *tdm1-4* allele. *Arabidopsis* genomic DNA is marked in blue, T-DNA in red and filler sequences at the fusion junction are marked in black.

Neither *tdm1-1* nor *tdm1-4* mutant lines produce pollen grains as shown by Alexander staining (figure 2.18). Instead we could only observe remnants of death microspores in anthers. Further we examined female fertility by reciprocal crosses with wild type. It was already shown in initial screen by Chaudhury and colleagues that *tdm1* mutant plants are female fertile (Chaudhury 1994). We could confirm this observation for both *tdm1* mutant alleles. No seeds were formed when we pollinated wild type plants with pollen from *tdm1-1* and *tdm1-4* mutants. In contrast, *tdm1* mutants pollinated with wild type developed long silliques with viable seeds. All progeny plants were heterozygous for *tdm1* mutation (data not shown).

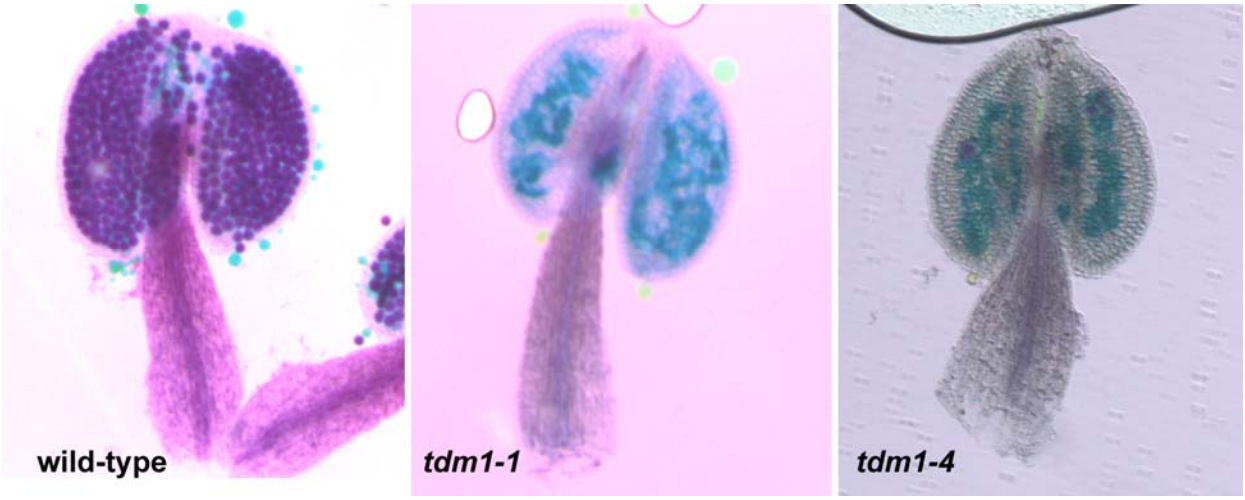

Figure 2.18: Pollen viability determined by Alexander staining of anthers. Viable pollen in wild-type is stained in purple. No viable pollen is detected in *tdm1-1* and *tdm1-4* mutants.

Ross and colleagues suggested that TDM1 dysfunction causes defect in meiotic exit and progression to third meiotic division without preceeding genome duplication (Ross et al. 1997). As only simple DAPI staining of chromosome spreads was used in this study, we wanted to verify this hypothesis and further describe the third meiotic division in details. The typical hallmark of metaphase is a formation of a spindle apparatus that later moves chromosomes in anaphase. We used immunostaining with antibodies against tubulin to visualize spindle in *tdm1-1* and *tdm1-4* meiosis. Consistently with previous description, in both *tdm1* mutant lines meiosis progressed until tetrade stage without any difference from wild type (figure 2.19A-C). After tetrade stage chromatids re-condensed and entered in stage that we called metaphase III because we could clearly detect formation of four regular spindles (figure 2.19D). In *tdm1-1* mutants is this stage followed by an anaphase-like stage characterized by spindle elongation, and stretching of chromatids resulting in anaphase bridges (figure 2.19E). In *tdm1-4* mutants, we observed anaphase III in part of meiocytes, the other part had elongated spindles but no stretching of chromatids and no anaphase bridges (figure 2.20). Eventually, in both alleles, this third meiotic division led to a formation of polyads – multinuclear cells that later degenerated.

To further characterize the third meiotic division we examined histone H3 phosphorylation at the serine 10 residue. Function of this phosphorylation is not well understood. In plant mitosis is H3 phosphorylation found in centromeric regions of metaphase chromosomes and disappears during anaphase. In meiosis, the phosphorylation pattern differs between the two meiotic divisions: in metaphase I whole chromosomes are phosphorylated, whereas this phosphorylation is restricted

to centromeres in metaphase II (Manzanero et al. 2000b; Riehs et al. 2008). We observed this phosphorylation pattern also in the first and second divisions in *tdm1* mutants. In the metaphase III, the histone H3 serine10 phosphorylation seems to localize to centromeres in both *tdm1* mutant alleles, suggesting some similarity with the second meiotic division (figure 2.21). Based on these results it is possible to conclude that in the absence of *TDM1* meiocytes re-enter a third meiotic division that in some aspects resembles the second division. *TDM1* protein is, therefore, critical for distinguishing meiotic interkinesis from meiotic exit.

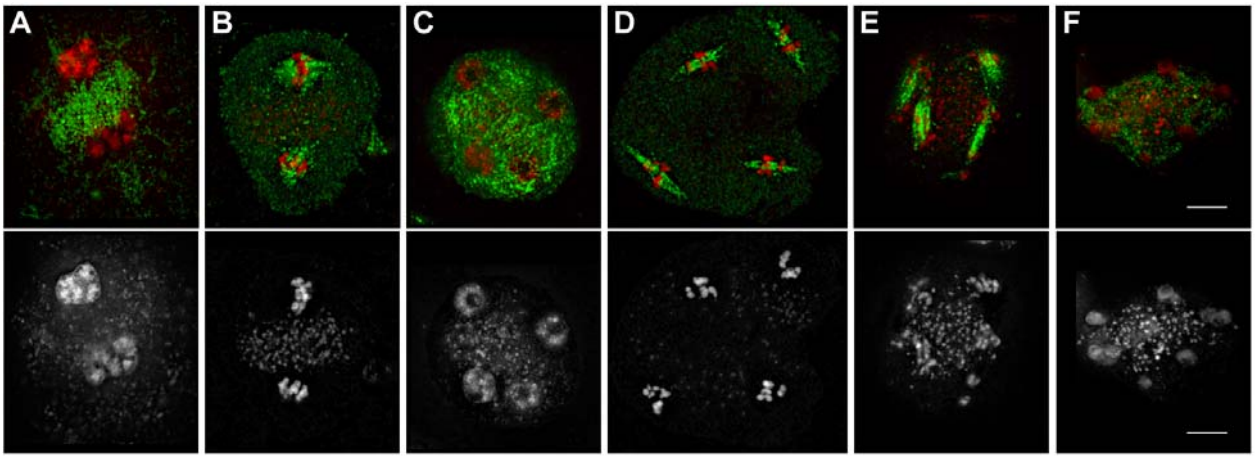

Figure 2.19: Meiosis in *tdm1-1* mutants. Progression of meiosis from interkinesis is shown. The spindle was detected by immunostaining with anti-α-tubulin antibody (green) and DNA was counterstained with DAPI (red). Only DAPI staining is shown in the bottom panel. **(A)** interkinesis, **(B)** metaphase II, **(C)** telophase II, **(D)** metaphase III, **(E)** anaphase III and **(F)** polyads. Scale bar: 5 µm.

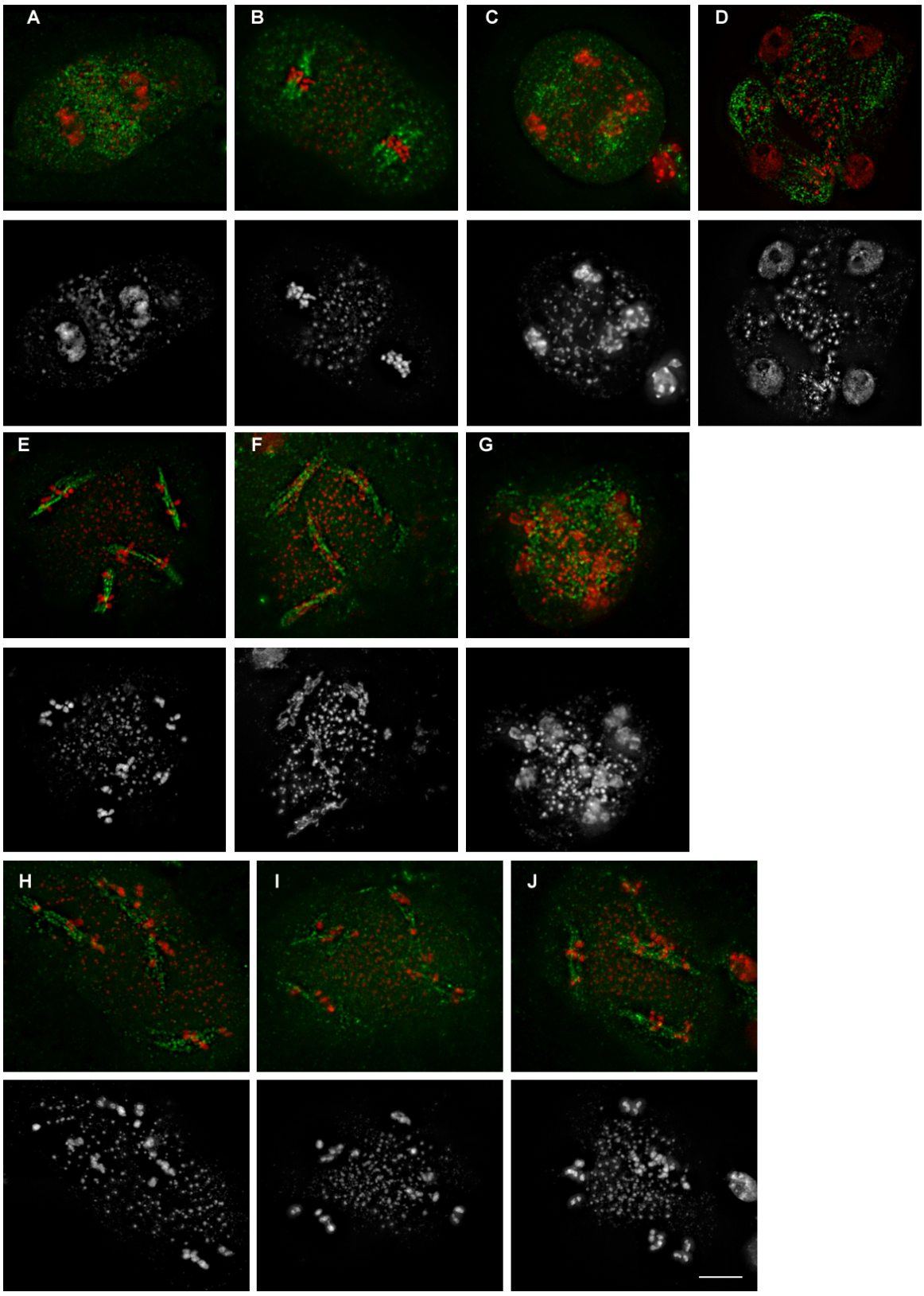

Figure 2.20: Meiosis in *tdm1-4* mutants. Progression of meiosis from interkinesis to polyad stage. The spindle was detected by immunostaining with anti-α-tubulin antibody (green) and DNA was counterstained with DAPI (red). Only DAPI staining is shown in the bottom panels. **(A)** interkinesis, **(B)** metaphase II, **(C)** telophase II, **(D)** tetrade, **(E)** metaphase III, **(F)** telophase III, **(G)** polyads and **(H-J)** irregular anaphases III. Scale bar: 10 µm.

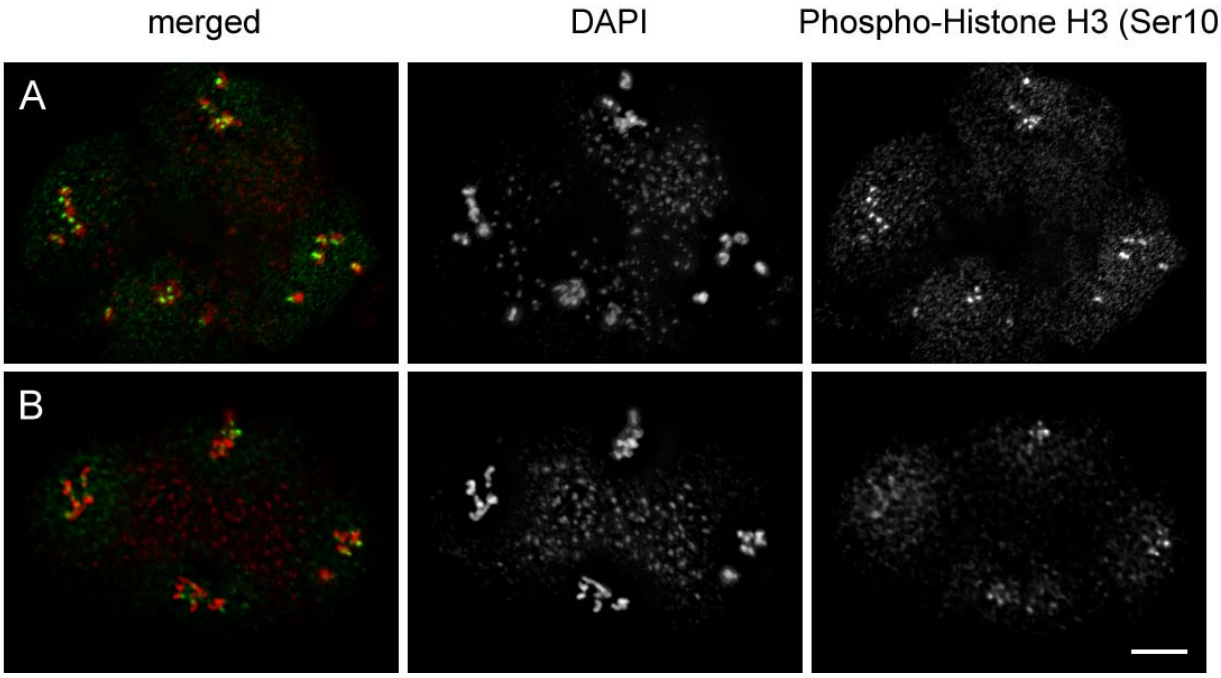

Figure 2.21: Histone H3 serine 10 phosphorylation during metaphase III in **(A)** *tdm1-1* and **(B)** *tdm1-4* mutants. Immunostaining with anti-Phospho-Histone H3 (Ser10) antibody (green) and DNA was counterstained with DAPI (red). Also separate DAPI and Phospho-Histone H3 (Ser10) staining are shown. Scale bar: 5 μm.

2.5.2. *smg7 tdm1* double mutants

To investigate relation between *SMG7* and *TDM1* in meiotic exit, we crossed plants heterozygous for *smg7* mutation with plants heterozygous either for *tdm1-1* or *tdm1-4* alleles. Double mutants segregating in F2 generation were sterile and exhibited the *smg7* vegetative phenotype. Strikingly, Alexander staining of anthers showed remnants of cells which was typical for *tdm1* single mutants rather than for *smg7* mutants (figure 2.22). Cytogenetic analysis of male meiosis showed that *smg7* arrest in anaphase II was completely suppressed, and instead meiocytes continued to the third meiotic division (figure 2.23). We confirmed this phenotype in both *smg7 tdm1-1* and *smg7 tdm1-4* double mutants. The third meiotic division in the double mutants looked very similar to *tdm1* single mutants as established by tubulin immunostaining (figure 2.23). We rarely detected stages in third division that were reminiscent of *smg7* phenotype – unequal numbers of clustered chromatids with irregular spindles instead of four groups per five chromatids (figure 2.23F). Thus, this analysis demonstrated that the *tdm1* mutant phenotype was dominant in male meiosis. Because *tdm1* affects only male fertility, while a *smg7* mutation impairs both male and female meiosis, we were interested what happens with female fertility in *tdm1 smg7* double mutants. Therefore, we pollinated double mutant plants with pollen from wild type plants. Pistils pollinated with wild type pollen developed into silliques with viable seeds (figure 2.24). All 44 analysed F1 plants were double heterozygous for *smg7*

and *tdm1* mutations confirming that they are a progeny from the cross. We conclude that *tdm1* mutation completely suppressed *smg7* anaphase II arrest in both male and female meiosis.

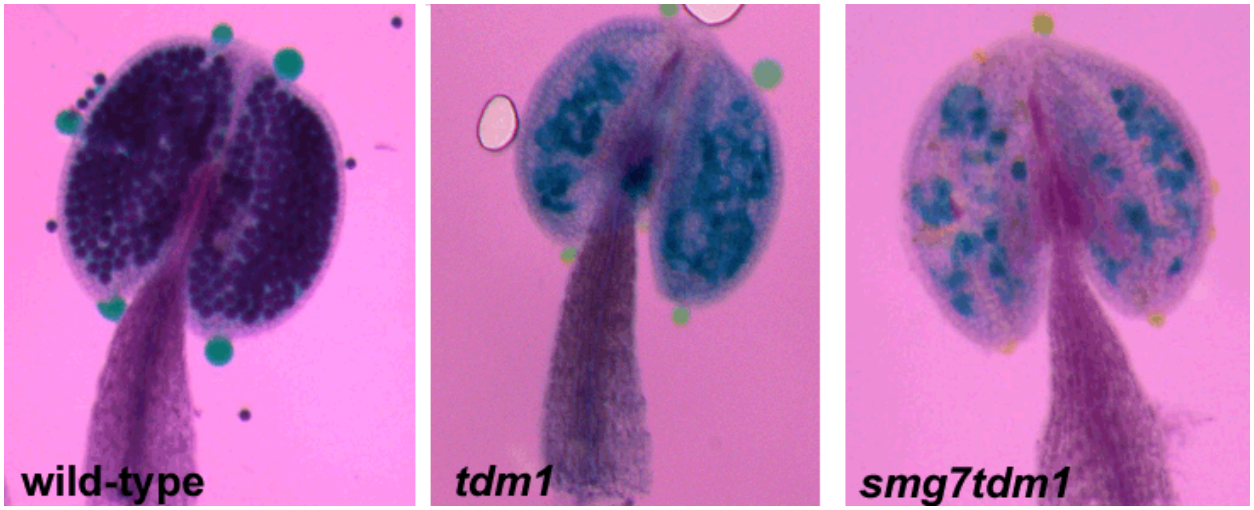

Figure 2.22: Pollen viability determined by Alexander staining of anthers. Viable pollen in wild-type is stained in purple; no viable pollen is detected in *tdm1* and *smg7 tdm1* double mutants.

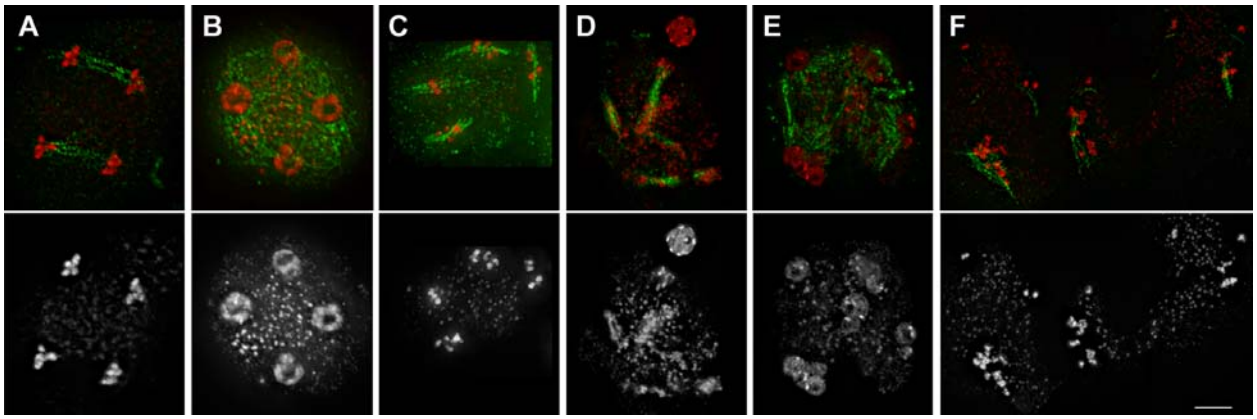

Figure 2.23: Meiosis in *smg7 tdm1-1* double mutants. Progression of meiosis from anaphase II is shown. The spindle was detected by immunostaining with anti-α-tubulin antibody (green) and DNA was counterstained with DAPI (red). Only DAPI staining is shown in the bottom panel. **(A)** anaphase II, **(B)** tetrade, **(C)** metaphase III, **(D)** anaphase III, **(E)** polyade and **(F)** *smg7*-like stage. Scale bar represents 5µm.

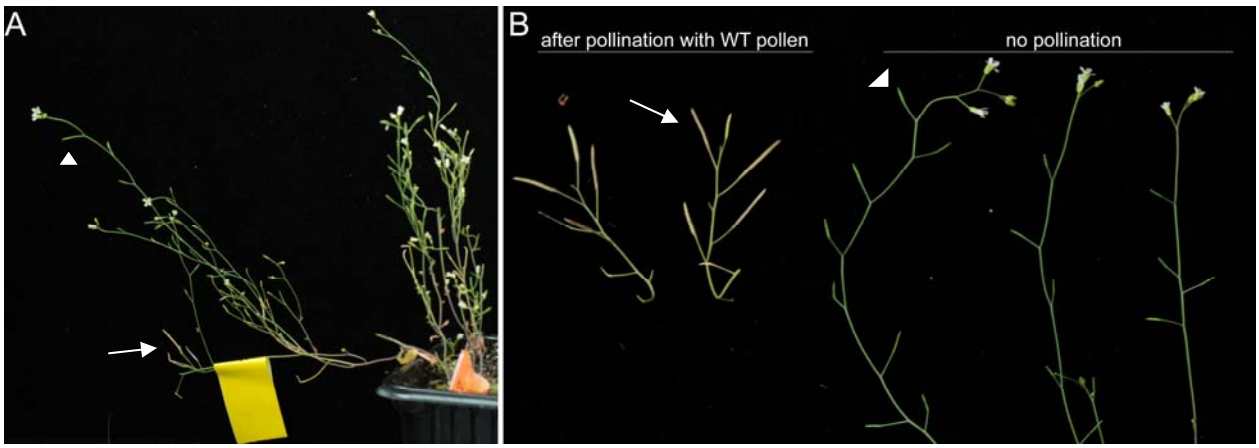

Figure 2.24: Female fertility in *smg7 tdm1* double mutants. Fertile silliques are marked by arrows, sterile by arrowheads. **(A)** *smg7 tdm1-1* plant – most stems harbour sterile silliques (arrowhead), but few fertile silliques are visible after pollination with wild type pollen (arrow) **(B)** detail of *smg7 tdm1-1* silliques: pollinated with wild type pollen (right) and without pollination (left).

2.5.3. TDM1 protein localization

The unexpected finding that *tdm1* mutation suppresses *smg7* anaphase II arrest suggests that *TDM1* functions in meiosis before manifestation of the mutant phenotype. For this reason we investigated TDM1 protein localization. As the *GUS* fusion strategy was successful in the case of *TAM* localization, we used it also for *TDM1*. We fused *TDM1* gene at the C-terminus with *GUS* and placed it under the *TDM1* native promoter. The TDM1:GUS fusion construct was transformed to plants heterozygous for the *tdm1-4* allele. We examined 58 independent lines in T1 generation. *TDM1:GUS* complemented mutant phenotype in 6 lines out of 9 segregating *tdm1-4* mutant lines. This demonstrated that the fusion TDM1:GUS construct is functionally equivalent to the native gene. GUS histochemical staining revealed *TDM1* expression in anthers of 2-3 young floral buds within one influorescence that were approximately at the stage that would correspond to meiosis in 38 T1 lines out of 58 examined (figure 2.25). Thus this staining pattern likely reflects expression of native TDM1 protein. Because genetic interaction with *SMG7* indicates that *TDM1* influences also female meiosis, we stained TDM1:GUS inflorescences under less stringent GUS assay conditions. Indeed, under these conditions we could detect weak staining also in pistils (data not shown). Based on the histochemical GUS assay we have chosen four representative lines – one wild type for *TDM1* endogenous gene, one heterozygous line and two *tdm1-4* mutant lines for further immunolocalization studies.

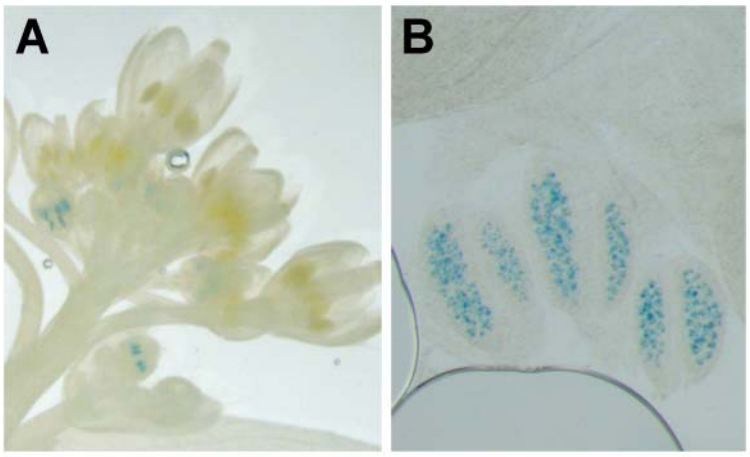

Figure 2.25. Expression of the TDM1:GUS fusion protein in anthers of young floral buds. Entire fluorescence **(A)** and close-up of dissected anthers **(B)** are shown. The *TDM1:GUS* construct was made by fusing the *TDM1* gene including promoter to the *GUS* reporter gene. Blue staining indicates activity of the GUS reporter.

Immunodetection showed that TDM1:GUS was expressed in pollen mother cells and microspores, and it was not detected in somatic cells. Signal appeared in cytoplasm already from the beginning of meiotic prophase I, than became stronger in metaphase I and persisted until microspore stage (figure 2.26). Interestingly, localization pattern of TDM1:GUS changed in the course of meiosis. As the signal was getting stronger during metaphase I, it started to form distinct foci (figure 2.26 B). Number of foci peaked in metaphase II, with more than 10 foci per meiocyte. However, during progression of anaphase II, the foci began to disappear and signal diffused throughout the cytoplasm (figure 2.26 E-G). One to two foci were still visible in tetrades and microspores (figure 2.26 G,H). We confirmed this pattern also with the *Arabidopsis* lines expressing TDM1:YFP fusion protein (data not shown). These dynamic changes in staining pattern imply that TDM1 localization probably plays a regulatory role.

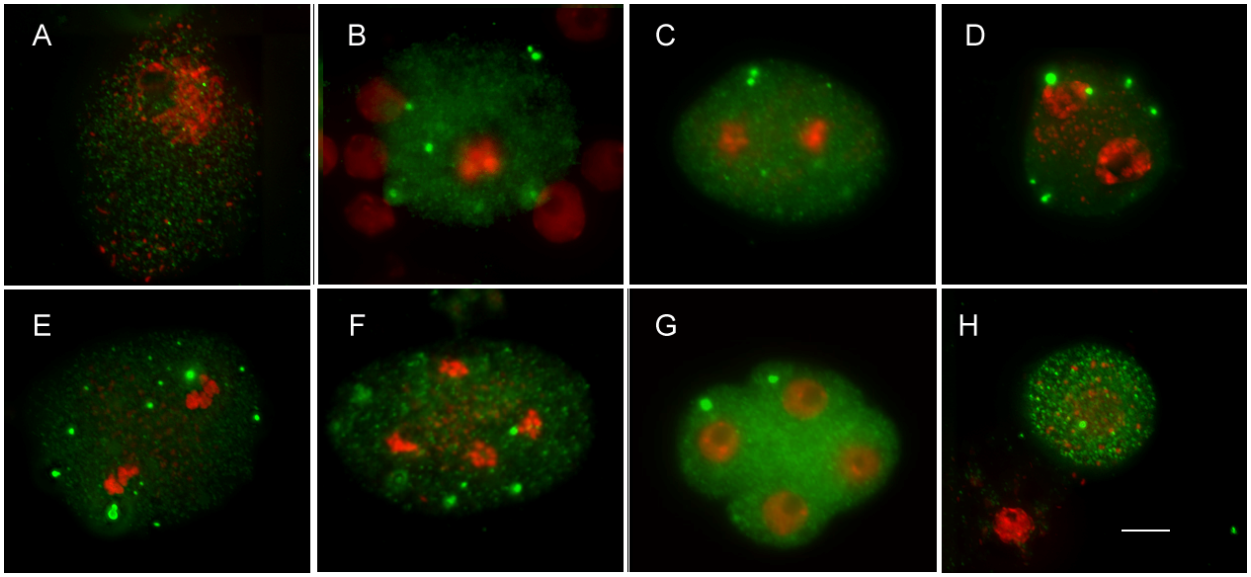

Figure 2.26: Localization of TDM1:GUS construct during meiosis. TDM1:GUS was detected with antibodies against GUS (green) and DNA was counterstained with DAPI (red). **(A)** prophase II, **(B)** metaphase I, **(C)** anaphase I, **(D)** interkinesis, **(E)** metaphase II, **(F)** anaphase II, **(G)** tetrade and **(H)** microspore. Scale bar represents 5µm.

2.6. Premature exit in *tam* null mutants depends on *TDM1*

Although *TDM1* dysfunction causes a phenotype only at the end of male meiosis, genetic interaction with *SMG7* indicate an earlier role in both male and female meiotic divisions. To test whether *TDM1* is required already during interkinesis we decided to follow its genetic interaction with *TAM*.

We examined double mutants segregating in F2 generation from crosses between *tam-1* and *tam-2* alleles and both *tdm1-1* and *tdm1-4* alleles. Because the phenotype was identical for all allele combinations, we show here only data on *tam-2 tdm1-1*. The *tam-2 tdm1-1* double mutant plants were male sterile and female fertile. Alexander staining of anthers showed that they do not contain any pollen grains but only remnants of death cell like *tdm1* single mutants (figure 2.27).

In male meiosis, the *tam-2* exit after the first meiotic division was completely suppressed (figure 2.28). Instead, all meiocytes continued to the third meiotic division typical for *tdm1* mutant (figure 2.28 G,H). The only difference from the *tdm1* phenotype was presence of meiocytes with irregular shape. A few cells in metaphase I and metaphase II stage had constriction reminding the beginning of cytokinesis (figure 2.28 I).

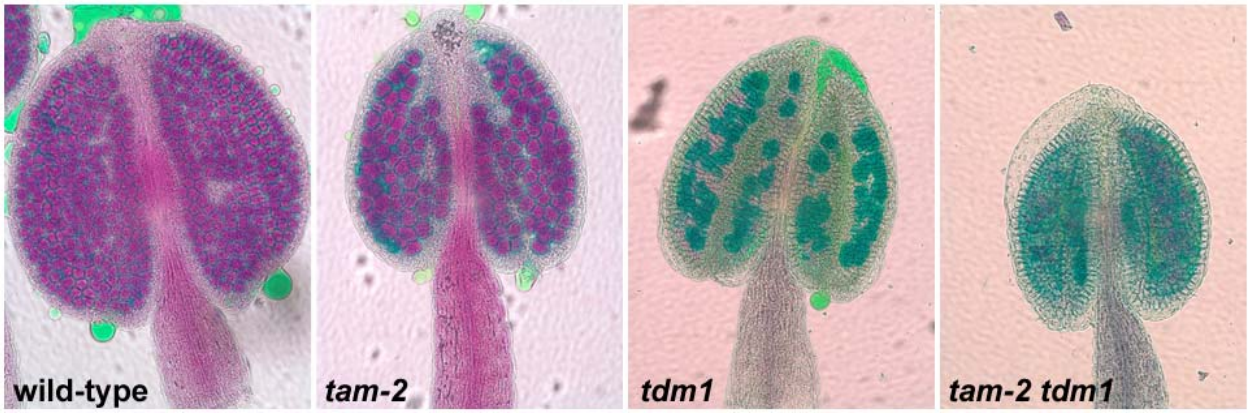

Figure 2.27: TDM1 deficiency suppresses premature exit after meiosis I caused by *tam-2* null allele. Pollen viability determined by Alexander staining of anthers. Viable pollen in wild-type and *tam-2* plants stain in red. No viable pollen is detected in *tdm1* and *tam-2 tdm1* mutants.

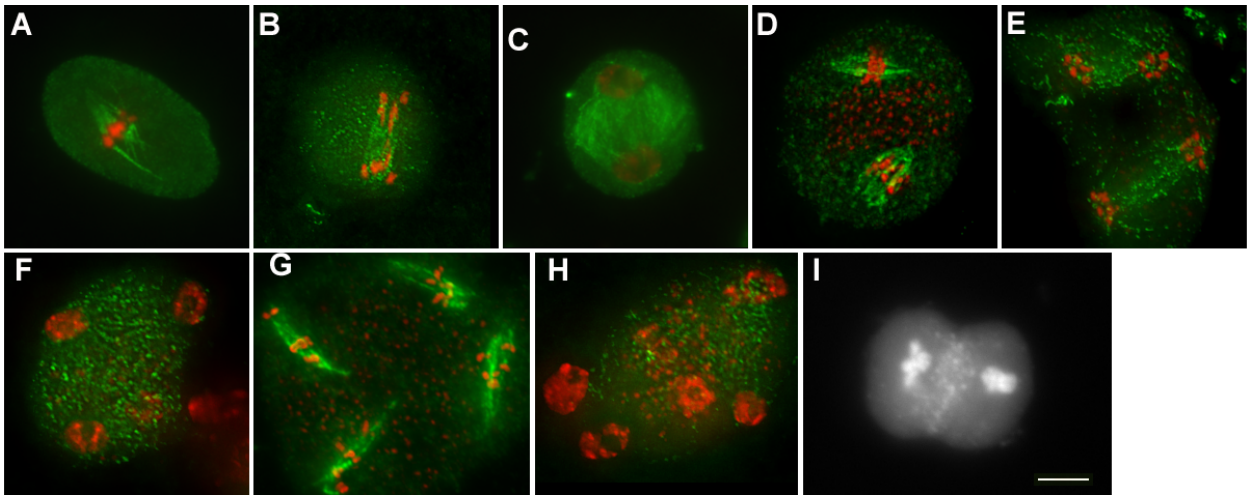

Figure 2.28: Meiosis in *tam-2 tdm1* mutants. Spindle is shown in green, DNA counterstained with DAPI in red. (A) metaphase I, (B) anaphase I, (C) interkinesis, (D) metaphase II, (E) anaphase II, (F) telophase II, (G) metaphase/ anaphase III (H) polyad and (I) metaphase II with irregular shape. Scale bar represents 10µm.

We also wanted to examine effect of *tdm1* mutation on *tam-2* female meiosis. Therefore we pollinated *tam-2* and *tdm1-1* single mutant as well as *tam-2 tdm1-1* double mutant plants with wild type pollen. If diploid gametes form in *tam-2 tdm1-1* we should obtain triploid plants in next generation. We analysed F1 plants by flow cytometry. All 12 F1 plants from cross with *tdm1-1* and 13 plants from *tam-2 tdm1-1* were diploid (figure 2.29 C and D). In a control cross when *tam-2* plants were pollinated with wild-type pollen we expected to find triploid progeny. Surprisingly, 18 out of 20 measured F1 plants from the cross with *tam-2* mutants were diploid

(figure 2.29 H). Flow cytometry of DNA content in nuclei revealed that one of the remaining plants had clear triploid and hexaploid peak, but also a broad peak that was between haploid and diploid DNA content (figure 2.29 F). The last plant had several peaks – strong diploid peak, smaller triploid and tetraploid peak and again a strong hexaploid peak (figure 2.29 G). It was already shown that plants can tolerate other ploidy levels than diploid, but it may cause genomic instability (Madlung et al. 2005; Wang et al. 2010). We suppose that a high number of diploid F1 plants reflects a weaker manifestation of *tam-2* phenotype in female meiosis together with a lower viability of triploid seeds due to disbalance of maternal to paternal genome contribution in the endosperm that might eventually result in endosperm failure (reviewed in Kohler et al.) Therefore, we can not draw a clear conclusion about the *tdm1* and *tam-2* interaction in female meiosis.

In conclusion, our demonstration that *tdm1* mutation suppresses *tam-2* phenotype in male interkinesis suggests that the premature meiotic exit in *tam-2* mutants requires TDM1 protein.

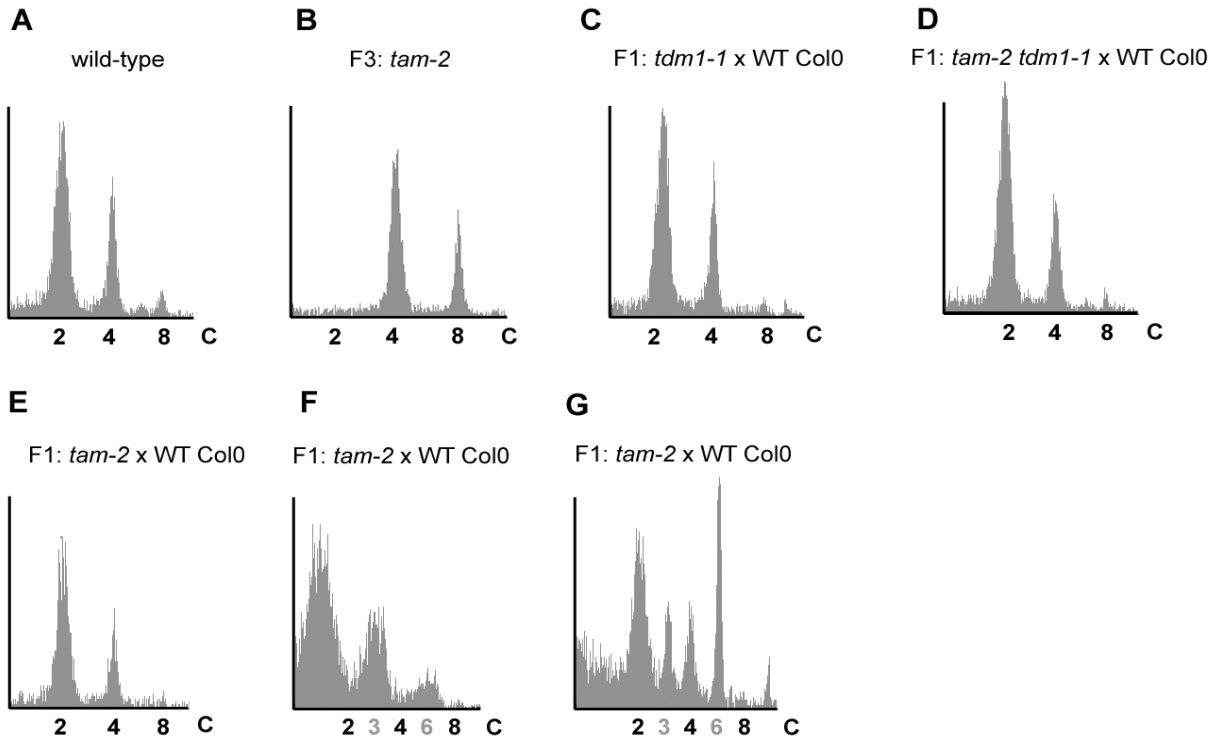

Figure 2.29: Flow cytometry analysis of DNA content in nuclei prepared from inflorescences of progeny of **(A)** wild-type, **(B)** *tam-2* **(C)** *tdm1-1* crossed with wild type Col0 **(D)** *tam-2 tdm1* crossed with wild type Col0 and **(E-G)** three examples of progeny from cross between *tam-2* with wild-type Col0.

2.7. Screen for meiotic B-type cyclin in *Arabidopsis*

Genetic analysis showed that *SMG7* and *TDM1* are critical regulators indispensable for proper meiotic cell cycle progression. Dysfunction in any of these proteins can suppress meiotic exit caused by the absence of the only known meiotic cyclin *TAM* and allows progression to second meiotic division. This argues that TAM is not target of TDM1 ad SMG7 regulation and that other cyclins besides TAM drive meiotic progression. To understand SMG7 and TDM1 role in meiotic cell cycle regulation, we need to first define the main components conferring the cdk activity – cyclin dependent kinases and cyclins. As already reasoned in previous sections, *CDKA;1* is clearly the major meiotic cdk. However, the B-type cdks have not yet been investigated in regards to meiosis. It was already shown that all *Arabidopsis* cdks are generally expressed in dividing tissues and their expression is not meiosis specific. Each cdk can be activated by distinct cyclins and one cyclin can form active complex with several cdks. Therefore we suppose that to identify meiosis-specific cdk complexes we first have to define meiotic cyclins

2.7.1. B-type cyclins in *Arabidopsis*

Plants show an unusually high redundancy in cell cycle-regulating proteins. Wang and colleagues (Wang et al. 2004a) identified in an *in silico* search 50 putative cyclin coding genes in *Arabidopsis thaliana* genome. Among them were 21 putative M-phase cyclins – 10 A-type cyclins and 11 B-type cyclins (figure 2.30). A-type cyclins are mainly required for S/G2 phase and contribute to entry into M-phase. Therefore we decided to focus on cyclin Bs because their activity is required for M-phase progression and their degradation is necessary for M-phase exit.

One way how to identify meiotic cyclins is through genetic analysis of cyclin mutants. However it was shown for at least some of *Arabidopsis* cyclins, that single knock-outs do not show any obvious phenotypes (Dr. Arp Schnittger, personal communication). This suggests high degree of redundancy and necessity to generate complex mutants to reveal cyclins with a meiotic function. This could be a very time-consuming taken into account number of B-type cyclins in *Arabidopsis*. We also anticipated that generation of mutants deprived of multiple cyclins will be lethal or that misregulation of previous mitotic divisions could cause a meiotic phenotype indirectly. Thereby we decided to identify meiotic cyclins by looking for cyclin candidates that are expressed in male meiocytes. For this purpose we decided to tag all B-type cyclin genes and examine their expression in meiotic cells.

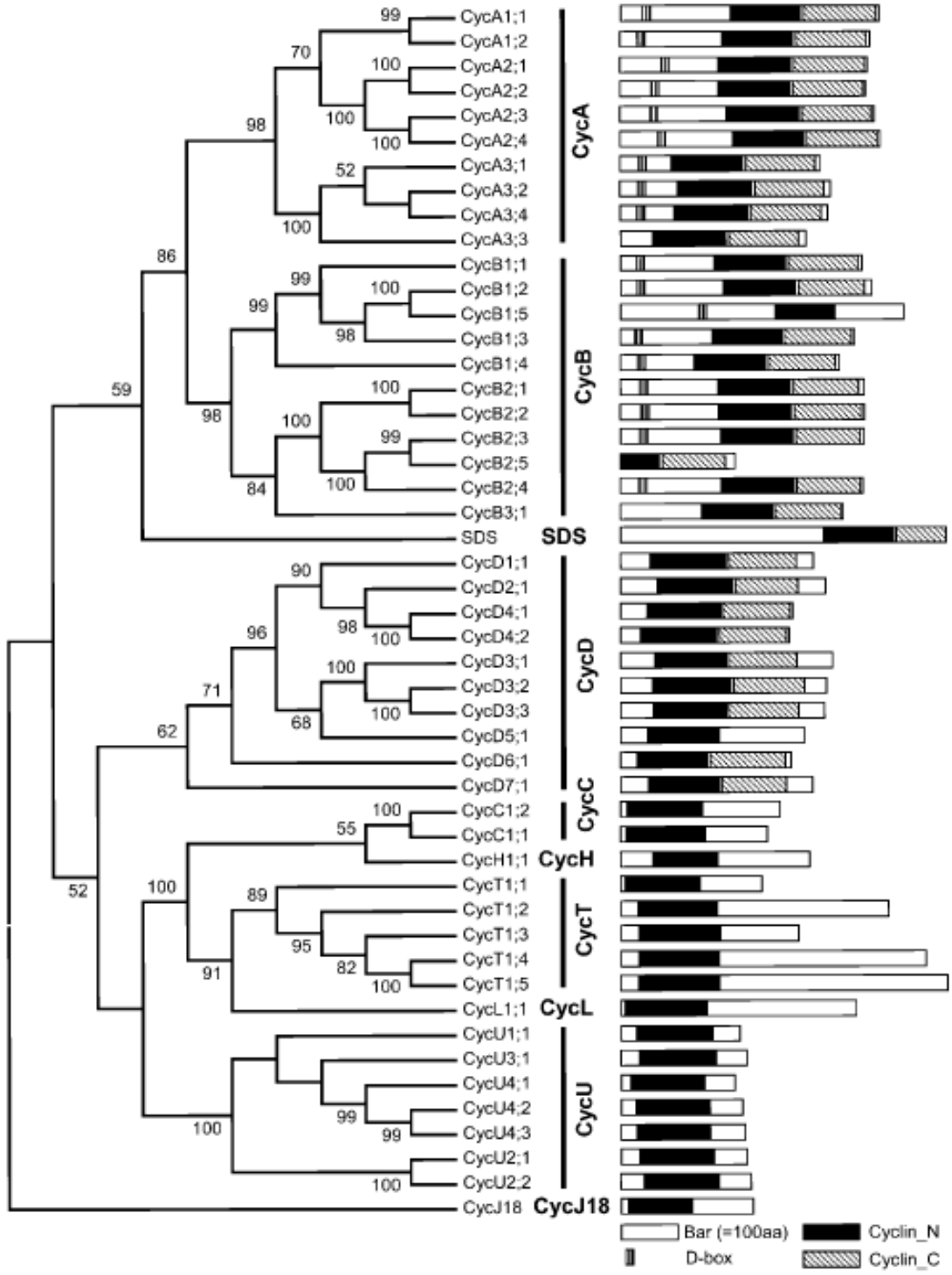

Figure 2.30: Copied from Wang et al. 2004a - Phylogenetic relationships and domain structure of the 49 Arabidopsis cyclins.

One very important feature that defines cyclin expression is their degradation during anaphase. It was already shown that construct with N-terminal fragment of *CYCLIN B1;1* containing the destruction box fused with GUS and driven by endogenous promoter is expressed from G2 to M-

phase and degraded during anaphase (Colon-Carmona et al. 1999). This is in agreement with typical cyclin B expression in other species and so we can suppose the CYCB1;1-GUS protein reflects native *CYCLIN B1;1* localization and degradation. We also successfully used similar strategy for determining meiotic expression of *TAM* and *TDM1*, demonstrating that GUS fusion proteins can be detected in meiosis. Therefore we decided to tag all B-type cyclins except *CYCLIN B1;1* at their C-terminus with GUS. Expression of CYCB1;1-GUS construct in meiosis was already examined by Nina Riehs in our lab (Riehs 2009). Using immunocytology with antibodies against GUS she could detect expression of this construct only in mitotic cells, and no expression during meiosis. To conserve all regulatory elements and possible alternative splicing isoforms we used a genomic DNA sequence including putative promoter, 5´UTR and all introns. The 3´UTR was replaced with the GUS gene.

Cyclin genes were amplified by PCR from genomic DNA with primers containing restriction sites and consequently cloned into entry pCR2.1 vector. We verified insert by sequencing and by cloned it trough restriction cloning to a final binary vector with the GUS tag. Next we transformed constructs to *Agrobacterium tumefaciens* and tested their functionality by transient expression in suspension culture. We infected growing *Arabidopsis* suspension cultures with *Agrobacteria* and subcultivated them for three days. We washed bacteria out and by GUS histochemical assay we determined expression of constructs in cultivated cells (figure 2.31). All tested cyclin constructs showed expression in the suspension culture, although staining in cultures transformed with *CYCLIN B2;1:GUS* and *CYCLIN B2;2:GUS* was rather weak and detectable only with binocular microscope (figure 2.31 E,F and P,Q). In contrast, staining of cultures expressing CYCLIN B2;3:GUS, CYCLIN B2;4:GUS and CYCLIN B2;5:GUS (figure 2.31 G, H and I) was stronger than control cultures, where GUS is driven by constitutively expressed *ACTIN* and *35S* promoters (figure 2.31 K,L).

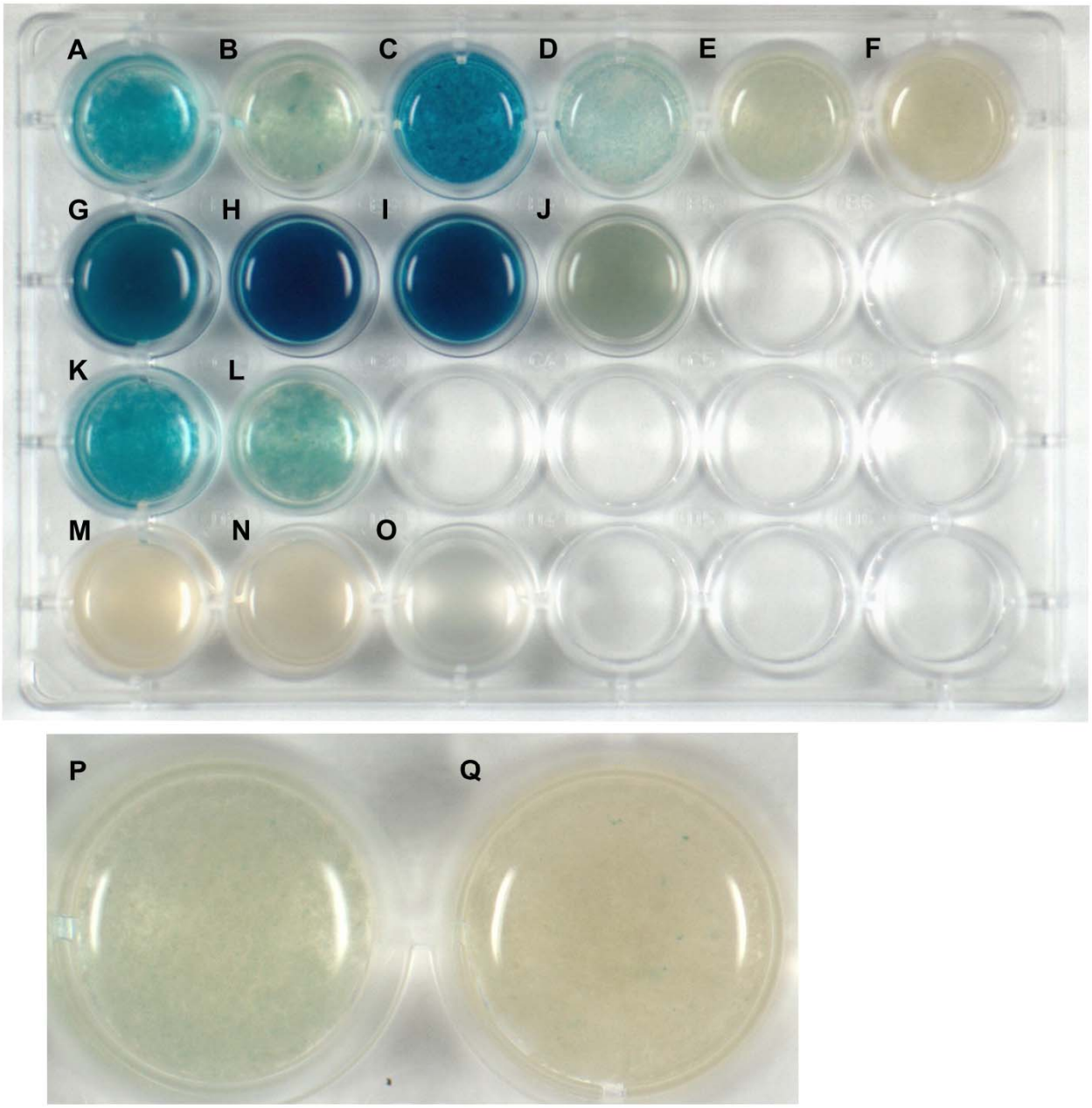

Figure 2.31: Transient expression of CYCLIN B:GUS in suspension culture. Blue staining indicates activity of the GUS reporter. **(A-J)** CYCLINB:GUS constructs: **(A)** CYCLIN B1;2:GUS, **(B)** CYCLIN B1;3:GUS, **(C)** CYCLIN B1;4:GUS, **(D)** CYCLIN B1;5:GUS, **(E)** CYCLIN B2;1:GUS, **(F)** CYCLIN B2;2:GUS, **(G)** CYCLIN B2;3:GUS, **(H)** CYCLIN B2;4:GUS, **(I)** CYCLIN B2;5:GUS, **(J)** CYCLIN B3;1:GUS, **(K,L)** positive controls : (K) 35S::GUS and (J) ACTIN::GUS **(M-O)** negative controls (empty vector) respective to individual rounds of transformations and **(P,Q)** zoom on **(P)** CYCLIN B2;1:GUS and **(Q)** CYCLIN B2;2:GUS suspension cultures.

After we confirmed that all constructs can be expressed in plant cells, we transformed wild type *Arabidopsis* plants. T1 transformed plants were selected for BASTA resistance and at least 15

individual lines were further analyzed for each construct. The only exception was CYCLIN B2;2 were only 12 transgenic lines were selected. In T2 generation we segregated resistant plants on plates and determined transgene segregation ratio for each line. To select representative lines and explore expression patterns of cyclins we performed GUS histochemical assay in 12 days old seedlings. Intensity of GUS staining in histochemical assay can be influenced by various factors, but in all our experiments the localization of expression and relative staining intensity of distinct cyclins remained the same.

We could divide cyclins into two groups based on their staining pattern. First group were highly expressed cyclins: *CYCLIN B1;1*, than *CYCLIN B1;2*, *CYCLIN B1;3*, *CYCLIN B1;4* and *CYCLIN B2;3*. All these cyclins showed expression in highly proliferating tissues such as shoot apex, young leaves and root tips. In the second group were the the remaining cyclins - *CYCLIN B1;5*, *CYCLIN B2;1*, *CYCLIN B2;2*, *CYCLIN B2;4*, *CYCLIN B2;5*, *CYCLIN B3;1* that exhibited either lower expression in the same parts of plant as highly expressed cyclins or no expression in some proliferating tissues where other cyclins were be detected. In the group of highly expressed cyclins, we selected three representative lines of each construct for furher analysis, in the second group of cyclins that showed weaker expression we analysed all lines.

For each construct we determined GUS staining pattern in young 12 days seedlings and in inflorescences and then we examined intracellular localization of the CYCLIN B:GUS proteins by immunostaining in cells prepared from young floral buds or root tips. For the first group of highly expressed cyclins we used squashes of young anthers and performed double immunostaining with antibodies against GUS and against alpha-TUBULIN to disclose eventual colocalization. For the second group of cyclins we performed only immunodetection with GUS antibody and besides anthers used also squashes of root tips and very young leaves surrounding shoot apical meristem. In the following sections are described staining patterns obtained for each cyclin with GUS histochemical assay and with the immunostaining.

2.7.2. Detection of cyclin expression in plant tissues

Expression in seedlings

In seedlings, expression of all cyclins from first group localized to the same organs – root tips, also in emerging lateral roots, in shoot apex and young leaves organs. In all cases the GUS staining had a form of single spots that represented single cells. The main difference was in the

number of stained cells. The *CYCLIN B1;1*, *CYCLIN B1;2*, *CYCLIN B1;3*, and *CYCLIN B1;4* were the highest expressed cyclins and they showed similar expression pattern (figure 2.32). *CYCLIN B2;3* was also highly expressed but its expression was detected in slightly less cells than in case of B1-type cyclins (figure 2.34 C). Although there was an overlapping expression of these cyclins, we could still distinguish some differences. In seedlings expressing *CYCLIN B1;2:GUS* a clear boundary was apparent in the proximal second third of leave distally of which cyclin expression was not detected (figure 2.33 A). We suppose that this may be a boundary between mitotically dividing cells and zone of endoreduplication. Staining pattern of *CYCLIN B1;3* in young leaves was the slightly different from *CYCLIN B1;2*. Whereas *CYCLIN B1;2:GUS* stained the first third of young leaves, in *CYCLIN B1;3:GUS* plants was the staining concentrated mainly in the marginal parts of leaves (figure 2.33 B).

Also *CYCLIN B2;1* and *CYCLIN B2;2* gave staining in root tips, shoot apical meristem and young leaves (figure 2.33 A and B). We could detect staining from CYCLIN B2;4:GUS only in shoot apical meristems and young leaves and not in root tips (figure 2.34 D). However, by using immunostaining with anti-GUS antibody we detected clear CYCLIN B2;4:GUS signal in root mitotic cells. The staining pattern of CYCLIN B2;4:GUS was similar to CYCLIN B2;1, CYCLIN B2;2 and CYCLIN B2;3 (figure 2.36 and figure 2.37.). Therefore, the immunodetection might present more reliable method of detection in the case of a very specific or weak expression of a construct than histochemical GUS assay. *CYCLIN B1;5*, *CYCLIN B2;5* *CYCLIN B3;1* did not show any detectable staining in seedlings (figure 2.35). Expression of all constructs in seedlings is summarized in table 2.17.

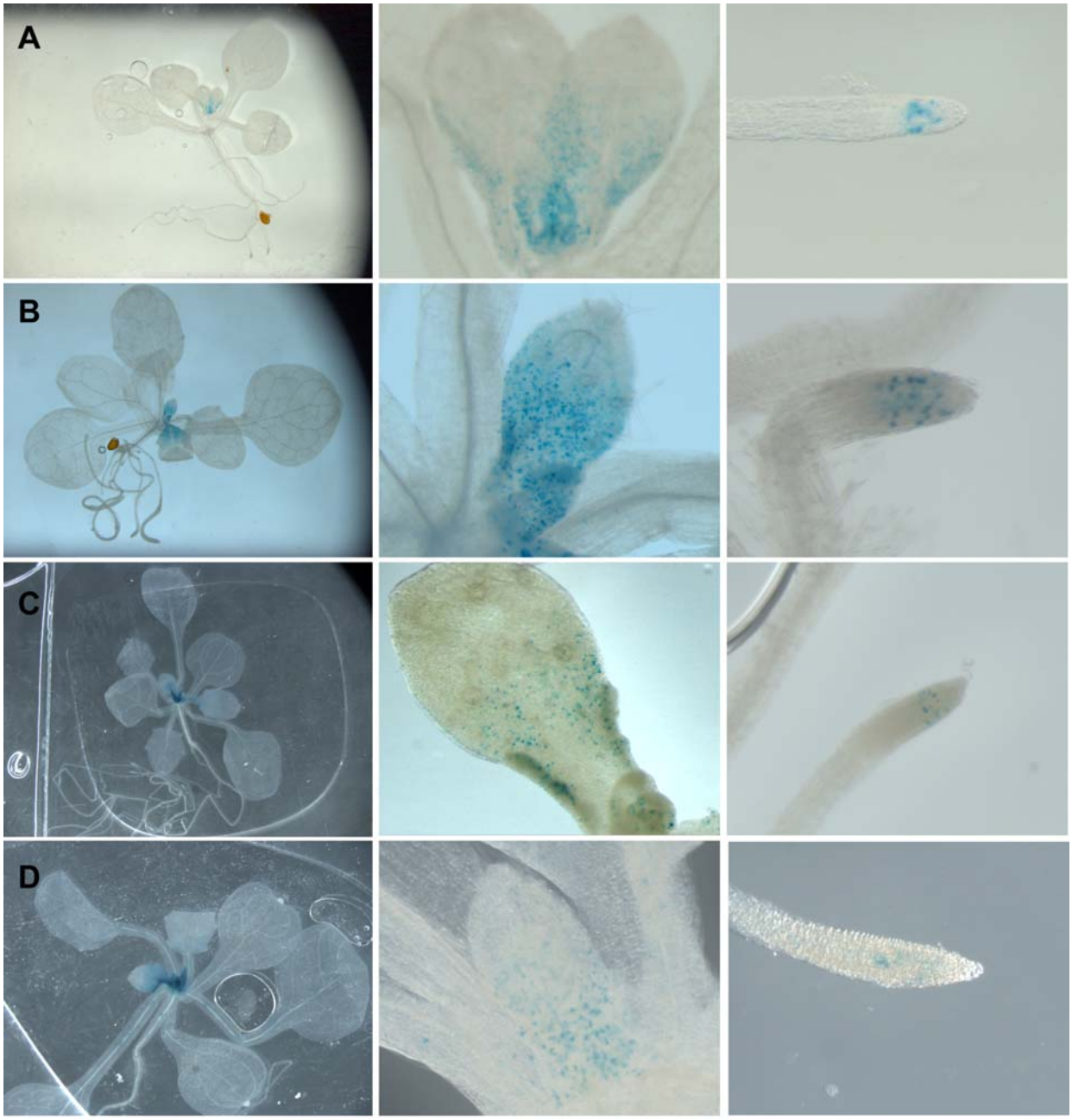

Figure 2.32: Expression pattern of B1-type CYCLIN:GUS constructs in seedlings visualized with GUS histochemical assay. Entire seedling, close-up of leaves and root tips. Blue staining indicates activity of the GUS reporter. **(A)** CYCLIN B1;1:GUS, **(B)** CYCLIN B1;2:GUS, **(C)** CYCLIN B1;3:GUS, **(D)** CYCLIN B1;4:GUS. As the blue GUS staining is in form of single spots, it was necessary to enhance contrast in some pictures in order to make it better visible.

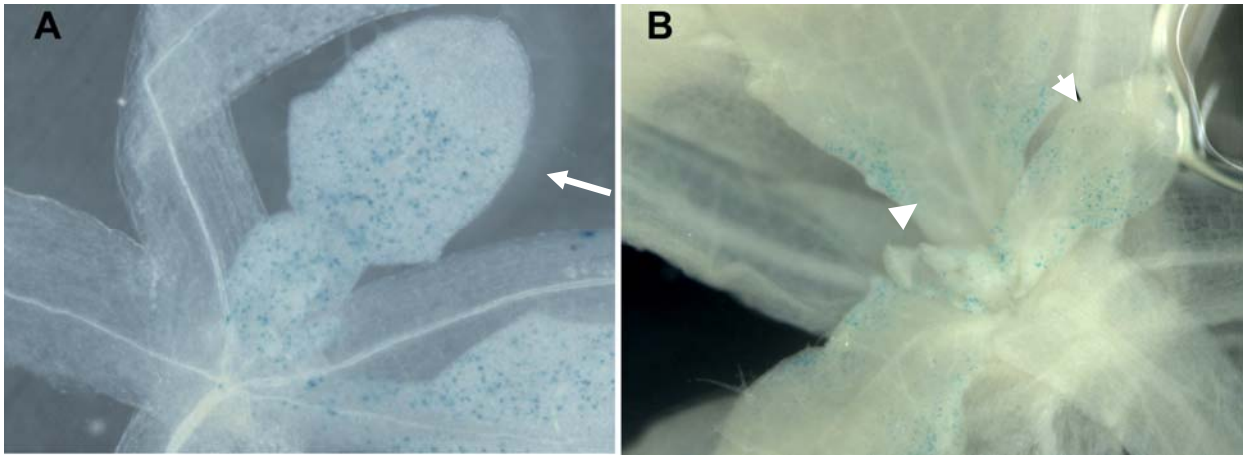

Figure 2.33: Comparison of staining pattern of CYCLIN B1;2:GUS and CYCLIN B1;3:GUS construct in young leaves. Blue staining indicates activity of the GUS reporter. **(A)** CYCLIN B1;2:GUS, **(B)** CYCLIN B1;3:GUS. Expression of CYCLIN B1;2:GUS is detectable in first two thirds of a young leave and zone of expression is separated by sharp boundary from the rest of leave (arrow), whereas expression of CYCLIN B1;3:GUS is limited to borders of leave (arrowheads).

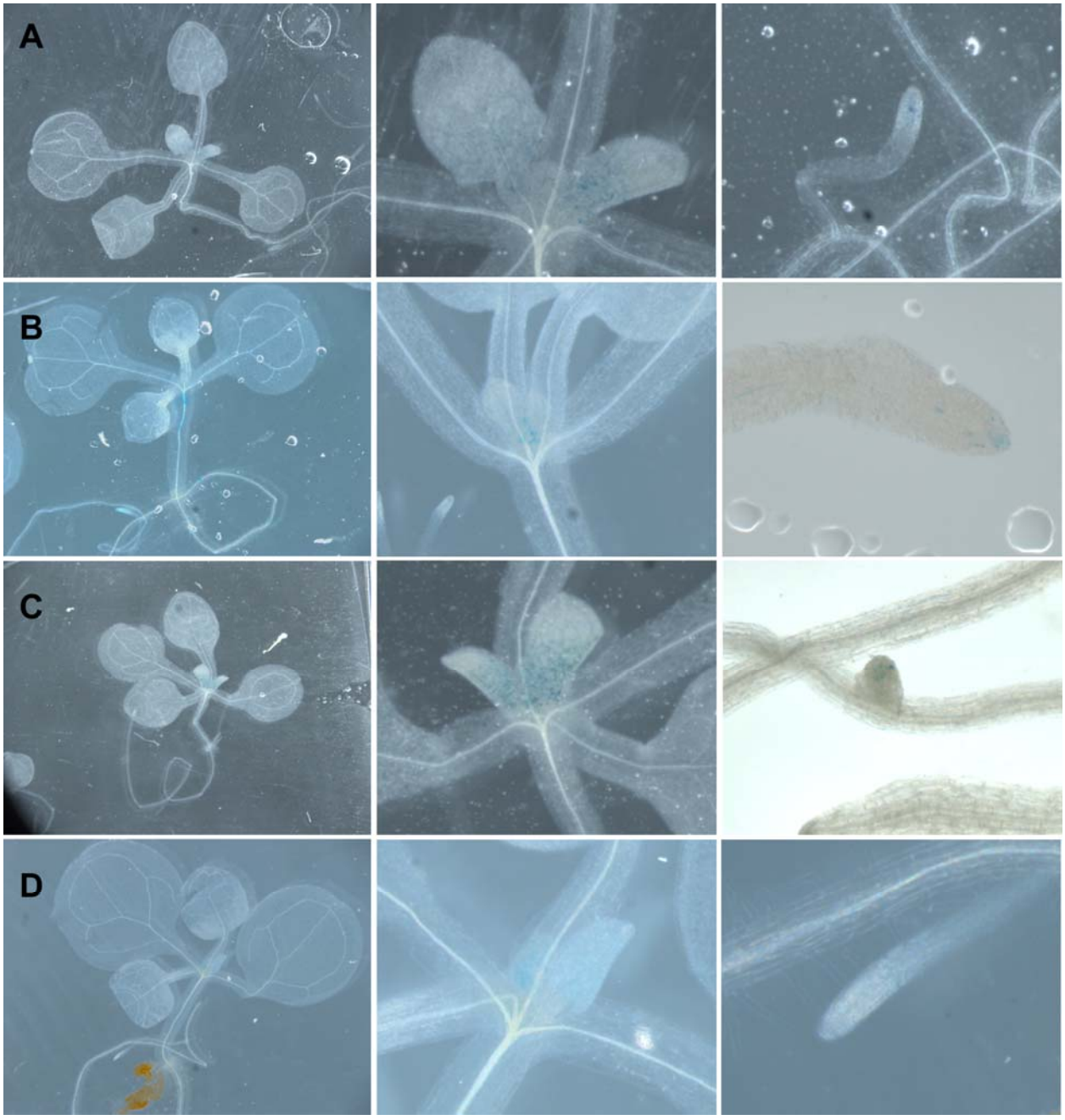

Figure 2.34: Expression pattern of B2-type CYCLIN:GUS constructs in seedlings visualized with GUS histochemical assay. Entire seedling, close-up of leaves and root tips. Blue staining indicates activity of the GUS reporter. **(A)** CYCLIN B2;1:GUS, **(B)** CYCLIN B2;2:GUS, **(C)** CYCLIN B2;3:GUS, **(D)** CYCLIN B2;4:GUS. As the blue GUS staining is in form of single spots, it was necessary to enhance contrast in some pictures in order to make it better visible.

Figure 2.35: Three cyclins with no detectable expression in seedlings by GUS histochemical assay. **(A)** CYCLIN B1;5:GUS, **(B)** CYCLIN B2;5:GUS, **(C)** CYCLIN B3;1:GUS.

Cyclin:	Root tips	Shoot apical meristem	Young leaves
CYCLIN B1;1	+++	+++	+++
CYCLIN B1;2	+++	+++	+++
CYCLIN B1;3	+++	+++	+++
CYCLIN B1;4	+++	+++	++
CYCLIN B1;5	-	-	-
CYCLIN B2;1	+	++	++
CYCLIN B2;2	++	++	++
CYCLIN B2;3	+++	+++	++
CYCLIN B2;4	-	+	+
CYCLIN B2;5	-	-	-
CYCLIN B3;1	-	-	-

Table 2.17: Summarized expression of CYCLIN B:GUS constructs in seedlings

Expression in inflorescences

Staining of inflorescences showed more variation between cyclins. In general, cyclins from the first group, and *CYCLIN B2;1*, *CYCLIN B2;2* and *CYCLIN B2;4* showed similar staining in stems of inflorescences and very young buds (stage 1-5) but the staining of anthers and pistils in older buds differed. Flower stages in following text are estimated based on (Smyth et al. 1990) and (Armstrong and Jones 2003).

CYCLIN B1;1 yielded prominent staining in young buds, pistils in all buds (figure 2.36 A) and

also in anthers of flowers in stage 12-13 (figure 2.36 A). *CYCLIN B1;2* was detected in young buds, anthers in flower stage 11-12 and pistils in open flowers – stage 13-14 (figure 2.36 B). *CYCLIN B1;3* showed the strongest expression in stems of inflorescences. It was detected also in young buds, anthers in flower stage 11-12 and pistils in most flower stages (figure 2.36 C). *CYCLIN B1;4* was widely expressed in young buds, stems of inflorescences and pistils, and also yielded very strong staining in anthers of flower stage 12-13 (figure 2.36 D). The last cyclin from the group of highly expressed cyclins, *CYCLIN B2;3,* was broadly expressed in inflorescences (figure 2.37 C).

All cyclins with lower expression were also detected in inflorescences. In order to increase the visibility of staining, we used a magenta- coloured X-GLUC substrate in some cases (figure 2.37 A). *CYCLIN B2;1* yielded expression in young buds (stage 1-5) and pistils up to stage 12 (figure 2.37 A). Expression of *CYCLIN B2;2* was detected in stems of inflorescences, prominent staining was also observed in buds up to stage 7-8, whereas in later stages it was seen mainly in pistils (figure 2.37 B). *CYCLIN B2;4* was expressed weakly in anthers of buds from stage 9 on and in and pistils in flower stage 15-16 (figure 2.37 D).

CYCLIN B1;5 and *CYCLIN B2;5* showed similar pattern of expression. We observed only relatively weak staining in anthers in few buds (figure 3.36 E and figure 3.37 E) starting from stage 8-9 approximately and weaker staining in older buds. *CYCLIN B3;1* also yielded a specific staining in buds at the stage 9, but than staining disappeared and was detectable in older anthers stage 13 (figure 2.37 F). As male meiosis in *Arabidopsis* is generally considered to take place in anthers of flowers at the stage 9 that range in size from 0,25 mm – 0,5 mm, these cyclins were considered to be promising candidates for meiotic expression. Expression of all constructs in inflorescences is summarized in table 2.18.

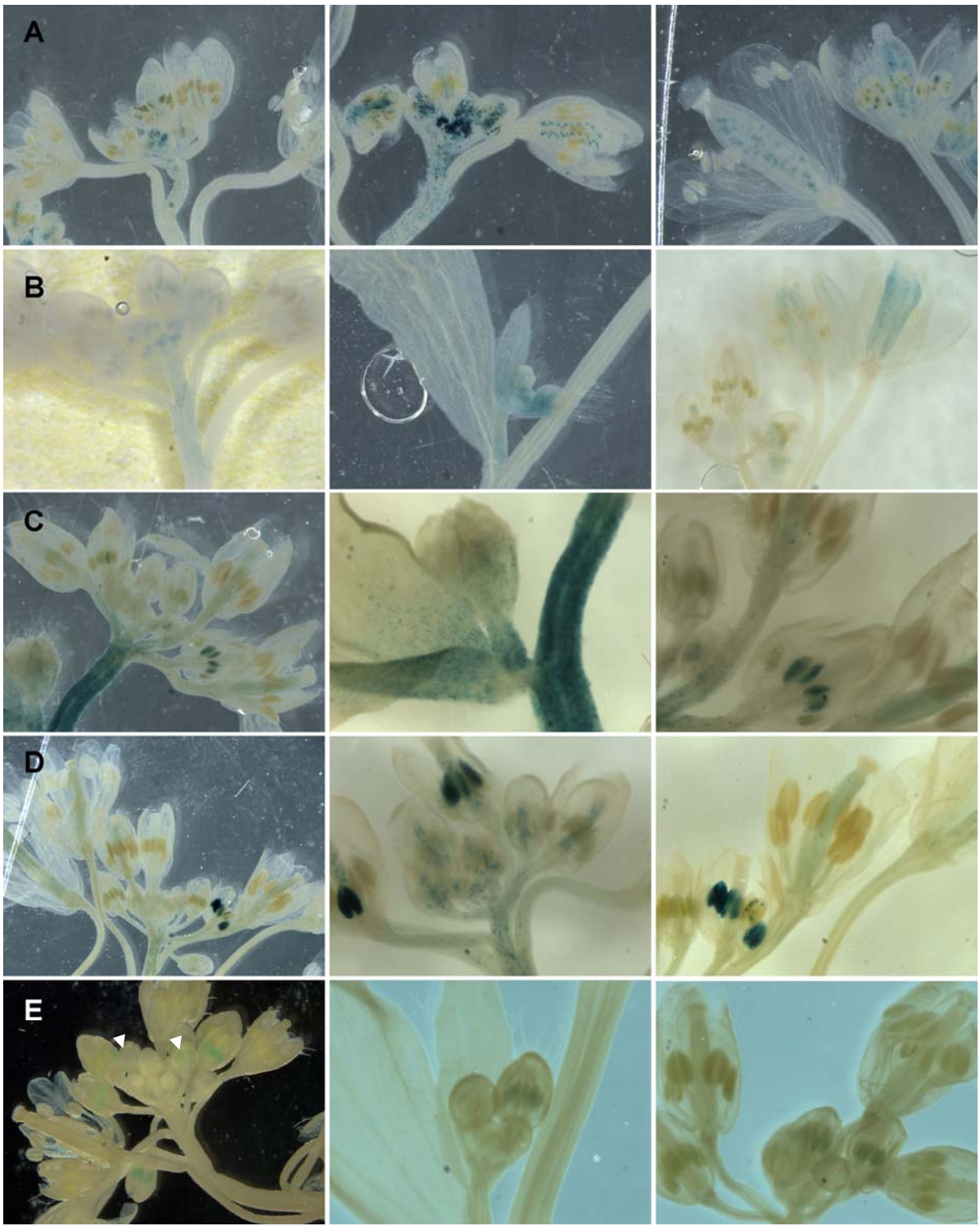

Figure 2.36: Expression pattern of B1 type cyclins in inflorescences visualized with GUS histochemical assay of CYCLIN:GUS constructs. Blue staining indicates activity of the GUS reporter. **(A)** CYCLIN B1;1:GUS, **(B)** CYCLIN B1;2:GUS, **(C)** CYCLIN B1;3:GUS, **(D)** CYCLIN B1;4:GUS and **(E)** CYCLIN B1;5:GUS. Stained buds with size corresponding to male meiosis are marked by arrowheads

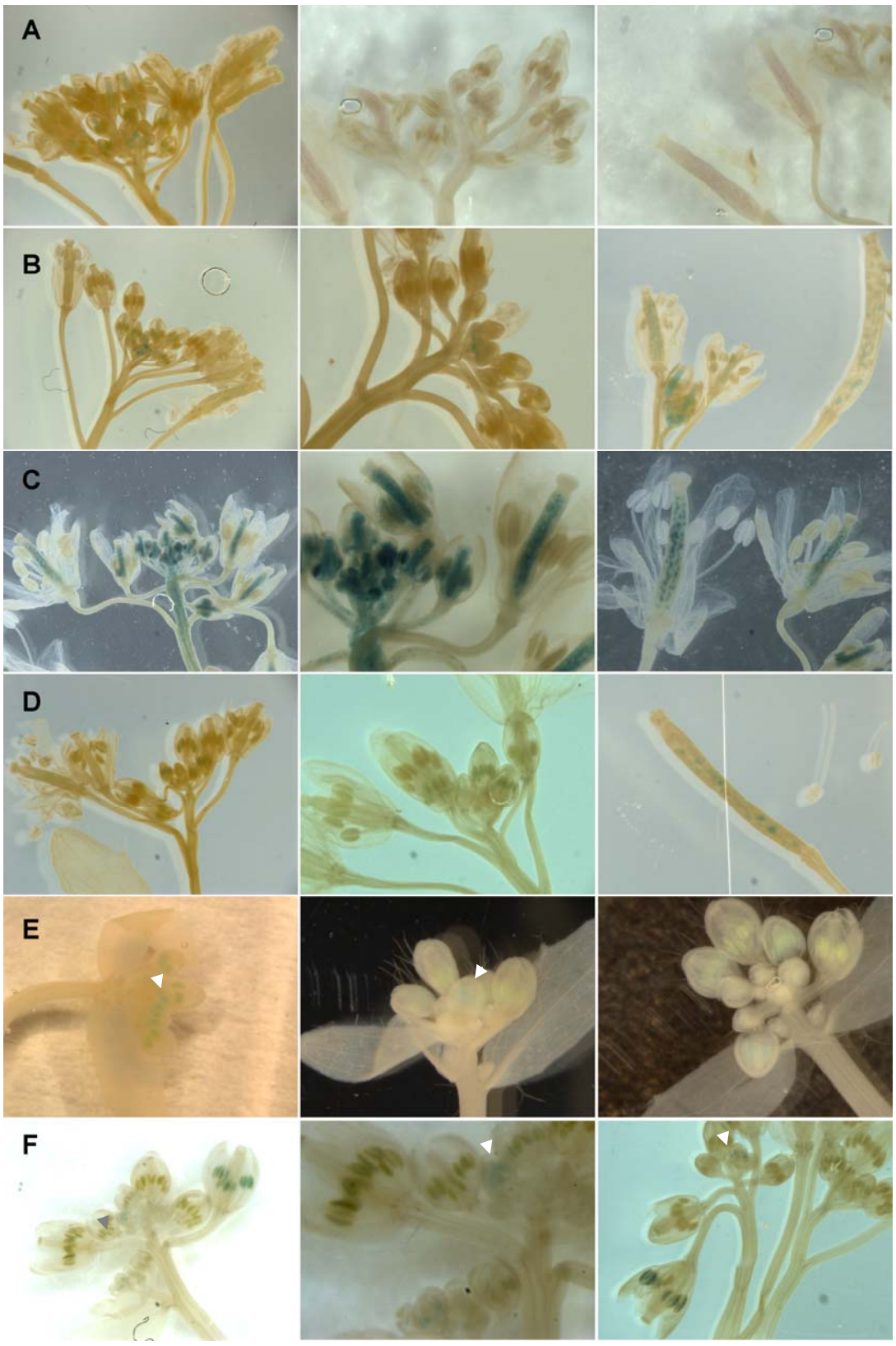

Figure 2.37: Expression pattern of B2 and B3 type cyclins in inflorescences visualized with GUS histochemical assay of CYCLIN:GUS constructs. Blue or magenta staining indicates activity of the GUS reporter. **(A)** CYCLIN B2;1:GUS, please note that first picture is stained with blue dye, the other with magenta dye **(B)** CYCLIN B2;2:GUS, **(C)** CYCLIN B2;3:GUS, **(D)** CYCLIN B2;4:GUS, **(E)** CYCLIN B2;5:GUS and **(F)** CYCLIN B3;1:GUS. As the blue GUS staining is in form of single spots, it was necessary to enhance contrast in some pictures in order to make it better visible. Stained buds with size corresponding to male meiosis are marked by arrowheads.

cyclin	stems	Stage 1-7 buds	Stage 8-9 buds	Stage 10-13 pistils	Stage 10-13 anthers
CYCLIN B1;1	+++	+++	+	+++	++
CYCLIN B1;2	+++	+++	+	+++	++
CYCLIN B1;3	+++	+++	+	++	+++
CYCLIN B1;4	++	+++	+	++	+++
CYCLIN B1;5	-	-	+	-	+
CYCLIN B2;1	++	+++	+	+	+++
CYCLIN B2;2	+	++	+	++	+
CYCLIN B2;3	+++	+++	+	+++	+
CYCLIN B2;4	-	-	-	++	++
CYCLIN B2;5	-	-	++	-	+
CYCLIN B3;1	-	-	+++	+	++

Table 2.18: Summarized expression of CYCLIN B:GUS constructs in inflorescences.

2.7.3. Subcellular localization B-type cyclins by immunocytology

2.7.3.1.Expression in mitotic cells

Immunodetection of CYCLIN B1;1:GUS in somatic cells from floral buds yielded a signal in cells undergoing mitosis (figure 2.38 A). We observed signal also in some interphase cells that most likely represented G2 phase. Signal in these cells was exclusively cytoplasmic and was excluded from nuclei. As chromosomes started to condense during prophase signal partially moved onto chromatin. The cyclin was enriched on chromatin during metaphase, but then disappeared during anaphase. No signal was detected in telophase cells.

CYCLIN B1;2 showed similar pattern as the *CYCLIN B1;1*. We observed cytoplasmic staining in interphase cells, relocalization to chromatin in prophase and very evident colocalization with chromatin in metaphase (figure 2.38 B). The signal disappeared during anaphase and was not detected during telophase. Immunodetection of CYCLIN B1;3:GUS also yielded cytoplasmic staining in interphase cells and the signal spread throughout the cell in prophase (figure 2.38 C). While major fraction of a signal was on chromatin during metaphase, there was still clearly

detectable signal in the cytoplasm. The signal disappeared during anaphase progression. CYCLIN B1;4 showed a strikingly different localization pattern compared to previously described cyclins. Signal from the CYCLIN B1;4 also appeared in cytoplasm of interphase cells, but remained exclusively cytoplasmic for the rest of mitosis (figure 2.38 C). This was particularly apparent during metaphase where no signal was detected on chromosomes. Again the signal cleared away during anaphase progression. CYCLIN B2;1, CYCLIN B2;2, CYCLIN B2;3 and CYCLIN B2;4 showed intracellular localization similar to CYCLIN B1;4 (figure 2.38 E and figure 2.39). Signal remained cytoplasmic from interphase to metaphase stage and vanished during anaphase. In summary all these cyclins showed similar pattern of expression in highly proliferating tissues, identical timing of expression from G2 to metaphase and disappearance during anaphase, but striking differences in intracellular localization during metaphase. Whereas CYCLIN B1;1 and CYCLIN B1;2 were enriched on chromatin, CYCLIN B1;3 showed also some localization in cytoplasm. In contrast CYCLIN B1;4 and all B2 cyclins were restricted to the cytoplasm only. Disappearance of the signal in anaphase reflects likely degradation of B-type cyclins by anaphase promoting complex. We could not detect any of these cyclins in meiotic cells.

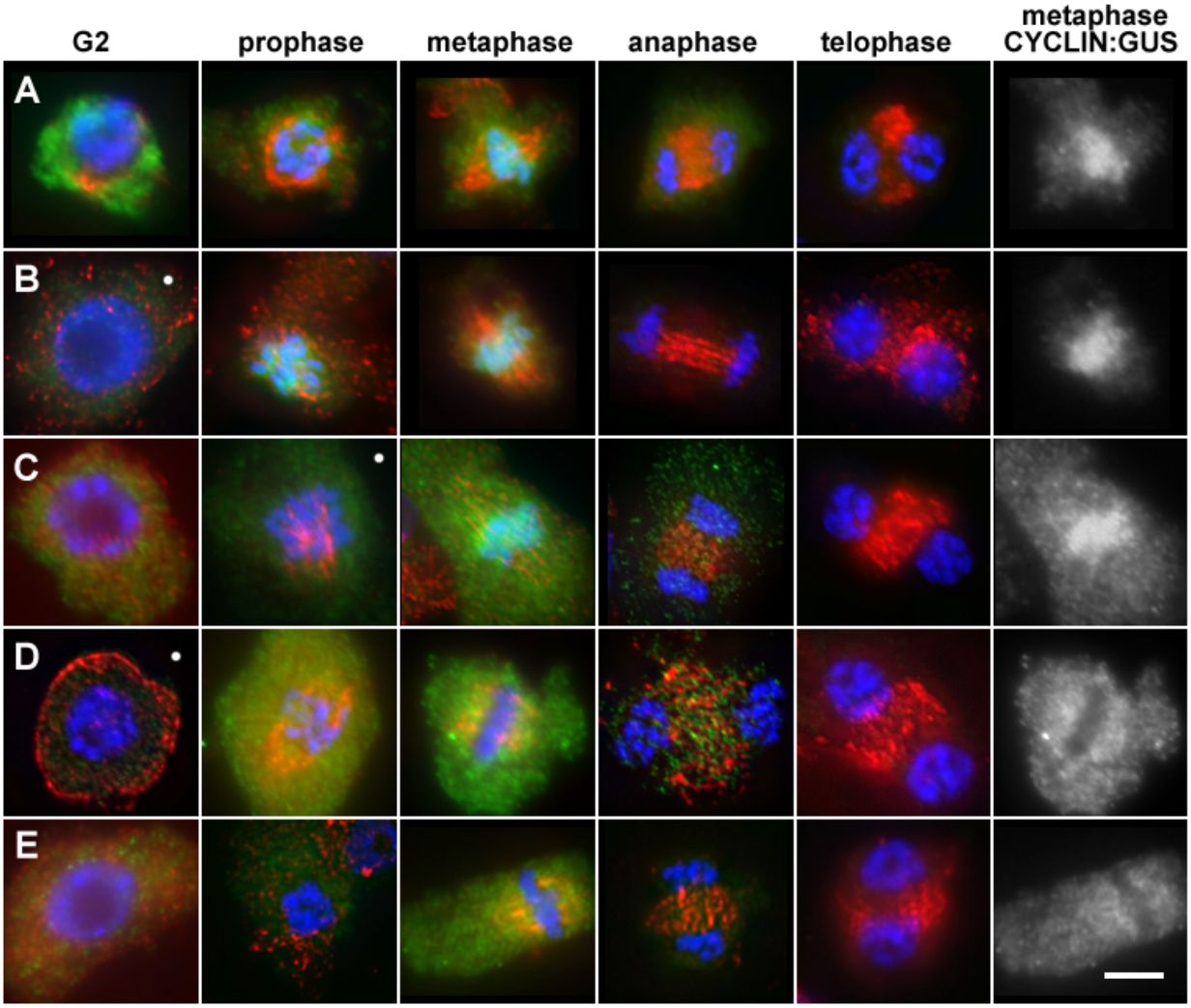

Figure 2.38: Immunodetection of highly expressed cyclins in squashes of anthers. CYCLIN:GUS was detected with antibodies against GUS (green), spindle is shown in red, DNA counterstained with DAPI in blue. **(A)** CYCLIN B1;1:GUS, **(B)** CYCLIN B1;2:GUS, **(C)** CYCLIN B1;3:GUS, **(D)** CYCLIN B1;4:GUS, **(E)** CYCLIN B2;3: GUS. Scale bar represents 5µm.

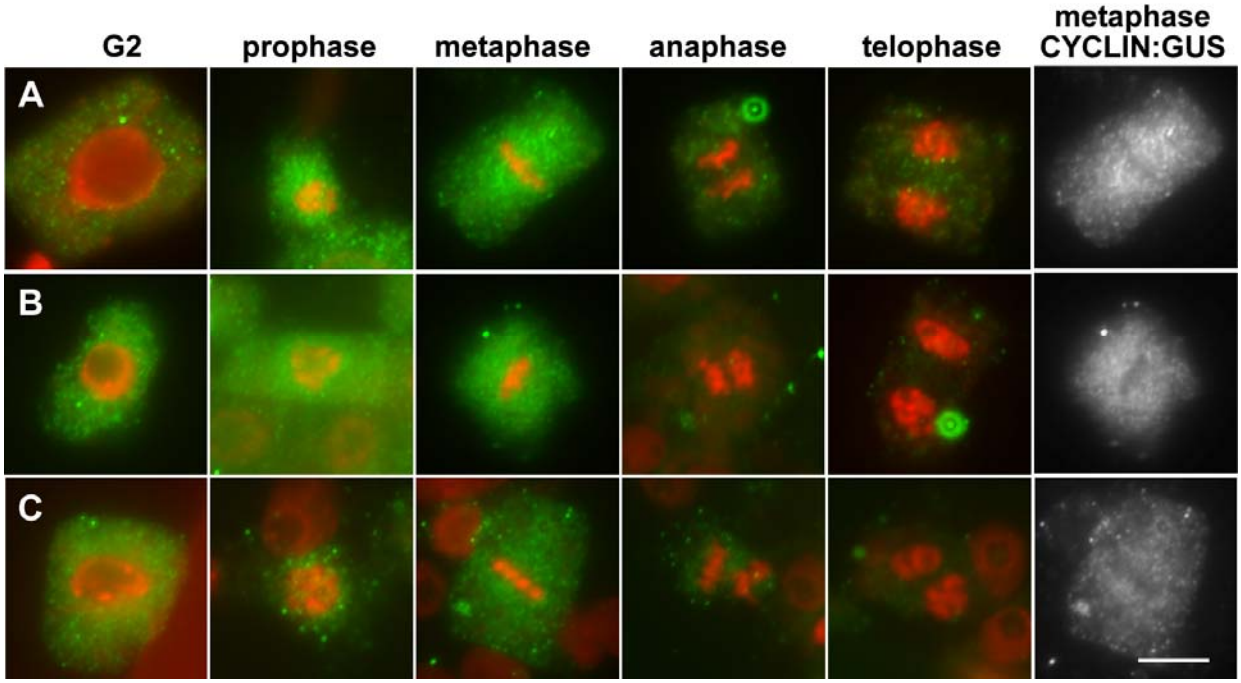

Figure 2.39: Immunodetection of cyclins with lower expression in squashes of root tips, shoot apical meristem or young buds. CYCLIN:GUS was detected with antibodies against GUS (green), DNA counterstained with DAPI in red **(A)** CYCLIN B2;1:GUS, **(B)** CYCLIN B2;2:GUS, **(C)** CYCLIN B2;4:GUS. Scale bar represents 10 µm.

2.7.3.2.Expression in meiotic cells

In contrast to above described cyclins, *CYCLIN B1;5, CYCLIN B2;5* and *CYCLIN B3;1* did not show any detectable staining mitosis. However expression of all these CYCLIN:GUS constructs was detected in meiosis. Staining was detectable from the beginning of prophase I and lasted throughout both meiotic divisions until tetrade stage (figure 2.40; figure 2.41; figure 2.42). The stability of CYCLIN:GUS constructs was unexpected because all mitotic cyclins were degraded during progression trough anaphase. Stability of CYCLIN B2;5 and CYCLIN B3;1 could be explained by the absence of predicted destruction box. However, predicted coding sequence of CYCLIN B1;5 included D-box. To understand whether these cyclins contribute to regulation of meiotic cell cycle we continued with their further characterization.

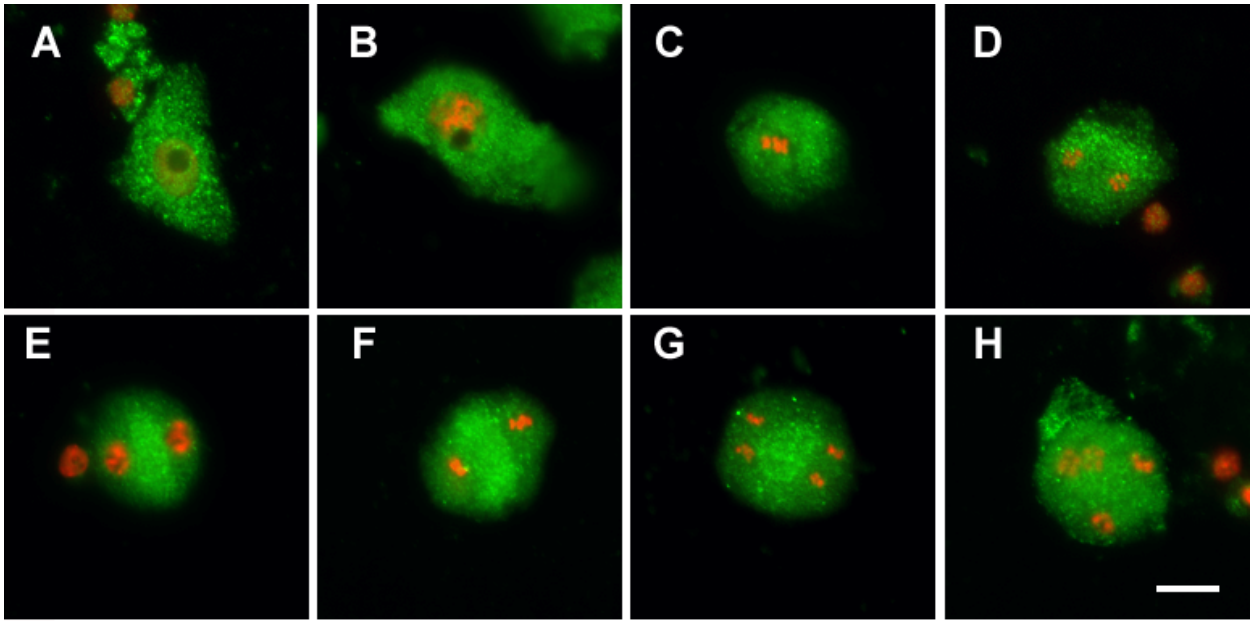

Figure 2.40: Immunolocalization of CYCLIN B1;5:GUS during progression of meiosis. CYCLIN B1;5:GUS was detected with antibodies against GUS (green), spindle is shown in red, DNA counterstained with DAPI in red. **(A)** zygotene, **(B)** pachytene, **(C)** metaphase I, **(D)** anaphase I, **(E)** interkinesis, **(F)** metaphase II, **(G)** anaphase II, **(H)** telophase II. Scale bar represents 10 µm.

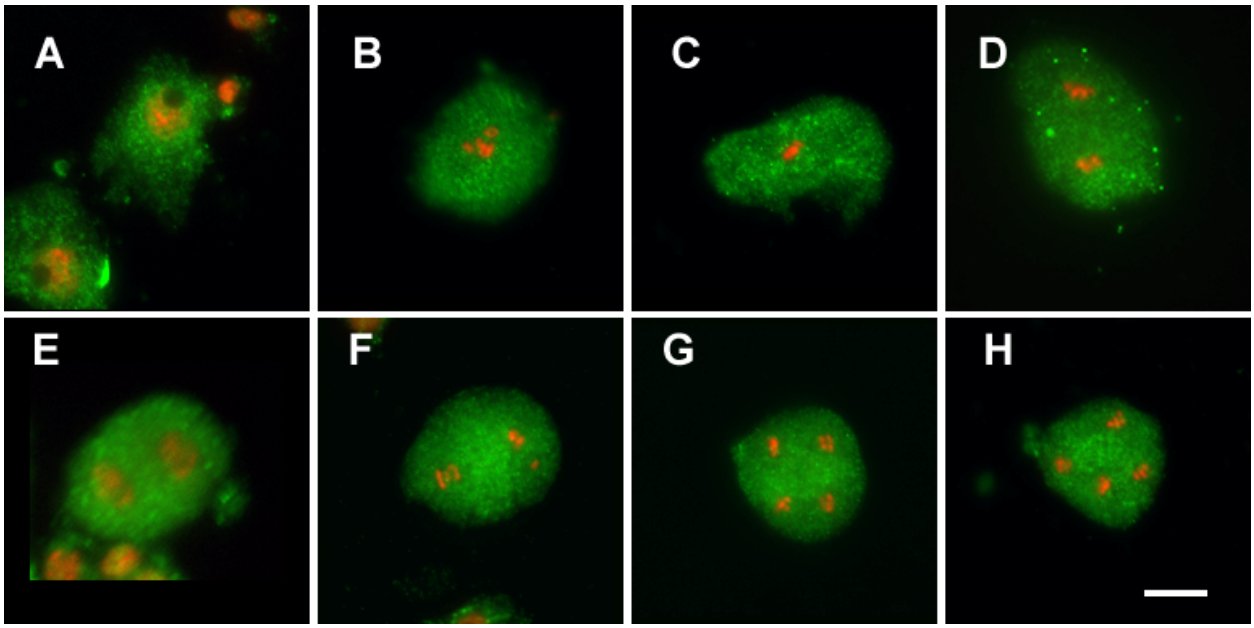

Figure 2.41: Immunolocalization of CYCLIN B2;5:GUS during progression of meiosis. CYCLIN B2;5:GUS was detected with antibodies against GUS (green), spindle is shown in red, DNA counterstained with DAPI in red. **(A)** pachytene, **(B)** diakinesis **(C)** metaphase I, **(D)** anaphase I, **(E)** interkinesis, **(F)** metaphase II, **(G)** anaphase II, **(H)** telophase II. Scale bar represents 10 µm.

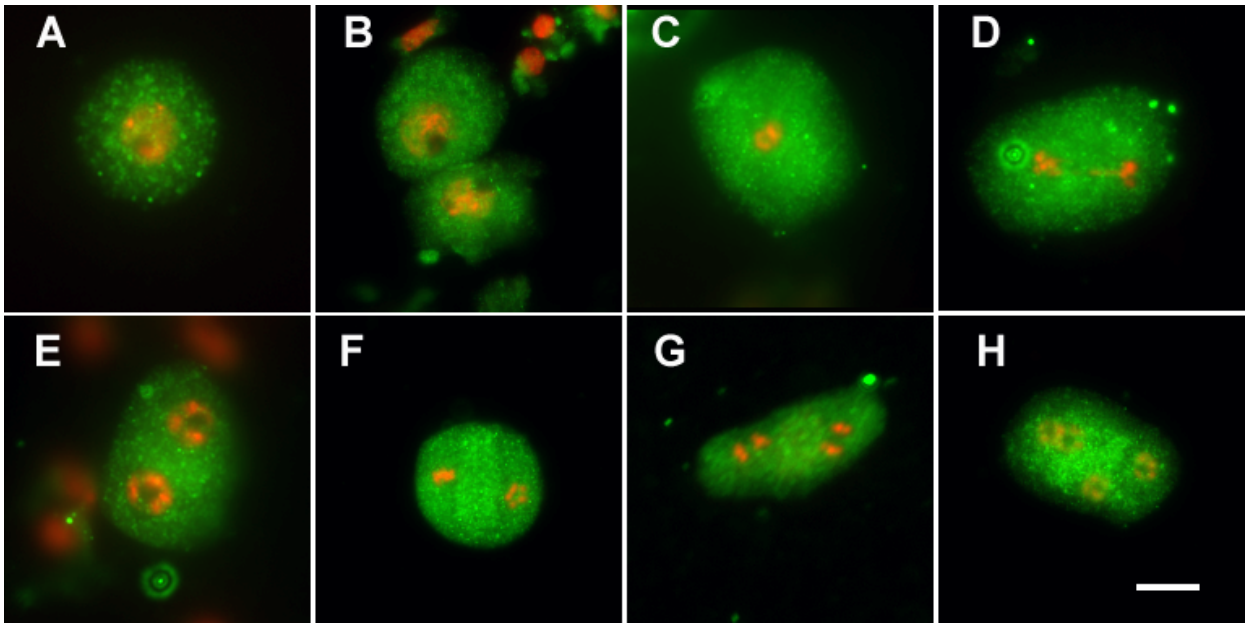

Figure 2.42: Immunolocalization of CYCLIN B3;1:GUS during progression of meiosis. CYCLINB3;1:GUS was detected with antibodies against GUS (green), spindle is shown in red, DNA counterstained with DAPI in red. **(A)** zygotene, **(B)** pachytene, **(C)** metaphase I, **(D)** anaphase I, **(E)** interkinesis, **(F)** metaphase II, **(G)** anaphase II, **(H)** tetrade. Scale bar represents 10 µm.

2.7.4. Characterization of cyclins expressed in meiosis

We found eight B-type cyclins to be expressed in mitotic cells and three B-type cyclins to be expressed during meiosis. Comparison of predicted protein sequences for these two groups revealed striking differences (figure 2.43). All mitotic B-type cyclins examined contained in their protein sequence three characteristic features – cyclin destruction box required for cyclin degradation during anaphase in the amino terminal part, cyclin amino terminal domain which is required for binding to a cyclin dependent kinase and cyclin carboxy terminal domain with not clear function. The predicted coding sequences for each cyclin with meiotic expression lacked at least one of these features. *CYCLIN B1;5* was predicted to contain destruction box and the cyclin amino terminal domain but lacked carboxy terminal domain. *CYCLIN B2;5* and *CYCLIN B3;1* lacked destruction box and *CYCLIN B2;5* has truncated cyclin amino terminal domain. To confirm these anotations we decided to analyze predicted cyclin cDNAs with reverse-transcription PCR.

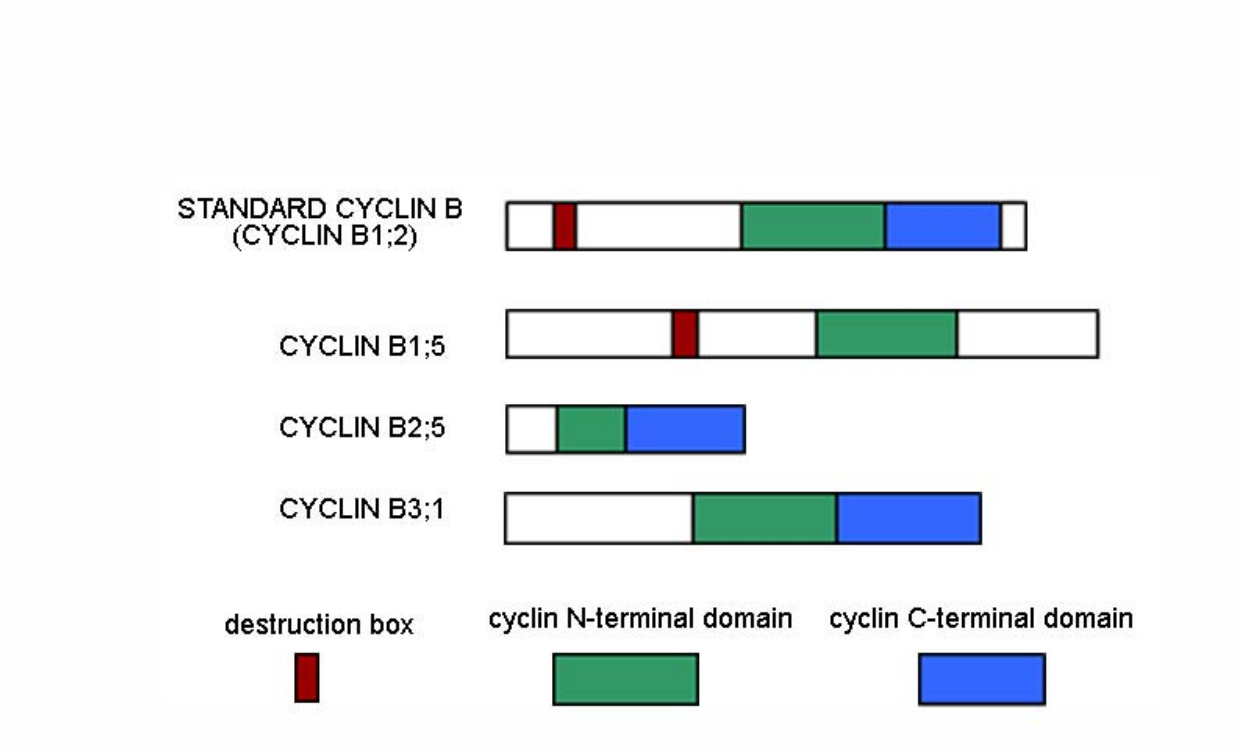

Figure 2.43: Graphical representation protein domain structure of standard Arabidopsis thaliana B-type cyclin (here example of CYCLIN B1;2) and predicted domain structures of three cyclins with meiotic expression: CYCLIN B1;5; CYCLIN B2;5and CYCLIN B3;1. Note absence of cyclin N-terminal domain in CYCLIN B1;5 predicted structure; absence of destruction box in CYCLIN B2;5 and CYCLIN B3;1 and shortened cyclin N-terminal domain in CYCLIN B2;5 predicted structure.

Based on histochemical GUS staining, these cyclins were specifically expressed in young buds. Therefore we used inflorescences as a source of RNA and for reverse transcription we used either oligo dT or a gene-specific primer. For each cyclin we used several primer combinations.

Despite our intensive effort we never succeeded to amplify full-length *CYCLIN B1;5* as predicted in the genome annotation (figure 2.44). Therefore we split the gene into three parts: first from exon one to exon five; second from exon six to intron eight/exon nine and third from exon nine to exon ten containing stop codon. Under these conditions we managed to amplify various cDNAs covering the whole predicted gene, but we did not obtained a cDNA that could possible encode the predicted protein. All amplified products were spliced, but the splicing sites did not correspond to the prediction. In the first part of cDNA, exons two and four were skipped and the fragment consisted of exons one, three and five and contained stop codons in all reading frames. In the second part of the gene, no predicted exon was skipped, instead intron six was retained. This part was amplified from the cDNA transcribed with oligo dT and we found a premature polyadenylation site in intron eight. The last part consisting of exon nine, intron nine and exon ten was extensively spliced and we found seven alternatively spliced variants. None of

these splice variants could produce a functional protein as the alternative splicing generated premature stop codons in all three possible reading frames.

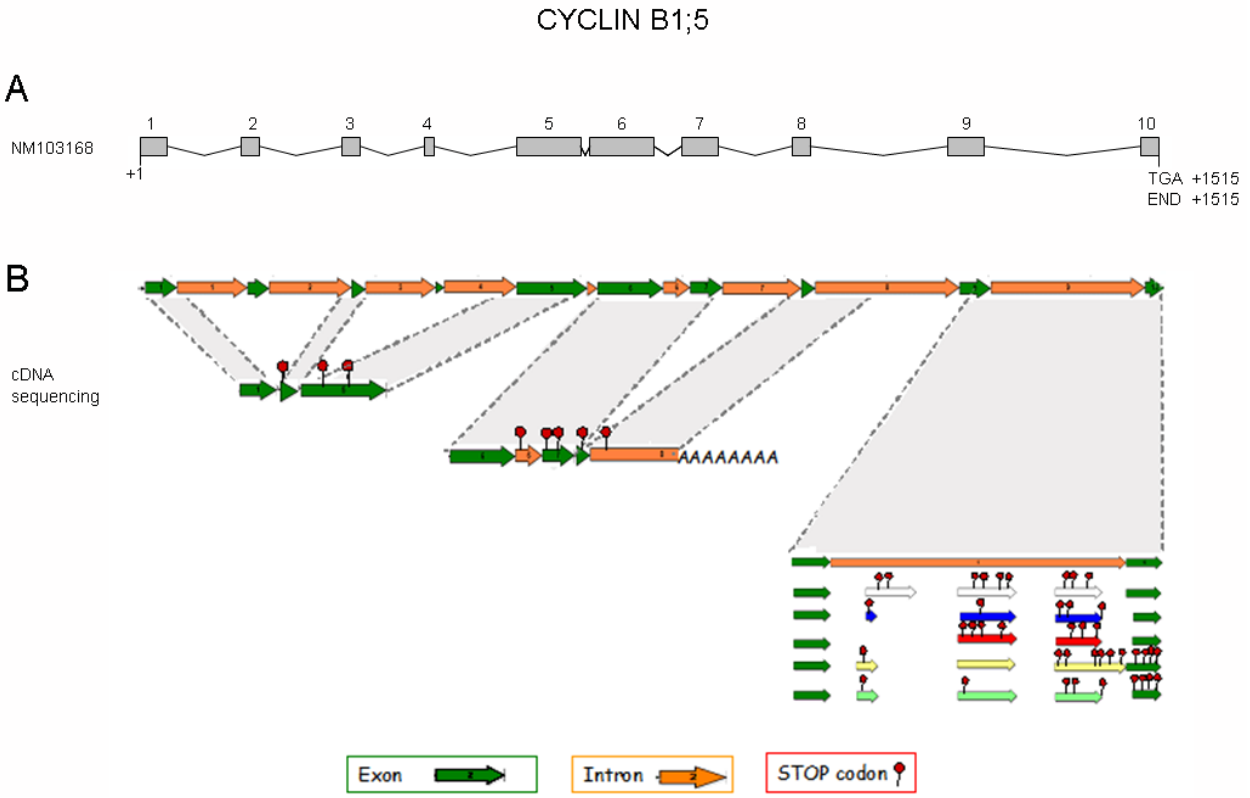

Figure 2.44.: Structure of *CYCLIN B1;5* mRNA **(A)** prediction in a database **(B)** inferred from cDNA sequencing. **(A)** The position of the transcriptional start point, the stop codon and the end of the 3´ UTR are numbered relative to the start codon. Exons are represented by gray boxes, 3´ UTR is represented by empty boxes. The number of the exon is indicated on top. **(B)** Graphical representation of sequenced *CYCLIN B1;5* cDNA clones. Upper lane represents genomic DNA, each bottom lane represents a sequenced cDNA clone. Exons are depicted as green arrows, introns are depicted as orange arrows and in-frame stop codons are represented by red circles

We obtained similar result also for the *CYCLIN B2;5*. We never managed to amplify the full length transcript according to the prediction (figure 2.45). We detected two distinct transcripts from the locus, both starting in exon #2 and retaining the intron #2. First transcript contained also correctly spliced exons # 3, 4, and 5, and could potentially encode a short protein with cyclin carboxy terminal domain. As this domain does not have a clear function we can not predict the role of such peptide. The second transcript contained only exons 3 and 5 and contained premature stop codons.

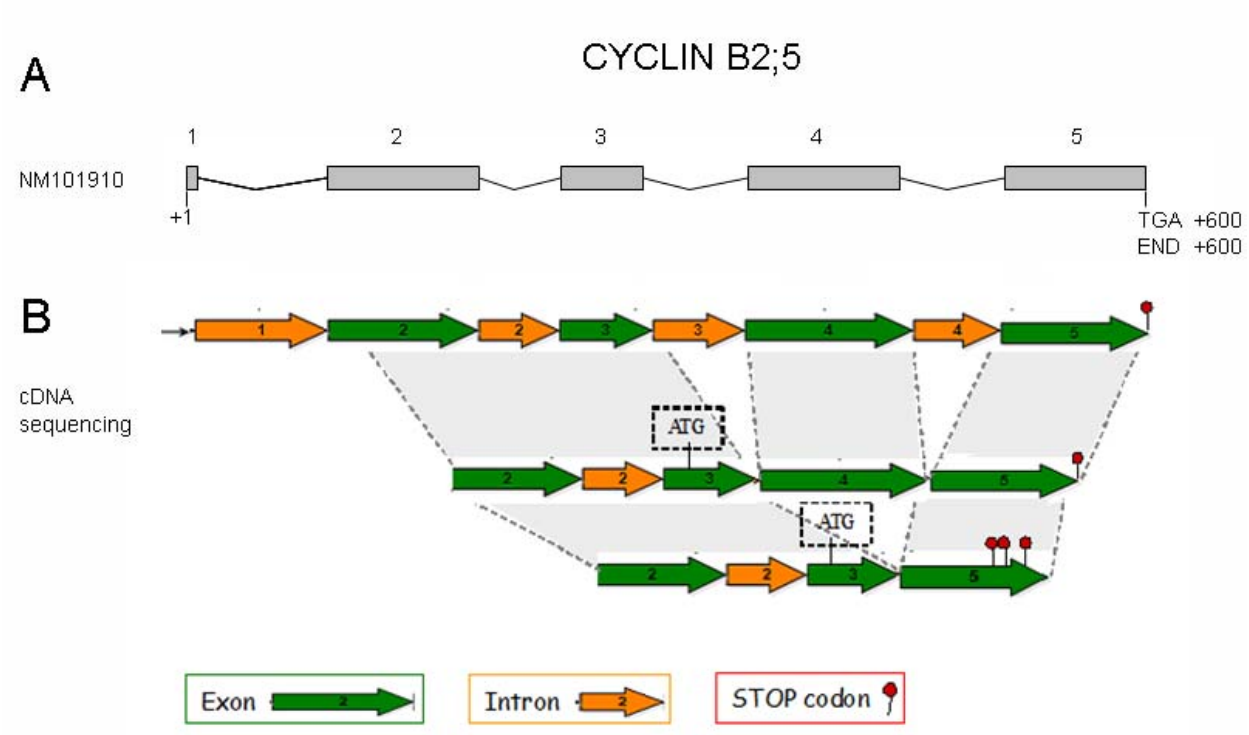

Figure 2.45: Structure of *CYCLIN B2;5* mRNA **(A)** prediction in a database **(B)** inferred from cDNA sequencing. **(A)** The position of the transcriptional start point, the stop codon and the end of the 3´ UTR are numbered relative to the start codon. Exons are represented by gray boxes, 3´ UTR is represented by empty boxes. The number of the exon is indicated on top. **(B)** Graphical representation of sequenced *CYCLIN B1;5* cDNA clones. Upper lane represents genomic DNA, each bottom lane represents a sequenced cDNA clone. Exons are depicted as green arrows, introns are depicted as orange arrows and in-frame stop codons are represented by red circles

The *CYCLIN B1;5* gene was very similar to mitotic *CYCLIN B1;2* as the parts coding for cyclin amino terminal domain were almost identical. The similarity was even more striking between *CYCLIN B2;5* and *CYCLIN B2;3*. These two cyclins were not only highly homologous in sequences of exons but also in introns and the whole structure of a gene. As the expected splice sites are identical in these cyclins, we also checked *CYCLIN B2;3* cDNA by RT-PCR and sequencing. In this case we obtained a correctly spliced cDNA and with no difference from prediction. The same predicted splice sites were used in *CYCLIN B2;3* but skipped in *CYCLIN B2;5*. The *CYCLIN B2;3* and *CYCLIN B2;5* genes are located in close proximity to each other on chromosome 1 with only 2.6 kb apart. This indicates that *CYCLIN B2;5* is probably a recent duplication of *CYCLIN B2;3*. Therefore, we checked conservation of the *CYCLIN B2;5* in the genome of a close relative of *Arabidopsis thaliana* which is *Arabidopsis lyrata.* Although *A. lyrata* has eight chromosomes whereas *A. thaliana* only five, there is a high synteny between these two genomes. The *CYCLIN B2;3* is located on chromosome 1 in both species. The genes in

its proximity from one side (centromere proximal) were conserved, but on the other side (telomere proximal) the closest gene and *CYCLIN B2;5* were missing (figure 2.46). Comparison of these two regions showed that part of the *CYCLIN B2;3* gene and other unknown gene was recently duplicated in *A. thaliana*. Therefore *CYCLIN B2;5* is a likely a pseudogene derived from the *CYCLIN B2;3* gene.

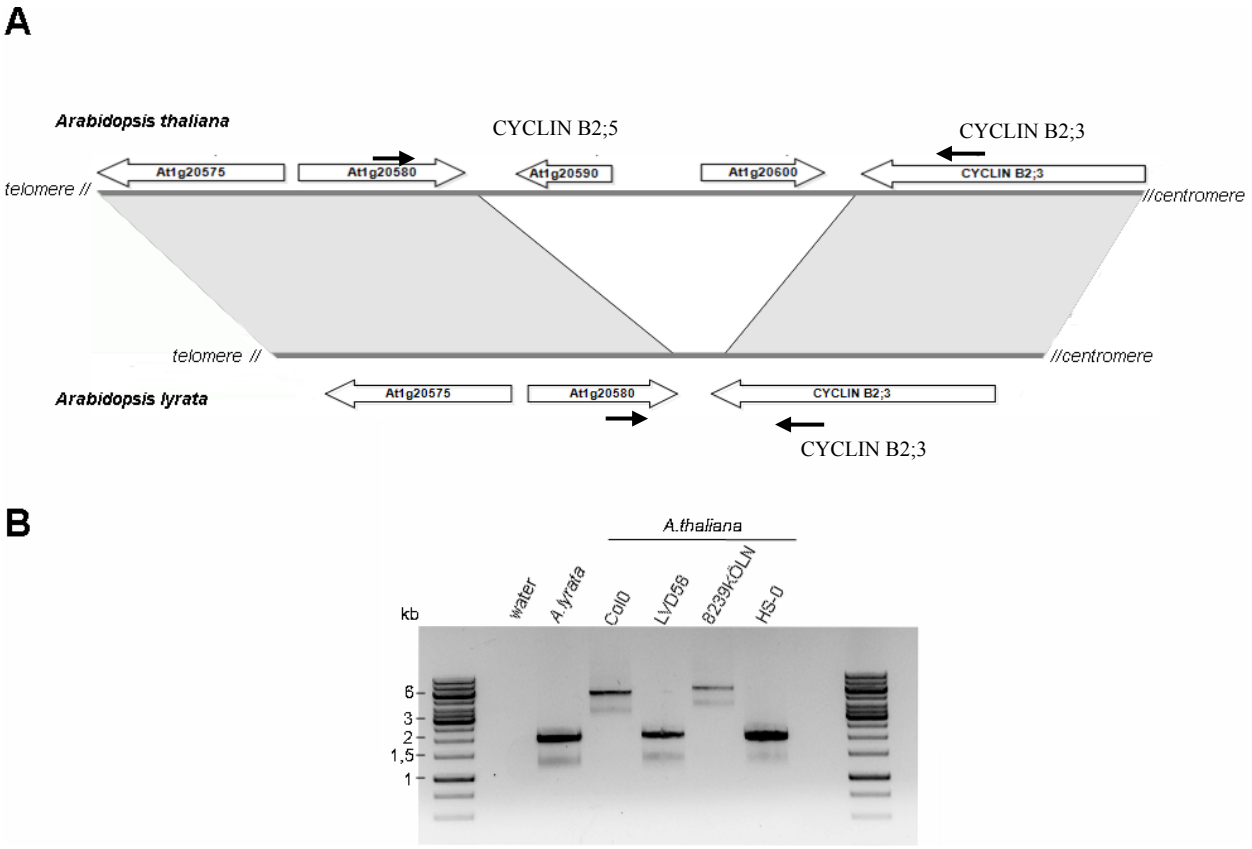

Figure 2.46: Genomic region containing *CYCLIN B2;5* and *CYCLIN B2;3* in *Arabidopsis thaliana* and *Arabidopsis lyrata*. **(A)** Scheme syntenic genomic regions containing *CYCLIN B2;5* and *CYCLIN B2;3* in *Arabidopsis thaliana* (upper) and *Arabidopsis lyrata* (bottom). Genes are represented by empty arrows, primers used for amplification are represented by black arrows and conserved regions are represented by gray-shading. **(B)** PCR amplification of region containing *CYCLIN B2;3* in *Arabidopsis lyrata* and several *Arabidopsis thaliana* ecotypes: Col0, LVD58, 8239KÖLN and HS-0.

In order to uncover whether there are some other duplications in cyclin B family, we searched for all B-type cyclin encoding genes in *A. lyrata* genome (table 2.19). Indeed we found that *CYCLIN B1;5* is also absent in *A. lyrata* genome. The synteny in the part of chromosome 1 around *CYCLIN B1;5* gene is not very well conserved, but we were not able to find this cyclin with several different BLAST (basic local alignment search tool) searches (Altschul et al. 1990)

elsewhere in *A. lyrata* genome. This suggest that *CYCLIN B1;5* also represents a recent duplication in *A. thaliana*. Interestingly we found 7 cyclin B-type genes in *A. lyrata* genome that are not present in *A. thaliana* (table 2.19) indicating rapid evolution of the cyclin B family.

Arabidopsis thaliana cyclin	Corresponding *Arabidopsis lyrata* cyclin –protein id	Related *Arabidopsis lyrata* pseudogene –predicted protein id
CYCLIN B1;1	Araly1:490869	
CYCLIN B1;2	Araly1:487418	Araly1:892412
CYCLIN B1;3	Araly1:478491	
CYCLIN B1;4	Araly1:901475	Araly1:901476
CYCLIN B1;5	-	
CYCLIN B2;1	Araly1:900109	
CYCLIN B2;2	Araly1:491085	
CYCLIN B2;3	Araly1:472290	
CYCLIN B2;4	Araly1:877739	Araly1:868823; Araly1:875306; Araly1:876301; Araly1:883572; Araly1:883575
CYCLIN B2;5	-	
CYCLIN B3;1	Araly1:312610	

Table 2.19: B –type cyclin predicted genes and pseudogenes in *A. thaliana* and *A. lyrata*.

To gain more information on evolution of B-type cyclins in *Arabidopsis* we examined the presence of *CYCLIN B1;5* and *CYCLIN B2;5* pseudogenes in different *A. thaliana* ecotypes. Due to the self-pollination, widespread distribution in the Northern hemisphere and in diverse range of environmental conditions, there is a high level of natural variation between *A. thaliana* ecotypes. In this part of work, we had a kind help from Dr. Thomas Turner, who examined for us Affymetrix genotyping array containing 250,000 SNPs (Atwell et al. 2010; Kim et al. 2007) for polymorphism in *CYCLIN B2;3* and *CYCLIN B2;5* region. He found three candidate *A. thaliana* ecotypes - LVD58, 8239 KÖLN and HS-0 with polymorphism in this region. We used PCR amplification with primers designed in conserved borders of duplicated regions of *CYCLIN B2;3 - CYCLIN B2;5* locus. This way we could distinguish longer allele with duplication characteristic

for *A. thaliana* Col-0 ecotype and shorter *A. lyrata* allele (figure 2.46). In two tested ecotypes – LVD58 and HS-0 we amplified the shorter variant. As we can find *A. thaliana* ecotypes that do not contain this duplication of *CYCLIN B2;3* locus, we suppose that this duplication arose after the split between *A. thaliana* and *lyrata* species and even after the split of some ecotypes in *A. thaliana*. We amplified also *CYCLIN B1;5* region in these ecotypes and found no difference. Based on these result we suppose that cyclin genes in *Arabidopsis* undergo very dynamic changes and are prone to duplications. Similar conclusion was drown also for mammalian cyclins (Lock et al. 1992; Nieduszynski et al. 2002) where numerous pseudogenes were found in mouse and human genomes. We show here the first evidence for specific expression of pseudogenes in *Arabidopsis* meiosis.

Cyclin B3;1

In contrast to *CYCLIN B1;5* and *CYCLIN B2;5*, region containing *CYCLIN B3;1* gene was preserved in *A. lyrata* and surrounding region was syntenic with corresponding region in *A. thaliana* genome. Predicted CYCLIN B3;1 protein from *A. lyrata* showed 94% identity with CYCLIN B3;1 in *A. thaliana*. We further checked conservation of *CYCLIN B3;1* in other plants with the BLAST search. We could clearly identify *CYCLIN B3;1* homologues in dicotyledonous plants. All identified CYCLIN B3;1 homologous proteins in dicotyledonous plants also lacked the sequence corresponding to destruction box. In monocotyledon plants the recognition of particular cyclins was more difficult due to the high similarity in conserved cyclin domains and variability in the other parts.

We managed to amplify *CYCLIN B3;1* cDNA and the 3' untranslated region (UTR) with 3'RACE procedure (figure 2.47). Cloning and sequencing revealed that splicing site at the 5`end of exon two is six base pairs upstream and as a consequence there are two amino acids more in *CYCLIN B3;1* sequence. We also found splicing in 3'UTR with 98 bp intron. The spliced 3`UTR has 248 bp and the total length of unspliced genomic is 346 bp in total length, which suggests possible regulation at RNA level. Otherwise *CYCLIN B3;1* cDNA matched the prediction and we could not detect destruction box in its protein sequence.

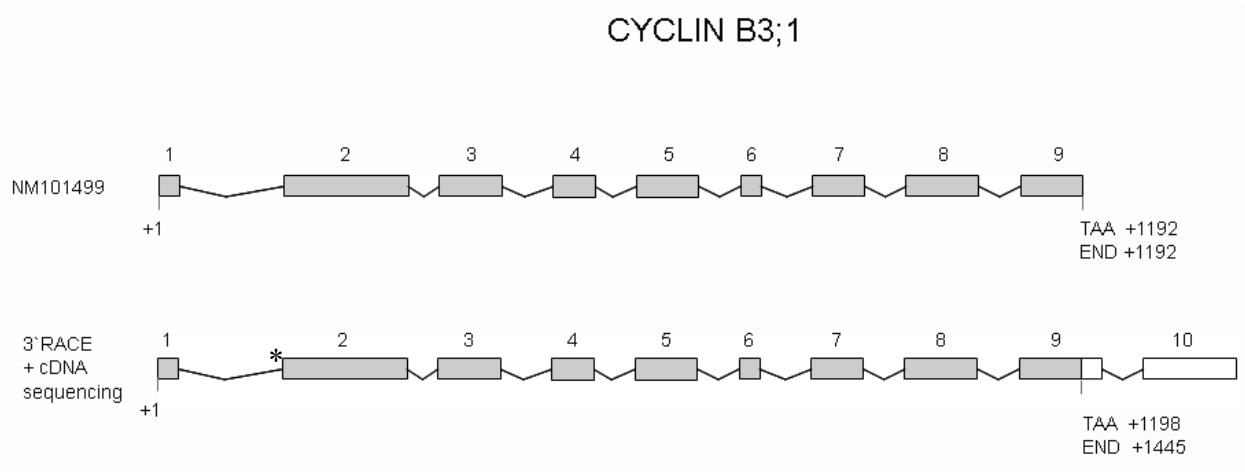

Figure 2.47: Structure of *CYCLIN B3;1* mRNA **(A)** prediction in a database **(B)** inferred from cDNA sequencing. The position of the transcriptional start point, the stop codon and the end of the 3´ UTR are numbered relative to the start codon. Exons are represented by gray boxes 3´ UTRs is represented by empty boxes. The number of the exon is indicated on top. The six nucleotide insertion (ATCCAG) at the position 64-69 is indicated by an asterisk.

In summary, we found one protein coding B-type cyclin gene, *CYCLIN B3;1* to be expressed during meiosis in *Arabidopsis* . The very striking feature is the lack of destruction box in which is required for cyclin degradation during progression of anaphase. Although we have to further investigate role of this cyclin in meiotic cell cycle, we hypothesize that there is a requirement for an alternative pathway to down-regulate cdk activity during anaphase that may involve SMG7 and TDM1 proteins.

3. DISCUSSION

3.1. *SMG7* is required for down-regulation of cdk activity during meiotic anaphase II

Regulation of meiotic cell cycle differs from mitosis in several aspects. Specialized mechanisms that ensure chromosome pairing followed by recombination, differential spindle attachment to chromosomes in the first and second divisions and mechanisms allowing execution of two nuclear divisions after only one round of DNA replication are examples of processes required for proper progression trough meiosis and subsequent formation of haploid gametes. Cell cycle regulation in meiosis is understood to much lesser extent than in mitosis. Available data indicate that each of studied model organisms employs a different strategy for regulation of cdk activity during meiosis. In plants, as in most others multicellular organism, entry into reproductive phase is part of developmental processes. Male and female gametes are in angiosperm plants formed by mitotic divisions that immediately follow after meiosis (McCormick 2004; Yadegari and Drews 2004). For proper progression trough these mitotic divisions, meiosis-specific machinery must be inactivated once meiosis is completed.

One gene possibly involved in this process in *Arabidopsis* is recently described *SMG7* gene which was shown to play role a critical role in progression trough meiotic exit, but not in mitosis (Riehs et al. 2008). Plants carrying a mutation in the *SMG7* gene are sterile due to unusual cell cycle arrest at anaphase II. There are only three known examples of anaphase arrest: 1) stabilization of cyclin B by removal of destruction box, 2) mutation of an APC subunit and 3) premature loss of sister chromatid cohesion due to shugoshin dysfunction (Holloway et al. 1993; Sigrist et al. 1995; Parry and O'Farrell 2001; Kitajima et al. 2004; Rabitsch et al. 2004; Salic et al. 2004; McGuinness et al. 2005; Swan et al. 2005; Swan and Schupbach 2005; Wolf et al. 2006). Here we present further insights into *SMG7* role in meiotic cell cycle. Possibility of premature loss of centromeric cohesion and chromosome biorientation were tested by (Riehs et al. 2008), and provided evidence that defect in *smg7* is caused neither by premature loss of sister chromatid cohesion nor by defective chromosome attachment to spindle and lack of tension. We extended this analysis to examine whether progression trough stages that precede anaphase II is not impaired due to spindle checkpoint dysfunction. Therefore we exposed *smg7* meiocytes to inhibitors of spindle polymerization to test the spindle checkpoint functionality. First we established conditions for effective spindle checkpoint induction in wild type plant meiosis by

scoring accumulation of cells in metaphase. Then we applied these experimental conditions to *smg7* mutant meiocytes. Similar to wild type, inhibitor treatment resulted in 10-fold accumulation of metaphases I compared to untreated control, suggesting that spindle checkpoint is fully functional during first division. The situation during the second meiotic division is more difficult to interpret because anaphase II in *smg7* mutants does not proceed to telophase stage but instead stay arrested. Indeed, data of Nina Riehs (Riehs et al. 2008) and this work showed that up to 75%-83% of untreated *smg7* meiocytes are in anaphase II arrest. So we assume that effect of spindle checkpoint induction is partially masked by presence of anaphase-II like stages and that the 2-fold increase in metaphase-anaphase ratio in treated samples compared to untreated ones, reflects accumulation of metaphases due to induction of spindle checkpoint.

Both other described examples of phenotypes similar to *smg7* are caused by problems to decrease cdk activity during meiosis, either by expressing cyclin A lacking destruction signal or by mutation of specific APC activator (Dr. Katja Wassmann, personal communication, Page and OrrWeaver 1996; Chu et al. 2001; Swan and Schupbach 2007). To test, whether artificial inhibition of cdk activity down-regulation will result in similar phenotype in wild type *Arabidopsis* meiocytes, we exposed them to proteasome inhibitor MG115 (Lee and Goldberg 1998; Planchais et al. 2000). Indeed we observed 18 meiocytes highly resembling *smg7* anaphase II arrest. It was already shown that a treatment of tobacco BY2 cultures with related compound, MG132, caused accumulation of metaphases and also presence of aberrant mitotic figures reminding anaphases with spread condensed chromatids (Genschik et al. 1998). As the two major targets of APC complex during metaphase are securin and cyclin B, accumulation of metaphases may be explained as a lack of destruction of securin that prevents entry to anaphase in cells that entered mitosis. In cells that are in anaphase during treatment, the stabilization of cyclin B is expected to keep elevated levels of cdk activity and thus prevents correct exit from mitosis.
Because spindle checkpoint appears to be functional during metaphase II and a phenotype similar to *smg7* anaphase II arrest can be induced in wild type by inhibiting proteasome, the plausible hypothesis is that *smg7* mutation interferes with cdk activity down-regulation at meiotic exit. Either the *smg7* mediated arrest may be caused by direct failure to down-regulate cdk activity which then permanently phosphorylates its target proteins or the cdk activity is already reduced but there is a defect in dephosphorylation of its target proteins. As it is impossible to biochemically test these predictions in *Arabidopsis* meiosis, we developed a new method to cytologically assess cdk activity.

A necessary condition for cdk activity is cdk-cyclin interaction that and phosphorylation of t-

loop (Gould and Nurse 1989; Jeffrey et al. 1995; Russo et al. 1996). Non-phosphorylated cdk-cyclin dimer is inactive because the catalytic site of cdk is hidden by t-loop. Upon phosphorylation mediated by cdk activating kinase, the dimer changes conformation and cdk-cyclin dimer becomes active (Gould and Nurse 1989; Jeffrey et al. 1995; Russo et al. 1996). This phosphorylation was first found by (Gould and Nurse 1989) in fission, and in the same study they also showed that it peaks in M phase but it disappears during anaphase. In following study (Gould et al. 1991) they showed that this phosphorylation is essential for cdk activity and seems to be conserved in all known cdks. Although later it was shown, that budding yeast cdk can remain permanently phosphorylated, even during anaphase (Lim et al. 1996), in vertebrates, fission yeast and plants the phosphorylation clearly disappears during anaphase (Gould and Nurse 1989; Lorca et al. 1992; Harashima et al. 2007, this work). One explanation for this difference is that budding yeast cdk can be phosphorylated in the absence of cyclin, whereas vertebrate cdk can only be phosphorylated after cyclin binding (Ducommun et al. 1991; Ross et al. 2000). In plants, biochemical analysis of synchronized plant cultures showed the activating t-loop phosphorylation gradually increases during progression trough the cell cycle, peaks in M phase but it disappears after the exit from mitosis (Harashima et al. 2007). This study further showed that cdk activity correlates with the t-loop phosphorylation. Therefore, we assume that in plants dephosphorylation of cdk during anaphase reflects its deactivation and therefore it can serve as a good marker for monitoring cdk activity in wild type and *smg7* meiocytes.

Arabidopsis genome encodes several cdk related genes including *CDKA;1* which is essential for mitosis (Dissmeyer et al., 2007). As no antibodies are available for phosphorylated *Arabidopsis* cdks, we took advantage of the high conservancy of cdk t-loop between species and tested antibody against human CDK2. Similar approach was taken by Harashima and collegues and Takatsuka and collegues (Harashima et al. 2007; Takatsuka et al. 2009), but they used antibody against human CDK1. Our reasoning for hsCDK2 was based on fact, that although t-loops of both human cdks differ from CDKA;1 t-loop, there are six substitutions in the case of hsCDK1 and some of them are in close proximity of threonine 161, whereas the hsCDK2 has only two substitutions and only one of them is in proximity of threonine 161. We confirmed that this antibody specifically recognizes phosphorylated form of CDKA;1. By using a CDKA;1:YFP fusion construct we established that CDKA;1 is also abundant in meiosis and likely represents the major meiotic cdk. Next we studied the distribution of phosphorylated CDKA;1 in meiosis by using immunostaining with an antibody that specifically recognizes the Thr161 phospho-epitope. We found that while CDKA;1 is constitutively expressed during meiosis, the Thr161-phosphorylation cycles, with the highest signal intensity in metaphase I and II. The

phosphorylation level decreases during subsequent anaphases and telophases. This oscillation of signal is in agreement with the biochemical measurement in *Xenopus* oocytes or synchronized meiotic cultures in yeast (Iwabuchi et al. 2000; Carlile and Amon 2008) and also provides the first evidence that cdk activity oscillates during the course of plant meiosis.

Interestingly we found enrichment of phosphorylated CDKA;1:YFP signal on organellar band in interkinesis, whereas the total CDKA;1 protein was rather enriched at chromatin in this meiotic stage. Similar pattern was observed in tapetum cells that undergo karyokinesis but not cytokinesis. It was shown that T161D substitution in the CDKA;1 t-loop causes strong meiotic defects including deregulated formation of cell wall formation in interkinesis (Dissmeyer et al. 2007). This suggests that cdk activity localized to organellar band may act to prevent cytokinesis in interkinesis. In contrast to wild type, Thr161 phosphorylation remains high in SMG7-deficient meiocytes that are arrested at the aberrant anaphase II. Therefore we conclude that *smg7* anaphase II arrest is caused by high levels of cdk activity and SMG7 protein is involved in downregulation of cdk activity at the end of meiosis.

3.2. TDM1 protein is required for anaphase arrest in *SMG7* mutant plants

The mechanism of *SMG7* contribution to control of cdk activity and whether it is a direct or indirect effect is not yet clear. One crucial problem is that the components and regulators of cdk activity are largely unknown in *Arabidopsis*. Besides *SMG7*, only few other genes were identified to be important for meiotic progression including *TDM1*, *TAM* and *OSD1* (Ross et al. 1997; Glover et al. 1998; Sanders et al. 1999; Magnard et al. 2001; Wang et al. 2004b; d'Erfurth et al. 2009; d'Erfurth et al. 2010). *TDM1* and *OSD1* are plant-specific genes with no clear homology to any other known cell cycle regulators. Pollen mother cells lacking TDM1 undergo the third round of chromosome segregation without an intervening S phase (Ross et al. 1997). Hence *TDM1* was particularly interesting for our analysis because similar to *SMG7*, it appears to be required for meiotic exit. To better characterize the role of *TDM1* in male meiosis, we analyzed a null allele of *TDM1* (*tdm1-4)* because the previously described *tdm1-1* allele has a semi-dominant phenotype (Chaudhury 1994; Ross et al. 1997; Glover et al. 1998). We found that entry into the third metaphase in *TDM1* deficient meiocytes is accompanied with formation of metaphase-like spindles around each group of re-condensed chromatids and with phosphorylation of histone H3 at serine 10 in centromeric regions. These observations argue that *tdm1* meiocytes indeed reinitiate another round of chromosome segregation which must be associated with re-activation of meiotic cdk-cyclin complexes. The histone H3 serine 10

phosphorylation is dispersed throughout whole chromosomes during the first meiotic division and restricted to centromeres during the second division (Kaszas and Cande 2000; Manzanero et al. 2000a). Because H3 serine 10 phosphorylation appears to be also restricted to centromeric region in the third meiotic division in *tdm1* mutants, we suppose that situation at the entry to third meiotic division shares some characteristics with interkinesis. *TDM1* is therefore a critical factor for distinguishing interkinesis and meiotic exit.

Only other gene with phenotype similar to *TDM1* so far been reported is *Drosophila Roughex*. Mutation in the *Roughex* gene results in the third meiotic division in male spermatocytes (Gonczy et al. 1994). Roughex is required also during mitotic divisions where it acts as inhibitor of M phase cdk- cyclin complexes during mitotic exit and in the following G1 phase (Thomas et al. 1994; Thomas et al. 1997; Foley et al. 1999; Avedisov et al. 2000, Foley and Sprenger 2001) Interestingly, Roughex does not have any known homologues outside the *Drosophila* genus, and it was shown to be one of the most quickly evolving genes between *Drosophila* species (Avedisov et al. 2001). Neither other known inhibitors required for M phase exit and G1 phase, namely Sic1p in *Saccharomyces cerevisiae* and Rum1p in *Schizosaccharomyces pombe*, show any homology at the protein level. Nevertheless, Sic1p and Rum1p proteins were shown to be functionally orthologous and they can substitute each other (Sanchez-Diaz et al. 1998). Similarly, Roughex function could be partially substituted by transient expression of Sic1p in *Drosophila* embryos (Sanchez-Diaz et al. 1998; Foley and Sprenger 2001). It is possible that *TDM1* might also belong to this group of cdk inhibitors that survey the down regulation of cdk activity at the end of M-phase.

To gain further insights to *TDM1* function, we localized this protein during male meiosis. Although *TDM1* acts at the meiotic exit, we found that it is expressed during whole meiosis. However, its localization pattern dramatically changes in the course of meiosis suggesting a possible regulatory function. Most of the TDM1 protein is localized to distinct foci until the onset of anaphase II, where the foci disappear and TDM1 is dispersed throughout the cytoplasm. The signal is clearly detectable in microspores further supporting the idea that TDM1 may also be important to establish G1 phase. Based on the *TDM1* phenotype, we suggest that the foci-located TDM1 presents an inactive form preventing TDM1 from acting prematurely, whereas the form spreading in the cytoplasm after the onset of anaphase may be an active version of TDM1. Similar localization based regulation of activity was described for Cdc14p phosphatase in budding yeast (Jaspersen et al. 1998; Visintin et al. 1998; Shou et al. 1999; Visintin et al. 1999; Stegmeier et al. 2002). This phosphatase is critical for mitotic and meiotic exit by

dephosphorylating cdk targets like APC activator Cdh1p, cdk inhibitor Sic1p and its transcription factor Swi5p (Shou et al. 1999; Visintin et al. 1999; Stegmeier et al. 2002; Marston et al. 2003). Cdc14p is bound by Cfi1/Net1 protein that keeps it sequestered to nucleolus until the onset of anaphase. After APC activation, the protein is released from nucleolus to cytoplasm and activated by FEAR and MEN networks where it contributes to further anaphase progression (reviewed in: Stegmeier and Amon 2004; Clifford et al. 2008b; Clifford et al. 2008a).

Localization of TDM1 supports the idea that both *SMG7* and *TDM1* play a role at the end of meiosis to downregulate cdk activity and thus, allowing the transition to G1 phase. To understand the relation between *SMG7* and *TDM1*, we examined *smg7 tdm1* double mutants. *SMG7* mutant phenotype is manifested earlier in meiosis, therefore we would expect that *SMG7* is dominant over *TDM1*. However, the opposite was true and *tdm1* mutation was epistatic to *smg7*. Similar to *tdm1* single mutants, *tdm1 smg7* plants were female fertile and male sterile due to progression to the third meiotic division. This suggests that *SMG7* is probably involved in the regulation of TDM1 during anaphase and that the anaphase II arrest in *smg7* mutants is executed trough TDM1 protein. It is not currently known, whether SMG7 inhibits TDM1 directly or indirectly. The much unexpected suppression of *smg7* phenotype in female meiosis implies that although the *tdm1* mutants are only male sterile, TDM1 protein plays a role in meiotic progression in female meiosis. Further we can deduce that the regulation of *TDM1* in female and male meiosis differs, but its relation to *SMG7* and role in anaphase II arrest in *smg7* mutants is similar. Different regulation of male and female meiosis is already described in several species. One reason could be a difference in developmental programs of female and male reproductive pathway in higher eukaryotes (reviewed in Orr-Weaver 1995; Hunt and Hassold 2002; Morelli and Cohen 2005). In most animal species studied so far, the female meiosis is arrested in prophase or metaphase of the first or second division until fertilization, whereas male meiosis is completed without such delay. However, even in organism like *Arabidopsis*, where meiotic arrest does not normally occur during male and female gametogenesis, and the gametophyte development immediately follows by several mitotic divisions, genes with mutant phenotypes only in male pathway such as *MMD/DUET* and *ASK1* were identified (reviewed in: Ma 2005; Liu and Qu 2008; Mercier and Grelon 2008).

Based on *TDM1* and *SMG7* genetic interaction, we can conclude that these two gene act in the same pathway required for down-regulation of cdk activity during meiosis. To further understand this interaction, it would be interesting to analyze TDM1 localization in *smg7* mutants and wild type female meiosis.

3.3. Neither *smg7* anaphase arrest nor *tdm1* re-entry into the third meiosis require TAM activity

To test our predictions that SMG7 and TDM1 facilitate downregulation of meiotic cdks, we intended to rescue the *smg7* and *tdm1* phenotypes by inactivating a meiotic cyclin to lower overall cdk activity. *Arabidopsis* has in total 50 predicted *Arabidopsis* cyclins, but only *TAM (CYCLIN A1;2*) and *CYCLIN SDS* are known to play a role during meiosis. *CYCLIN SDS* is required for pairing of homologous chromosomes, but there are no data suggesting that this cyclin has other effects on the meiotic progression (Azumi et al. 2002). *TAM* is therefore the only *Arabidopsis* cyclin that has been shown to play a role in progression of meiosis. This data were based on characterization of a hypomorphic, temperature sensitive *tam-1* allele that carries a point mutation in the conserved cyclin amino domain (Magnard et al. 2001; Wang et al. 2004b). Growth of *tam-1* mutant plants at restrictive temperatures results in formation a cell wall during interkinesis and asynchronous second meiotic division in the two divided cells. According to our analysis, null mutation of *TAM* has a more severe phenotype. Cells also form a cell wall after the first meiotic division, but instead continuing in meiosis II they exit meiotic cell cycle producing unreduced spores. This was confirmed by scoring ploidy of *tam-2* mutant plant progeny. Because anaphase I results in formation of two nuclei with chromosomes composed of two chromatids, gametes formed after the first meiotic division are diploid. Our finding that around 85% of self-pollinated *tam-2* progeny are tetraploids implies that both female and male meiosis are affected. It was suggested that the order of events during M-phase exit is dependent on the relative dose of cdk activity (reviewed in Wolf et al. 2007). For example, stabilization of cyclin B3 blocked exit from mitosis without blocking cytokinesis (Parry and O'Farrell 2001). Therefore we expect that cell wall formation in interkinesis is possible under low cdk activity, whereas exit from the M-phase requires that the M-phase specific cdk activity is completely switched off. This implies that protein produced in *tam-1* mutant plants has a residual activity as cells are still able to enter the second meiotic division. In *tam-2* allele, deletion of upstream part of a gene by T-DNA insertion prevents production of a functional protein; we suppose that the complete loss of TAM dependent cdk activity causes premature meiotic exit. This phenotype has recently been confirmed also in two other independent studies where other *TAM* null alleles were characterized (d'Erfurth et al. 2010; Wang et al. 2010).

Thus, *TAM* was an obvious candidate for testing genetic interaction with *SMG7* and *TDM1*. We assumed that *tam* mutation would be epistatic to *smg7* and *tdm1* mutations. However, neither the

smg7 anaphase II arrest nor the entry into the third meiotic division in *tdm1* mutants was suppressed by *tam* mutant alleles. In contrast, formation of cell wall in *tam-1* mutants and premature meiotic exit in *tam-2* were completely abolished. These data suggest that in double mutants meiosis can proceed to second division in the absence of TAM-dependent cdk activity. Thereby, other cyclins form active cdk-complexes during interkinesis and drive the progression through the second meiotic division. We suppose that *TAM* rather plays a regulatory role in this process. We further confirmed this hypothesis by localizing of TAM protein during meiosis. Similar to mitotic cells, TAM expression peaked during prophase. The highest signal was observed in pachytene cells, decreased in later stages and completely disappeared during anaphase I. There was no detectable expression during interkinesis and in second meiotic division. Therefore TAM seems to be meiosis I specific cyclin and it probably influences progression trough later stages indirectly.

Although A-type cyclins are considered to be involved mainly in the S phase, it was shown that they play also an important role in entry into M-phase, likely through activation of CDK-cyclin B complexes (Lehner and O'Farrell 1990; Knoblich and Lehner 1993; Fung et al. 2007; Deibler and Kirschner 2010). Consistent with this suggestion, degradation of A-type cyclins is animals initiated already in pro-metaphase independently on spindle checkpoint (Wolthuis et al. 2008; van Zon and Wolthuis 2010). Our observation that TAM:GUS signal peaks in prophase in both mitotic and somatic cells indicates that plant A-type cyclins are regulated in a similar manner.

Although TAM is not detectable during interkinesis, genetic analysis provides strong evidence that it plays an important regulatory role in progression from the first to the second meiotic division. We observed a very striking difference between the *smg7 tam-1* and *smg7 tam-2* mutants in proportion of meiocytes in interkinesis. In wild type and *smg7 tam-2* mutants we found that 13% and 12% respectively of counted meiocytes were in interkinesis. In the case of *smg7 tam-1* it was only 1,2% and these cells had a strange morphology with hypercondensed chromosomes (work by Nina Riehs). This suggests that in *smg7 tam-1* double mutants the cell cycle progression from the first to second meiotic division is accelerated. The chromatin decondensation requires first drop of cdk-cyclin B activity and then of the Aurora B kinase activity (reviewed in Meyer et al. 2010). Therefore, the condensation of chromosomes in *smg7 tam-1* interkinesis points to increased cdk activity. How can we explain this phenomenon and the difference in *SMG7* interaction with the two *TAM* alleles? It was shown that on one hand, A-type cyclins promote entry into M-phase in human cells by phosphorylating and inhibiting WEE1 kinase, and therefore allowing accumulation of active cyclin B complexes (Fung et al. 2007;

Deibler and Kirschner 2010). On the other hand, downregulation of cyclin A in *Xenopus* oocytes led to the earlier appearance of cdk-cyclin B activity and premature entry into mitosis (Walker and Maller 1991). A complementary experiment was done by overexpressing cyclin A in human cell line what caused a delayed prometaphase probably by the stability of cyclin B (den Elzen and Pines 2001). This suggests that cyclin A has an inhibitory effect on mitotic progression in animals. We hypothesize that *TAM* also plays a dual role in interkinesis by having both activating and inhibiting effect on the total cdk activity in meiosis (figure 3.1 A). *SMG7* is required for down regulation of cdk activity. Suppression of *TAM* phenotype suggests that SMG7 could execute this function already during interkinesis. In *smg7 tam-1* specific activity of TAM containing cdk complex is not fully down-regulated (figure 3.1 D) whereas in *smg7 tam-2* is completely missing. So both activating and inhibiting effect are missing in *tam-2* null allele and they are probably balanced by the absence of *SMG7* which prevents exit from meiosis. *tam-1* mutants maintain partial TAM-dependent cdk activity, probably lacks its inhibitory function, but still has some activating function, as deduced from the capability of *tam-1* mutants to enter into second meiotic division after extended interkinesis (figure 3.1 C). Thus absence of *SMG7* inhibitory effect on cdk activity with *tam-1* allele could result in upregulated cdk activity in interkinesis, premature condensation of chromosomes and rapid transition from meiosis I to meiosis II.

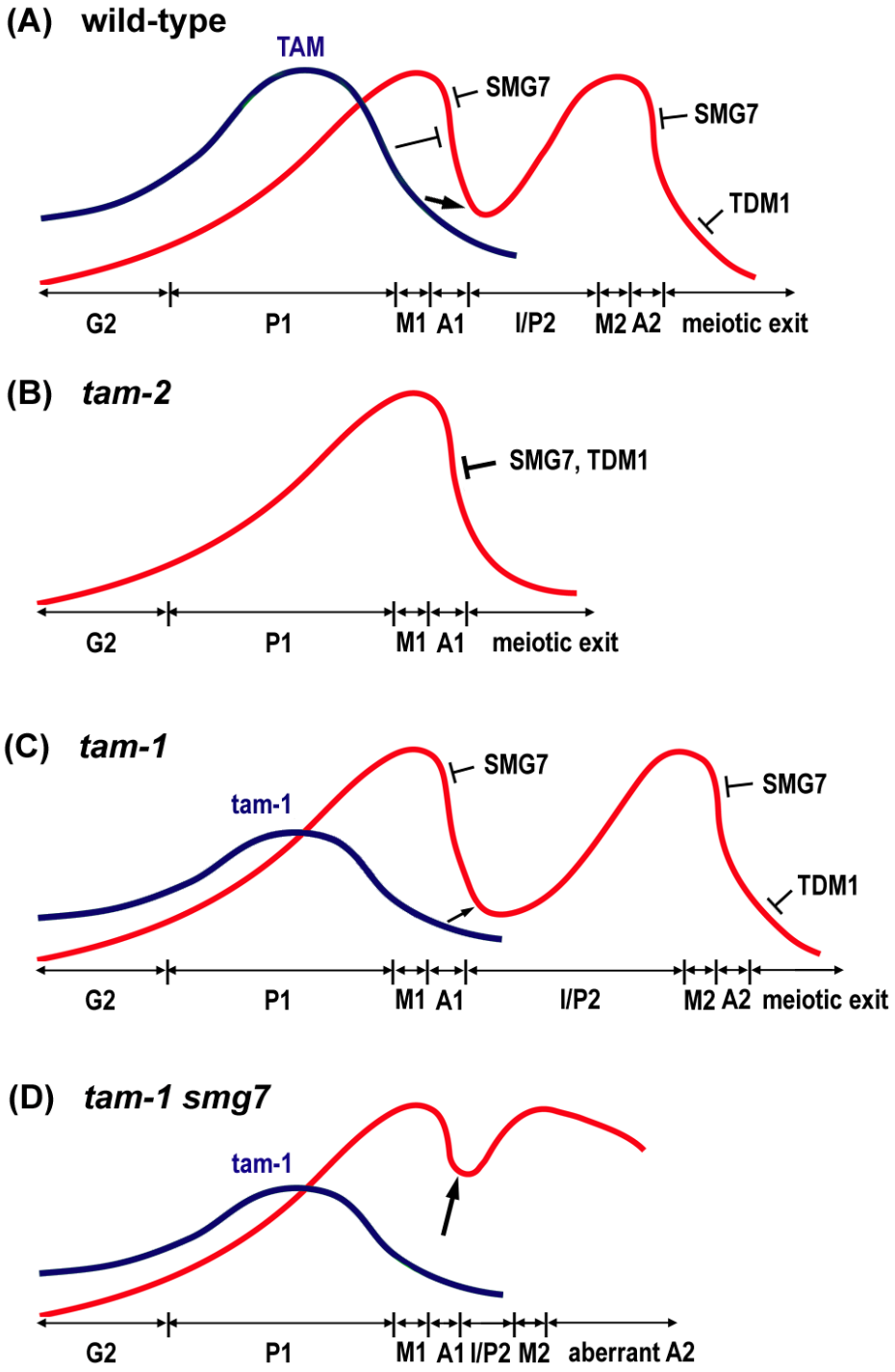

Figure 3.1: Models of cdk regulation in male meiosis in **(A)** wild-type, **(B)** *tam-2*, **(C)** *tam-1* and **(D)** and *smg7 tam-1* mutants. The red line illustrates activity of the hypothetical cdk-cyclin kinase(s) in the course of meiosis. Blue line depicts activity of TAM as inferred from TAM:GUS localization data. Stages of meioses and their approximate durations are indicated on the X axis (P1 - prophase I, M1 - metaphase I, A1 - anaphase I, I/P2 - interkinesis/ prophase II, M2 – metaphase II, A2 - anaphase II). CDK activities and durations of meiotic stages reflect only hypothetical values and are not based on any exact measurements.. In wild-type **(A)** inhibiting and activating effect of TAM are balanced with SMG7 In *tam-2* mutants **(B)** complete loss of TAM functions together with inhibitory effect of SMG7 leads to exit after first meiotic division. In *tam-1* mutants **(C),** decreased level of activating TAM-cdk activity together with SMG7 inhibiting effect causes extended interkinesis. **(D)** Lack of *tam-1* inhibiting function together with lack of *smg7* inhibitory effect in *smg7 tam-1* double mutants causes increased cdk activity and shortening of interkinesis.

As TAM is not detectable during interkinesis, we suggest that its regulation is indirectly, most likely by phosphorylation of target proteins. One possible TAM target, which would help to explain its phenotype and difference between *tam-1* and *tam-2* alleles, is TDM1. Suppression TAM phenotype in both *tam1-1 tdm1* and *tam-2 tdm1* double mutants implies that *TDM1* is required for premature cell wall formation or meiotic exit in *TAM* single mutants (model - figure 3.2). TDM1 protein sequence contains 5 predicted putative cdk phosphorylation sites (NetPhosK software prediction (Blom et al. 1999) so we hypothesize that TDM1 may be a inhibited by TAM–cdk mediated phosphorylation. Appearance of TDM1 during meiotic prophase and subsequent formation of foci correlate with high abundance of TAM protein. One possibility is that TAM- mediated phosphorylation targets TDM1 to foci. Therefore it would be interesting to examine TDM1 localization in *tam-1* and *tam-2* mutants. Similar regulation undergoes Sic1 protein in *S. cerevisiae*. As already mentioned, Sic1 is an important inhibitor of M-phase cdk activity at meiotic exit and in G1 phase. Sic1p is phosphorylated by Cdc28p kinase when cdk activity is high. This phosphorylation targets Sic1p for degradation. After activation of Cdc14 phosphatase during anaphase, Sic1p is stabilized by dephosphorylation and contributes to the irreversibility of mitotic exit by inhibiting Cdc28/Clb complexes (Donovan et al. 1994; Schwob et al. 1994; Visintin et al. 1998; Lopez-Aviles et al. 2009).

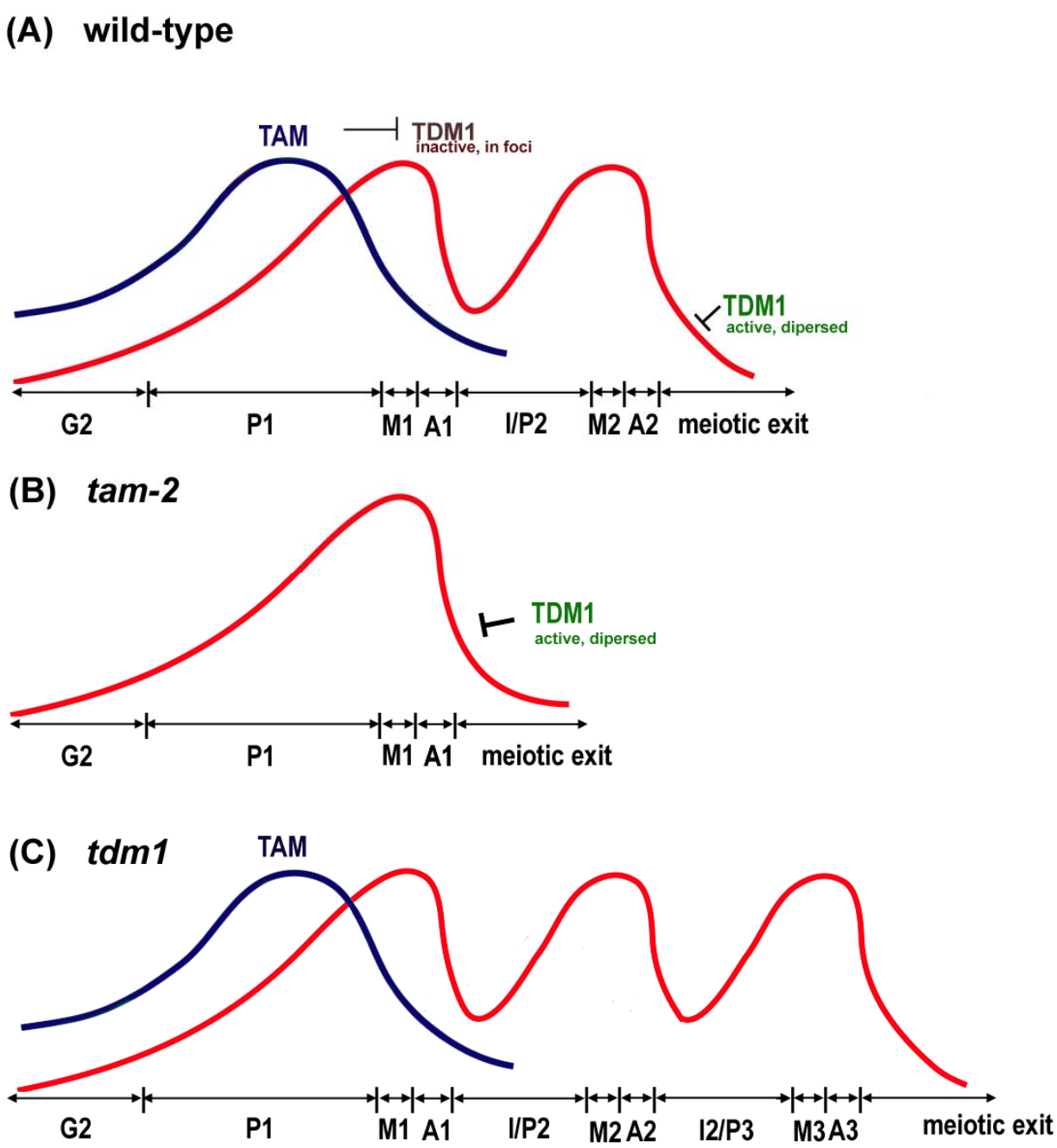

Figure 3.2: Hypothetical model of interaction between TAM and TDM1 proteins in male meiosis in **(A)** wild-type, **(B)** *tam-2* and **(C)** *tdm1* mutants. The red line illustrates activity of the hypothetical cdk-cyclin kinase(s) in the course of meiosis. Blue line depicts activity of TAM as inferred from TAM:GUS localization data. Stages of meioses and their approximate durations are indicated on the X axis and labelled in the same manner like on Figure 3.1. cdk activities and durations of meiotic stages reflect only hypothetical values and are not based on any exact measurements. In wild-type **(A)** TDM1 is inactivated during meiosis I by TAM. This inactivation is released by unknown signal at the meiotic exit. In *tam-2* mutant **(B)** TDM1 protein is not inhibited by TAM and therefore cause meiotic exit already after first division. In tdm1 mutants **(C),** loss of TDM1 inhibitory effect causes 3rd meiotic division.

3.4. Two cyclin pseudogenes and *CYCLIN B3;1* are expressed during meiosis in *Arabidopsis thaliana*

Progression through the M-phase relies on A and B-type cyclins. In budding yeast, 6 cyclin B-like genes exist, but they share also properties with A-type cyclin (Epstein and Cross 1992; Fitch et al. 1992; Richardson et al. 1992; Stuart and Wittenberg 1998). It is likely due to the fact that G2 and M phase overlap in this organism. In fission yeast, only one cyclin B-like gene, cdc13, is sufficient to drive mitotic progression (Fisher and Nurse 1996). In metazoans, the A-type cyclins are required for promoting entry into mitosis and early mitotic events, whereas B-type cyclins stimulate the major mitotic processes from mid-prophase on (Minshull et al. 1990; Furuno et al. 1999; Gong et al. 2007). Most studied organism posses several members of A and B-type cyclin families, indicating that distinct members of the same cyclin family may have non-redundant functions. Indeed, in several organisms a specialized meiotic cyclins were found, such as Rem1p and Crs1p in fission yeast, CYCLIN A1 and CYCLIN B3 in mammals and *CYCLIN SDS* in plants (Liu et al. 1998; Azumi et al. 2002; Nguyen et al. 2002b; Averbeck et al. 2005; Malapeira et al. 2005). Nevertheless in most cases, cyclins play overlapping roles in both mitosis and meiosis. It has recently been shown that five out of six mitotic Clb cyclins in budding yeast are involved in meiosis; only the major mitotic cyclin Clb2 is not meiotically expressed (Carlile and Amon 2008). These cyclins undergo a very precise regulation by translation, as well as on the posttranscriptional and posttranslational level. Misregulation of these processes as well as contrived expression of Clb2 during meiosis severely perturbs meiosis.

Based on presented results, we suppose that *SMG7*, *TAM* and *TDM1* are involved in regulation of core cdk-cyclin activity in meiosis. To understand their precise role we would need to examine their interaction with meiotic cdk complexes in *Arabidopsis*. As functional characterization of distinct *Arabidopsis* cyclins is largely missing, we sought to identify cyclins that are involved in meiosis. *Arabidopsis* has clearly distinguishable family of A-type cyclins with ten members, and of B-type cyclins with eleven members (Wang et al. 2004a). The only cyclin sharing properties of both groups is *CYCLIN SDS* which was already found to promote meiotic chromosome pairing. As both *SMG7* and *TDM1* operate during meiotic exit, we focused on B-type cyclins.

We examined localization of all 11 *Arabidopsis* B-type cyclin in both mitotic and meiotic cells. We found that eight out of eleven cyclins showed a strong signal in mitotic cells and no signal

over background in meiotic cells. Based the on localization during metaphase, we could distinguish two categories of mitotic cyclins – those that localize to chromatin and those that localize to cytoplasm. Similar differences in localization were reported for human and mouse CYCLIN B1 and B2 during prophase. CYLIN B2 resides in cytoplasm during G2 and M phase. CYCLIN B1 is cytoplasmic until late prophase then moves to nucleus, promotes further mitotic events (Jackman et al. 1995; Yang et al. 1998; Yang and Kornbluth 1999; Gavet and Pines 2010a, 2010b). During metaphase is CYCLIN B1 enriched on spindle and only a weaker signal is found on chromatin during metaphase (Pines and Hunter 1991; Girard et al. 1995). In *Arabidopsis,* we observed a similar distribution of localization during prophase; all mitotic CYCLIN B2s localized to cytoplasm, all but one CYCLIN B1 localized to nucleus during prophase. Interestingly CYCLIN B1;1 and CYCLINB1;2 localization was restricted to chromatin during metaphase, CYCLIN B1;3 was enriched on chromatin but showed also some signal in cytoplasm. Interestingly, the last CYCLIN B1;4 was excluded from chromatin and showed a similar localization pattern like cyclin B2s. The *CYCLIN B1;4* clearly clusters with other B1 cyclins in protein alignments, but we suppose that there has be a motif that is responsible for cyclin localization during mitosis. *CYCLIN B1;4* could probably share a localization motif with B2 cyclins.

Complementary genetic interaction between *Arabidopsis* B1 cyclins was carried in Arp Schnittgers´ laboratory. According to their unpublished data, combination of mutations in two chromatin-localized cyclins is either lethal or severely harms plant development, while combination of *cyclin B1;4* mutation with any other B1 cyclin does not have any effect on plant growth (Arp Schnittger, personal communication).

Last three B-type cyclin were found to be expressed in meiocytes. However, we failed to amplify any protein coding transcripts from *CYCLIN B1;5* and *CYCLIN B2;5* loci; only detected transcripts were products of extensive alternative splicing containing numerous premature stop codons. We further found that these two cyclins are not present in the genome of *Arabidopsis lyrata*, which is the closest relative of *Arabidopsis thaliana*. This suggests that these two cyclins likely represent pseudogenes that arose by a recent duplication. We found seven other similar pseudogenes in *A. lyrata* genome. In addition, *CYCLIN B2;5* is missing even in some *A. thaliana* ecotypes. This implies that cyclins in plants are prone to a very rapid evolution and that there are differences in number of cyclin-related genes even within ecotypes of one species. How these cyclin pseudogenes acquired expression during meiosis and whether they fulfil some regulatory function is currently unknown. Existence of cyclin pseudogenes was reported already in mouse

and humans (Lock et al. 1992; Nieduszynski et al. 2002). Interestingly, in mouse genome are dispersed nine sequences derived from CYCLIN B1 whereas in human genome is only one sequence derived from the CYCLIN B2. Whether these pseudogenes have some function was not investigated so far. An intriguing example of functional relationship between gene and derived pseudogene was described for human tumour-suppressor PTEN (Poliseno et al. 2010). Here, the transcripts arising from PTENP1 locus buffers the effect of microRNAs targeting PTEN transcripts. Mutations causing loss of PTENP1 transcription affects abundance of PTEN due to enhanced micro RNA binding followed by mRNA cleavage and degradation.

As all sequenced transcript derived from the *CYCLIN B1;5* and *CYCLIN B2;5* pseudogenes contained premature stop codons, we speculate that they could be a potential targets for non-sense mediated RNA decay. *SMG7* is a conserved nonsense-mediated mRNA decay factor and its requirement in this process in *Arabidopsis* and tobacco was already shown by Riehs and collegues and Kerenyi and collegues (Riehs et al. 2008, Kerenyi et al. 2008). Therefore if transcripts of these pseudogenes are directly or indirectly required for regulation of cdk activity during meiosis, their deregulation in *SMG7* mutant plants may cause anaphase II arrest. The other possibility is that as these pseudogenes are missing in close *A. thaliana* relatives, they are not executing a special function. Rather, non-sense mediated RNA decay could be widely used for removal of premature stop codon containing transcripts arising from duplicated loci. Upregulation of these transcripts may impair correct processing of other cyclin mRNAs and cause their further deregulation during meiosis.

RNA processing mechanisms appear to play an important role in regulation of meiosis. In *Schizosaccharomyces pombe*, expression of cell cycle regulators including meiotic cyclins is under strict posttranscriptional control that includes splicing, polyadenylation and mRNA stability (Kishida et al. 1994; Izawa et al. 2005; Malapeira et al. 2005; Moldon et al. 2008; McPheeters et al. 2009). Posttranscriptional regulation was shown to operate also in *Xenopus* eggs, where three rounds of translation of stored mRNAs are executes during meiosis (Barkoff et al. 1998; Gillian-Daniel et al. 1998; Barkoff et al. 2000; Belloc and Mendez 2008; Belloc et al. 2008). In budding yeast, so far unknown mechanism restricts translation of Clb3 mRNA to the second meiotic division (Carlile and Amon 2008). Therefore it is reasonable to propose that the meiotic role of *SMG7* is related to processing meiotic RNA transcripts. Support for the role of RNA processing in meiotic control is provided by recent discovery of *AtPS1,* which is another gene with predicted function in RNA metabolism that is required for meiosis. *AtPS1* gene encodes a meiosis-specific protein that contains RNA degradation PIN domain and is required

for proper spindle orientation in second meiotic division (d'Erfurth et al. 2008). RNase PIN domain is found in human SMG5 and SMG6 proteins which are homologous to SMG7 and also act in NMD but are missing in *Arabidopsis*. SMG6 contains a PIN domain that was shown to have a nuclease activity (Glavan et al. 2006). Therefore, one possibility is that *SMG7* and *AtPS1* play synergistical roles in RNA stability regulation during meiosis.

The only cyclin gene expressed in meiosis that was confirmed to encode a functional protein is *CYCLIN B3;1*. Plant cyclin gene duplication arose after split of plant lineage from other eukaryotes, therefore *Arabidopsis CYCLIN B3;1* is not related to mammalian CYCLIN B3 (Wang et al. 2004a). This gene does not cluster with neither group of B1-type cyclins nor with B2-type cyclins. By sequencing *CYCLIN B3;1* cDNA, we found an intron in 3´ untranslated region, which points to a possible regulation at the mRNA stability level. Non-sense mediated RNA decay was shown to influence the stability of transcripts with spliced 3´UTR in mammalian cells (Banihashemi et al. 2006; Hansen et al. 2009), therefore we can assume that *CYCLIN B3;1* could be regulated in *SMG7*-dependent manner. The more surprising feature of this cyclins is the absence of sequence motives corresponding neither to the D-box, a recognition signal for the APC^{Cdc20}-mediated degradation, nor to the KEN-box, which is sequence recognized by APC^{cdh1} that mediates protein degradation later during meiotic exit (Pfleger and Kirschner 2000). Therefore, CYCLIN B3;1 protein is probably resistant to the APC-mediated degradation. This assumption was further supported by the constant level of the CYCLIN B3; 1:GUS protein during meiotic progression. The CYCLIN B3;1:GUS signal was detected at meiotic exit at the tetrad stage as well as in other stages of meiosis (figure 2.39). There is no other report of B-type cyclin lacking destruction box so far. The only other M-phase cyclin without destruction box described so far is the mammalian CYCLIN F (Bai et al. 1994). This cyclin is related to both A and B-type cyclins, it oscillates during the cell cycle in a similar manner as other cyclins (Bai et al. 1994), but its degradation is based on the presence of the PEST motif, which targets proteins to proteolysis by metalloproteases (Fung et al. 2002). CYCLIN F was the first protein found to contain an F-box. Later on, F-box proteins were shown to act as substrate-recognition components of the Skp1–Cul1–F-box-protein (SCF) ubiquitin ligase (Bai et al. 1996; Feldman et al. 1997; Skowyra et al. 1997, reviewed in Cardozo and Pagano 2004). CYCLIN F was recently shown to play a role in control of centrosome homeostasis by targeting the CP110 protein for degradation (D'Angiolella et al. 2010). CYCLIN B3;1 does not contain an F-box, therefore we suppose that it will not function in similar manner like CYCLIN F. However CYCLIN B3;1 has two predicted poor PEST motifs in its sequence (prediction: ePESTfind software), that suggest possible proteolytic degradation (Rogers et al. 1986). Nevertheless CYCLIN B3;1 is stable

during meiotic progression, therefore we can expect the proteolytic degradation to occur only after meiosis is finished. Further examination of other putative M-phase cyclins showed that neither CYCLIN SDS and CYCLIN A3;3 contain a destruction box. *CYCLIN SDS* was already shown to play a role during meiosis (Azumi et al. 2002). Although there is no evidence for its involvement in other process than pairing of homologous chromosomes, we cannot exclude that it plays also more prevalent role. There are no information about *CYCLIN A3;3* so far, but expression profile published at Genevestigator software (Hruz et al. 2008) suggest that its expression is detectable in anthers and pistils and thereby could be a candidate gene for further examination. We suggest that CYCLIN B3;1- dependent and probably also CYCLIN SDS-dependent cdk activity requires an alternative pathway for inactivation during anaphase than cyclin destruction. A similar alternative pathway must also operate during *Saccharomyces cerevisiae* meiosis where level of two Clb proteins does not change during meiosis (Carlile and Amon 2008). Clb4p was shown to be stable at the protein level but the associated cdk activity oscillated and peaked during both metaphases. Clb1p protein was also stable until exit from meiosis, but showed associated cdk activity was detectable only during the first meiotic division.

Although this hypothesis needs further support from experimental data, we can postulate that *SMG7* and *TDM1* may be directly involved in this pathway. TDM1 is a good candidate for being a direct interaction partner with cyclins, as it contains eight cyclin-binding motifs. TDM1 which shows a similar localization pattern during anaphase II in like *CYCLIN B3;1* could therefore deactivate cdk-cyclin complex by direct binding.

There are several possibilities for the role of *SMG7* in meiosis. One is already above mentioned regulation of the recently duplicated cyclin pseudogenes. Another possibility is that *SMG7* is involved in a pathway that mediates down-regulation of cdk activity dependent on cyclins without D-box trough *TDM1*. But we could mimic the *smg7* phenotype using proteasome inhibitor MG115, what points to requirement of protein degradation during anaphase II. Thus another possibility is that the whole cascade of events leading to deactivation of cdk activity could be dependent on both alternative non-proteolytic pathway required for cdk activity down-regulation probably involving TDM1 and SMG7 and APC mediated protein degradation by proteasome.

4. CONCLUSION

In this work, we have focused on the role of SMG7 protein in meiotic cell cycle progression. Hypomorphic mutation of this protein causes a specific cell cycle arrest during anaphase of second meiotic division. Data obtained in our laboratory by Nina Riehs excluded the possibility that this arrest is caused by premature loss of cohesion. Using spindle inhibitors, we could determine that the checkpoint mechanism in *smg7* mutants is functional and therefore the anaphase II arrest phenotype is not caused by premature separation of improperly chromosomes. Thus, the defect observed in *smg7* mutants is most likely not a consequence of an error during previous meiotic stage, but rather is specific for anaphase II

We hypothesised that *smg7* phenotype might reflect a problem with downregulation of cdk activity during anaphase or aberrant dephosphorylation of cdk substrates. To test the first possibility, we established a cytogenetic method for detection of cdk activity during meiosis by detection of activating phosphorylation of the major Arabidopsis cdk, *CDKA;1*. We found that CDKA;1 protein is ubiquitously present during meiosis but the activating phosphorylation cycles with highest signal intensity in metaphase I and II. During anaphase and in telophase the intensity of signal decreased. In contrast, we detected high levels activating phosphorylation in *smg7* meiocytes arrested at aberrant anaphase II. Therefore we conclude that SMG7 protein functions in downregulation of cdk activity at the end of meiosis.

To experimentally test whether we can suppress high levels of cdk activity in anaphase II arrested meiocytes, we aimed to combine *smg7* deficiency with mutation of a meiotic cyclin. The only known cyclin known to be involved in meiotic progression in Arabidopsis is an A-type cyclin called *TAM*. We show that *TAM* deficiency causes exit from meiosis after first division, but this phenotype is suppressed by inactivation of *SMG7*. To explain this genetic interaction we localized tagged TAM protein in meiocytes and we can show that *TAM* is specifically expressed during first meiotic division. Therefore *TAM* is most likely not required for cdk activity during second meiotic division.

We further show that *SMG7* arrest in anaphase II is dependent on a plant specific protein TDM1. *smg7* mutant phenotype is suppressed in *smg7 tdm1* double mutants. *TDM1* is also required for premature meiotic exit in *tam* mutants because this phenotype is suppressed in double mutant plants.

As *tam* mutation can be suppressed by both *smg7* and *tdm1* mutation and the meiosis continues to second division, we suppose that there has to be driven by another cdk-cyclin complex independent in absence of *TAM*. For this reason we focused on identification of B-type cyclins expressed during male meiosis in *Arabidopsis*. By generating marker lines for each B-type cyclin, we detected expression of three B-type cyclins during meiosis. Further analysis showed that two of them are not-conserved pseudogenes. The only protein-coding gene *CYCLIN B3;1* differs from standard B-type cyclins by lack of destruction box sequence that is required for cyclin degradation during anaphase. This suggests existence of an alternative pathway for inactivation of cdk activity than APC mediated cyclin proteolysis and we speculate that *SMG7* might be involved in regulation of this pathway.

5. MATERIAL AND METHODS

All reagents and chemicals were purchased from Sigma.Aldrich, if not otherwise stated.

5.1. Plant material

5.1.1. Plant cultivation

Wild-type and mutant *Arabidopsis* plants were grown in mix of three parts of soil with one part of vermiculite (Gramoflor) at 22°C under long day conditions (16h light, 8h dark). Plants carrying *smg7* mutation were grown in higher humidity (50-60%) for first three weeks. Phenotype of plants with *tam1* mutation was induced by transfer to 27 ° C before flowering.

5.1.2. *In vitro* plant culture

Seeds of plants for in vitro growth were first sterilized. Seeds were shortly washed with 70% ethanol, then ethanol was replaced with 1 ml of freshly made 50% bleaching solution (~ 6% sodium hypochloride "DanKlorix" (Colgate-Palmolive); few drops of Triton-X-100) and incubated for 7 minutes. Bleaching solution was then removed and seeds were washed five times with water under sterile conditions. Sterilized seeds were transferred with pipette on ½ MS plates (2,21g/l MS complete salts, 0.5 g/l MES monohydrate (2-(N)-morpholino methansulfonic acid), 8g/l plant agar, (all from Duchefa), 10g/l sucrose, pH adjusted with 1M KOH to 5.8, autoclaved). Plates were sealed with Leucopore tape and incubated for 24 h at 4°C, then transferred to standard conditions (22°C, 16h light, 8h dark).

5.1.3. T-DNA insertion lines

T-DNA insertion lines used in this study are listed in table 5.1. All lines were obtained from NASC stock centre except for *tdm1-1* line which was a kind gift from Dr. Susan Armstrong (University of Birmingham, UK).

Allele	AGI code	Insertion line	Reference
smg7-1	At5g19400	SALK_073354	(Riehs et al. 2008)
tam-1	At1g77390		(Magnard et al. 2001)
tam-2	At1g77390	SAIL_505_C06	
tdm1-1	At4g20900	Feldmann line 178	(Chaudhury 1994; Ross et al. 1997; Glover et al. 1998)
tdm1-4	At4g20900	SALK_123139	

Table 5.1. T-DNA insertion lines used in this study.

5.2. Genotyping

DNA for genotyping was isolated from 3 weeks old plants with. Leaves or flowers were ground in 200µl of DNA extraction buffer (200mM Tris pH 7.5, 250mM NaCl, 0,5% SDS, 25mM EDTA pH 8.0) either with IKA RW 20n overhead stirrer (Ika) or with Retsch mixer mill MM 400 (Retsch). Then another 200 µl of DNA extraction buffer were added and samples were centrifuged at 16,000 rcf at room temperature for 5 minutes. Supernatant was transferred to a new tube and DNA was precipitated by addition of 1 volume of isopropanol. After gentle mixing and 10 minutes incubation at room temperature, samples were again spinned at 16,000 rcf at room temperature for 5 minutes. Supernatant was decanted and pellet containing DNA was washed with 500 µl of 70% ethanol. DNA was air-dried and pellet was resuspended in 50µl of nuclease-free water.

T-DNA insertion lines were genotyped with home-made Taq polymerase and home-made buffer. PCR reaction consisted of 2 µl of 10 x PCR buffer (500 mM KCl, 15 mM $MgCl_2$, 1.5 mg/ml BSA, 200 mM Tris HCl pH 8.3), 2 µl of 0.2 mM dNTPs, 1 µl of 10 µM of each gene specific oligo (table 5.1 and table 5.3), water up to 18,8 µl , 0.2 µl of home-made Taq polymerase and 1 µl of genomic DNA. Samples were denatured in PTC100 Peltier Thermo Cycler (BioRad) at 95 °C for 3 min, followed by 32 cycles of denaturation 95°C for 30 seconds, primer annealing at 56°C for 30 seconds and extension at 72°C for 1:30 minutes with a final extension step at 72°C for 3 minutes. PCR products were separated by electrophoresis in a 1% agarose gel with Ethidium Bromide.

5.2.1. Allele specific PCR for *tam-1* allele:

Tam-1 allele carries a point mutation in exon 5 that changes C to T (Wang et al. 2004b). In order to discriminate these alleles, allele-specific primers CycA1,2-2W for WT allele and CycA1,2-2M for mutant were designed. Both primers contain the corresponding polymorphic nucleotide at the 3´end and also one more mismatch in the 3rd nucleotide from the 3´end to destabilize the primer annealing. So these mismatches at the 3′ end possibly reduce annealing to the other allele, but more importantly it prevents *Taq* DNA polymerase from extending the mismatched primer because *Taq* needs a perfect match at the 3′ end for further extension. As an internal control in reaction each sample contained primers for *MRE11* gene (Mre1 and Mre3) that gives a PCR product of different size. For each allele was therefore run a separate reaction with 2 primer pairs. Only reactions with band from control reaction were evaluated. The PCR reaction was the same as for the other genotyping, but the concentration of $MgCl_2$ was increased to 3 mM.

Allele	**Wild type allele**	**Mutant allele**
smg7-1	Est1b-1 + Est1b-4 (1520 bp)	Est1b-4+ Lbc1 (1256 bp)
tam-1	CycA1,2-3 + CycA1,2-W (503 bp), Mre1+ Mre3 (702 bp)	CycA1,2-3 + CycA1,2-M (503 bp), Mre1 + Mre3 (702)
	Allele – specific PCR – description in text	
tam-2	CycA12-1 + cycA_r_nonspec (626 bp)	cycA_r_nonspec + SAIL-LB3 (437 bp)
tdm1-1	TDM-1 + TDM-3 (743 bp)	TDM-1 +TDM-2 (495 bp)
tdm1-4	TDM-5 + TDM-11 (500bp)	TDM-11 + Lbc1 (309bp)

Table 5.2: Primer combinations used for genotyping.

Primer name	Primer sequence in 5´ - 3´direction
Est1b-1	GACCTTGGTAGCTGGTCCTGAG
Est1b-4	AGTCGAGAAGCAGCTAGTGAT
Lbc1	TGGACCGCTTGCTGCAACTCT
CycA1,2-3	ATGGAGCGTATCGAAGCATAGCGT
CycA1,2-2W	GCGCGTGGAGGATTTCTGTTACATAAC
CycA1,2-M	GCGCGTGGAGGATTTCTGTTACATAAT
MRE-1	CCAATGGATGAGGCCTGAAGTT
MRE-3	GTCTGCCACCACCATAACAT
CycA12-1	ATGGAAAGAACTCAGTCAAGCATCA
cycA_r_nonspec	GAACAGAAGACTCCATCTCCAA
SAIL-LB3	TAGCATCTGAATTTCATAACCAATCTCGATACAC
TDM-1	TAGGGAACTTGGGCTGGGTTCATT
TDM-2	ATCTTGCTAACAGCTGGTAT
TDM-3	TCTTCTGCGATATCTGCCCAGCTT
TDM-5	TCATTACAACGGCCATATCCTTCAA
TDM-11	CACCATGTGTCCCTGCGTAGAGCGTCGT

Table 5.3: Names and sequences of primers used for genotyping.

5.3. Crossing

Plants used for crossing were grown in soil for 4-5 weeks. Young inflorescence from a mother plant was immobilized under Leica MZ6 stereomicroscope (Leica). All silliques, opened flowers and small buds were excised and discarded; only 2-3 biggest unopened buds were left. Buds were carefully opened and anthers were dissected out with forceps. Anthers from opened flowers of father plant were excised with forceps and the pollen was tapped on the pistil of mother plants. Afterwards, stem with pollinated pistils was carefully attached to a wooden stick to keep it in upright position. After development and maturation of silliques, they were harvested in to eppendorf tubes.

5.4. Analysis of gene expression

5.4.1. RNA isolation

For RNA isolation, 100 mg of inflorescences were collected in liquid nitrogen and ground to fine powder. Powder was mixed with 1 ml of Tri-Reagent and vortexed. After 10 minute incubation at room temperature 0,2 ml of chloroform was added, mixed by vortexing and again incubated for 10 minutes at room temperature. Samples were then centrifuged at 16,000 rcf at 4°C for 10 minutes. Supernatant containing RNA was transferred to a new eppendorf tube and precipitated with 0,4 volume of isopropanol. Pellet was washed with 500 µl of 70% ethanol and dried. RNA was resuspended in 50 µl of nuclease-free water.

5.4.2. RNA concentration and integrity control

5.4.2.1. RNA concentration estimation

RNA concentration was measured with Qubit quantification platform (Invitrogen). System was calibrated and used according to manufacturers instructions. 1µl of Quant-iT RNA reagent was mixed with 199 µl of Quant-iT RNA buffer to prepare working solution. 1 µl of RNA sample was mixed with 199 µl of working solution and shortly vortexed. Sample concentration was then measured on Qubit fluorometer.

5.4.2.2.RNA mini gel

RNA integrity was accessed on TBE mini gel. 2 µl or 1 µg of RNA were adjusted with water to 5 µl and mixed with 5 µl of 2 x urea loading buffer (0.26 g urea, 500 µl 6x loading buffer III, 200 µl of 5xTBE and 150 µl of nuclease-free water) and incubated at 65 °C for 3 minutes. Samples were then incubated ice for 1 minute and separated on 1,5 % TBE gel (1 x TBE (90 mM Tris-base, 90 mM boric acid, 2mM EDTA, pH 8.0) , 1,5% weight/volume agarose, 0,5 µg/ml ethidium bromide).

5.4.3. RT-PCR

5.4.3.1.DNAse treatment

1-2 µg of RNA were adjusted with nuclease-free water to 16 µl, mixed with 1µl of RiboLock RNAse inhibitor, 2µl of 10 x DNAse buffer and 1µl of 1u/µl DNAse (all Fermentas). Samples were incubated at 37 °C for 40 minutes. Reaction was stopped by adding 1 µl of 25 mM EDTA (Fermentas) and heating 65 ° C for 10 minutes.

5.4.3.2. cDNA synthesis

RNA samples after DNAse treatment were subjected to reverse transcription. For further amplification of control gene *ACTIN2* and TAM cDNAs, we used standard reverse transcriptase with no thermostability and oligo dT primer. Amplification of cyclins with meiotic expression required thermostable reverse transcriptase or 3`SMART RACE kit.

cDNA synthesis with standard reverse transcriptase

1 µg of DNAse treated RNA was reverse transcribed with RevertAid™ H Minus First Strand cDNA Synthesis Kit (Fermentas) according to manufacturers instructions. First, RNA was mixed in eppendorf tube with 1µl of 5µg/µl oligo dT primer and total volume adjusted to 12 µl with nuclease-free water. Solution was then incubated at 65 °C for 5 minutes and cooled on ice and mixed with 4 µl of 5x reaction buffer, 1 µl of 20u/µl RiboLock RNase Inhibitor and 2 µl 10mM dNTPs (all reagents were supplied in a kit). After gently mixing and short spin, reaction was incubated at 42 °C for 60 minutes. Reaction was stopped by heating to 70 °C for 5 minutes.

cDNA synthesis with thermostable reverse transcriptase

For low expressed genes or transcripts that were predicted to contain secondary structures it was necessary to use thermostable reverse transcriptase. 1µg of DNAse treated RNA mixed with 1µl of 20u/µl RiboLock RNase Inhibitor, 2 µl of 10 mM dNTPs (both Fermentas), 1 µl of 5µg/µl primer (either oligo dT or gene-specific primer), 1µl of 0.1 M DTT, 4 µl of 5x cDNA synthesis buffer, nuclease-free water up to 19 µl and 1µl of ThermoScript reverse transcriptase (all Invitrogen). Reaction was gently mixed and short spinned and incubated at 65 °C for 80

minutes. Reaction was terminated by incubation at 85 °C for 5 minutes.

5.4.3.3. PCR amplification of cDNAs

Amplification of TAM cDNA in WT and tam-2 mutant plants

All cDNAs were amplified using GoTaq DNA Polymerase (Promega). 1µl of cDNA from each sample was used for control PCR reaction on *ACTIN2* gene (At5g0980) with Actin 2-1 and Actin 2-2 primers. PCR reaction mix consisted of 1 µl cDNA, 4 µl 5 x GoTaq Reaction buffer containing $MgCl_2$ (Promega), 2 µl of 2 mM dNTPs, 1 µl of forward and reverse 10 µM primer, nuclease-free water up to 19,8 µl and 0,2 µl of 5u/µl GoTaq DNA polymerase. Reaction mix was shortly spinned and run under program consisting of initial denaturation at 95 °C for 2 minutes, followed by 24 cycles of denaturation at 95°C for 30 seconds, primer annealing at 56°C for 30 seconds and extension at 72 °C for 1 minute and final extension at 72 degrees for 5 minutes. PCR products were loaded and resolved on 1% agarose gel with Ethidium bromide and signal from different samples was compared. In case if signals were not equal, amount of template cDNA was adjusted and procedure was repeated until signals from all samples were equal.

TAM cDNA was amplified with the same protocol as described above for *ACTIN2*, but with 32 cycles instead of 24. Full-length TAM cDNA was amplified using primers CycA1.2-3b and CycA1,2-R1, region spanning T-DNA border was amplified with primers CycA12-1 and cycA_r_nonspec and the region downstream of T-DNA insertion was amplified with primers CycA1,2-R1 and cycA_f_nonspec. All primer sequences are listed in table 5.4.

Primer name	Primer sequence in 5´ - 3´direction
Actin 2-1	CTGCCGCTGTTGTTTCTCCT
Actin 2-2	CGTTGTAGAAAGTGTGATGCCA
CycA1.2-3b	AACCCTAAATCTCACCGGAAAAC
CycA1,2-R1	GAGGAAAAGCTCTTGCGGTA
CycA12-1	ATGGAAAGAACTCAGTCAAGCATCA
cycA_r_nonspec	GAACAGAAGACTCCATCTCCAA
cycA_f_nonspec	TGTTACCTGCATGATGATAGCA

Table 5.4: Names and sequences of primers used for RT-PCR amplification of *ACTIN2* and *TAM* transcripts.

Amplification of cyclins with meiotic expression

CYCLIN B1;5

1-5 µl of cDNA transcribed with thermostable reverse transcriptase either with oligo dT or CycB15-27 primer localized in putative 3´UTR was amplified by PCR with following primer pairs: CycB15-9 in and CycB15-5 for region containing exons 1 to 5, CycB15-17 and oligo dT for region from exon 6 to intron 8 / exon9 and CycB15-14 with B15Rev/NheI for region from exon 9 to the stop codon in exon 10. Primer sequences are listed in table 5.5. PCR was either performed with GoTaq polymerase as described above for *ACTIN2* and TAM genes, but with 40 cycles, or with Phusion polymerase (Finnzymes). For PCR with Phusion polymerase, 4 µl of 5x Phusion HF Buffer (Finnzymes), 2 µl of 2mM dNTPs, 1µl of each forward and reverse 10 µM primer, nuclease-free water up to 19,8 µl and 0,2 µl Phusion Polymerase were mixed in a PCR tube. Although HF buffer already contains 1.5 mM $MgCl_2$ (final concentration in PCR), it was necessary to supplement some of reaction with additional $MgCl_2$ up to 3 mM. Reaction was denatured for 2 minutes at 98 °C, followed by 36 cycles of denaturation at 98°C for 10 seconds, primer annealing at 60°C for 30 seconds and extension at 72 °C for 1 minute and 1 cycle of final extension at 72 °C for 5 minutes. Amplified PCR products were cloned to pCR2.1 vector (Invitrogen) and sequenced with T7 and TOPO-1 primers as described in chapter 5.5.3.1.6.

Primer name	Primer sequence in 5´ - 3´direction
CycB15-27	CTTCATCAATCACCATACCTTTGAATAG
CycB15-9	ATGGCCCATTACATTAACATCTA
CycB15-5	CCGATGTCACCGAGGGCACGCCGATT
CycB15-17	CCTTGAAACTCTGTACCTCACTGTTA
CycB15-14	CAAGAAGTGACGGCCCCTGCTTCAGAAT
B15Rev/NheI/	GATCTTCTTTGCAGCTAAACACT

Table 5.5: Names and sequences of primers used for RT-PCR amplification of *CYCLIN B1;5* transcripts.

CYCLIN B2;5

CYCLIN B2;5 c DNA was amplified with the same procedure as *CYCLIN B1;5* cDNA. Primers used for reverse transcription were either oligo dT or CycB25-16. Attempts to amplify full-length predicted cDNA with CycB25-9 and CycB25-16 primers failed. Combination of CycB25-6 and CycB25-16 primers yielded 2 splice variants as described in chapter Results.

Primer name	Primer sequence in 5´ - 3´direction
CycB25-16	CTTATTATAGTTTTTTCCTCCCTT
CycB25-9	TCTGTTTCTTGATACCATGTC
CycB25-6	GGTGTTACTGCTTTGTTGCTCGCAT

Table 5.6: Names and sequences of primers used for RT-PCR amplification of *CYCLIN B2;5* transcripts.

5.4.4. 3´ RACE

CYCLIN B3;1 cDNA and 3`UTR was amplified with SMART RACE cDNA amplification kit (Clontech) according to provided instructions. 3µl RNA sample were mixed with 1µl of 12 µM 3´-CDS primer A (Clontech) and 1 µl of nuclease-free water and denatured at 70°C for 2 minutes and cooled on ice. Following reagents were added to cooled mix: 2µl of 5x First-Strand synthesis

buffer, 1µl of 20 mM DTT, 1µl of 10 mM dNTP mix (all Clontech) and 1µl of MMLV Reverse Transcriptase (Fermentas). Reaction was incubated at 42 °C for 90 minutes after short mixing and spinning. Then reaction was diluted with 20 µl of Tricine-EDTA buffer (Clontech) and stopped by heating at 72 °C for 7 minutes.

PCR amplification of full-length cDNA including 3`end was performed in 50 µl volume reaction: 34,5 µl nuclease-free water, 5 µl of 10 x Advantage 2 PCR buffer, 1 µl of 10 mM dNTP mix, 5 µl of 10 x UPM primer mix, 1 µl of 50 x Advantage 2 Polymerase mix (all Clontech), 1 µl of 10 µM CycB31-8 primer with 2,5 µl of transcribed cDNA. cDNA was further amplified by touchdown PCR consisting of 5 cycles of denaturation at 94 °C for 30 seconds and annealing/extension at 72 °C for 3 minutes, 5 cycles of denaturation at 94 °C for 30 seconds, annealing at 70 °C for 30 seconds and extension at 72 °C for 3 minutes and 25 cycles of denaturation at 94 °C for 30 seconds, annealing at 68 °C for 30 seconds and extension at 72 °C for 3 minutes. PCR product was checked on 1% agarose gel with Ethidium bromide and then cloned to pCR2.1 TOPO vector (Invitrogen) and sequenced with T7 and TOPO-1 primers.

Primer name	**Primer sequence in 5´ - 3´direction**
3`-CDS primer A	AAGCAGTGGTATCAACGCAGAGTAC$(T)_{30}$
UPM – long	CTAATACGACTCACTATAGGGCAAGCAGTGGTATCAACGCAGAGT
UPM - short	CTAATACGACTCACTATAGGGC
CycB31-8	ATGCTTAGGGACGGCAATAAGCA

Table 5.7: Names and sequences of primers used for 3´RACE and PCR amplification of *CYCLIN B3;1* transcripts.

5.5. Generation of transgenic lines

5.5.1. Cloning strategy for TAM:GUS and TDM:GUS constructs

TAM and *TDM1* were fused with *GUS* gene at their C-terminus in pMDC163 vector (Curtis and Grossniklaus 2003) by Gateway® recombination cloning technology (Invitrogen). Gateway technology is based on site-specific recombination properties of bacteriophage lambda (Landy 1989). This allows recombining the gene of interest between vectors if they contain appropriate

recombination sequences. To obtain a construct that would reflect the localization of native protein as close as possible we used a genomic DNA sequence of a gene. Therefore forward primer was designed into beginning of putative promoter. In case *TAM* it was region between *TAM* start codon and the closest upstream gene (total 1665 bp upstream of start codon). As *TDM 1* is only 418 bp downstream from stop codon of *HEN1* gene (At4g20910), we used a 520 bp genomic fragment according that includes also last exon of HEN1 gene. Both inserts were first PCR amplified; blunt–ended PCR fragment was cloned with topoisomerase to entry vector (pENTR/D/TOPO) that contains attL1 and attL2 recombination sites. For further recombination with pMDC163 vector it was necessary to have the insert in correct orientation, therefore the forward primer contained CACC sequence at its 5` end that is complementary to GTGG sequence in pENTR vector and allows a directional cloning. pMDC163 vector contains *GUS-A* gene in reading frame B, therefore reverse primer was designed to the last exon of cDNA, omitting the stop codon and 3´ÚTR. Insert was verified by sequencing in pENTR/D/TOPO vector and subcloned to pMDC163 vector by recombination of attL1 and attL2 sites in pENTR/D/TOPO with attR1 and attR2 sites in pMDC163 mediated by LR Clonase II enzyme mix (Invitrogen). The fusion site between the gene of interest and GUS was again sequenced to verify whether they are in the same the reading frame.

5.5.2. Cloning strategy for CYCLIN B:GUS constructs

CYCLIN B genes also were also fused at C-terminus with GUS gene, but they were cloned into pCBK04 by restriction cloning. The reason to do not use gateway system was relatively high price and limited lifespan of Clonase enzyme. Again a genomic DNA of a promoter and cyclin gene was used for cloning to include possible alternative splicing sites and regulation at RNA level.

Restriction sites used in pCBK04 vector were the same for all cyclins, PstI at 5´end of and XbaI at 3´end of insert. Therefore all forward primers contained SbfI site which have compatible ends with PstI and all reverse primers contained NheI site at 5´end which have compatible ends with XbaI. Forward primer was positioned at the beginning of putative promoter region – either up to 2,5 kilobase if the upstream gene was farther, or the sequence between the end of upstream gene and start codon, if it was shorter than 2,5 kilobase. Reverse primer was designed to the last exon and did not included 3'UTR and stop codon.

Amplified PCR products were cloned to pCR2.1 TOPO vector by topoisomerase reaction using adenine overhangs added by Taq polymerase. Insert was verified by sequencing and subcloned to pCBK04 by restriction cloning. The fusion site between cyclin and GUS sequenced to verify whether they are inn the same reading frame.

5.5.3. Cloning of TAM:GUS and TDM1:GUS constructs

5.5.3.1.1. PCR amplification of inserts

All inserts were amplified with iProof Polymerase (BioRad). As a template was used 1 µl of genomic DNA isolated as described in chapter 5.2. Conditions for particular constructs are in table 5.8 and primer sequences in table 5.9. Reaction mix with total volume 20 µl consisted of 4 µl of 5x iProof HF buffer (BioRad), 2 µl of 2 mM dNTPs, 1µl of 10 mM forward and reverse primer (table 5.9), 1µl of genomic DNA, water up to 19,8 µl and 0,2 µl of iProof polymerase. iProof HF buffer already contains 7.5 mM $MgCl_2$, so it was added into reaction only if necessary. Products were amplified in a reaction consisting of initial denaturation at 98 °C for 2 minutes, 30 cycles of denaturation for 10 seconds at 98°C, annealing for 30 seconds at particular annealing temperature (table 5.8) and extension at 72°C for 30 seconds counted for 1 kilobase of expected product (table 5.8), followed by final extension at 72°C for 20 minutes.

Gene	**Primers**	**Product length**	**PCR conditions**	
			Annealing temperature	Extension
TAM	CycA12-F1 + CycA12-R1	3900 bp	62 °C	2:00 min.
TDM1	TDM-g3 + TDM-12	2263 bp	60 °C	1:30 min.

Table 5.8: Conditions for amplification of *TAM* and *TDM1* fragment for cloning: names of primers, product length and PCR conditions

Primer name	Primer sequence in 5´ - 3´direction (sequence required for directional cloning is underlined)
CycA12-F1	CACCATGACGAGAGGGGAGAGTGAT
CycA12-R1	GAGGAAAAGCTCTTGCGGTA
TDM-g3	CACCCACCATCTGTTGAGAATGTTGCAGAAA
TDM-12	CATCTCTGCGGTTTTAAGCTCTCCCTGCAA

Table 5.9: Names and sequences of primers used for amplification of *TAM* and *TDM1* products for cloning.

5.5.3.1.2. Cloning to pENTR/D/TOPO vector

2µl of PCR reaction were checked on a agarose gel with ethidium bromide. If there was a single strong band, the reaction was directly used for cloning; if there were several bands, the expected band was purified from gel with QIAEXII Gel Extraction Kit (Qiagen) according to manufacturer's instructions. Topoisomerase cloning reaction consisted of 4,8 µl of PCR reaction or purified PCR product, 1 µl of salt solution and 0,2 µl of pENTR/D/TOPO vector (both Invitrogen). Reaction was incubated at 25 °C for 1 hour and then transformed to *Escherichia coli* TOP10F´ cells.

5.5.3.1.3. Heat-shock transformation of *Escherichia coli*

100 µl of *Escherichia coli* (*E. coli*) competent TOP10F´cells were thawed on ice. Whole topoisomerase cloning reaction was added to cells; gently mixed with tip of pipette and let stand for 5 minutes on ice. Afterwards, eppendorf tubes with cells were transferred to a thermomixer (Eppendorf) heated to 42°C for 45 seconds and then immediately transferred back on ice for 2 minutes. 900 µl of LB medium (1% Peptone, 0,5% Yeast Extract, 1% NaCl) without antibiotics was added to cells and they were incubated at 37^{o}C with shaking for 1 hour. Cells were collected by centrifugation at 2500 rcf (5200 rpm) in a table centrifuge for 2 minutes. 900 µl of supernatant were removed, cells were resuspended in the remaining 100 µl of supernatant and plated on a LB plate (LB with 1,5% bacterial agar) with appropriate antibiotics – 50 mg/ml of kanamycin for all used vectors. Plates were incubated overnight at 37 °C.

5.5.3.1.4. Glycerol stock preparation and plasmid extraction

For verification and further cloning, plasmids were extracted with isopropanol precipitation method. 4 ml of LB medium with antibiotics were inoculated with 1 single colony and grown overnight at 37 °C with shaking. In case if it was necessary to make glycerol stock, 700 µl of culture were transferred to a sterile eppendorf tube with 300 µl of sterile 50 % glycerol and tube was frozen at - 80°C. For plasmid extraction, 2 times 1,5 ml of culture were transferred to an eppendorf tube and centrifuged at 16 000 rcf (14,000 rpm) in a table centrifuge for 30 seconds. Supernatant was discarded and cell pellet was resuspended in 250 µl of resuspension buffer (50 mM Tris-Cl pH 8.0; 10 mM EDTA; 200 µg/ml RNase A) by vortexing, lysed by addition of 250 µl of lysis solution (200 mM NaOH; 1% SDS) and gentle flipping of a tube. Cell debris were precipitated by addition of 300 µl of neutralization buffer (3M potassium acetate, pH 5.5) and gentle mixing. Tubes were centrifuged at 16,000 rcf (14,000 rpm) for 6 minutes at room temperature and supernatant containing plasmid was transferred to a new tube. Plasmid DNA was precipitated with 600 µl of isopropanol, gentle mixing and centrifugation for 10 minutes at 16,000 rcf (14,000 rpm) at room temperature. Supernatant was discarded and pellet was washed by addition of 500 µl of 70% ethanol and centrifugation for 5 minutes at 16,000 rcf (14,000 rpm) at room temperature. Ethanol was discarded, pellet was air dried and resuspended in 50 µl of nuclease-free water.

5.5.3.1.5. Verification of plasmids by restriction digest

The presence of insert was verified by restriction digest of plasmids with enzymes that cut once in plasmid backbone and once in insert. Predicted restriction patterns were investigated with SeqBuilder program (DNASTAR). Restriction reaction was composed of 1-5 µl of plasmid DNA, 2 µl of 10 x restriction buffer, water up to 19 µl and 1 µl of restriction enzyme. Reaction was incubated at appropriate temperature depending on particular enzyme for 1-2 hours. DNA was then resolved on 1% agarose gel with ethidium bromide. Most enzymes were purchased from Fermentas or New England Biolabs.

5.5.3.1.6. Sequencing of plasmids

If plasmid were supposed to be sequenced, they were further purified with precipitation by PEG solution. 30 µl of PEG solution (20 % PEG 6000, 2.5 M NaCl) was added to plasmid

resuspended in 50 µl of nuclease-free water after isopropanol extraction and incubated on ice for 1 hour. Samples were centrifuged at 16, 000 rcf (14, 00 rpm) at 4°C for 15 minutes. DNA pellet was washed with 70 % ethanol, air-dried and dissolved in 20 µl H_2O.

Sequencing reaction was performed with BigDye kit (Applied Biosystems). Reaction had total volume 10 µl and was composed of 5,5 µl plasmid DNA, 1,5 µl 5x Sequencing Buffer, 1.0µl BigDye (both Applied Biosystems) and 2,0µl 10µM primer. Samples were incubated in a PCR thermocycler at 96 °C for 2 minutes, followed by 25 cycles of denaturation at 96°C for 2 minutes, annealing at 45 °C for 15 seconds and extension at 60 °C for 4 minutes. Reaction was adjusted to 20 µl total volume with water and was send to VBC genomics. Sequences were analysed by SeqBuilder and MegAlign programs (both DNASTAR). Primers used for sequencing of pENTR/D/TOPO are listed in table 5.10.

Primer name	**Primer sequence in 5´ - 3´direction**
M13 forward	GTAAAACGACGGCCAG
M13 reverse	CAGGAAACAGCTATGAC

Table 5.10: Names and sequences of primers used for sequencing of inserts cloned into pENTR/D/TOPO vector

5.5.3.1.7. Gateway recombination to pMDC163 vector

pENTR/D/TOPO plasmids with verified inserts were recombined with pMDC163 binary vector. As both plasmids have kanamycin as a selection marker, it was necessary to digest pENTR/D/TOPO before recombination as it could cause a con*tam*ination by growing on plates with recombined plasmids. pENTR/D/TOPO was therefore digested overnight with enzyme that cuts vector backbone outside of att recombination sites and insert according to protocol described in chapter 5.5.3.1.5. Fragment containing insert and att sites was purified from gel with QIAEXII Gel Extraction Kit (Qiagen) according to manufacturer's instructions and dissolved in 1 x TE buffer (10mM Tris-Cl, 1mM EDTA pH 8.0). Concentration of isolated fragment of entry vector and destination vector was measured with NanoDrop spectrophotometer (ThermoScientific) and adjusted to approximately 150 ng/µl either with water or by concentration plasmid with additional precipitation. Recombination reaction was performed in 5

µl total volume and consisted of 1 µl of purified insert, 1 µl of destination vector, 2µl of 1 x TE buffer (10mM Tris-Cl, 1mM EDTA pH 8.0) and 1 µl of Gateway® LR Clonase® II enzyme mix (Invitrogen). Reaction was incubated for 1- 2 hours at room temperature and afterwards stopped by addition of 1 µl of proteinase K and incubation at 37 °C for 10 minutes at room temperature. Whole reaction was transformed by heat-shock to *E. coli* GT116 cells (InvivoGen) as described in chapter 5.5.3.1.3. Clones were verified again by restriction digest and fusion between the gene of interest and GUS was verified by sequencing with GUS-1 primer (TCCCACCAACGCTGATCAAT)

5.5.4. Cloning of CYCLIN B : GUS constructs

5.5.4.1.1. PCR amplification of inserts

PCR amplification of inserts followed the same protocol as in case of cloning of TAM:GUS and TDM1:GUS constructs. Inserts were amplified with iProof Polymerase (BioRad) as described in chapter 5.5.3.1.1. Conditions for particular constructs are in table 5.11 and primer sequences in table 5.12.

Gene	Primers	Product length	PCR conditions	
			Annealing temperature	Extension
CycB1;2	B12For(SdaI) + B12Rev(NheI)	2827 bp	62 °C	1:30 min.
CycB1;3	B13For(SdaI) + B13Rev(NheI)	3130 bp	62 °C	1:30 min.
CycB1;4	B14For(SdaI) + B14Rev(NheI)	4420 bp	67 °C	2:30 min.
CycB1;5	B15For(SdaI) + B15Rev(NheI)	7365 bp	60 °C	3:30 min.
CycB2;1	B21For(SdaI) + B21Rev(NheI)	4675 bp	67 °C	2:30 min.
CycB2;2	B22For(SdaI) + B22Rev(NheI)	3548 bp	64 °C	2:00 min.
CycB2;3	B23For(SdaI) + B23Rev(NheI)	4809 bp	64 °C	2:30 min.
CycB2;4	B24For(SdaI) + B24Rev(NheI)	3265 bp	66 °C	2:00 min.
CycB2;5	B25For(SdaI) + B25Rev(NheI)	1931 bp	63 °C	2:30 min.
CycB3;1	B31For(SdaI) + B31Rev(NheI)	4583 bp	64 °C	1:30 min.

Table 5.11: Conditions for amplification of CYCLIN Bs fragment for cloning: names of primers, product length and PCR conditions

Primer name	Primer sequence in 5´ - 3´direction (restriction site is underlined)
B12For(SdaI)	CCTGCAGGTGTAAGAATCAATCACTAAAGTTTTCA
B12Rev(NheI)	GCTAGCAGAAGAAACAGGCTTCTTCCAAT
B13For(SdaI)	CCTGCAGGTGTTTAGGAAAAAGTTTAATTCAT
B13Rev(NheI)	GCTAGCTGGAGCAGATGACATAAGAGA
B14For(SdaI)	CCTGCAGGAAACCCGTCAATTCTACGATT
B14Rev(NheI)	GCTAGCTGCACAAGAAACAGAGAAGT
B15For(SdaI)	CCTGCAGGTCTCTCCTTTTCCCATCTCTTC
B15Rev(NheI)	GCTAGCGATCTTCTTTGCAGCTAAACACT
B21For(SdaI)	CCTGCAGGATGTCGGGTCAAAAGTGCCTAA
B21Rev(NheI)	GCTAGCAGAATGATGAGACTCAGACACTA
B22For(SdaI)	CCTGCAGGTCGCACTTTAGTCTAGGGATTG
B22Rev(NheI)	GCTAGCGTGAGAATCTGACACAAGAAAGT
B23For(SdaI)	CCTGCAGGTCACTTGTAGGATTACTCAT
B23Rev(NheI)	GCTAGCAATCAGAAACCCAGCTGGTTCAGTT
B24For(SdaI)	CCTGCAGGTCTTCACCGGAATTGTTTTTGA
B24Rev(NheI)	GCTAGCCAGCAGAAGAAACCCAGCT
B25For(SdaI)	CCTGCAGGTCGATCTCTCACGTTCTCTCTAT
B25Rev(NheI)	GCTAGCCTTATTATAGTTTTTTCCTCCCT
B31For(SdaI)	CCTGCAGGAACAGTGAGTACTAGGAGTT
B31Rev(NheI)	GCTAGCGAGAGGGAGTTTATCTAAGGGC

Table 5.12: Names and sequences of primers used for amplification of CYCLIN Bs products for cloning

5.5.4.1.2. Cloning to pCR2.1 TOPO vector

As already described for cloning to pENTR/D/TOPO, 2µl of PCR reaction were checked on a agarose gel. For samples containing single strong band of expected size the PCR reaction was used further, if case of several bands, the expected band was purified from gel with QIAEXII Gel Extraction Kit (Qiagen) according to manufacturer's instructions. Cloning to pCR2.1 TOPO is based on topoisomerase catalyzed reaction between 3´T overhangs in vector and 3´A overhangs on PCR products. To add adenines at 3´ ends of the PCR product, 0,2 µl of home-made Taq

polymerase was added to samples, in case of purified fragment from a gel and also 1 µl of 10 mM dNTPs and samples were incubated at 72 °C for 10 minutes in a thermal cycler. Topoisomerase cloning reaction consisted of 4,8 µl of PCR reaction or purified PCR product after addition of 3´adenines, 1 µl of salt solution and 0,2 µl of pCR2.1 TOPO vector (both Invitrogen). Reaction was incubated at 25 °C for 30 minutes and then transformed to *Escherichia coli* TOP10F´ cells as described in chapter 5.5.3.1.3.
Presence of inserts in clones was examined by restriction digest as described in chapter 5.5.3.1.5. Selected plasmids were sequenced with T7 and TOPO-1 primers (table 5.13) according to protocol described in chapter 5.5.3.1.6.

Primer name	**Primer sequence in 5´ - 3´direction**
T7	TAATACGACTCACTATAGGG
TOPO-1	ATGATTACGCCAAGCTTGGTA

Table 5.13: Names and sequences of primers used for sequencing of inserts cloned into pCR2.1 TOPO vector

5.5.4.1.3. Restriction cloning to pCBK04 vector

Verified inserts were subcloned from pCR2.1 TOPO plasmids to pCBK04 by restriction cloning. As both plasmids contain kanamycin as a selection marker and some of cyclin genes have bigger size than vector backbone, it was necessary to digest pCR2.1 TOPO backbone as it could be self-ligated during cloning and cause a con*tam*ination by growing on plates with pCBK04 plasmids. Therefore, all pCR2.1 TOPO plasmids containing cyclin gene were digested with BglI enzyme (New England Biolabs) that cuts twice in vector backbone but not in any of inserts.
Verified pCR2.1 TOPO plasmids were digested with SbfI, NheI and BglI enzymes in one reaction overnight. Reaction consisted of 2-3 µg of plasmid DNA, 2 µl of 10x NEB buffer 4, 0,1 µl of 10 mg/ ml BSA (both New England Biolabs), nuclease-free water up to 17 µl, 1µl of 10u/µl SbfI, 1µl of 10u/µl of NheI and 1µl of 10u/µl BglI (all enzymes from New England Biolabs). Reaction was incubated at 37°C overnight. Restriction fragments were then separated on 1% agarose gel and fragment containing insert was extracted using QIAEXII Gel Extraction Kit (Qiagen) according to manufacturer's instructions. pCBK04 plasmid is a low-copy number, therefore plasmids from 5 isolations were pooled together. For restriction digest 2-3 µg of plasmid DNA, 2 µl of 10x Tango buffer (Fermentas), nuclease-free water up to 18,5 µl, 1µl of

10u/µl PstI, 0,5 µl of 10u/µl of XbaI (Fermentas) were pipetted together and incubated overnight 37°C. Next day samples were treated 1 µl of 1u/µl shrimp alkaline phosphatase (SAP, Fermentas) for 30 minutes at 37°C. Reaction was stopped by heating to 65°C for 15 minutes. Reaction was then run on a 1% agarose gel with ethidium bromide and appropriate band containing vector backbone was extracted using QIAEXII Gel Extraction Kit (Qiagen) according to manufacturer's instructions. Eluted insert and vector fragments were compared on agarose gel by running 1 µl of each sample side by side. Ligation was performed with 1:1 – 3:1 ratio of insert : vector DNA, 2 µl of 10 x T4 DNA Ligation buffer (Fermentas), water up to 19 µl and 1 µl of T4 DNA ligase (Fermentas) either for 1 hour at room temperature or at 4 °C overnight. Reaction was then transformed by heat-shock to *E. coli* TOP10F´cells as described in chapter 5.5.3.1.3 and cells were plated on LB plates with 50 mg/ ml kanamycin. Single colonies were verified by restriction digest and sequencing.

5.5.5. Electroporation of plasmid to *Agrobacterium tumefaciens*

Verified plasmids were transformed to *Agrobacterium tumefaciens* GV3101 strain. Competent *Agrobacterium* cells were thaw on ice, 1 µl of plasmid was added and the content of a tube was mixed with pipette tip. Agrobacterium suspension was pipetted into to a pre-cooled Gene Pulser Cuvette (BioRad) on ice, and all bubbles were removed by gently tapping on cuvette. Cuvette was then inserted into BioRad Gene Pulser X-Cell PC module (BioRad) adjusted to 400 Ω, 25 µF and 2.5 kV and pulsed for 10 ms. Cells were then mixed with 0,9 ml of LB medium without antibiotics, they were transferred back to original tube and let stand on room temperature for 1 hour. 100 µl of cell suspension was then plated on LB plates with appropriates antibiotics (50 mg/ml gentamycin and 50 mg/ml kanamycin for all constructs) and they were let grow for 3 days at 28°C. Presence of plasmid was checked by PCR on colonies. Eventually, a glycerol stock was made in the same way as described for *E. coli* cells in 5.5.3.1.4.

5.5.6. Transformation of plants with *Agrobacterium tumefaciens*

A single colony of *A. tumefaciens* harbouring individual constructs was inoculated to 5 ml of LB medium with appropriate antibiotics (for all constructs: 50 mg/ml gen*tam*ycin and 50 mg/ml kanamycin) and grown overnight at 28°C with shaking. Next day 1 ml of starter culture was used to inoculate 500ml LB medium with antibiotics and culture was again grown overnight at 28°C with shaking. Bacteria were harvested by centrifugation at 2831 rcf (4000 rpm) in Avanti J-26 XP centrifuge (Beckman Coulter) at 4°C for 10 minutes and resuspended in 250 ml water with

5% sucrose and 200µl/L Silwett 77 (Lehle Seeds). 3 weeks old healthy plants either TAM-2+/- for TAM:GUS construct, TDM1-4+/- for TDM1:GUS or WT Col0 for CYCLIN B:GUS lines were used fro transformation. In a day of first transformation, all silliques were cut off. Plants were dipped into resuspended *Agrobacterium* cells for 30 seconds. Transformation was repeated after 3-4 days. In between transformation and 3 days after, plants were kept lying in a tray which was covered with transparent plastic lid. Afterwards, plants were grown in standard conditions and seeds were harvested.

5.5.7. Selection of representative plant lines

Transformed plants were selected on Grodan (Delta Technology) according to (Hadi et al. 2002). Grodan was cut into pieces of appropriate size and autoclaved for 20 minutes at 125 °C. Autoclaved pieces of Grodan were placed into a tray and soaked with water supplement with ½ MS with vi*tam*ins (Duchefa) and either 5 mg/l hygromycin (Calbiochem) for pMDC163 based constructs or 20 mg/ml BASTA (phosphinotricin) for pCBK04 based constructs. Seeds from transformed plants were spread on a surface and let growing for three weeks. Resistant seedlings were than transferred with forceps to soil. At least 15 different resistant seedlings were transferred for each construct, only for *CYCLIN B2;2* there were only 8 seedling resistant. TDM1:GUS plants were genotyped for endogenous *tdm1-4* allele. Seeds from individual F1 plants were harvested and grown on ½ MS plates either with 10 mg/l hygromycin or 10 mg/l BASTA as described in chapter 5.1.2. A segregation ration between resistant and sensitive plants was counted for every plant line. Few resistant seedlings were then transferred to a GUS staining solution and stained as described in chapter 5.7. Other 8-10 resistant seedlings were transferred to a soil and grown to maturity. Inflorescences were stained with GUS - staining protocol. In case of strong staining,
4 representative lines were selected with the segregation ratio as close to 3:1 for resistant: sensitive plants (therefore most likely heterozygous for one construct). Seeds from each plant were segregated in T3 generation to obtain homozygous plants and these lines were used for further work. In case of weak staining, it was not possible to choose a representative line; therefore all lines were processed further.

5.6. Alexander staining

Alexander staining (Alexander 1969) was used to differentiate viable and non-viable pollen

grains. 2 biggest unopened buds from inflorescence were cut off with forceps and transferred to a drop of 1x Alexander staining solution (50x stock: 10 ml of 95% Ethanol, 1 ml of 1% malachite green in 95% ethanol, 50 ml of distilled water, 25 ml of glycerol, 5 g of phenol, 5g of chloral hydrate, 5 ml of acid fuschsin 1% in water, 0,5 ml of Orange G 1% in water, 2 ml of acetic acid). Anthers were dissected out and the rest of bud was discarded. Slides were covered with cover slips, sealed with glue and incubated at 50°C for 24 hours. Slides were then examined under Leica MZ6 stereomicroscope (Leica).

5.7. Histochemical GUS staining

For detection of GUS fusion proteins, 12 days old seedlings and inflorescences were infiltrated with GUS staining buffer (50mM Na-phosphate buffer pH 7, 10mM EDTA pH8, 0,1% Triton-X-100, 2mM potassium ferricyanide ($K_3(Fe(CN)_6)$ and 1mM X-Gluc) and incubated at 37˚C. Length of incubation varied, based on the strength of expression of particular construct. Afterwards, samples were washed in ethanol series (20%, 35%, 50%) for 30 minutes each at room temperature, post fixed with FAA (50% ethanol, 10% acetic acid and 5% formaldehyde) for 30 minutes and washed in 70% ethanol for 1 hour.

5.8. Transpiration stream delivery

Stems of young plants were cut with scissors (stem length was more than 5 cm) and transferred immediately into water. Leaves and silliques were removed from stems by cutting. Stems measured, submerged under water and cut to length of 5 cm with a sharp razor blade. They were carefully transferred to a small glass bottle with water, and when all samples were ready, water was exchanged with treatment solution. Particular conditions of incubation are described in chapter 2.1. In brief, samples were incubated for 2, 4 or 6 hours with spindle inhibitors - oryzalin, 8-hydroxyquinoline, colchicine, nocodazol, propyzamide or their combination (all provided by Dr. Boris Vyskot, Brno, Czech republic or purchased from Sigma- Aldrich). Treatment with cold was done in water in cold room at 4 °C under standard light conditions for 6, 8 or 24 hours. Combined treatment with cold and 2,5 mM 8-hydroquinoline was also done in cold room for 2, 4 or 6 hours. After treatment inflorescences were fixed in 3:1 mixture of ethanol: acetic acid under vacuum and stored at – 20 °C until preparation of slides. Slides were prepared as described in chapter 5.9.1 by squashing young buds to score effects on mitosis or from anthers from young buds to score effects on meiosis

5.9. Cytogenetic analysis

5.9.1. Preparation of slides for scoring mitotic and meiotic stages

Inflorescences were fixed in 3:1 ethanol: acetic acid, infiltrated with vacuum for 30 minutes and fixative was several times replaced. Fixed inflorescences were stored at – 20°C until preparation of slides. Prior preparations of slides, samples were washed two times in water and three times with 1 x citrate buffer (4 mM citric acid, 6 mM tri-sodium citrate, pH4.6) for 10 minutes. Samples were digested in enzymatic mixture of 0.5% cellulose and 0.5% pectolyase in 1x citrate buffer at 37 °C for 45-90 minutes according to batch of enzymes. Enzymatic mixture was than washed 3 times with 1x citrate buffer. Inflorescences were then transferred to a drop of 45% acetic acid. For preparation of mitotic cells, pistils and anthers were dissected from unopened floral buds. For preparation of meiotic cells anthers were dissected from buds 0.2-0.5 mm in length. Dissected anthers and pistils were covered by a cover slip; cells were spread by tapping with rubber gum on a pencil and finally specimens were gently squashed. Slides were dipped liquid nitrogen and cover slip was removed Slides were air-dried and chromatin was stained and mounted in 1µg/ml DAPI in Vectashield mounting medium (Vector Laboratories). Samples were examined under Zeiss Axioscope fluorescence microscope (Zeiss) equipped with a cooled CCD camera (Visitron). Pictures were acquired and analyzed using MetaVue software (Universal Imaging Corporation) Zeiss.

5.9.2. Preparation of slides for detection of CDKA:YFP and immunodetection from inflorescences

Inflorescences were fixed in 3,7% formaldehyde in PEM buffer (50 mM PIPES pH 6.9, 5 mM EGTA pH 8.0, 5 mM $MgSO_4$, 0.1 % Triton X-100) for 15 minutes under vacuum and then for 45 minutes at 4°C. Inflorescences were then washed three times for 10 minutes in PEM buffer and transferred to a slide coated with 1% gelatine. For preparation of mitotic cells, pistils and anthers were dissected from unopened floral buds, for preparation of meiotic cells anthers were dissected from buds 0.2-0.5 mm in length. Slides were then covered with cover slips and cells were spread with rubber gum tapping and squashing. Cells were frozen to slides in liquid nitrogen and cover slip was removed with sharp razor blade. Slides were air-dried for 30-60 minutes and then rehydrated in PEM buffer. Cell walls were digested with of 1.4% beta-glucuronidase (w/v), 7% sucrose (w/v) in PEM buffer for 30 minutes at room temperature. Slides were covered with parafilm and kept in moist chamber during digestion. Enzymes were washed out by incubation of

slides in coplin jars with PEM buffer, three times 10 minutes. In case of immunodetection, immediately followed blocking of slides (see chapter 5.9.4). For CDKA;1:YFP detection, slides were stained and mounted in 1µg/ml DAPI in Vectashield mounting medium (Vector Laboratories) and examined within two days under Zeiss Axioscope fluorescence microscope (Zeiss) equipped with a cooled CCD camera (Visitron). Pictures were acquired and analyzed using MetaVue software (Universal Imaging Corporation) Zeiss.

5.9.3. Preparation of slides for immunodetection in cells from roots

Squashes of root tips were prepared from 12 days old seedlings grown on plates. Plantlets were carefully released from plates and roots were fixed in 3,7% formaldehyde in PEM buffer for 15 minutes under vacuum. After carefully washing roots with three times for 10 minutes in PEM buffer, roots were transferred to a gelatine coated slide, root tips were separated with forceps and the rest of roots were discarded. Next steps were done according to protocol for inflorescences but for enzymatic digestion was used 2% driselase in 1x PEM buffer for 30 minutes at 37 °C.

5.9.4. Immunodetection

Slides prepared from formaldehyde-fixed material were used immediately after enzymatic digest and washing. Conditions for blocking, primary and secondary antibodies and conditions for incubations are listed in table 5.14. Slides were blocked with 3-10% BSA in PEM buffer for 1 hour at room temperature. Blocking and all other solutions were applied on specimens, covered with parafilm and slides were kept during all incubations in moist chamber. Immediately after blocking was applied primary antibody diluted in blocking solution and incubated overnight at 4°C. Antibody was washed out with PEM buffer three times for 5 minutes. Afterwards was applied secondary antibody diluted in 3% BSA in PEM and slides were incubated for 2 hours at room temperature. Slides were again washed three times 5 minutes with PEM buffer. Slides were then slides were stained and mounted in 1µg/ml DAPI in Vectashield mounting medium (Vector Laboratories) and examined within two days under Zeiss Axioscope fluorescence microscope (Zeiss) equipped with a cooled CCD camera (Visitron). Pictures were acquired and analyzed using MetaVue software (Universal Imaging Corporation) Zeiss.

Antibody	Blocking	Dilution (in blocking solution)	Detection with secondary antibody
Anti Phospho-CDK2 (Thr160) (Cell Signaling Technology)	10% BSA	1:50; with 100µg/ml non - phosphorylated blocking peptide	Anti rabbit-CY3
Anti β-glucuronidase (Molecular Probes, Invitrogen)	3 % BSA	1:200	Anti rabbit-FITC
Anti alpha-tubulin (Serotec)	3% BSA	1:50	Anti rat-CY3
Anti histone H3 Ser10phospho (Upstate Biotechnology)	3% BSA	1:200	Anti rabbit-FITC
Anti rabbit-CY3 (Jackson ImmunoResearch)	3% BSA	1:2000	
Anti rabbit-FITC (Sigma Aldrich)	3% BSA	1:200	
Anti rat-CY3 (Chemicon)	3% BSA	1:500	

Table 5.14: Antibodies used in this study: conditions for blocking, dilution and eventually detection with secondary antibody.

5.10. Analysis of ploidy

Inflorescences of 4-5 weeks old plants were chopped with a sharp razor blade in 250 µl CyStain UV Precise P nuclei extraction buffer and mixed with 750µl of CyStain UV Precise P Staining buffer containing propidium iodide (both Partec). Released nuclei were purified by sieving through CellTrics filter columns (Partec). Fluorescence of the nuclei was measured by CyFlow space (Partec).

5.11. Protein analysis

5.11.1. Protein extraction

Proteins were extracted according to (Peck 2006). Plant tissues was crushed in liquid nitrogen and mixed with extraction buffer for phosphorylated proteins (50mM HEPES-KOH pH7.5, 5% glycerol, 50mM sodium pyrophosphate, 1mM sodium molybdate, 25mM sodium fluoride, 10mM EDTA, 0,5% PVP, 1% Triton-X-100, 150mM NaCl and immediately before use were added Complete Protease Inhibitor Cocktail Tablets and PhosSTOP Phosphatase Inhibitor Cocktail Tablets (both from Roche)). Extracts were centrifuged for 10 minutes at 16,000 rcf (14 000 rpm) at 4°C and the supernatant containing proteins was transferred to a new tube. Protein concentration was estimated with Qubit quantification platform (Invitrogen). System was calibrated with BSA standards and used according to manufacturers instructions. 1µl of Quant-iT Protein reagent was mixed with 199 µl of Quant-iT Protein buffer to prepare working solution. 1 µl of RNA sample was mixed with 199 µl of working solution, shortly vortexed and incubated for 15 minutes at room temperature. Sample concentration was then measured on Qubit fluorometer.

5.11.2. Western blot

50 µg of total proteins were run on 10% polyacrylamide gel (10% Acrylamide/Bisacrylamide, 0,375 M Tris-Cl pH 8.7, 0,1% SDS, 0,1% APS, 0,1% Temed; Stacking gel: 5% Acrylamide/Bisacrylamide, 0,125 M Tris-Cl pH6.8, 0,1% SDS, 0,1% APS, 0,1% Temed) at 150V for 90 minutes in 1x protein electrophoresis buffer (6,2 mM Tris base, 48 mM Glycine, 0,25% SDS). Gel was then washed with distilled water and soaked in transfer buffer (190 mM Glycine, 25 mM Tris, 20 % methanol) together with filter papers. PVDF transfer membrane (Thermo Scientific #88518) was soaked for 15 seconds in methanol, washed with water and also soaked in transfer buffer. Transfer sandwich was built up from gel, membrane, filter papers and fiber pads and fixed in Mini Trans-Blot transfer cell filled with transfer buffer. Transfer was done at 420 mA for 1 hour at 4°C. Membrane was washed in 1x TBS-T buffer (136 mM NaCl, 2,7 mM KCl, 24 mM Tris, 0,5% Tween-20, pH7.4).

Detection of total CDKA;1 *and* KU70

Membrane was blocked in 1% milk in TBS-T for 1 hour at room temperature. To detect total CDKA;1, membrane was incubated with anti-PSTAIR antibody (Sigma Aldrich) diluted 1:5000 in 1% milk in TBS-T buffer overnight at 4˚C with shaking. KU70 was detected with anti-AtKU70 antibodies (Zellinger and Riha, unpublished) diluted 1:30 000 in 1% milk in TBS-T overnight at 4˚C with shaking. Both antibodies were washed with TBS-T 3x10 minutes. To detect anti-PSTAIR antibody, membrane was incubated with Anti-Mouse IgG + IgM, (H+L), conjugated to HRP (Pierce) diluted 1:50000 in 1% milk in TBS-T. For KU70 detection, anti-Rabbit IgG, (H+L), conjugated to HRP (Pierce) secondary antibody was diluted 1:100 000 in 1% milk in TBS-T and incubated with membrane for 2 hours at room temperature with shaking. Membrane was washed 3x10 minutes with TBS-T and incubated with ECL Western Blotting Substrate (Pierce) for 5 minutes and then exposed to Hyperfilm ECL (Amersham).

Detection of phosphorylated CDKA;1 *on threonine 161*

For detection of CDKA;1 Thr161(p), membrane was blocked in 5-10% BSA (depending on batch of antibody) in 1x TBS-T for 1 h at room temperature. Anti-Phospho-CDK2 (Thr160) Antibody (Cell Signalling Technology) was diluted 1:1000 in blocking solution and incubated with membrane overnight at 4˚C with shaking. Membrane was washed in TBS-T 3 x 10 minutes and incubated with Anti-Rabbit IgG, (H+L), conjugated to HRP (Pierce) secondary antibody diluted 1:100 000 in 1% milk in TBS-T and incubated with membrane for 2 hours at room temperature with shaking. Membrane was then processed as described above.

9.1.1. Antibody specificity testing with competitive peptides

To confirm specificity of Thr161 phospho detection antibody was mixed with 1, 10 or 100 µg/ml of non-phosphorylated blocking peptide (GIP VRT FTH EVV TLW) or phosphorylated blocking peptide **(**GIP VRT FT(PO3H2)H EVV TLW) (both synthesized by Eurogentec) 30 minutes before incubation with membrane.

3.4.1. Phosphatase treatment

WT and CDKA;1:YFP total proteins were isolated from flowers as described above with or

without PhosSTOP Phosphatase Inhibitor Cocktail Tablets. Extracts containing 400 µg of total protein (WT) and 200 µg of total protein (CDKA;1:YFP) were incubated with 1200 units of Lambda Protein Phosphatase (New England Biolabs) for 0 or 60 minutes at 30 ˚C. Reaction was stopped by addition of 2 x SDS loading buffer and boiling 5 min 95 ˚C. Proteins were resolved on 10% SDS-PAGE gel and detected by Western blotting as described above.

3.5. *In silico* analysis

All sequences of genes were down-loaded from NCBI web page (http://www.ncbi.nlm.nih.gov/), sequences of commercial vectors were provided by manufacturing companies. Sequences were annotated and processed in SeqBuilder program (DNASTAR), pairwise and multiple alignments of 2-4 sequences were performed in MegAlign program (DNASTAR).

3.5.1. Annotation of *Arabidopsis lyrata* B-type cyclins

All searches in *Arabidopsis lyrata* genome were performed on DOE Joint Genome Institute web page (http://genome.jgi-psf.org/Araly1/Araly1.home.html). *Arabidopsis lyrata* cyclin genes were identified in a TBLASTN search (Altschul et al. 1990; Gertz et al. 2006) using individual *Arabidopsis thaliana* cyclin B protein sequences as a query against *Arabidopsis lyrata* v1.0 all model transcripts database. To uncover possible pseudogenes, a BLASTN search was performed against *Arabidopsis lyrata* v1.0 assembly scaffolds with individual cyclin B genomic sequences from *Arabidopsis lyrata*. All searches were performed with BLOSUM62 scoring matrix and low complexity region filter.

6. REFERENCEES

Alexander MP (1969) Differential staining of aborted and nonaborted pollen. Stain Technol 44(3): 117-122.

Altschul SF, Gish W, Miller W, Myers EW, Lipman DJ (1990) Basic local alignment search tool. J Mol Biol 215(3): 403-410.

Armstrong SJ, Jones GH (2001) Female meiosis in wild-type Arabidopsis thaliana and in two meiotic mutants. Sexual Plant Reproduction 13(4): 177-183.

Armstrong SJ, Jones GH (2003) Meiotic cytology and chromosome behaviour in wild-type Arabidopsis thaliana. J Exp Bot 54(380): 1-10.

Armstrong SJ, Franklin FCH, Jones GH (2001) Nucleolus-associated telomere clustering and pairing precede meiotic chromosome synapsis in Arabidopsis thaliana. Journal of Cell Science 114(23): 4207-4217.

Armstrong SJ, Franklin FCH, Jones GH (2003) A meiotic time-course for Arabidopsis thaliana. Sexual Plant Reproduction 16(3): 141-149.

Atwell S, Huang YS, Vilhjalmsson BJ, Willems G, Horton M et al. Genome-wide association study of 107 phenotypes in Arabidopsis thaliana inbred lines. Nature 465(7298): 627-631.

Avedisov SN, Krasnoselskaya I, Mortin M, Thomas BJ (2000) Roughex mediates G(1) arrest through a physical association with cyclin A. Mol Cell Biol 20(21): 8220-8229.

Avedisov SN, Rogozin IB, Koonin EV, Thomas BJ (2001) Rapid evolution of a cyclin A inhibitor gene, roughex, in Drosophila. Mol Biol Evol 18(11): 2110-2118.

Averbeck N, Sunder S, Sample N, Wise JA, Leatherwood J (2005) Negative control contributes to an extensive program of meiotic splicing in fission yeast. Molecular Cell 18(4): 491-498.

Azumi Y, Liu DH, Zhao DZ, Li WX, Wang GF et al. (2002) Homolog interaction during meiotic prophase I in Arabidopsis requires the SOLO DANCERS gene encoding a novel cyclin-like protein. Embo Journal 21(12): 3081-3095.

Bai C, Richman R, Elledge SJ (1994) Human cyclin F. Embo J 13(24): 6087-6098.

Bai C, Sen P, Hofmann K, Ma L, Goebl M et al. (1996) SKP1 connects cell cycle regulators to the ubiquitin proteolysis machinery through a novel motif, the F-box. Cell 86(2): 263-274.

Banihashemi L, Wilson GM, Das N, Brewer G (2006) Upf1/Upf2 regulation of 3' untranslated region splice variants of AUF1 links nonsense-mediated and A+U-rich element-mediated mRNA decay. Mol Cell Biol 26(23): 8743-8754.

Barkoff A, Ballantyne S, Wickens M (1998) Meiotic maturation in Xenopus requires polyadenylation of multiple mRNAs. Embo J 17(11): 3168-3175.

Barkoff AF, Dickson KS, Gray NK, Wickens M (2000) Translational control of cyclin B1 mRNA during meiotic maturation: coordinated repression and cytoplasmic polyadenylation. Dev Biol 220(1): 97-109.

Bell SP, Dutta A (2002) DNA replication in eukaryotic cells. Annu Rev Biochem 71: 333-374.

Belloc E, Mendez R (2008) A deadenylation negative feedback mechanism governs meiotic metaphase arrest. Nature 452(7190): 1017-1021.

Belloc E, Pique M, Mendez R (2008) Sequential waves of polyadenylation and deadenylation define a translation circuit that drives meiotic progression. Biochem Soc Trans 36(Pt 4): 665-670.

Blom N, Gammeltoft S, Brunak S (1999) Sequence and structure-based prediction of eukaryotic protein phosphorylation sites. J Mol Biol 294(5): 1351-1362.

Booher R, Beach D (1988) Involvement of cdc13+ in mitotic control in Schizosaccharomyces pombe: possible interaction of the gene product with microtubules. Embo J 7(8): 2321-2327.

Borg M, Twell D (2010) Life after meiosis: patterning the angiosperm male gannetophyte. Biochemical Society Transactions 38: 577-582.

Borgne A, Murakami H, Ayte J, Nurse P (2002) The G1/S cyclin Cig2p during meiosis in fission yeast. Mol Biol Cell 13(6): 2080-2090.

Bousset K, Diffley JF (1998) The Cdc7 protein kinase is required for origin firing during S phase. Genes Dev 12(4): 480-490.

Cardozo T, Pagano M (2004) The SCF ubiquitin ligase: insights into a molecular machine. Nat Rev Mol Cell Biol 5(9): 739-751.

Carlile TM, Amon A (2008) Meiosis I is established through division-specific translational control of a cyclin. Cell 133(2): 280-291.

Chaudhury AM, Lavithis, M.,Taylor, P. E.,Craig, S.,Singh, M. B.,Signer, E. R.,Knox, R. B.,Dennis, E. S. (1994) Genetic control of male fertility in Arabidopsis thaliana: structural analysis of premeiotic developmental mutants. Sexual Plant Reproduction 7: 17-28.

Chevalier S, Couturier A, Chartrain I, Le Guellec R, Beckhelling C et al. (1996) Xenopus cyclin E, a nuclear phosphoprotein, accumulates when oocytes gain the ability to initiate DNA replication. J Cell Sci 109 (Pt 6): 1173-1184.

Chu T, Henrion G, Haegeli V, Strickland S (2001) Cortex, a Drosophila gene required to complete oocyte meiosis, is a member of the Cdc20/fizzy protein family. Genesis 29(3): 141-152.

Clifford DM, Wolfe BA, Roberts-Galbraith RH, McDonald WH, Yates JR, 3rd et al. (2008a) The Clp1/Cdc14 phosphatase contributes to the robustness of cytokinesis by association with anillin-related Mid1. J Cell Biol 181(1): 79-88.

Clifford DM, Chen CT, Roberts RH, Feoktistova A, Wolfe BA et al. (2008b) The role of Cdc14 phosphatases in the control of cell division. Biochem Soc Trans 36(Pt 3): 436-438.

Colon-Carmona A, You R, Haimovitch-Gal T, Doerner P (1999) Technical advance: spatio-temporal analysis of mitotic activity with a labile cyclin-GUS fusion protein. Plant J 20(4): 503-508.

Connolly T, Beach D (1994) Interaction between the Cig1 and Cig2 B-type cyclins in the fission yeast cell cycle. Mol Cell Biol 14(1): 768-776.

Cross FR, Yuste-Rojas M, Gray S, Jacobson MD (1999) Specialization and targeting of B-type cyclins. Mol Cell 4(1): 11-19.

Curtis MD, Grossniklaus U (2003) A gateway cloning vector set for high-throughput functional analysis of genes in planta. Plant Physiol 133(2): 462-469.

D'Angiolella V, Donato V, Vijayakumar S, Saraf A, Florens L et al. (2010) SCF(Cyclin F) controls centrosome homeostasis and mitotic fidelity through CP110 degradation. Nature 466(7302): 138-142.

d'Erfurth I, Jolivet S, Froger N, Catrice O, Novatchkova M et al. (2009) Turning meiosis into mitosis. PLoS Biol 7(6): e1000124.

d'Erfurth I, Jolivet S, Froger N, Catrice O, Novatchkova M et al. (2008) Mutations in AtPS1 (Arabidopsis thaliana parallel spindle 1) lead to the production of diploid pollen grains. PLoS Genet 4(11): e1000274.

d'Erfurth I, Cromer L, Jolivet S, Girard C, Horlow C et al. (2010) The CYCLIN-A CYCA1;2/TAM Is Required for the Meiosis I to Meiosis II Transition and Cooperates with OSD1 for the Prophase to First Meiotic Division Transition. Plos Genetics 6(6): -.

Dahmann C, Diffley JF, Nasmyth KA (1995) S-phase-promoting cyclin-dependent kinases prevent re-replication by inhibiting the transition of replication origins to a pre-replicative state. Curr Biol 5(11): 1257-1269.

De Wulf P, Montani F, Visintin R (2009) Protein phosphatases take the mitotic stage. Curr Opin Cell Biol 21(6): 806-815.

Deibler RW, Kirschner MW (2010) Quantitative reconstitution of mitotic CDK1 activation in somatic cell extracts. Mol Cell 37(6): 753-767.

den Elzen N, Pines J (2001) Cyclin A is destroyed in prometaphase and can delay chromosome alignment and anaphase. J Cell Biol 153(1): 121-136.

Di Fiore B, Pines J (2010) How cyclin A destruction escapes the spindle assembly checkpoint. J Cell Biol 190(4): 501-509.

Dirick L, Goetsch L, Ammerer G, Byers B (1998) Regulation of meiotic S phase by Ime2 and a Clb5,6-associated kinase in Saccharomyces cerevisiae. Science 281(5384): 1854-1857.

Dissmeyer N, Nowack MK, Pusch S, Stals H, Inze D et al. (2007) T-loop phosphorylation of Arabidopsis CDKA;1 is required for its function and can be partially substituted by an aspartate residue. Plant Cell 19(3): 972-985.

Donaldson AD, Fangman WL, Brewer BJ (1998) Cdc7 is required throughout the yeast S phase to activate replication origins. Genes Dev 12(4): 491-501.

Donovan JD, Toyn JH, Johnson AL, Johnston LH (1994) P40SDB25, a putative CDK inhibitor, has a role in the M/G1 transition in Saccharomyces cerevisiae. Genes Dev 8(14): 1640-1653.

Ducommun B, Brambilla P, Felix MA, Franza BR, Jr., Karsenti E et al. (1991) cdc2 phosphorylation is required for its interaction with cyclin. Embo J 10(11): 3311-3319.

Duesbery NS, Vande Woude GF (1998) Cytoplasmic control of nuclear behavior during meiotic maturation of frog oocytes. Biol Cell 90(6-7): 461-466.

Elledge SJ (1996) Cell cycle checkpoints: preventing an identity crisis. Science 274(5293): 1664-1672.

Epstein CB, Cross FR (1992) CLB5: a novel B cyclin from budding yeast with a role in S phase. Genes Dev 6(9): 1695-1706.

Evans T, Rosenthal ET, Youngblom J, Distel D, Hunt T (1983) Cyclin: a protein specified by maternal mRNA in sea urchin eggs that is destroyed at each cleavage division. Cell 33(2): 389-396.

Fang G, Yu H, Kirschner MW (1999) Control of mitotic transitions by the anaphase-promoting complex. Philos Trans R Soc Lond B Biol Sci 354(1389): 1583-1590.

Feldman RM, Correll CC, Kaplan KB, Deshaies RJ (1997) A complex of Cdc4p, Skp1p, and Cdc53p/cullin catalyzes ubiquitination of the phosphorylated CDK inhibitor Sic1p. Cell 91(2): 221-230.

Ferby I, Blazquez M, Palmer A, Eritja R, Nebreda AR (1999) A novel p34(cdc2)-binding and activating protein that is necessary and sufficient to trigger G(2)/M progression in Xenopus oocytes. Genes Dev 13(16): 2177-2189.

Ferreira PC, Hemerly AS, Villarroel R, Van Montagu M, Inze D (1991) The Arabidopsis functional homolog of the p34cdc2 protein kinase. Plant Cell 3(5): 531-540.

Fisher DL, Nurse P (1996) A single fission yeast mitotic cyclin B p34cdc2 kinase promotes both S-phase and mitosis in the absence of G1 cyclins. Embo J 15(4): 850-860.

Fitch I, Dahmann C, Surana U, Amon A, Nasmyth K et al. (1992) Characterization of four B-type cyclin genes of the budding yeast Saccharomyces cerevisiae. Mol Biol Cell 3(7): 805-818.

Foley E, Sprenger F (2001) The cyclin-dependent kinase inhibitor Roughex is involved in mitotic exit in Drosophila. Curr Biol 11(3): 151-160.

Foley E, O'Farrell PH, Sprenger F (1999) Rux is a cyclin-dependent kinase inhibitor (CKI) specific for mitotic cyclin-Cdk complexes. Curr Biol 9(23): 1392-1402.

Follette PJ, Duronio RJ, O'Farrell PH (1998) Fluctuations in cyclin E levels are required for multiple rounds of endocycle S phase in Drosophila. Curr Biol 8(4): 235-238.

Frank-Vaillant M, Haccard O, Ozon R, Jessus C (2001) Interplay between Cdc2 kinase and the c-Mos/MAPK pathway between metaphase I and metaphase II in Xenopus oocytes. Developmental Biology 231(1): 279-288.

Fung TK, Ma HT, Poon RY (2007) Specialized roles of the two mitotic cyclins in somatic cells: cyclin A as an activator of M phase-promoting factor. Mol Biol Cell 18(5): 1861-1873.

Fung TK, Siu WY, Yam CH, Lau A, Poon RY (2002) Cyclin F is degraded during G2-M by mechanisms fundamentally different from other cyclins. J Biol Chem 277(38): 35140-35149.

Furuno N, den Elzen N, Pines J (1999) Human cyclin A is required for mitosis until mid prophase. J Cell Biol 147(2): 295-306.

Furuno N, Nishizawa M, Okazaki K, Tanaka H, Iwashita J et al. (1994) Suppression of DNA replication via Mos function during meiotic divisions in Xenopus oocytes. Embo J 13(10): 2399-2410.

Gavet O, Pines J (2010a) Progressive activation of CyclinB1-Cdk1 coordinates entry to mitosis. Dev Cell 18(4): 533-543.

Gavet O, Pines J (2010b) Activation of cyclin B1-Cdk1 synchronizes events in the nucleus and the cytoplasm at mitosis. J Cell Biol 189(2): 247-259.

Genschik P, Criqui MC, Parmentier Y, Derevier A, Fleck J (1998) Cell cycle -dependent proteolysis in plants. Identification Of the destruction box pathway and metaphase arrest produced by the proteasome inhibitor mg132. Plant Cell 10(12): 2063-2076.

Gerhart J, Wu M, Kirschner M (1984) Cell cycle dynamics of an M-phase-specific cytoplasmic factor in Xenopus laevis oocytes and eggs. J Cell Biol 98(4): 1247-1255.

Gertz EM, Yu YK, Agarwala R, Schaffer AA, Altschul SF (2006) Composition-based statistics and translated nucleotide searches: improving the TBLASTN module of BLAST. BMC Biol 4: 41.

Gillian-Daniel DL, Gray NK, Astrom J, Barkoff A, Wickens M (1998) Modifications of the 5' cap of mRNAs during Xenopus oocyte maturation: independence from changes in poly(A) length and impact on translation. Mol Cell Biol 18(10): 6152-6163.

Girard F, Fernandez A, Lamb N (1995) Delayed cyclin A and B1 degradation in non-transformed mammalian cells. J Cell Sci 108 (Pt 7): 2599-2608.

Glavan F, Behm-Ansmant I, Izaurralde E, Conti E (2006) Structures of the PIN domains of SMG6 and SMG5 reveal a nuclease within the mRNA surveillance complex. Embo J 25(21): 5117-5125.

Glotzer M (2001) Animal cell cytokinesis. Annu Rev Cell Dev Biol 17: 351-386.

Glotzer M, Murray AW, Kirschner MW (1991) Cyclin is degraded by the ubiquitin pathway. Nature 349(6305): 132-138.

Glover J, Grelon M, Craig S, Chaudhury A, Dennis E (1998) Cloning and characterization of MS5 from Arabidopsis: a gene critical in male meiosis. Plant Journal 15(3): 345-356.

Goldberg RB, Beals TP, Sanders PM (1993) Anther development: basic principles and practical applications. Plant Cell 5(10): 1217-1229.

Gonczy P, Thomas BJ, DiNardo S (1994) roughex is a dose-dependent regulator of the second meiotic division during Drosophila spermatogenesis. Cell 77(7): 1015-1025.

Gong D, Pomerening JR, Myers JW, Gustavsson C, Jones JT et al. (2007) Cyclin A2 regulates nuclear-envelope breakdown and the nuclear accumulation of cyclin B1. Curr Biol 17(1): 85-91.

Gould KL, Nurse P (1989) Tyrosine phosphorylation of the fission yeast cdc2+ protein kinase regulates entry into mitosis. Nature 342(6245): 39-45.

Gould KL, Moreno S, Owen DJ, Sazer S, Nurse P (1991) Phosphorylation at Thr167 is required for Schizosaccharomyces pombe p34cdc2 function. Embo J 10(11): 3297-3309.

Gross SD, Schwab MS, Taieb FE, Lewellyn AL, Qian YW et al. (2000) The critical role of the MAP kinase pathway in meiosis II in Xenopus oocytes is mediated by p90(Rsk). Curr Biol 10(8): 430-438.

Hadi MZ, Kemper E, Wendeler E, Reiss B (2002) Simple and versatile selection of Arabidopsis transformants. Plant Cell Reports 21(2): 130-135.

Hagan I, Hayles J, Nurse P (1988) Cloning and sequencing of the cyclin-related cdc13+ gene and a cytological study of its role in fission yeast mitosis. J Cell Sci 91 (Pt 4): 587-595.

Hansen KD, Lareau LF, Blanchette M, Green RE, Meng Q et al. (2009) Genome-wide identification of alternative splice forms down-regulated by nonsense-mediated mRNA decay in Drosophila. PLoS Genet 5(6): e1000525.

Harashima H, Shinmyo A, Sekine M (2007) Phosphorylation of threonine 161 in plant cyclin-dependent kinase A is required for cell division by activation of its associated kinase. Plant Journal 52(3): 435-448.

Hartwell LH, Culotti J, Reid B (1970) Genetic control of the cell-division cycle in yeast. I. Detection of mutants. Proc Natl Acad Sci U S A 66(2): 352-359.

Henderson KA, Kee K, Maleki S, Santini PA, Keeney S (2006) Cyclin-dependent kinase directly regulates initiation of meiotic recombination. Cell 125(7): 1321-1332.

Hinchcliffe EH, Li C, Thompson EA, Maller JL, Sluder G (1999) Requirement of Cdk2-cyclin E activity for repeated centrosome reproduction in Xenopus egg extracts. Science 283(5403): 851-854.

Hirayama T, Imajuku Y, Anai T, Matsui M, Oka A (1991) Identification of two cell-cycle-controlling cdc2 gene homologs in Arabidopsis thaliana. Gene 105(2): 159-165.

Hochegger H, Klotzbucher A, Kirk J, Howell M, le Guellec K et al. (2001) New B-type cyclin synthesis is required between meiosis I and II during Xenopus oocyte maturation. Development 128(19): 3795-3807.

Holloway SL, Glotzer M, King RW, Murray AW (1993) Anaphase is initiated by proteolysis rather than by the inactivation of maturation-promoting factor. Cell 73(7): 1393-1402.

Hruz T, Laule O, Szabo G, Wessendorp F, Bleuler S et al. (2008) Genevestigator v3: a reference expression database for the meta-analysis of transcriptomes. Adv Bioinformatics 2008: 420747.

Hunt PA, Hassold TJ (2002) Sex matters in meiosis. Science 296(5576): 2181-2183.

Iino Y, Yamamoto M (1985) Negative control for the initiation of meiosis in Schizosaccharomyces pombe. Proc Natl Acad Sci U S A 82(8): 2447-2451.

Iino Y, Hiramine Y, Yamamoto M (1995) The Role of Cdc2 and Other Genes in Meiosis in Schizosaccharomyces-Pombe. Genetics 140(4): 1235-1245.

Iwabuchi M, Ohsumi K, Yamamoto TM, Sawada W, Kishimoto T (2000) Residual Cdc2 activity remaining at meiosis I exit is essential for meiotic M-M transition in Xenopus oocyte extracts. Embo J 19(17): 4513-4523.

Izawa D, Goto M, Yamashita A, Yamano H, Yamamoto M (2005) Fission yeast Mes1p ensures the onset of meiosis II by blocking degradation of cyclin Cdc13p. Nature 434(7032): 529-533.

Jackman M, Firth M, Pines J (1995) Human cyclins B1 and B2 are localized to strikingly different structures: B1 to microtubules, B2 primarily to the Golgi apparatus. Embo J 14(8): 1646-1654.

Jaspersen SL, Charles JF, Tinker-Kulberg RL, Morgan DO (1998) A late mitotic regulatory network controlling cyclin destruction in Saccharomyces cerevisiae. Mol Biol Cell 9(10): 2803-2817.

Jeffrey PD, Russo AA, Polyak K, Gibbs E, Hurwitz J et al. (1995) Mechanism of CDK activation revealed by the structure of a cyclinA-CDK2 complex. Nature 376(6538): 313-320.

Jurgens G (2005) Cytokinesis in higher plants. Annu Rev Plant Biol 56: 281-299.

Kanki JP, Donoghue DJ (1991a) Progression from Meiosis-I to Meiosis-Ii in Xenopus Oocytes Requires Denovo Translation of the Mosxe Protooncogene. Proceedings of the National Academy of Sciences of the United States of America 88(13): 5794-5798.

Kanki JP, Donoghue DJ (1991b) Progression from meiosis I to meiosis II in Xenopus oocytes requires de novo translation of the mosxe protooncogene. Proc Natl Acad Sci U S A 88(13): 5794-5798.

Kassir Y, Granot D, Simchen G (1988) IME1, a positive regulator gene of meiosis in S. cerevisiae. Cell 52(6): 853-862.

Kaszas E, Cande WZ (2000) Phosphorylation of histone H3 is correlated with changes in the maintenance of sister chromatid cohesion during meiosis in maize, rather than the condensation of the chromatin. J Cell Sci 113(18): 3217-3226.

Kerenyi Z, Merai Z, Hiripi L, Benkovics A, Gyula P et al. (2008) Inter-kingdom conservation of mechanism of nonsense-mediated mRNA decay. Embo J 27(11): 1585-1595.

Kim S, Plagnol V, Hu TT, Toomajian C, Clark RM et al. (2007) Recombination and linkage disequilibrium in Arabidopsis thaliana. Nat Genet 39(9): 1151-1155.

Kim SY, Ferrell JE, Jr. (2007) Substrate competition as a source of ultrasensitivity in the inactivation of Wee1. Cell 128(6): 1133-1145.

Kimata Y, Trickey M, Izawa D, Gannon J, Yamamoto M et al. (2008) A mutual inhibition between APC/C and its substrate Mes1 required for meiotic progression in fission yeast. Developmental Cell 14(3): 446-454.

Kishida M, Nagai T, Nakaseko Y, Shimoda C (1994) Meiosis-dependent mRNA splicing of the fission yeast Schizosaccharomyces pombe mes1+ gene. Curr Genet 25(6): 497-503.

Kitajima TS, Kawashima SA, Watanabe Y (2004) The conserved kinetochore protein shugoshin protects centromeric cohesion during meiosis. Nature 427(6974): 510-517.

Knoblich JA, Lehner CF (1993) Synergistic action of Drosophila cyclins A and B during the G2-M transition. Embo J 12(1): 65-74.

Kohler C, Mittelsten Scheid O, Erilova A The impact of the triploid block on the origin and evolution of polyploid plants. Trends Genet 26(3): 142-148.

Landy A (1989) Dynamic, structural, and regulatory aspects of lambda site-specific recombination. Annu Rev Biochem 58: 913-949.

Lanker S, Valdivieso MH, Wittenberg C (1996) Rapid degradation of the G1 cyclin Cln2 induced by CDK-dependent phosphorylation. Science 271(5255): 1597-1601.

Lee DH, Goldberg AL (1998) Proteasome inhibitors: valuable new tools for cell biologists. Trends Cell Biol 8(10): 397-403.

Lehner CF, O'Farrell PH (1990) The roles of Drosophila cyclins A and B in mitotic control. Cell 61(3): 535-547.

Lenormand JL, Dellinger RW, Knudsen KE, Subramani S, Donoghue DJ (1999) Speedy: a novel cell cycle regulator of the G2/M transition. Embo J 18(7): 1869-1877.

Lilly MA, Spradling AC (1996) The Drosophila endocycle is controlled by Cyclin E and lacks a checkpoint ensuring S-phase completion. Genes Dev 10(19): 2514-2526.

Lim HH, Loy CJ, Zaman S, Surana U (1996) Dephosphorylation of threonine 169 of Cdc28 is not required for exit from mitosis but may be necessary for start in Saccharomyces cerevisiae. Mol Cell Biol 16(8): 4573-4583.

Liu D, Matzuk MM, Sung WK, Guo Q, Wang P et al. (1998) Cyclin A1 is required for meiosis in the male mouse. Nat Genet 20(4): 377-380.

Liu J, Qu LJ (2008) Meiotic and mitotic cell cycle mutants involved in gametophyte development in Arabidopsis. Mol Plant 1(4): 564-574.

Lock LF, Pines J, Hunter T, Gilbert DJ, Gopalan G et al. (1992) A single cyclin A gene and multiple cyclin B1-related sequences are dispersed in the mouse genome. Genomics 13(2): 415-424.

Lopez-Aviles S, Kapuy O, Novak B, Uhlmann F (2009) Irreversibility of mitotic exit is the consequence of systems-level feedback. Nature 459(7246): 592-595.

Lorca T, Labbe JC, Devault A, Fesquet D, Capony JP et al. (1992) Dephosphorylation of cdc2 on threonine 161 is required for cdc2 kinase inactivation and normal anaphase. Embo J 11(7): 2381-2390.

Ma H (2005) Molecular genetic analyses of microsporogenesis and microgametogenesis in flowering plants. Annu Rev Plant Biol 56: 393-434.

Madlung A, Tyagi AP, Watson B, Jiang H, Kagochi T et al. (2005) Genomic changes in synthetic Arabidopsis polyploids. Plant J 41(2): 221-230.

Magnard JL, Yang M, Chen YCS, Leary M, McCormick S (2001) The Arabidopsis gene tardy asynchronous meiosis is required for the normal pace and synchrony of cell division during male meiosis. Plant Physiology 127(3): 1157-1166.

Malapeira J, Moldon A, Hidalgo E, Smith GR, Nurse P et al. (2005) A meiosis-specific cyclin regulated by splicing is required for proper progression through meiosis. Molecular and Cellular Biology 25(15): 6330-6337.

Mandel S, Robzyk K, Kassir Y (1994) IME1 gene encodes a transcription factor which is required to induce meiosis in Saccharomyces cerevisiae. Dev Genet 15(2): 139-147.

Manzanero S, Arana P, Puertas MJ, Houben A (2000a) The chromosomal distribution of phosphorylated histone H3 differs between plants and animals at meiosis. Chromosoma 109(5): 308-317.

Manzanero S, Arana P, Puertas MJ, Houben A (2000b) The chromosomal distribution of phosphorylated histone H3 differs between plants and animals at meiosis. Chromosoma 109(5): 308-317.

Marston AL, Amon A (2004) Meiosis: Cell-cycle controls shuffle and deal. Nature Reviews Molecular Cell Biology 5(12): 983-997.

Marston AL, Lee BH, Amon A (2003) The Cdc14 phosphatase and the FEAR network control meiotic spindle disassembly and chromosome segregation. Dev Cell 4(5): 711-726.

Martin-Castellanos C, Labib K, Moreno S (1996) B-type cyclins regulate G1 progression in fission yeast in opposition to the p25rum1 cdk inhibitor. Embo J 15(4): 839-849.

Masui Y, Markert CL (1971) Cytoplasmic control of nuclear behavior during meiotic maturation of frog oocytes. J Exp Zool 177(2): 129-145.

Matos J, Lipp JJ, Bogdanova A, Guillot S, Okaz E et al. (2008) Dbf4-dependent CDC7 kinase links DNA replication to the segregation of homologous chromosomes in meiosis I. Cell 135(4): 662-678.

McCormick S (2004) Control of male gametophyte development. Plant Cell 16 Suppl: S142-153.

McGuinness BE, Hirota T, Kudo NR, Peters JM, Nasmyth K (2005) Shugoshin prevents dissociation of cohesin from centromeres during mitosis in vertebrate cells. PLoS Biol 3(3): e86.

McPheeters DS, Cremona N, Sunder S, Chen HM, Averbeck N et al. (2009) A complex gene regulatory mechanism that operates at the nexus of multiple RNA processing decisions. Nat Struct Mol Biol 16(3): 255-264.

Mercier R, Grelon M (2008) Meiosis in plants: ten years of gene discovery. Cytogenet Genome Res 120(3-4): 281-290.

Meyer H, Drozdowska A, Dobrynin G (2010) A role for Cdc48/p97 and Aurora B in controlling chromatin condensation during exit from mitosis. Biochem Cell Biol 88(1): 23-28.

Minshull J, Golsteyn R, Hill CS, Hunt T (1990) The A- and B-type cyclin associated cdc2 kinases in Xenopus turn on and off at different times in the cell cycle. Embo J 9(9): 2865-2875.

Minshull J, Murray A, Colman A, Hunt T (1991) Xenopus oocyte maturation does not require new cyclin synthesis. J Cell Biol 114(4): 767-772.

Moldon A, Malapeira J, Gabrielli N, Gogol M, Gomez-Escoda B et al. (2008) Promoter-driven splicing regulation in fission yeast. Nature 455(7215): 997-U983.

Morelli MA, Cohen PE (2005) Not all germ cells are created equal: aspects of sexual dimorphism in mammalian meiosis. Reproduction 130(6): 761-781.

Musacchio A, Hardwick KG (2002) The spindle checkpoint: structural insights into dynamic signalling. Nat Rev Mol Cell Biol 3(10): 731-741.

Nebreda AR (2006) CDK activation by non-cyclin proteins. Curr Opin Cell Biol 18(2): 192-198.

Nguyen TB, Manova K, Capodieci P, Lindon C, Bottega S et al. (2002a) Characterization and expression of mammalian cyclin B3, a prepachytene meiotic cyclin. Journal of Biological Chemistry 277(44): 41960-41969.

Nguyen TB, Manova K, Capodieci P, Lindon C, Bottega S et al. (2002b) Characterization and expression of mammalian cyclin b3, a prepachytene meiotic cyclin. J Biol Chem 277(44): 41960-41969.

Nieduszynski CA, Murray J, Carrington M (2002) Whole-genome analysis of animal A- and B-type cyclins. Genome Biol 3(12): RESEARCH0070.

Nishiyama T, Ohsumi K, Kishimoto T (2007) Phosphorylation of Erp1 by p90rsk is required for cytostatic factor arrest in Xenopus laevis eggs. Nature 446(7139): 1096-1099.

Nurse P (1990) Universal control mechanism regulating onset of M-phase. Nature 344(6266): 503-508.

Nurse P, Thuriaux P (1980) Regulatory genes controlling mitosis in the fission yeast Schizosaccharomyces pombe. Genetics 96(3): 627-637.

Obara-Ishihara T, Okayama H (1994) A B-type cyclin negatively regulates conjugation via interacting with cell cycle 'start' genes in fission yeast. Embo J 13(8): 1863-1872.

Ohe M, Inoue D, Kanemori Y, Sagata N (2007) Erp1/Emi2 is essential for the meiosis I to meiosis II transition in Xenopus oocytes. Dev Biol 303(1): 157-164.

Ohsumi K, Yamamoto TM, Iwabuchi M (2006) Oocyte extracts for the study of meiotic M-M transition. Methods Mol Biol 322: 445-458.

Orr-Weaver TL (1995) Meiosis in Drosophila: seeing is believing. Proc Natl Acad Sci U S A 92(23): 10443-10449.

Page AW, OrrWeaver TL (1996) The Drosophila genes grauzone and cortex are necessary for proper female meiosis. Journal of Cell Science 109: 1707-1715.

Parry DH, O'Farrell PH (2001) The schedule of destruction of three mitotic cyclins can dictate the timing of events during exit from mitosis. Curr Biol 11(9): 671-683.

Peck SC (2006) Analysis of protein phosphorylation: methods and strategies for studying kinases and substrates. Plant J 45(4): 512-522.

Perez-Hidalgo L, Moreno S, Martin-Castellanos C (2007) Modified cell cycle regulation in meiosis. Genome Dyn Stab 2: 307-353.

Peters JM (2006) The anaphase promoting complex/cyclosome: a machine designed to destroy. Nat Rev Mol Cell Biol 7(9): 644-656.

Pfleger CM, Kirschner MW (2000) The KEN box: an APC recognition signal distinct from the D box targeted by Cdh1. Genes Dev 14(6): 655-665.

Philpott A, Yew PR (2008) The Xenopus cell cycle: an overview. Mol Biotechnol 39(1): 9-19.

Pines J, Hunter T (1989) Isolation of a human cyclin cDNA: evidence for cyclin mRNA and protein regulation in the cell cycle and for interaction with p34cdc2. Cell 58(5): 833-846.

Pines J, Hunter T (1991) Human cyclins A and B1 are differentially located in the cell and undergo cell cycle-dependent nuclear transport. J Cell Biol 115(1): 1-17.

Pinsky BA, Biggins S (2005) The spindle checkpoint: tension versus attachment. Trends Cell Biol 15(9): 486-493.

Planchais S, Glab N, Inze D, Bergounioux C (2000) Chemical inhibitors: a tool for plant cell cycle studies. Febs Letters 476(1-2): 78-83.

Poliseno L, Salmena L, Zhang J, Carver B, Haveman WJ et al. (2010) A coding-independent function of gene and pseudogene mRNAs regulates tumour biology. Nature 465(7301): 1033-1038.

Rabitsch KP, Gregan J, Schleiffer A, Javerzat JP, Eisenhaber F et al. (2004) Two fission yeast homologs of Drosophila Mei-S332 are required for chromosome segregation during meiosis I and II. Curr Biol 14(4): 287-301.

Radford HE, Meijer HA, de Moor CH (2008) Translational control by cytoplasmic polyadenylation in Xenopus oocytes. Biochim Biophys Acta 1779(4): 217-229.

Rhind N, Russell P (1998) Mitotic DNA damage and replication checkpoints in yeast. Curr Opin Cell Biol 10(6): 749-758.

Richardson H, Lew DJ, Henze M, Sugimoto K, Reed SI (1992) Cyclin-B homologs in Saccharomyces cerevisiae function in S phase and in G2. Genes Dev 6(11): 2021-2034.

Riehs N (2009) Functional characterization of the Arabidopsis SMG7 protein. University of Vienna, Dissertation.

Riehs N, Akimcheva S, Puizina J, Bulankova P, Idol RA et al. (2008) Arabidopsis SMG7 protein is required for exit from meiosis. Journal of Cell Science 121(13): 2208-2216.

Rogers S, Wells R, Rechsteiner M (1986) Amino acid sequences common to rapidly degraded proteins: the PEST hypothesis. Science 234(4774): 364-368.

Ross KE, Kaldis P, Solomon MJ (2000) Activating phosphorylation of the Saccharomyces cerevisiae cyclin-dependent kinase, cdc28p, precedes cyclin binding. Mol Biol Cell 11(5): 1597-1609.

Ross KJ, Fransz P, Armstrong SJ, Vizir I, Mulligan B et al. (1997) Cytological characterization of four meiotic mutants of Arabidopsis isolated from T-DNA-transformed lines. Chromosome Research 5(8): 551-559.

Russo AA, Jeffrey PD, Pavletich NP (1996) Structural basis of cyclin-dependent kinase activation by phosphorylation. Nat Struct Biol 3(8): 696-700.

Salic A, Waters JC, Mitchison TJ (2004) Vertebrate shugoshin links sister centromere cohesion and kinetochore microtubule stability in mitosis. Cell 118(5): 567-578.

Sanchez-Diaz A, Gonzalez I, Arellano M, Moreno S (1998) The Cdk inhibitors p25rum1 and p40SIC1 are functional homologues that play similar roles in the regulation of the cell cycle in fission and budding yeast. J Cell Sci 111 (Pt 6): 843-851.

Sanders PM, Bui AQ, Weterings K, McIntire KN, Hsu Y-C et al. (1999) Anther developmental defects in Arabidopsis thaliana male-sterile mutants. Sexual Plant Reproduction 11(6): 297-322.

Schwob E, Nasmyth K (1993) CLB5 and CLB6, a new pair of B cyclins involved in DNA replication in Saccharomyces cerevisiae. Genes Dev 7(7A): 1160-1175.

Schwob E, Bohm T, Mendenhall MD, Nasmyth K (1994) The B-type cyclin kinase inhibitor p40SIC1 controls the G1 to S transition in S. cerevisiae. Cell 79(2): 233-244.

Sherr CJ, Roberts JM (1999) CDK inhibitors: positive and negative regulators of G1-phase progression. Genes Dev 13(12): 1501-1512.

Shou W, Seol JH, Shevchenko A, Baskerville C, Moazed D et al. (1999) Exit from mitosis is triggered by Tem1-dependent release of the protein phosphatase Cdc14 from nucleolar RENT complex. Cell 97(2): 233-244.

Sigrist S, Jacobs H, Stratmann R, Lehner CF (1995) Exit from mitosis is regulated by Drosophila fizzy and the sequential destruction of cyclins A, B and B3. Embo J 14(19): 4827-4838.

Skaar JR, Pagano M (2008) Cdh1: a master G0/G1 regulator. Nat Cell Biol 10(7): 755-757.

Skowyra D, Craig KL, Tyers M, Elledge SJ, Harper JW (1997) F-box proteins are receptors that recruit phosphorylated substrates to the SCF ubiquitin-ligase complex. Cell 91(2): 209-219.

Smith HE, Mitchell AP (1989) A transcriptional cascade governs entry into meiosis in Saccharomyces cerevisiae. Mol Cell Biol 9(5): 2142-2152.

Smyth DR, Bowman JL, Meyerowitz EM (1990) Early flower development in Arabidopsis. Plant Cell 2(8): 755-767.

Stalder L, Muhlemann O (2008) The meaning of nonsense. Trends Cell Biol 18(7): 315-321.

Stegmeier F, Amon A (2004) Closing mitosis: the functions of the Cdc14 phosphatase and its regulation. Annu Rev Genet 38: 203-232.

Stegmeier F, Visintin R, Amon A (2002) Separase, polo kinase, the kinetochore protein Slk19, and Spo12 function in a network that controls Cdc14 localization during early anaphase. Cell 108(2): 207-220.

Strausfeld UP, Howell M, Descombes P, Chevalier S, Rempel RE et al. (1996) Both cyclin A and cyclin E have S-phase promoting (SPF) activity in Xenopus egg extracts. J Cell Sci 109 (Pt 6): 1555-1563.

Stuart D, Wittenberg C (1998) CLB5 and CLB6 are required for premeiotic DNA replication and activation of the meiotic S/M checkpoint. Genes Dev 12(17): 2698-2710.

Swan A, Schupbach T (2005) Drosophila female meiosis and embryonic syncytial mitosis use specialized Cks and CDC20 proteins for cyclin destruction. Cell Cycle 4(10): 1332-1334.

Swan A, Schupbach T (2007) The Cdc20 (Fzy)/Cdh1-related protein, Cort, cooperates with Fzy in cyclin destruction and anaphase progression in meiosis I and II in Drosophila. Development 134(5): 891-899.

Swan A, Barcelo G, Schupbach T (2005) Drosophila Cks30A interacts with Cdk1 to target Cyclin A for destruction in the female germline. Development 132(16): 3669-3678.

Takatsuka H, Ohno R, Umeda M (2009) The Arabidopsis cyclin-dependent kinase-activating kinase CDKF;1 is a major regulator of cell proliferation and cell expansion but is dispensable for CDKA activation. Plant J 59(3): 475-487.

Tang WL, Wu JQ, Guo YX, Hansen DV, Perry JA et al. (2008) Cdc2 and Mos regulate Emi2 stability to promote the meiosis I-meiosis II transition. Molecular Biology of the Cell 19(8): 3536-3543.

Thomas BJ, Gunning DA, Cho J, Zipursky L (1994) Cell cycle progression in the developing Drosophila eye: roughex encodes a novel protein required for the establishment of G1. Cell 77(7): 1003-1014.

Thomas BJ, Zavitz KH, Dong X, Lane ME, Weigmann K et al. (1997) roughex down-regulates G2 cyclins in G1. Genes Dev 11(10): 1289-1298.

Tung JJ, Padmanabhan K, Hansen DV, Richter JD, Jackson PK (2007) Translational unmasking of Emi2 directs cytostatic factor arrest in meiosis II. Cell Cycle 6(6): 725-731.

van Zon W, Wolthuis RM (2010) Cyclin A and Nek2A: APC/C-Cdc20 substrates invisible to the mitotic spindle checkpoint. Biochem Soc Trans 38(Pt 1): 72-77.

Visintin R, Hwang ES, Amon A (1999) Cfi1 prevents premature exit from mitosis by anchoring Cdc14 phosphatase in the nucleolus. Nature 398(6730): 818-823.

Visintin R, Craig K, Hwang ES, Prinz S, Tyers M et al. (1998) The phosphatase Cdc14 triggers mitotic exit by reversal of Cdk-dependent phosphorylation. Mol Cell 2(6): 709-718.

Waga S, Stillman B (1998) The DNA replication fork in eukaryotic cells. Annu Rev Biochem 67: 721-751.

Walker DH, Maller JL (1991) Role for cyclin A in the dependence of mitosis on completion of DNA replication. Nature 354(6351): 314-317.

Wang GF, Kong HZ, Sun YJ, Zhang XH, Zhang W et al. (2004a) Genome-wide analysis of the cyclin family in Arabidopsis and comparative phylogenetic analysis of plant cyclin-like proteins. Plant Physiology 135(2): 1084-1099.

Wang YX, Magnard JL, McCormick S, Yang M (2004b) Progression through meiosis I and meiosis II in Arabidopsis anthers is regulated by an A-type cyclin predominately expressed in prophase I. Plant Physiology 136(4): 4127-4135.

Wang YX, Jha AK, Chen RJ, Doonan JH, Yang M (2010) Polyploidy-Associated Genomic Instability in Arabidopsis thaliana. Genesis 48(4): 254-263.

Welcker M, Singer J, Loeb KR, Grim J, Bloecher A et al. (2003) Multisite phosphorylation by Cdk2 and GSK3 controls cyclin E degradation. Mol Cell 12(2): 381-392.

Wolf F, Sigl R, Geley S (2007) '... The end of the beginning': Cdk1 thresholds and exit from mitosis. Cell Cycle 6(12): 1408-1411.

Wolf F, Wandke C, Isenberg N, Geley S (2006) Dose-dependent effects of stable cyclin B1 on progression through mitosis in human cells. Embo J 25(12): 2802-2813.

Wolthuis R, Clay-Farrace L, van Zon W, Yekezare M, Koop L et al. (2008) Cdc20 and Cks direct the spindle checkpoint-independent destruction of cyclin A. Mol Cell 30(3): 290-302.

Won KA, Reed SI (1996) Activation of cyclin E/CDK2 is coupled to site-specific autophosphorylation and ubiquitin-dependent degradation of cyclin E. Embo J 15(16): 4182-4193.

Yadegari R, Drews GN (2004) Female gametophyte development. Plant Cell 16 Suppl: S133-141.

Yang J, Kornbluth S (1999) All aboard the cyclin train: subcellular trafficking of cyclins and their CDK partners. Trends Cell Biol 9(6): 207-210.

Yang J, Bardes ES, Moore JD, Brennan J, Powers MA et al. (1998) Control of cyclin B1 localization through regulated binding of the nuclear export factor CRM1. Genes Dev 12(14): 2131-2143.

7. ABBREVIATIONS

APC	anaphase promoting complex
ATP	adenosine triphosphate
BLAST	basic local alignment search tool
cdk	cyclin dependent kinase
cDNA	complementary DNA
CDS	coding sequence
Col 0	Columbia – Arabidopsis ecotype
DAPI	4',6-diamidino-2-phenylindole
D-box	destruction box
dH_2O	distilled water
dNTP	deoxyribonucleotide triphosphate
DTT	dithiothreitol
EDTA	Ethylenediaminetetraacetic acid
FISH	fluorescent *in situ* hybridization
gDNA	genomic DNA
GFP	green fluorescent protein
GUS	beta-glucuronidase
h	hour
kDa	kilodalton
MES	2-(N-morpholinoethane- sulphonic acid)
MFP	maturation promoting factor
min	minute
mRNA	messenger RNA
MS medium	Murashige and Skoog medium
NC	negative control
OD	optical density
PCR	polymerase chain reaction
RACE	rapid amplification of cDNA ends
RT	reverse transcriptase
RT PCR	Reverse transcription polymerase chain reaction
SDS	sodium dodecyl sulphate
sec	second

T-DNA	transfer DNA
Thr	threonine
u	unit
UTR	untranslated region
X-GLUC	5-bromo-4-chloro-3-indolyl-beta-D-glucuronic acid cyclohexylammonium salt
YFP	yellow fluorescent protein

8. ACKNOWLEDGEMENT

First of all, I would like thank Karel. I would like to thank for his patience, his never ending enthusiasm for scientific questions and positive view on any problems I needed to solve. Under his supervision I had a unique chance to work on a project that I was interested in. I always had enough freedom but when it was necessary he shifted the research in right direction. And besides it, I also had a great chance to spend four years of my life in a place with a great scientific atmosphere where I could learn and develop.

I would like to thank to my PhD committee members: Marie-Therese Hauser, Franz Klein and Jan-Michael Peters for their feedback on my work, for their inputs and advices.

I would like to thank in advance to Dr. Ortrun Mittelsten Scheid and Prof. Boris Vyskot for reviewing my thesis.

I have to thank our collaborators: Dr. Arp Schnittger and Dr. Moritz Nowack for providing *CDKA;1:YFP* complemented plants, Dr. Susan Armstrong for plants carrying *tdm1-1*mutant allele and Dr. Thomas Turner for the analysis of Affymetrix tilling arrays for polymorphism in cyclin genes in *Arabidopsis* ecotypes

I want to thank Sveta for all her help during my PhD, uncountable number of practical advices about protocols but also being a great friend, open-minded and experienced.

I would like to thank people who worked on this project with me: Nina for sharing a data about *SMG7* with me and also sharing a non-telomeric topic in a telomere oriented lab. Clemens for his work on histological examination of GUS tagged constructs and also for many non-scientific discussions.

I would like thank my friends Iva and Aleš with his family simply for being great friends.

I want to thank Matt for being always ready and happy to help with whatever (mainly correcting my English texts).

I would like to thank all the current and former lab members that I did not mention so far - Babsi,

Martina, Anita, Astrid, Elisa, Soňa, Max, Honza, Christian, Jiradet and Nick for making our lab a nice place to work. I want to thank them and also Gudrun for many discussions on scientific as well as non scientific topics.

And last but not least I want to thank my family – my parents Eva and Peter and my sister Kristína for their support and love over all the years. I have to thank Braňo for so many things that I cannot even name them all here - simply for all the time he is living with me.

Finally, I want to apologize to anyone I forgot to mention.

9. CURRICULUM VITAE

Name: Petra Bulánková

Birth: 17.03.1981, Bratislava, Slovak Republic

Address: GMI – Gregor Mendel Institute of Molecular Plant Biology
Dr. Bohrgasse 3
1030 Vienna, Austria

E-mail: petra.bulankova@gmi.oeaw.ac.at

Education:

1996 – 2001 – High school Gymnázium Metodova 2, French – Slovak bilingual section, Bratislava, Slovak Republic

2001 – 2004 – Masaryk University in Brno
Bachelors degree studies in Biology, Faculty of Science, Czech Republic

2004 – 2006 – Masaryk University in Brno,
Masters degree studies in Molecular Biology and Genetics, Czech Republic

2004 - 2006 – diploma student in the Laboratory of Plant Developmental Genetics, Institute of Biophysics, Brno, Czech Republic
Supervisor: Dr. Jiri Siroky
Title of diploma thesis: Genomic instabilities induced by telomerase dysfunction in *Arabidopsis*.

2006 – 2010 – PhD student at the Gregor Mendel Institute of Molecular Plant Biology (GMI), Vienna, Austria
Supervisor: Dr. Karel Riha
Title of thesis:
Regulation of meiotic progression in *Arabidopsis*

Publications

Bulankova P, Riehs-Kearnan N, Nowack MK, Schnittger A, Riha K.: Meiotic Progression in *Arabidopsis* Is Governed by Complex Regulatory Interactions between SMG7, TDM1, and the Meiosis I-Specific Cyclin TAM. Plant Cell. 2010 Nov 30. [Epub ahead of print]

Riehs N, Akimcheva S, Puizina J, Bulankova P, Idol RA, Siroky J, Schleiffer A, Schweizer D, Shippen DE, Riha K.: *Arabidopsis* SMG7 protein is required for exit from meiosis. J Cell Sci. 2008 Jul 1;121(Pt 13):2208-16.

Watson JM, Bulankova P, Riha K, Shippen DE, Vyskot B: Telomerase-independent cell survival in *Arabidopsis thaliana*. Plant J. 2005 Sep;43(5):662-74.

Presentations at meetings and conferences:

Arabidopsis EST1/SMG7-like protein is a novel regulator of meiotic cell cycle progression.
4th Tri-National Arabidopsis Meeting
Vienna, Austria, September 12-15th 2007
poster presentation

Immunodetection of active CDK complexes during Arabidopsis meiosis
The EMBO Conference on Meiosis
Isle sur la Sorgue, France, September 19-26th 2009
poster presentation

Meiosis: the cell cycle between sporophyte and gametophyte
12 th Conference of Experimental Plant Biology
Prague, Czech Republic, September 14-17th 2010
oral presentation